

Fundamentals of the Host-Virus Evolutionary Arms Race

Efrem S. Lim

A dissertation
submitted in partial fulfillment of the
requirements for the degree of

Doctor of Philosophy

University of Washington

2012

Michael Emerman, Chair

Harmit S. Malik

Shiu-lok Hu

Program Authorized to Offer Degree:

Microbiology

University of Washington

Abstract

Fundamentals of the Host-Virus Evolutionary Arms Race

Efrem S. Lim

Chair of the Supervisory Committee:
Affiliate Professor Michael Emerman
Microbiology

The immune system has been battling viral infections over the course of millions of years in primate evolution. The constant evolution of hosts and viruses to defeat the other has led to a high stakes genetic arms race. Here I present a detailed study of three antiviral proteins locked in antagonistic viral conflict called Tetherin, Viperin and SAMHD1. Using a combined approach of virology and evolutionary biology, I have reconstructed their evolutionary arms race between primates and lentiviruses, including HIV-1, HIV-2 and related SIVs. The broad themes that emerge from my research are two-fold. First, lentiviruses are able to evolve new functions within existing gene repertoires to counteract rapidly evolving host antiviral genes. Second, hosts escape from viral pressure either by single amino acid changes or by deletions of a 'susceptibility domain'. Thus, my thesis research has helped define the rules by which host-virus arms races ensue. Based on my findings, we contend that the host evolutionary framework is a fundamental pillar of antiviral restriction.

TABLE OF CONTENTS

	Page
LIST OF FIGURES.....	ii
LIST OF TABLES	iv
CHAPTER ONE.....	1
CHAPTER TWO.....	45
CHAPTER THREE.....	66
CHAPTER FOUR.....	91
CHAPTER FIVE.....	124
CHAPTER SIX.....	150
CHAPTER SEVEN.....	182
REFERENCES	194

LIST OF FIGURES

Figure Number	Page
Figure 1	4
Figure 2	5
Figure 3	15
Figure 4	16
Figure 5	19
Figure 6	23
Figure 7	33
Figure 8	35
Figure 9	38
Figure 10	39
Figure 11	44
Figure 12	69
Figure 13	72
Figure 14	75
Figure 15	78
Figure 16	81
Figure 17	84
Figure 18	86
Figure 19	90
Figure 20	98
Figure 21	101
Figure 22	106
Figure 23	107
Figure 24	112
Figure 25	116
Figure 26	118
Figure 27	131
Figure 28	133
Figure 29	138
Figure 30	139
Figure 31	142
Figure 32	144
Figure 33	146

Figure 34	154
Figure 35	160
Figure 36	161
Figure 37	164
Figure 38	167
Figure 39	170
Figure 40	171
Figure 41	174
Figure 42	175
Figure 43	179
Figure 44	181
Figure 45	187
Figure 46	191

LIST OF TABLES

	Page
Table 1.....	157

Acknowledgements

First and foremost, I am grateful to my mentor and role model, Michael Emerman. Thank you for giving me the opportunity to learn from you and the intellectual freedom to explore diverse challenges (We covered 3 restriction factors and nearly all the accessory genes within a PhD!) After all these years, I have finally discovered the secret to your success – your dedicated passion and realistic optimism. (No wonder you could also bike from Seattle to Portland, I feel sore just thinking about that!) Your scientific acumen and unwavering support has made a lasting impression. I hope that someday I will be a purposeful scientist like yourself and emulate your success.

I am also grateful to Harmit Malik. There's a saying that to 'teach a man to fish, you feed him for a lifetime'. Not only did you teach me to fish, you taught me 99 ways to cook it (metaphorically, of course). Your creativity is phenomenal. Thank you for your guidance and mentorship. By your example, I have learned the importance of communicating fantastic scientific concepts in simplicity.

I would like to acknowledge and thank members of the Emerman and Malik lab for their contribution to this experience. In particular, I would like to thank Lily Wu. Thanks for being there when I needed help and being my confidante. I have also been very fortunate to be surrounded by many brilliant scientists, and would like to acknowledge the following people:

(Emerman Lab) Alex Compton, Nisha Duggal, Oliver Fregoso, Semih Tareen
and Masahiro Yamashita

(Malik Lab) Nels Elde, Raymond Malfavon-Borja, Patrick Mitchell and Maulik Patel
(Collaborators) Erick Matsen and Connor McCoy

I wish to thank my PhD Committee for their advice and guidance that has shaped my research and honed my scientific thinking:

Evan Eichler, Shiu-lok Hu, Julie Overbaugh and Rolland Strong.

My research has been generously supported by the Fred Hutchinson Cancer Research Center Interdisciplinary Fellowship and the University of Washington Helen Riaboff Whiteley Graduate Fellowship Award.

Finally, I would like to sincerely thank my family for their love and support. Thanks for giving me the opportunity to pursue my PhD in the US. Sorry for not always replying your emails as promptly as I should have! So, thanks for being understanding and supportive.

CHAPTER ONE

INTRODUCTION

RETROVIRUSES AND LENTIVIRUSES

Retroviruses are a broad family of viruses that package a dimer of positive-sense single-stranded RNA genomes. The hallmark of a retrovirus is the reverse-transcription stage in its life cycle that transcribes DNA from RNA genetic material during its replication. Based on their genomes, retroviruses can be classified as simple retroviruses – alpha, beta and gamma retroviruses; or complex retroviruses – delta, epsilon, spuma and lentiviruses. The genome of simple retroviruses encodes the *gag*, *pol* and *env* genes within flanking long terminal repeat sequences (LTRs). In contrast, complex retroviruses encode accessory genes in addition to the *gag*, *pol*, *env* genes within their LTRs. While these accessory genes are dispensable for producing infectious virions, they afford utility in enhancing viral replication in different cell types

HIV-1 and other primate lentiviruses encode accessory genes that serve to enhance virus replication and counteract host immune factors (151). Studies of these accessory proteins have led to the identification of important antiviral effector proteins encoded by host genomes called host restriction factors (123). Human immunodeficiency virus (HIV) and its close relative simian immunodeficiency virus (SIV) are prominent members of the lentivirus subfamily whose accessory genes have been characterized substantially.

There are five accessory genes in primate lentiviruses – Vif, Vpx, Vpr, Vpu and Nef (reviewed extensively in (151)).

- Virion infectivity factor (Vif) plays an important role in HIV-1 replication in primary T cells, but is dispensable in certain cell types. The cellular gene called APOBEC3G is the target of Vif antagonism.
- Viral protein R (Vpr) is encoded by all extant primate lentiviruses. Vpr is best associated with the phenotype of exerting arrest at the G2 phase of the cell cycle. While the cellular protein targeted by Vpr is still unknown, multiple lines of evidence point to the degradation of this factor that leads to the cell cycle arrest.
- Viral protein X (Vpx) is a paralog of Vpr. While all extant primate lentiviruses encode a *vpr*, *vpx* is only found in 3 lineages of primate lentiviruses. This is a unique feature of HIV-2 and is absent from HIV-1. Vpx targets the cellular protein called SAMHD1 for degradation resulting in enhanced infection of monocyte-derived dendritic cells and macrophages, with the former having the highest effect.
- Negative factor (Nef) is encoded by all primate lentiviruses. Nef displays pleiotropic effects that include cell surface receptor modulation, cholesterol biosynthesis, infectivity enhancement and immunoregulatory effects (12, 281, 318). In several lineages, Nef antagonizes the host restriction factor called tetherin to enhance virus release.

- Finally, Viral protein U (Vpu) is encoded by HIV-1 and SIVmus/gsn lineages, but is absent from HIV-2 and several other lineages. Vpu also modulates the expression levels of cell surface proteins such as CD4 and NTB-A (243). Vpu encoded by some of these viruses have also evolved to antagonize tetherin.

Due to their different origins, HIV-1 and HIV-2 are phylogenetically distinct and also differ in their genomic organization. HIV-1 encodes Vif, Vpr, Vpu and Nef accessory genes, while the related HIV-2 virus has a different repertoire of Vif, Vpx, Vpr and Nef (Figure 1). Another difference is that HIV-1 Nef open reading frame does not overlap with Env, whereas HIV-2 Nef maintains an overlap with the c-terminal portion of Env (196).

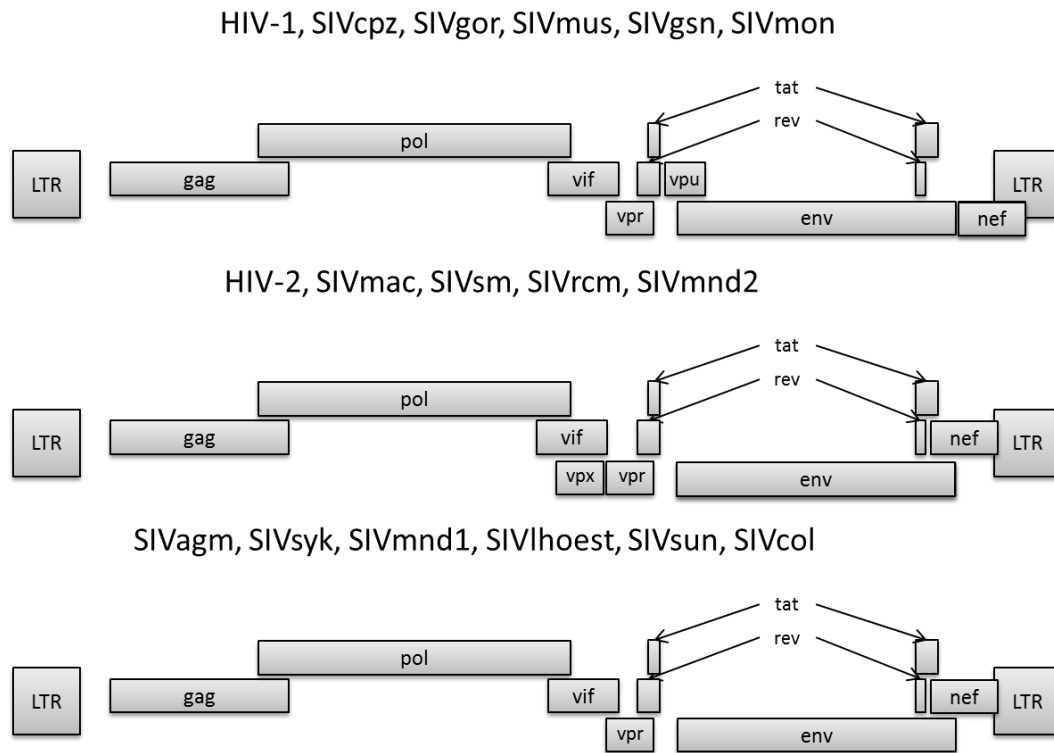
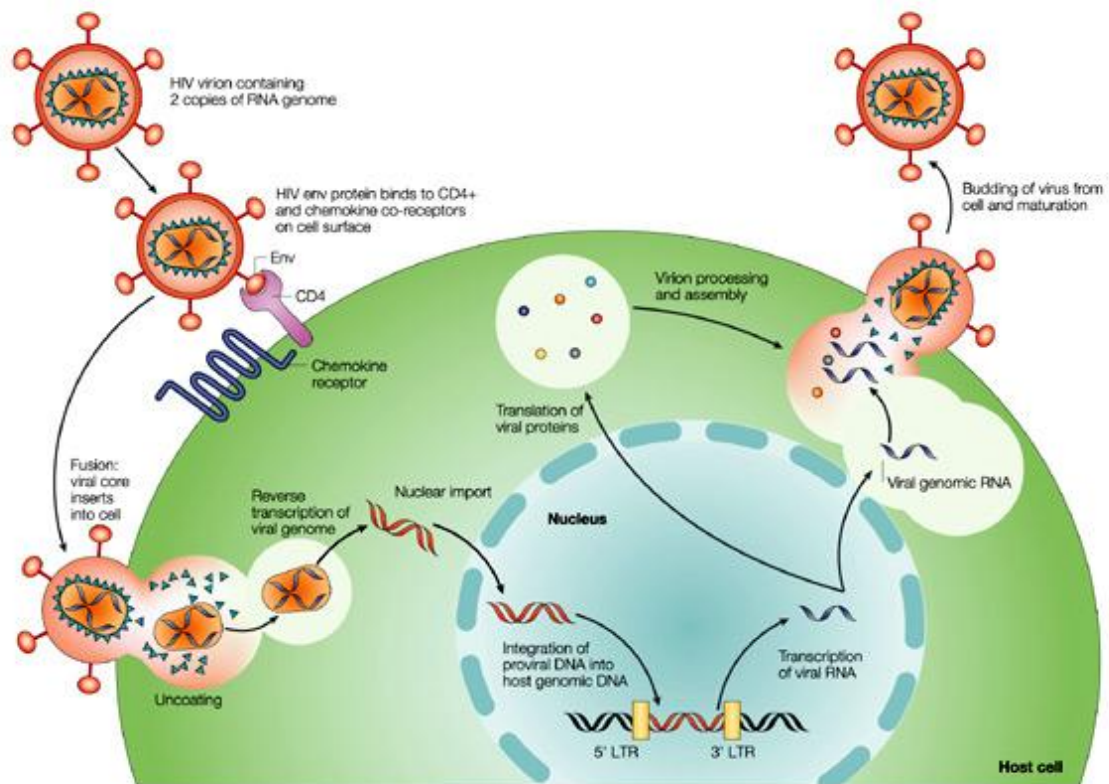


Figure 1

Genomic organization of primate lentiviruses.

HIV-1/SIVcpz lineages encode a unique *vpu* gene. HIV-2/SIVmac lineages encode a unique *vpx* gene. The third group of viruses including SIVagm lineages lacks *vpx* and *vpu* genes.



Nature Reviews | Genetics

Figure 2

This figure summarizes the HIV-1 life cycle. HIV-1 entry is mediated by binding to cell surface CD4 and co-receptors, followed by fusion. Virion uncoating occurs and reverse transcription proceeds in the cytoplasm. After provirus integration, viral transcription and translation lead to synthesis of viral proteins. Virion particles are assembled and bud from the plasma membrane.

This figure is from (214) with permission (License number 2798930993888).

HIV LIFE CYCLE

Entry of HIV and SIV into target cells is mediated by the envelope protein (Figure 2). The Env protein is initially produced as a precursor glycoprotein 160 (gp 160) that is subsequently cleaved by cellular furin-like proteases into glycoprotein 120 (gp120) and glycoprotein 41 (gp 41). The gp 120 subunit is the surface unit (SU) that binds to the receptor and co-receptors and gp41 subunit is the transmembrane unit (TM) that allows for membrane fusion. The maturation process includes post-translational modifications that include disulfide bond formations and extensive glycosylation. Finally, the heterodimer of gp 120 and gp 41 are displayed on the virion membrane surface as trimers.

While HIV-1 fusion is thought to occur at the plasma membrane, there is evidence fusion may also occur in endosomes upon endocytosis (170). Upon membrane fusion, which is mediated by the gp 41 glycoprotein, the viral core is delivered into the cytoplasm. The conical viral core is comprised of mature p24 capsid (CA) proteins that harbor within it the dimer of RNA viral genome, nucleocapsid (NC), reverse transcriptase (RT), integrase (IN) and Vpr. The viral core undergoes an uncoating step that is linked to the formation of the reverse transcription complex (RTC). While the specific subcellular location of where uncoating occurs is unclear (10).

HIV-1 binds cell surface CD4 molecule via gp120 that leads to a conformational change that allows the subsequent binding to the co-receptor CCR5 or CXCR4 (reviewed extensively in (83)). Thus, the target cells of HIV-1 are primarily CD4+ T cells and macrophages which express CD4 and either co-receptor molecules. However, virus isolates

may vary in their co-receptor tropism. In fact, the viruses established in early infections are predominantly CCR5 using. During progression towards late stage infections, there is often either a switch to CXCR4 specificity or to dual-tropic variants that have CCR5 and CXCR4 usage (233). As such, humans who are homozygous for the CCR5 Δ 32 allele (a 32 bp deletion within CCR5 that results in a frameshift mutation) are protected from HIV-1 infection (160, 225). Other well-documented instances of selection on the co-receptor include red capped mangabeys (RCM), which are hosts of SIVrcm, that have a 24 bp deletion in CCR5 (CCR5 Δ 24) at an allele frequency of 87% (83). Sooty mangabeys (SM), which are hosts of SIVsm, also have a 2 bp deletion in CCR5 (CCR5 Δ 2) at 26% allele frequency (217).

Cellular co-factors contribute to the uncoating process. Cyclophilin A (CypA), a host protein, binds CA at a proline-rich binding loop (66, 149, 271). It is hypothesized that the prolyl isomerase activity of CypA catalyzes the cis/trans isomerization of CA, resulting in conformational changes that regulate uncoating (29, 100). Inhibition of CypA by cyclosporine, a competitive inhibitor of the CypA, results in a marked decrease in infectivity due to a decrease in HIV-1 reverse transcripts in certain cell types (32, 221, 292). Pin1, also a prolyl isomerase like CypA, binds CA at a site neighboring the CypA-binding loop and facilitates the uncoating process (167). Overall, studies of host proviral factors involved in this process are largely based on mutations within CA. Nonetheless, they strongly suggest that CA is directly involved in early stages of infection.

Reverse transcription in RTC is mostly completed in the cytoplasm, with a minor portion occurring in the nucleus (reviewed in (295)). The RTC is minimally comprised of viral genomic RNA, tRNA (Lys3) and RT. The tRNA(Lys3), notably of cellular origin, acts as a primer and is bound to the primer binding site (PBS) near the 5' end of the viral genome (reviewed extensively in (1)). Reverse transcription is initiated and extends to the 5' R by RT. This intermediate negative strand DNA, also referred to as (-)ssDNA, is released from the complementary RNA template by the RNase H activity of RT which degrades the template RNA strand. The first strand transfer occurs with this initial (-)ssDNA annealing to the complementary 3'R near the 3' end of the viral genome, thus serving as the primer for the (-) strand synthesis. Reverse transcription proceeds to generate the full length (-) strand cDNA, couple with the same RNase H activity to degrade RNA template. However, two regions are resistant to RNase H degradation: the 3' polypurine tract within U3 (3'-PPT) and central polypurine tract (cPPT). These serve as the primers for the (+) strand cDNA synthesis. Following which, the second strand transfer occurs that anneals the (+) ssDNA to the 3' end of the full length (-) strand cDNA. This allows for reverse transcription to proceed, generating the final full length (+) strand cDNA. Thus, double-stranded cDNA of the viral genome is produced with a 99 bp DNA flap in the center, flanked by two long terminal repeats (LTRs).

The PIC is composed of the double-stranded viral genome DNA, MA, RT, IN and NC. Upon completion of reverse transcription, IN processes the 3'- ends of each LTR within the pre-integration complex (PIC) and proceeds with nuclear import for integration into the host genome. The mechanism of nuclear import is highly debated. In fact, multiple proteins

have been implicated in this process. TNPO3, a transportin involved in nuclear import of splicing factors, was identified through a yeast two-hybrid screen as factor that mediated nuclear import of the PIC (44). HIV-1 CA is the main determinant for TNPO3 dependency (128, 305). Several other proteins including NUP153, NUP155 and CPSF6 may also be involved in nuclear import (60, 128, 136). While the details remain unclear, it is evident that HIV-1 has multiple alternative pathways that facilitate nuclear import. Nonetheless, upon nuclear import, the 3'-processed viral DNA is inserted into host cellular chromatin by DNA strand transfer reaction (61). This is mediated by IN and always results in a 5 bp spacing between viral genome and host genome at each end. There is a high preference for integration at sites of actively transcribed genes (235).

The integrated provirus serves as the template for viral transcription in a highly regulated process involving viral and cellular proteins. Transcription from HIV-1 provirus is regulated in 2 phases (Reviewed in (17, 138)). Initially, the transcription is driven by the 5' LTR which has sequences that are recognized as cis-acting elements by cellular transcriptional machinery. The LTR promoter contains a TATAA box, 3 SP1 binding sites and a region of NF- κ B binding site (197). The second phase is marked by Tat trans-activation that results in a dramatic increase in transcription up to several thousand times higher (138). Tat is synthesized early from a multiply spliced viral mRNA and binds to a stem-loop structure (TAR) on the RNA leader sequence. Through a series of kinase activity and phosphorylation events with the help of Tat-associated kinase (TAK), cyclin T1 and CDK9, the RNAPII complex is hyperphosphorylated at the carboxyl-terminal domain (CTD) resulting in promoter clearance and processive elongation.

Alternative splicing of viral transcripts regulates the translation of HIV-1 (Reviewed in (303)). Transcription of the provirus leads to full-length mRNA transcripts that are either unspliced, singly spliced or multiply spliced. The multiply spliced mRNA encodes for early regulatory proteins Tat, Rev and Nef. Singly spliced transcripts encode Vpu, Vpr, Vif and Env. Finally, the unspliced transcripts encodes for the GagPol polyprotein. Unspliced and singly-spliced transcripts have a Rev Response Element (RRE) which is a secondary structure within an intron region. Intron-containing viral transcripts are retained in the nucleus by cellular splicing factors. As such, nuclear export of these RRE-containing transcripts is dependent on the viral protein Rev. Thus, in the initial stages of transcription, Rev is absent and only multiply spliced transcripts that no longer contain introns are exported out and proceed with translation (Tat, Rev and Nef). Tat transactivation coupled with increasing amounts of Rev shuttling back by importin- β into the nucleus regulate the nuclear export. Rev binds to the RRE and multimerizes to form a complex with cellular exportin 1 (CRM-1) and RAN GTPase (263). Hence, the cellular protein nuclear export machinery is usurped with the aid of the viral Rev protein to export the singly spliced and unspliced viral transcripts for protein translation.

The full length unspliced viral transcript functions as the mRNA template for translating the GagPol polyprotein and the genomic RNA to be packaged within virion particles (Reviewed in (16)). Translation initiation occurs by ribosomal assembly at the 5'-capped end of the mRNA (6, 36). Gag is synthesized most of the time, but a -1 frameshifting event occurs at about 5-10% frequency resulting in a GagPol precursor polyprotein. This results in about 20:1 ratio of Gag : GagPol intracellularly (248).

The expression of Gag protein alone is sufficient for the formation of virus-like particles and mediates the recruitment of other virion components for assembly. A dimer of full length genomic RNA associates with the nucleocapsid (NC) of Gag through the RNA packaging signal (Ψ) located in the 5' end of the viral RNA (reviewed extensively in (192)). The RNA dimerization occurs in the cytoplasm and is mediated by a dimerization initiation site (DIS) also called as the kissing loop (146, 171). Additionally, viral proteins (Vpr) and cellular proteins (tRNA-Lys3 not a protein, CypA, HSP70 hsp70 not that much either and others) are recruited into the nascent virion (Reviewed in (189)).

Assembly of HIV-1 occurs at the plasma membrane (115). The N-terminal myristoylated matrix (MA) domain targets Gag to phosphoinositide $PI(4,5)P_2$ at the plasma membrane. Multimerization occurs with other Gag molecules, and notably, genomic viral RNA associated with NC is important in establishing the early-intermediate membrane-bound assembly complex (117). While oligomerization of Gag occurs intrinsically, the cellular endosomal sorting complex required for transport (ESCRT) complexes are required for the completion of assembly and budding. Virion particles that fail to engage the ESCRT complexes result in the formation of partially assembled immature particles that are arrested at the plasma membrane as stalks best described as lollipop-like structures.

The late domain encoded within p6 of Gag (PTAP and YPLTSL) determine the recognition of TSG101 and ALIX (ESCRT-binding proteins) respectively. The PTAP motif is the predominant motif for budding and directly binds TSG101 and recruits the ESCRT-I complex (73). Gag-bound ESCRT-I complex recruits the ESCRT-III complex (also called as CHMP6,

CHMP4A-4C, CHMP3, CHMP2A and 2B) which is responsible for the scission of membrane neck. Finally, Vps4A arrives to disassemble the ESCRT-III complex via its ATPase activity. While PTAP is likely utilized in most instances of assembly, the alternative recruitment of ALIX by YPLTSL motif can serve as an intermediate complex that directly recruits ESCRT-III (63, 118). However, while ESCRT-III is recycled with the help of Vps4A, ALIX does not appear to be recycled (118). Curiously, some primate lentiviruses exclusively rely on the ALIX-mediated recruitment of ESCRT-III (22, 259). Nonetheless, virion particles are released from the plasma membrane by hijacking host cellular machinery normally involved in multivesicular body formation and cytokinesis.

The immature virion is initially non-infectious and requires the proteolytic maturation by viral protease (PR). PR is activated after budding and cleaves Gag at 5 sites resulting in MA, CA, SP1, NC, SP2, and p6. CA forms a fullerene cone formed that is made up of about 250 hexameric subunits and 12 pentamers. The other newly processed proteins re-assemble within the virion particle to form the MA layer at the inner viral membrane and NC is found associated with the viral RNA genome (Reviewed in (35, 69)). This structural morphology is a defining trait of retroviruses and the electron-dense conical core is a hallmark of the maturation process. Thus, the matured and infectious virion particle is ready to infect another target cell.

PRIMATE LENTIVIRUSES

There are eight major lineages of primate lentiviruses (shown in Figure 3): (i) HIV-1/SIVcpz, (ii) HIV-2/SIVsmm, (iii) SIVagm, (iv) SIVsun/lst/mnd1, (v) SIVsyk, (vi) SIVcol/olc/wrc, (vii) SIVmus/gsn/mon, (viii) SIVrcm/mnd2. These SIVs have been isolated from at least 30 different nonhuman primate species in sub-Saharan Africa (9, 22). This number is likely to increase further as better methods of detection are developed and more survey efforts are initiated. There are several key differences between primate lentiviruses.

First, lentivirus infections can have disparate outcomes in their primate hosts. For instance, Sooty mangabeys (SM) and African green monkeys (AGM) are found to be infected with SIVs that do not resolve the infection, and that do not lead to a pathogenic outcome. This is in contrast to HIV-1 that leads to a pathogenic outcome in humans (152, 253). Rhesus macaques experimentally infected with SIVmac also progress to immunodeficiency and develop AIDS-like symptoms (155, 172). Furthermore, HIV-1 infection of humans usually results in chronic IFN stimulation (152), whereas there is an absence of chronic stimulation of IFN production in SIVagm infection in naturally infected AGMs despite equivalent high levels of virus titers (54). In Chapter Three, I will present conclusive evidence that these differences in cellular immune environment during viral replication directly impact the role of viral factors to counteract host restriction factors that are induced by such responses.

Second, besides gross differences in their genomic organization mentioned above (Figure 1), phylogenetic analyses of the 5' coding sequences (gag or pol) and 3' coding sequences (env or nef) reveal strong discordance suggesting that recombination occurred

between several lineages (111, 196, 224). For instance, SIVagm.Sabaeus is a recombinant of SIVagm and SIVsm/HIV-2 lineages (111). The recombinant origin of SIVcpz will be discussed in detail below.

The precise evolutionary history of primate lentiviruses is further complicated by virus transmission between different primate species. In fact, cross-species transmission of primate lentiviruses is well-documented. For example, SIVagm has been detected in chacma baboons, and SIVsm was found in infected humans (71, 285). This is also supported by phylogenetic analyses which show that several phylogenetic relationships between SIV lineages are not congruent with their host species phylogeny (40). HIV-1 is the result of three independent cross-species transmission of SIVcpz from chimpanzees and one transmission of SIVgor from gorilla (itself the descendant of transmission from SIVcpz) (Figure 4); and HIV-2 arose from eight independent cross-species transmission of SIVsm from sooty mangabeys to humans (48, 70, 120, 208, 267, 284).

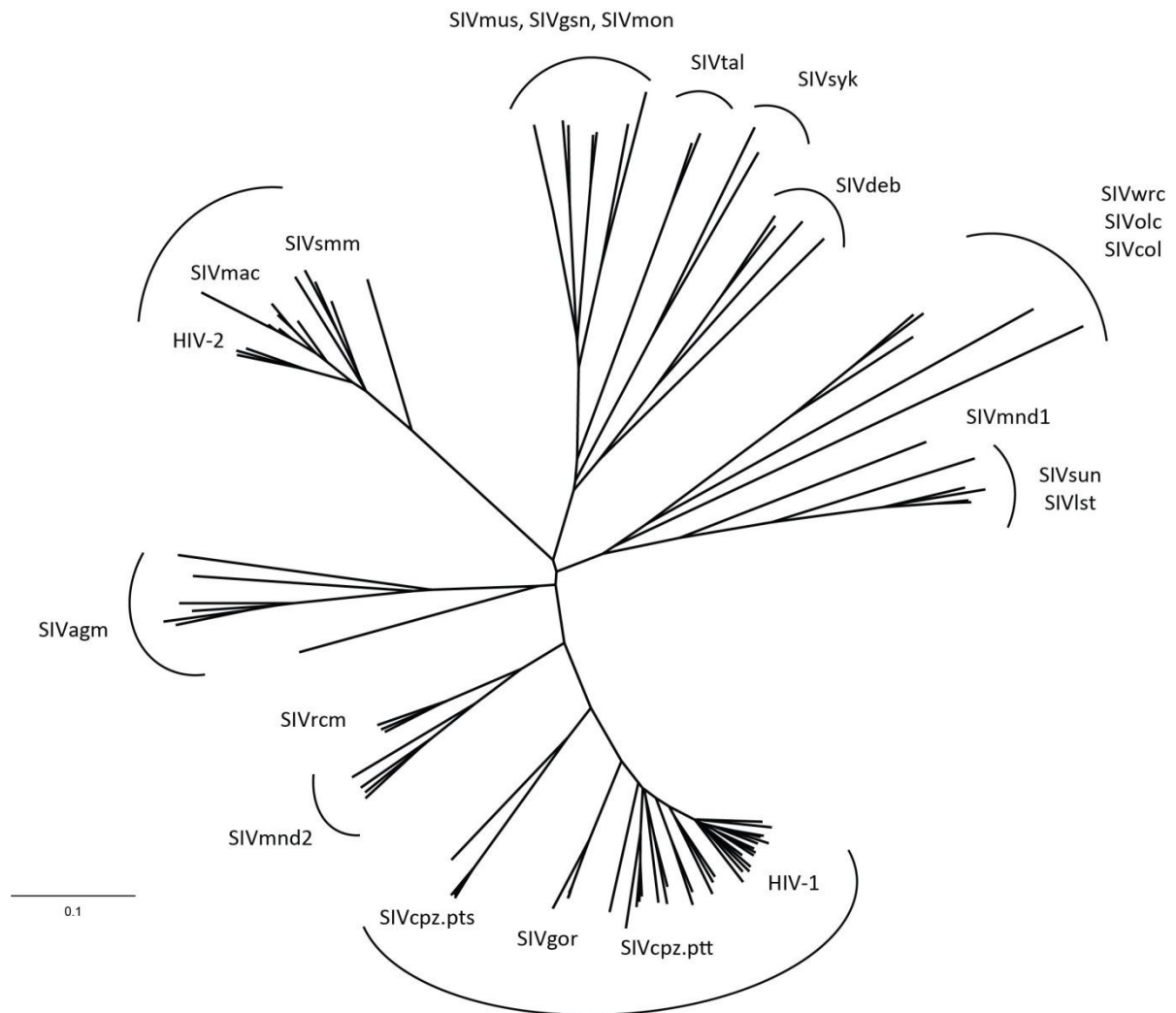


Figure 3

There are eight major lineages of primate lentiviruses. This phylogeny was constructed from 93 HIV and SIV pol sequences (amino acids). However, the phylogenies constructed using other genes yield incongruent topologies due to recombination.

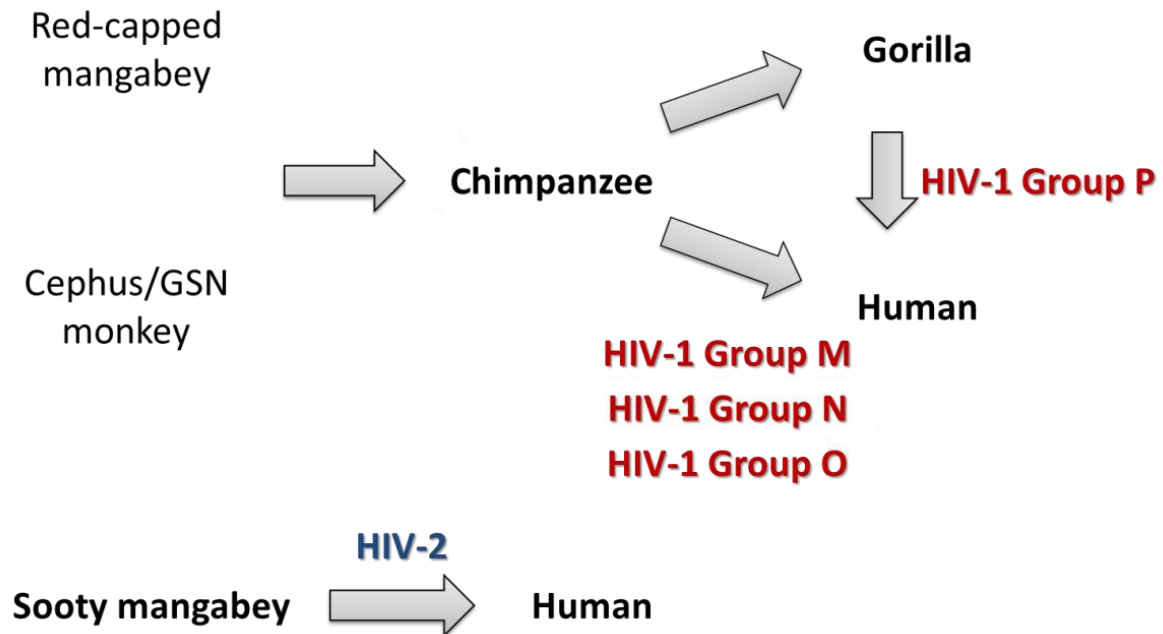


Figure 4

HIV-1 is the result of three independent cross-species transmission of SIVcpz from chimpanzees and one transmission of SIVgor from gorilla (itself the descendant of transmission from SIVcpz); and HIV-2 arose from eight independent cross-species transmission of SIVsm from sooty mangabeys to humans.

SIVcpz, the immediate precursor of HIV-1, is of hybrid origin (15). The 5' region and 3' end of SIVcpz is derived from SIVrcm, but the middle region clusters more closely with SIVmus/gsn/mon viruses. A closer look at the genomic structure shows that the recombinant SIVcpz only has a single Vpr (compared to SIVrcm which has Vpx and Vpr) and Vpu (clearly acquired from SIVmus/gsn/mon that is absent in SIVrcm). Thus, the HIV-1 and SIVcpz lineages have an intriguing evolutionary history that traces to a unique recombination event and involves several cross-species transmissions.

In west Africa, both *Pan troglodytes schweinfurthii* and *Pan troglodytes troglodytes* species are infected with subspecies-specific SIVcpz. However, no SIVcpz has been found in either *Pan troglodytes vellerosus* or the geographically isolated *Pan troglodytes verus* species despite extensive surveying efforts (212, 226). Interestingly, all the HIV-1 viral sequences are more closely related to the SIVcpz that infects *P.t.t.*, and no SIVcpz from *P.t.s.* that has been found in humans to date. This strongly suggests that HIV-1 originated from the SIVcpz-harboring *P.t.t.* species. Based on molecular clock estimates, the date of the most recent common ancestor of SIVcpz is about 1492 (1266–1685) (298). Therefore, SIV transmission into chimpanzees was likely a recent event.

There are four groups of HIV-1: Group M (major), Group N (non-major), Group O, (outlier) and Group P (to be designated after Paris, the origin of the lab that discovered it). HIV-1 Group M is the pandemic virus accounting for more than 90% of current HIV infections, and can be further classified into at least 9 phylogenetically distinct subtypes (clades) and a growing list of circulating recombinant forms (CRFs). In comparison, HIV-1 Group O accounts for about 1% and is mostly isolated to Central Africa, while Group N constitutes about 0.1% of infections (38). There are only 2 strains of HIV-1 Group P identified to date (208, 280). HIV-2 accounts for 1% of infections and is predominantly in West Africa (38).

This raises the question: why is HIV-1 Group M the pandemic virus? This could be due to a combination of sociological factors and intrinsic viral properties. First, studies using molecular clock estimates place the inception of HIV-1 Group M at a time that coincides

with high population growth. The time of most recent common ancestor (tMRCA) for HIV-1 Group M is around 1908 (1884 – 1924), whereas the tMRCA of HIV-1 Group O is about 1920 (1890 – 1940) and HIV-1 Group N tMRCA is about 1963 (1948 – 1977) (298, 301).

Demographic data from the early 1900s looking at the cities around the zone of cross-species transmission (Cameroon, Central African Republic, DRC, Republic of Congo, Gabon and Equatorial Guinea) suggest that the early HIV infections coincided at a time when there was a surge in population size and expansion within these major cities (301). It is important to emphasize that HIV-1 infections were mostly undetected until its discovery in 1983 (68). Thus, the growth of cities in that region might have unknowingly provided a sufficient host-population size and transmission network that facilitated the establishment of HIV-1.

Secondly, there is also evidence of intrinsic properties of HIV-1 Group M strains that might allow for its more effective viral replication. Specifically, HIV-1 virus isolates from Group M have a higher replicative capacity and more effective viral countermeasures that antagonize host restriction factors (13, 229). My thesis research (presented in Chapter Four) will demonstrate that another key difference is the neofunctionalization of HIV-1 Vpu to antagonize Tetherin.

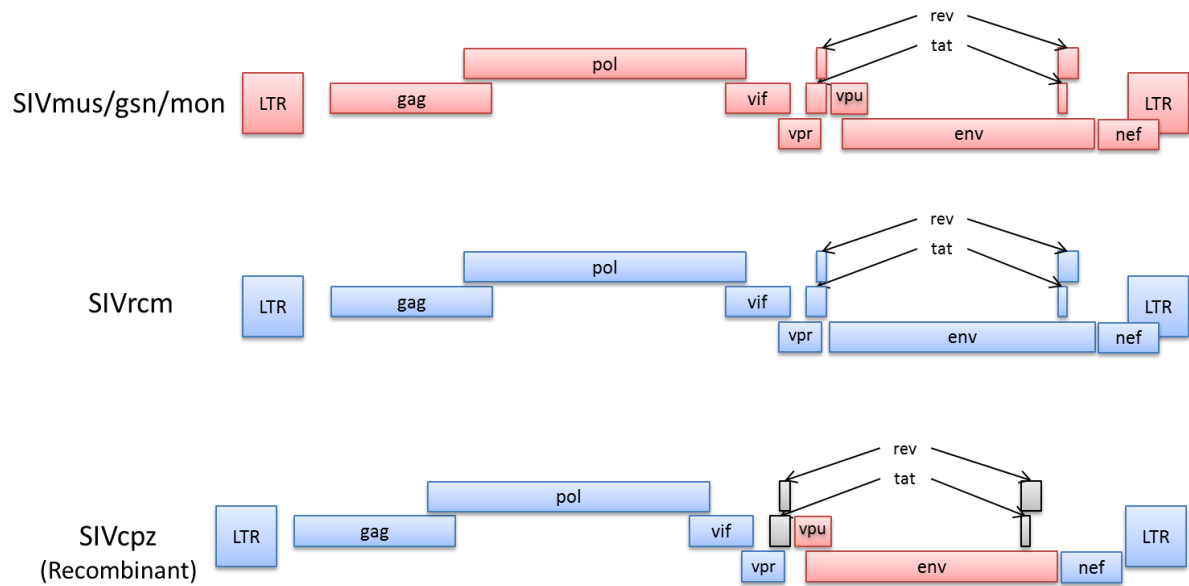


Figure 5

This figure shows the recombinant origin of SIVcpz. The flanking 5' and 3' regions of SIVcpz are more closely related to the SIVrcm sequences (blue). However, SIVcpz Vpu and Env are more closely related to sequences from the SIVmus/gsn/mon lineages (red).

INNATE IMMUNITY

The innate immune response is the front line defense against pathogen invasion. Recognition and efficient control during the early stages of pathogen invasion is dictated by the innate immune response. This also provides the framework for the innate control of the adaptive immunity, a model proposed by Charles Janeway (106, 107, 164). The key concept is that the innate immune system uses germline-encoded pattern recognition receptors to mediate pathogen sensing, which instructs the adaptive immunity cells based on the pathogen recognition or costimulatory signals.

The first phase of the innate immune response is pathogen sensing. This was initially characterized in *Drosophila* as the Toll receptor which is responsible for the sensing and signaling of the antifungal defense (137). It quickly became apparent that the mammalian homologs, toll-like receptors (TLR), were important for activating the NF- κ B signaling cascade (165, 219). In fact, the TLR family and C-type lectins have specificities for different microbial ligands: TLR1/TLR2 and TLR2/TLR6 recognize lipoteichoic acids of Gram-positive bacteria and bacterial lipoproteins; TLR3 detects double-stranded RNA (dsRNA); TLR4 directly senses lipopolysaccharide (LPS) of Gram-negative bacteria; TLR5 recognizes flagellin; TLR7/8 detects single-stranded RNA (ssRNA); and TLR9 detects dsDNA (TLR9) (Reviewed in (106, 266)). Thus, TLRs can be organized as cell-surface TLRs (TLR1,2,4,5 and 6) that mostly recognize bacterial protein products, and the endosomal TLRs (TLR 3, 7, 8 and 9) detect microbial nucleic acids.

Upon engagement of pathogen-associated molecular patterns (PAMPs) with TLRs, a signaling pathway is initiated and is mediated by either MyD88 or TRIF. A series of

phosphorylation and ubiquitination leads to the activation and nuclear translocation of NF- κ B and AP1 transcription factors, triggering the expression of many cytokines, chemokines, chemokine receptors and costimulatory molecules.

Cytosolic pathogen recognition receptors are composed of the retinoic acid-inducible gene I (RIG-I)-like receptors (RLRs) and the nucleotide-binding domain and leucine-rich repeat-containing receptors (NLRs) (159, 205). While most TLRs and dectins are expressed on the specialized immune cells such as macrophages and dendritic cells, the cytosolic RLRs and NLRs are expressed in most cell types. This is likely due to the 'cell-intrinsic' nature of the pathogen recognition that requires the cells themselves to be infected. The RLRs RIG-I and MDA5 primarily detect viral pathogens. Upon ligand binding and recruitment of the adaptor MAVS/IPS1, downstream activation of NF- κ B, AP1 and IRF3 occurs through a series of phosphorylation and ubiquitination events. IRF3 activation drives the transcription of interferon- β (IFN β), leading to the production and secretion of IFN β .

IFN signaling is critical in establishing an 'antiviral state' in cells. Secreted IFN β can act in an autocrine or paracrine fashion, and this happens by binding to type I IFN receptors. Upon engagement of IFN receptors, the JAK/STAT signaling pathway is activated through several kinases that culminate in the formation of ISGF3 complex – STAT1/STAT2/IRF9. The ISGF3 complex translocates into the nucleus and induces the transcription of numerous genes by binding to the IFN-stimulated response element (ISRE) within the promoter/enhancer region. These genes are collectively labeled as IFN-stimulated genes (ISGs). IRF7, itself a transcription factor that is interferon-induced, is produced. Upon

phosphorylation, IRF7 is thereby activated to bind virus-responsive elements (VRE) in the promoter of IFN α , leading to the production of IFN α . Thus, these signaling pathways lead to rapid amplification of IFN production and gene induction.

There are three types of interferon: type I includes α (13 isotypes), β , δ , ϵ , κ , τ , and ω ; type II IFN γ and type III IFN λ . Different sets of genes, sometimes up to several hundred genes, are induced by the various types of IFNs (18, 49, 52, 157). In fact, variation is also observed depending on the cell type used and might also partly be due to technical details or cutoff methodology. Nonetheless, many of these ISGs are potent antiviral effectors. Hence, interferon-stimulation is associated with an antiviral response or an 'antiviral state'.

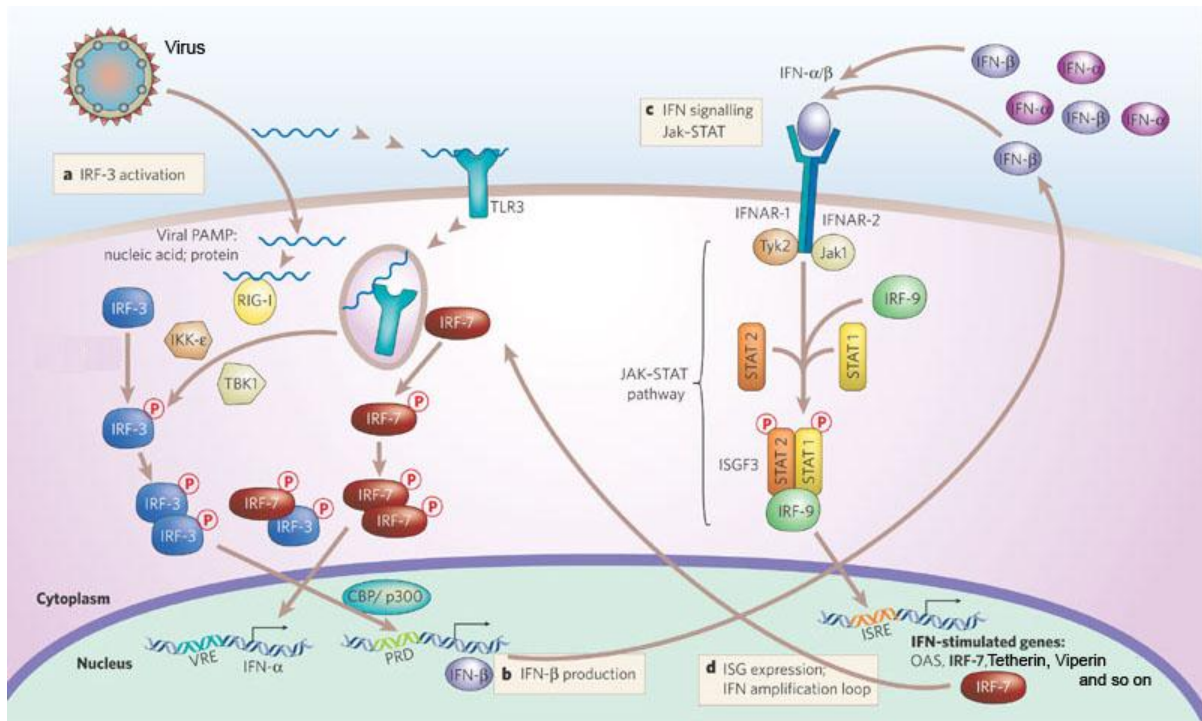


Figure 6

Innate immunity signaling. Pathogen sensing triggers a signaling cascade that leads to IFN β production and induction of ISGs such as Tetherin and Viperin. This figure is adapted from (67).

HOST RESTRICTION FACTORS

There are several host restriction factors of HIV-1 and other retroviruses (also called antiviral effectors) that have been identified to date. The main function of host restriction factors is to provide protection at the cellular level against incoming viral pathogens. In contrast to the adaptive immune response, which involves somatic learning and memory, host restriction factors are germline-encoded. Many of these proteins are highly induced upon interferon stimulation as part of switch to an 'antiviral state' of the cell. However, their mode of action differs at the stage of infection targeted and mechanism which can be highly specific or autonomous in some cases. It is unlikely that the role of these restriction factors is solely limited to target retroviruses. Nonetheless, host restriction factors of retroviruses is still the most studied model system.

FV1 AND FV4

Fv1 and Fv4 were the first host restriction factors to be discovered. Friend murine leukemia virus (F-MLV) is a retrovirus that causes erythroleukemia in susceptible strains of mice. Resistance to F-MLV infection between resistant and sensitive mice strains was chromosomally mapped to the Fv4 locus (formerly called Akvr-1). Fv4 encodes a MLV-related envelope protein that directly interferes with the ectopic receptor, thus preventing incoming virus from binding and infecting the cell. Indeed, expression of Fv4 in transgenic mice provided potent protection against F-MLV infection. Importantly, Fv4 is genetically dominant. Likewise, Fv1 also exerts a genetically dominant trait. Mice that were homozygous for the Fv1ⁿ allele were susceptible to N-tropic MLV strains but resistant

against B-tropic MLVs. Conversely, mice homozygous for the Fv1^b allele could be infected by B-tropic MLV but were resistant to N-tropic MLV infection. The viral determinant of Fv1 restriction specificity is the viral capsid protein at residue 110. Furthermore, Fv1 activity can be saturated at high amounts of virus. Surprisingly, Fv1 and Fv4 are of retroelement origin that arose from endogenization in the mouse lineages only. Thus, *Fv1* and *Fv4* are only found in mice and are absent from all other mammalian species.

TRIM5 α AND TRIMCYP

Although humans have no ortholog of Fv1, several human cell lines restricted N-tropic MLV (analogous to the Fv1^b allele) in a manner that was dependent on viral capsid residue 110 and could be saturated. This restriction factor was called Ref 1 (restriction factor 1). On the other hand, nonhuman primates expressed a restriction factor that was called Lv1 (lentivirus restriction factor 1). Lv1 restricted HIV-1 and its specificity was determined by the viral capsid. Furthermore, Lv1 was saturable not only by paralogous lentiviruses but even by some distantly-related retroviruses. However, Lv1 was clearly species-specific in its restriction profile. Most importantly, Lv1 was a dominant protective trait that could be conferred to permissive cells through heterokaryon experiments. Finally, 2004 marked the exciting discovery that Trim5 α in rhesus macaques was responsible for the Lv1 phenotype. In fact, Trim5 α was also responsible for the Ref1 activity in human cells (94, 202).

Trim5 α is composed of an N-terminal tripartite motif (TRIM) defined by a RING, B-Box2 and a coiled-coil domain, and a C-terminal PRY-SPRY (B30.2) domain (Reviewed in (24,

77, 228)). Trim5 α binds and multimerizes around incoming viral capsid proteins to cause an accelerated uncoating of the viral core (201, 261). This results in an impaired reverse transcription and nuclear import (7, 260, 276). The exact mechanism of viral restriction is still poorly understood. The RING domain functions as an E3 ubiquitin ligase and is required for the antiviral activity of Trim5 α , although the role of the ubiquitination is unclear. The B-Box2 and coiled-coil domains are important for the high-order multimerization and low-order dimerization of Trim5 α – which is necessary for the restriction function. Nonetheless, the binding and recognition of viral capsid is clearly determined by the PRY-SPRY domain (150, 184, 239, 262, 309, 317). Amino acid differences within the PRY-SPRY domain are sufficient to account for the species-specific restriction profile of Trim5 α (94, 231, 262, 309). In fact, a single amino acid change within the PRY-SPRY domain can cause human Trim5 α to gain the ability of recognizing HIV-1 and thus acquire potent HIV-1 restriction capability (309).

As an example of convergent evolution, owl monkeys encode a different variant called TRIMCyp in which the PRY-SPRY domain is replaced by Cyclophilin A (180, 232). In essence, the C-terminal role of capsid recognition is now determined by Cyclophilin A binding specificity. Surprisingly, this occurred independently at least twice in primate evolutionary history. In owl monkeys, the generation of TRIMCyp arose from a direct LINE-1-mediated retrotransposition of Cyclophilin A into intron 7 of TRIM5 (180, 232). Yet, in macaque sub-species, the retrotransposition of Cyclophilin A within the 3' UTR of TRIM5 in combination with a novel splice acceptor mutation leads to TRIMCyp expression (34, 139, 289, 299). Analogous to the Trim5 α PRY-SPRY domain, CypA determines the species

specificity of these fusion TRIMCyp proteins. Changes at two residues in the CypA domain allow rhesus macaque TRIMCyp to restrict HIV-1 to a similar potency of owl monkey TRIMCyp (289). Thus, the spectrum of viral recognition by Trim5 α and TRIMCyp is dictated and refined by changes in the C-terminal domain (be it PRY-SPRY or CypA).

Trim5 α also functions in innate immune signaling. Trim5 α stimulates AP1 and NF κ B signaling by activating the TAK1 kinase complex (203, 270). The RING and B-BOX2 domains mediate the synthesis of K63-linked ubiquitin chains synthesis by E2 UBC13–UEV1A, which leads to TAK1 kinase complex activation. Furthermore, NF κ B signaling by TRIM5 α appears to be an evolutionary conserved property as the mouse homolog is also capable of performing this function (249). Signaling can be triggered by LPS treatment or retroviral capsid recognition. The strongest evidence that viral recognition correlates with signaling function comes from Human Trim5 α which recognizes N-MLV at a higher avidity than B-MLV. NF κ B- and MAPK-dependent genes were induced at a higher level by Trim5 α upon N-MLV infection, compared to the unrestricted B-MLV infection (203). Since Trim5 α recognizes the interface of the inter-hexamer capsid lattice (69, 317), it has been proposed that Trim5 α could also be a pathogen recognition receptor that detects viral (capsid) proteins (203).

APOBEC3G

APOBEC3G (also known as CEM15) was identified because of its antagonism by HIV-1 Vif (247). APOBEC3G is a host cellular cytidine deaminase enzyme that causes G to A hypermutations (93). In the absence of HIV-1 Vif, APOBEC3G is packaged into nascent virion particles and restricts the virus upon its next round of infection (247). APOBEC3G restriction

leads to a decrease in virus infectivity (247). APOBEC3G can induce hypermutations on the retroviral cDNA during reverse transcription that leads to an error catastrophe (92, 154, 316). Indeed, APOBEC3G also causes hypermutations on hepatitis B virus (182). However, there is also evidence that APOBEC3G can also exert deaminase-independent restriction (25, 177). This could be caused by a simple physical block to RT, preventing reverse transcription elongation (26). In support of this, catalytically inactive mutants of APOBEC3G are capable of restricting HIV-1 and HTLV-1 (25, 227).

APOBEC3G restriction of HIV-1 is antagonized by Vif (Reviewed in (81)). In the target cell, Vif directly binds to APOBEC3G and recruits the cellular E3 ubiquitin complex of Cullin-5/elonginB/elonginC/Rbx1. This leads to the polyubiquitination of APOBEC3G, targeting it for the degradation by the 26S proteasome. However, there is species-specificity between APOBEC3G:Vif interactions. For example, human APOBEC3G can be targeted by HIV-1 Vif but not by SIVagm Vif; reciprocally, AGM APOBEC3G can be targeted by SIVagm Vif but not by HIV-1 Vif (158). A single amino acid change on APOBEC3G can toggle the species-specific switch of Vif sensitivity (28, 236). This means that host evasion from Vif antagonism requires a single adaptive change and consequently imposes a species-specific barrier. Thus, HIV-1 Vif acts as an adaptor protein that targets the host cellular machinery to remove APOBEC3G. As a result, APOBEC3G is not packaged into virion particles and virus is infectious in the next round of infection.

TETHERIN

Tetherin is a host restriction factor capable of inhibiting the release of a broad range of viruses from the plasma membrane of infected cells (Figure 7). Tetherin, also called BST-2/CD317/HM1.24, was first identified as a marker for cells involved in B-cell differentiation and was subsequently found to be overexpressed on multiple myeloma cells (84, 104, 190). Upon the discovery of its antiviral activity, the name “tetherin” was coined to describe the tethering phenotype that BST-2/CD317/HM1.24 causes during virion budding from the plasma membrane (176). In addition to inhibiting the release of HIV particles, tetherin also inhibits the release of filoviruses (Ebola and Marburg viruses), arenaviruses (Lassa virus), and other retroviruses including gammaretroviruses (murine leukemia virus) and spumaretroviruses (foamy virus) (90, 114, 176, 223). HeLa, Jurkat, and CEM cells constitutively express high levels of tetherin; however, in cells that express low levels of tetherin, such as 293T or HT1080 cells, tetherin can be upregulated by type I IFN (176). This results in permissive 293T cells becoming nonpermissive to infection by HIV-1 and Ebola virus (175).

Tetherin restricts virus release by physical linkage between nascent virion and the cell plasma membrane (200). The tetramer structure is formed by two coiled coil-mediated parallel dimers of tetherin. Structural studies support an anti-parallel four-helix bundle configuration that is stabilized by three disulfide bridges, and allows for pronounced flexibility (237, 264, 306). In fact, restriction activity by an artificial “tetherin” demonstrates that the intrinsic protein topology determines its function rather than the coding amino acid (200).

Retroviruses have developed at least three strategies to counteract tetherin (62, 135) (Figure 7). First, the Vpu protein from HIV-1 abrogates the retention phenotype in cells that express tetherin and has been observed to be colocalized with tetherin (176, 282). Vpu displays species specificity and counteracts human tetherin by targeting it for degradation (78, 163). Notably, Vpu is encoded by a unique lineage of primate lentiviruses, including HIV-1, SIVcpz from chimpanzees, and SIVmus, SIVgsn, and SIVmon from mustached monkeys (*Cercopithecus cephus*), greater spot-nosed monkeys (*Cercopithecus nictitans*), and Mona monkeys (*Cercopithecus mona*), respectively (46), but is not encoded by the other lineages of primate lentiviruses. HIV-1 Vpu directly binds to tetherin via their transmembrane domains (105, 125, 163, 183, 220, 251, 288, 311). Vpu recruits the β -TrCP subunit of a Skp1-Cullin1-F-box ubiquitin ligase complex leading to the ubiquitination of tetherin at the lysine and serine/threonine residues in the cytoplasmic tail domain (80, 274). This leads to the lysosomal degradation that is mediated by HRS, a component of the ESCRT-0 complex (108). It should be noted that tetherin overexpression studies can also lead to an artifactual proteasomal degradation phenotype due to excessive protein accumulation (8).

Second, lentiviruses from the SIVsmm/SIVmac lineage have evolved the ability to counteract tetherin through the Nef protein (109, 315). The Nef proteins from SIVsmm and SIVmac display species specificity in their ability to counteract their hosts, sooty mangabey and rhesus macaque, respectively, and closely related tetherins. Nef binds to the cytoplasmic tail domain of tetherin via its C-terminal domain and recruits the AP-2 clathrin adaptor complex (314). Thus, Nef counteraction leads to internalization of cell-surface

tetherin and intracellular retention. This raises an intriguing question about viruses that encode both Vpu and Nef: what determines their choice of tetherin antagonist? In Chapter Four, I will resolve this by tracing the tetherin antagonist viral evolution from HIV-1 back to when the switch occurred and reconstruct the evolutionary events that shaped its trajectory.

Third, the HIV-2 envelope enhances virion particle release and is able to complement HIV-1 that lacks Vpu (31). HIV-2 Env antagonism of tetherin promotes the cell surface downregulation of tetherin, similar to Vpu. However, Env does not result in protein degradation, but leads to the intracellular sequestration of tetherin (95, 134). While the mechanistic details of antagonism are unclear, the gp41 cytoplasmic tail of Env might be involved (134). More convincingly, a revertant SIVmac that lacked Nef (the native tetherin antagonist) was isolated from infected rhesus macaques and found to have evolved Env to antagonize tetherin (242). Another case was identified in a strain of SIVagm that was capable of antagonizing tetherin through Env (89).

Tetherin can also be antagonized by other viruses besides retroviruses. Kaposi's sarcoma-associated herpesvirus (KSHV) is able to counteract Tetherin with its K5 protein (156, 193). KSHV K5 promotes the downregulation of cell surface tetherin through the ESCRT-mediated pathway. Tetherin is delivered to the late endosomes and undergoes endosomal degradation (193). Ebola virus, a member of the family Filoviridae, has a means to counteract tetherin through its full-length glycoprotein (GP) (119). However, the mechanism of tetherin antagonism by Ebola virus GP is unique in that it could antagonize

multiple primate species' tetherin and can even antagonize the “artificial” tetherin (132, 147). Importantly, this mechanism does not require the downregulation of cell surface tetherin nor does it result in decreased tetherin protein expression levels. Given the broad spectrum activity of tetherin, it is likely that other virus might evolve novel antagonism strategies. There is strong evidence that influenza might encode an antagonist as it has been shown that while tetherin can restrict influenza VLPs, tetherin restriction is circumvented in experiments using infectious influenza virus (296, 310). This might also be the case for vaccinia virus, a member of the poxvirus family. Vaccinia virus release was found to be unaffected by tetherin expression (252). While cell surface and total intracellular levels of tetherin were found to be unchanged (252), this phenotype would be expected if the antagonist mechanism is similar to that of Ebola and Marburg virus GP (132, 147). In conclusion, the independent acquisitions of a viral tetherin antagonist by multiple viruses emphasize the role of tetherin and the strong selective pressure imposed by its potent restriction.

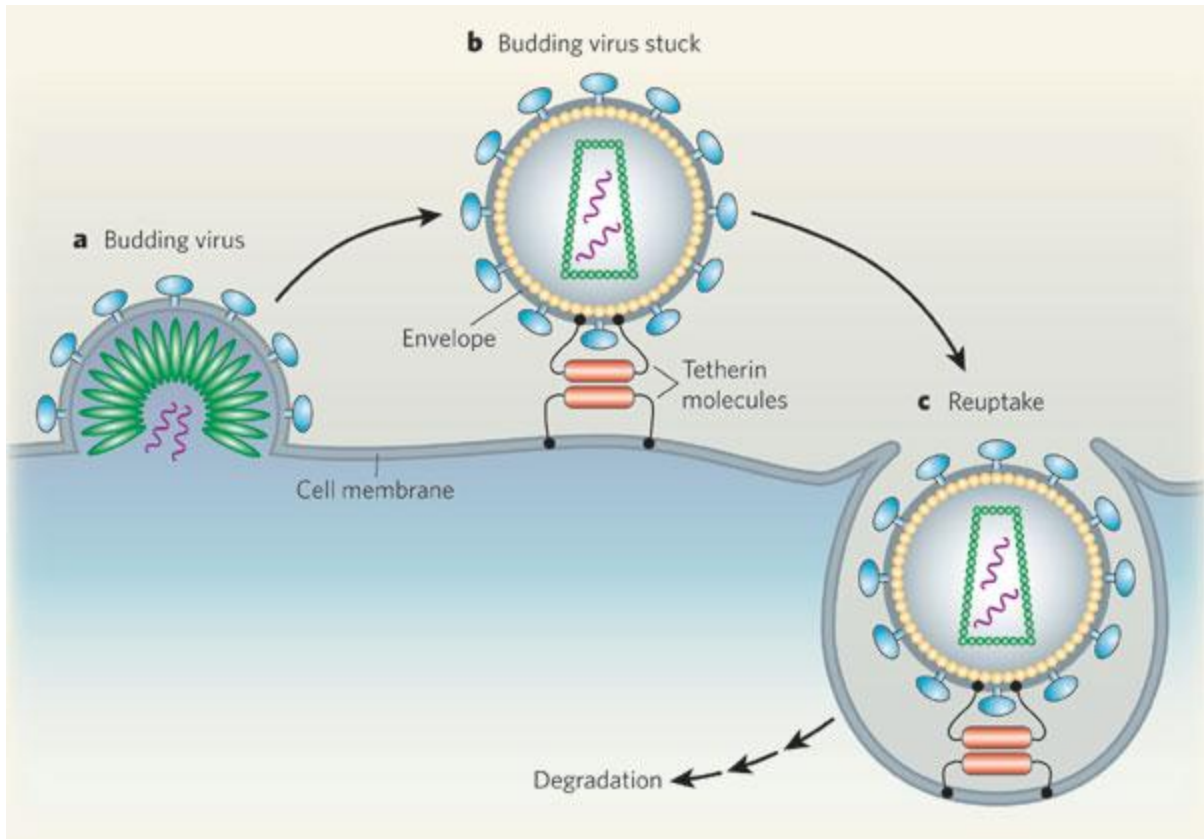


Figure 7

Tetherin restricts virus release. Tetherin forms anti-parallel dimers that tethers nascent virions to the plasma membrane, and subsequently internalized by endocytosis.

This figure is from (91) with permission (License number 2818340284014).

VIPERIN

A host protein with broad antiviral activity called Viperin (Virus inhibitory protein, endoplasmic reticulum-associated, interferon-inducible, also known as *RSAD2*) has been shown to modulate lipid rafts (43, 110, 293). Viperin inhibits the release of a wide range of viruses in cell culture including Influenza virus (293), Hepatitis C virus (96, 110), and Japanese Encephalitis virus (39) (Figure 8). Moreover, Viperin knockout mice show that this protein plays a role in controlling West Nile Virus pathogenesis in vivo (265). In the case of CMV, Viperin has been reported not only to inhibit expression CMV late viral gene products (43) but also to enhance CMV infectivity by remodeling cellular actin cytoskeleton (241).

Lipid rafts are sphingolipid- and cholesterol-enriched microdomains on the plasma membrane that have been implicated in a number of processes including membrane signaling, polarization, and immunological synapse function (186, 250). Lipid rafts also play an important role in the entry and assembly stages of viral replication (162, 186). Indeed, the host sterol biosynthesis pathway is downregulated in response to viral infections as part of the innate immune response via type I interferon signaling (27). This suggests that the disruption of virus budding through host-encoded lipid rafts may represent a host defense against viruses.

HIV is thought to assemble and bud from lipid rafts and depletion of cellular cholesterol leads to a reduction in HIV production (185, 187, 291). In addition to its other activities, Nef, an accessory gene encoded by HIV, has been shown to lead to an increased synthesis of cholesterol (281, 318), which may be related to the ability of Nef to increase

virus infectivity (318). Thus, cellular cholesterol and lipid raft integrity is important for HIV replication.

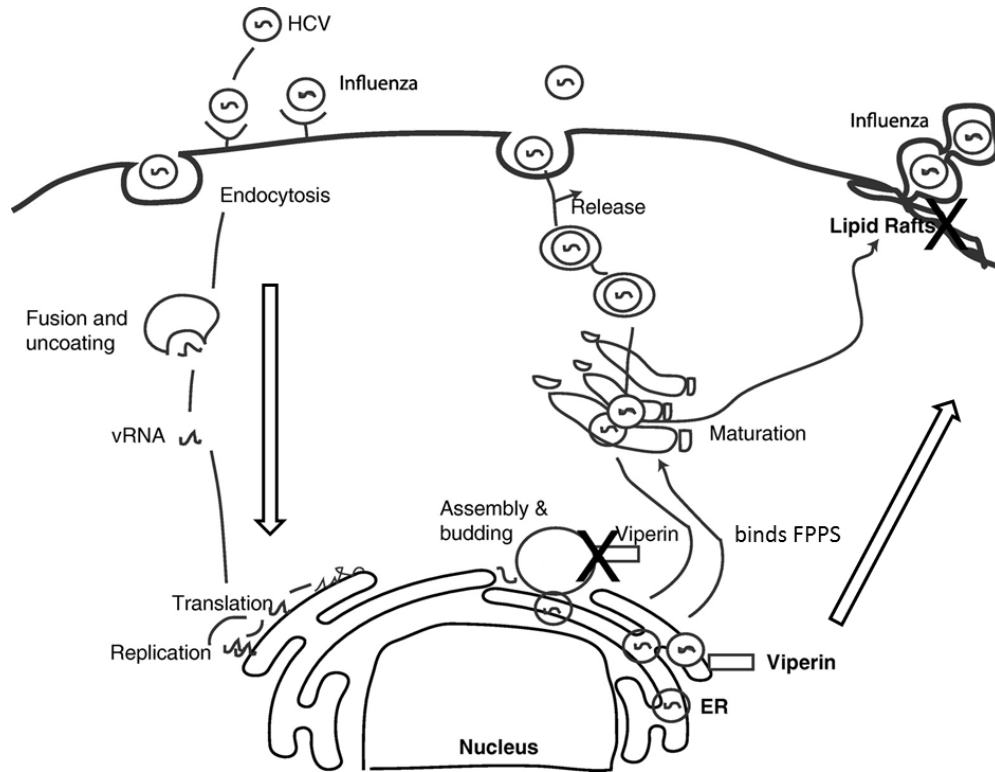


Figure 8

Schematic representation of the antiviral action of Viperin against influenza and HCV.

Viperin prevents HCV assembly and/or budding by binding to lipid droplets. Influenza restriction is mediated by viperin binding to farnesyl diphosphate synthase, and thereby disrupts lipid rafts to prevent virus release.

This figure is adapted from (64)

SAMHD1

The accessory protein Vpx was previously shown to be critical for the ability of primate lentiviruses to efficiently infect monocytes, dendritic cells, and mature macrophages (14, 244). Recently, the target of Vpx has been identified as the restriction factor SAMHD1 (101, 133), where the binding of Vpx to SAMHD1 leads to the proteasomal degradation of SAMHD1 (Figure 9). Humans with missense mutations in SAMHD1 are associated with Aicardi Goutieres Syndrome (AGS), an encephalitis syndrome which mimics a state of viral infection leading to interferon production and an autoimmune syndrome (216, 256).

SAMHD1 is a deoxynucleoside triphosphate triphosphohydrolase. Dimeric SAMHD1 binds to dGTP, which acts as both substrate and activator, and hydrolyses deoxynucleotides using the HD domain (82, 211). As a result, in myeloid cells where SAMHD1 is highly expressed (302), cellular deoxynucleotide pools are suppressed and retrovirus reverse transcription would be hampered due to the limited deoxynucleotide substrate availability. Therefore, in AGS patients with defective SAMHD1 mutations, the aberrant availability of deoxynucleotide pools fuels endogenous reverse transcription activity that triggers an autoimmune response, resulting in the AGS clinical phenotype (Figure 10). Likewise, Vpx antagonism of SAMHD1 relieves the suppression of deoxynucleotide to allow for viral reverse transcription. Thus, Vpx appears to degrade a host restriction factor that allows primate lentiviruses to infect key immunomodulatory cells types.

Despite this important function, only two of the eight major lineages of primate lentiviruses (reviewed in (196)) encode Vpx: HIV-2/ SIVsm-related viruses and a lineage represented by SIV from red-capped mangabeys (SIVrcm). On the other hand, all extant primate lentivirus lineages encode a paralogous gene called Vpr that causes cell cycle arrest (246, 277, 278). Both Vpr and Vpx are incorporated in the core of budding viruses (312, 313), and both bind to the Cul4 complex through interactions with DDB1 and DCAF1 (reviewed in (14)). Despite its limited representation in primate lentiviruses, Vpx appears to be more critical than Vpr for replication of SIV in monkeys (74, 98). The important role played by Vpx has led to a conundrum as to why this protein is missing in lentiviruses like HIV-1. Therefore, is SAMHD1 antagonism an ancestral trait that was lost in some lineages or a newly acquired function? In Chapter Six, I will answer this by combining an extensive functional characterization of SAMHD1 and Vpr/Vpx with a detailed phylogenetic framework of primate lentivirus evolution.

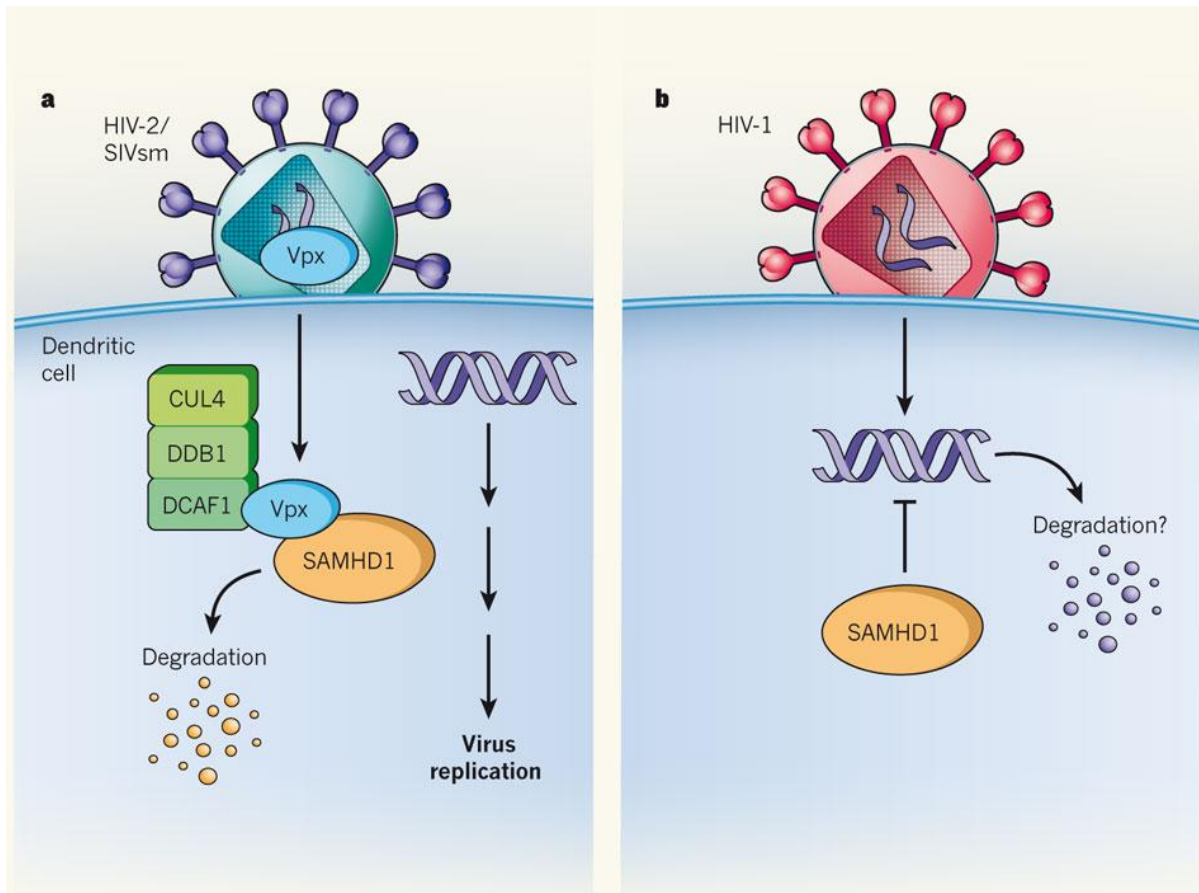


Figure 9

On infecting dendritic cells, retroviruses such as HIV-2 and sooty mangabey SIV (SIVsm) deliver their Vpx protein into the cell cytoplasm, where it could bind to SAMHD1. Vpx also recruits the CUL4–DDB1–DCAF1 protein complex, leading to the degradation of SAMHD1. The virus can now replicate unhindered. b, By contrast, when HIV-1, or other viruses that do not express Vpx, infect dendritic cells, SAMHD1 inhibits their replication, perhaps by recognizing viral nucleic acids and mediating their degradation.

This figure is from (143).

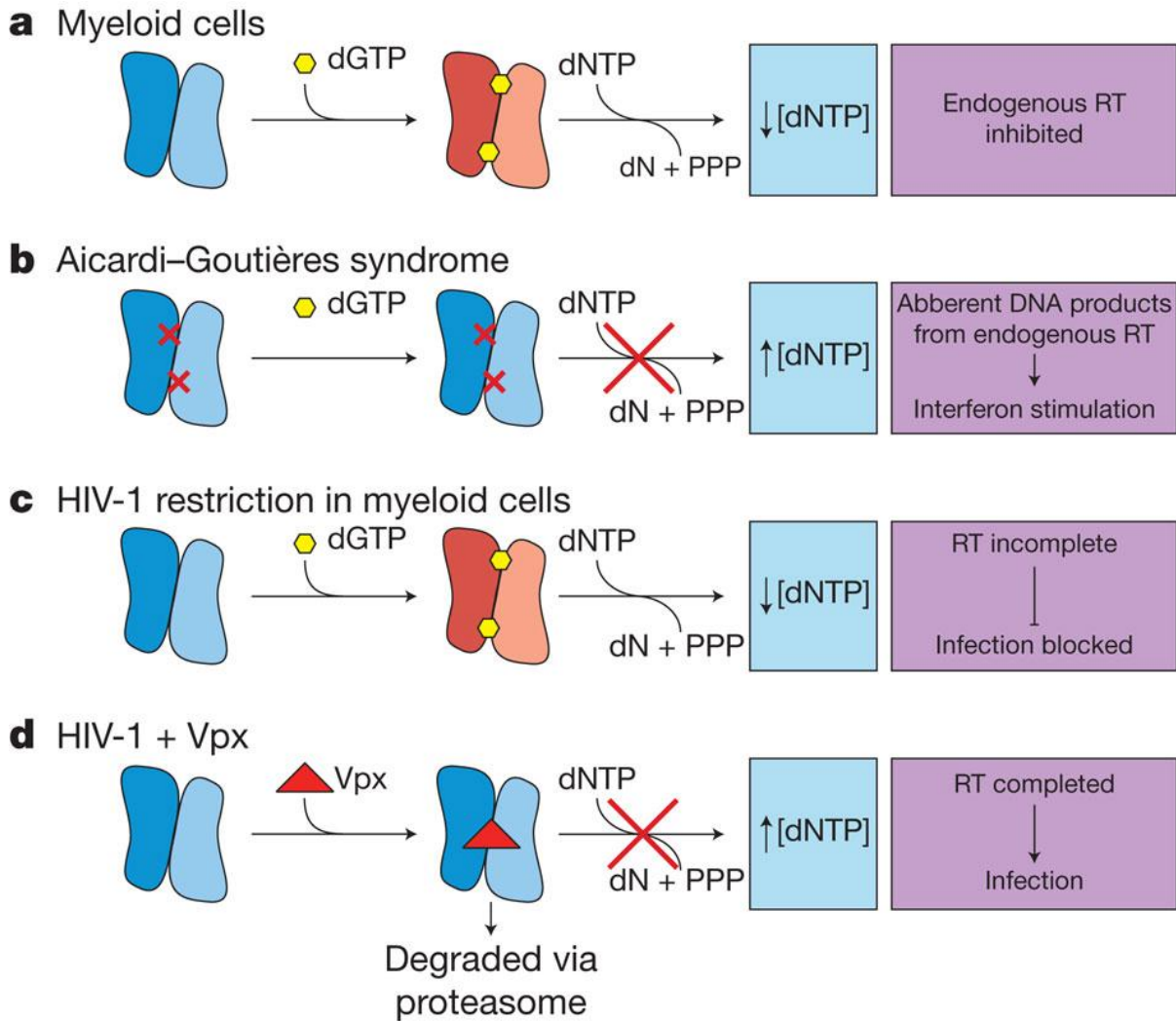


Figure 10

Dimeric SAMHD1 binds dGTP to activate the enzymatic cleavage activity of dNTPs

Suppression of dNTPs pools protect terminally differentiated cells like myeloids cells from endogenous RT activity (a). Abberant endogenous RT results from the defective SAMHD1 activity, leading to autoimmune AGS symptoms (b). HIV-1 restrction results from SAMHD1-mediated suppression of dNTP pools (c), and can be alleviated by Vpx counteraction (d). Figure is from (82) with permission (License number 2798951082907).

EVOLUTION OF HOST RESTRICTION FACTORS

The “Red Queen” hypothesis was proposed by Leigh Van Valen to describe an evolutionary system where continuous adaptation is required to maintain relative fitness levels (286). The underlying argument is that since every improvement in a species leads to a selective advantage in that species, genetic variation will normally continuously result in an increased fitness. However, in a system that involves two species sharing the same resources, improvement in one species implies a competitive advantage over the other species. Since resources are limited, this leads to a fitness advantage of one species that comes at the expense of the second species. Therefore, the only way for the second species to maintain its relative fitness while involved in a competition is to adapt in turn.

Virus-host interactions are a prime example of where this “Red Queen” competition plays out. Host antiviral genes exert a potent selective pressure on virus fitness, and viruses encode antagonists in turn to counteract the effects of host restriction factors. Mutations that allow the host restriction factor to evade antagonism provides an increased fitness to the host. This imposes a selective pressure on the virus to evolve its antagonist to re-establish the interaction (Figure 11). As a result, the selective pressure is shifted back on the host. Thus, this creates an escalating “arms race” dynamic.

The evolutionary “arms race” between host antiviral genes and the virally encoded antagonists of these antiviral genes can be inferred by observing adaptive evolution (also called positive selection) signatures in the antiviral genes that are indicative of repeated episodes of Darwinian selection due to ancient viral infections (59). In fact, the exact amino

acids under positive selection can describe the sites of host-virus interactions (231). When there are multiple viral antagonists, such detailed evolutionary analyses focused on positive selection can also reveal which type of viral antagonist exerted the greatest selective pressure during the course of primate evolution. These evolutionary signatures can also be used to infer the domains involved in the host-virus interaction. For instance, the Zinc Finger Antiviral Protein (ZAP) was shown to inhibit retroviruses, alphaviruses and filoviruses by specifically recognizing and degrading viral messenger RNAs (23, 72, 174). However, the positive selection on ZAP acts on a domain separate from the RNA-binding zinc finger domain, suggesting that rapid alterations of viral mRNA binding did not affect ZAP evolution, and some other (antagonistic) interaction did (121).

The nature of the antagonistic interactions determine the selective pressures, and hence, the distribution of the signals of positive selection. Some host restriction factors use a non-discriminating mechanism of action. For instance, the APOBEC3 cytidine deaminases or tetherin can restrict a wide array of viruses, an activity that is not dependent on the recognition of specific viral components (discussed above). Because of its non-discriminating mechanism of restriction, the expectation is for multiple lineages of viruses to employ different modes of antagonism against these host restriction factors. Indeed, several groups have identified more than five viral strategies to antagonize tetherin. These antagonist-antiviral interactions are also akin to 'arms-races' and also result in positive selection of the antiviral genes. In most instances, a single difference at the amino acid level is sufficient to disrupt the binding interaction and lead to evasion. However, these interactions often result in a more diffuse signature of positive selection, as the pressure to

avoid many antagonists has shaped the evolution of antiviral factors. For instance, in APOBEC3G which can be susceptible to Vif antagonism in some species (28, 236), avoidance of Vif-interactions cannot explain the majority of positively selected residues in Apobec3 proteins (230). Hence, under antagonism evasion conditions, the sites of positive selection will be seen at the residues directly targeted by the antagonist but will vary depending on the antagonist specificity.

In contrast, when the mechanism of the host restriction factor is dependent on discriminatory recognition for viral targets, the selective pressures are for adaptations that acquire new recognition specificities. For instances, restriction by TRIM5 α and Fv1 requires the specific recognition of viral components by the restriction factors (discussed above). In such instances, 'arms-races' are played out by the evolution of viral variants to avoid restriction, and restriction factors to restore restriction (166). Thus, at the molecular level, specific domains or clusters of residues of the host restriction factors recurrently evolve under positive selection. Thus, the selective pressures exerted by antagonist evasion or viral recognition lead to different consequences for the host gene.

Thus, a detailed look at how positive selection has affected an antiviral gene can thus provide valuable information about the history of antagonism, and even possibly the domains involved in the host-virus interaction. Such insights can complement the original findings of antiviral activity and trace the evolutionary history of the "arms race".

In this dissertation, I will present a three-dimensional perspective of the evolutionary host-virus arms race. In the following chapters, I will reconstruct two specific

examples that convincingly show how host genetics evolve barriers to cross-species transmission, and how viruses ultimately counter-evolve to their new hosts (Chapter Four and Six). I will also present conclusive evidence that the host immune environment directly impacts the role of viral factors (Chapter Three). Finally, I will demonstrate how to exploit the evolutionary signatures of host restriction factors to identify and characterize novel candidates (Chapter Five). My studies have helped define the rules of host-virus arms races. Based on my findings, we contend that the **host evolutionary framework is a fundamental pillar of antiviral restriction.**

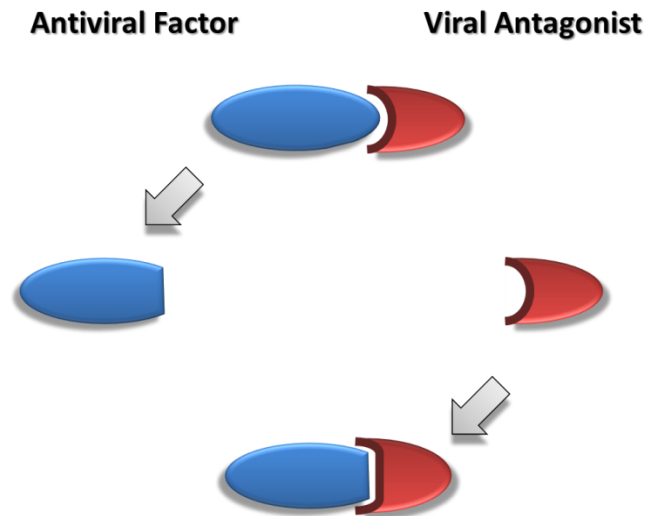


Figure 11

Genetic conflict between virus and host leads to an escalating “arms race”. Host antiviral genes (blue) evasion from viral antagonists (red) leads to rapid adaptive evolution of hosts genes.

CHAPTER TWO

MATERIALS AND METHODS

CELLS

293T, COS-7, and TZM-bl cells were maintained in a solution containing Dulbecco's modified Eagle's medium, 8% bovine growth serum, and 1% penicillin-streptomycin in a 5% CO₂ atmosphere at 37°C. TZM-bl cells were obtained from the AIDS Research and Reference Reagent Program, Division of AIDS, NIAID, NIH. *Chlorocebus sabaues* fibroblasts were obtained from the Coriell Institute and were maintained in a solution containing Dulbecco's modified Eagle's medium, 10% fetal bovine serum, and 1% penicillin-streptomycin. SupT1 and U937 cells were maintained in a solution containing RPMI 1640 medium, 10% fetal bovine serum, and 1% penicillin-streptomycin.

PLASMIDS

The SIVagm molecular clones pSAB-1 (SIVagmSab) and pSIVagmTan-1 (SIVagmTan) were obtained from the AIDS Research and Reference Reagent Program, Division of AIDS, NIAID, NIH. The SIVagmTan Env⁻ Nef⁻ provirus was a gift from Ned Landau (158). The HIV1VpuFS construct, containing a frameshift mutation in Vpu, is based on a molecular clone of HIV-1 described previously (87). The HIV1VpuFSLuc2 double mutant reporter clone was constructed by replacing the Nef gene of HIV1VpuFS with the Nef gene containing an insertion of the modified firefly luciferase, as described previously (304). Codon-optimized

HIV-1 Vpu was a gift from Stephen Bour (178), and codonoptimized (Genscript) SIVmus Vpu was constructed from a calculated ancestral sequence constructed from four SIVmus Vpu sequences reported previously (3). Both Vpu constructs were inserted into a pCDNA3.1 expression vector as HindIII and NotI fragments. The empty pCDNA3.1 vector was used as a negative control. The Nef proteins from SIVagmTan and SIVagmSab were PCR amplified from pSIVagmTan-1 and pSAB-1, respectively, flanked by HindIII and XhoI restriction sites, and ligated into a pCDNA3.1 expression vector. Human, *Cercopithecus cephus*, AGM, and chimpanzee tetherins were cloned from human cDNA, *C. cephus* genomic DNA (Coriell Cell Repository), cDNA from CV-1 cells, and chimpanzee cDNA, respectively. Tetherin was amplified by PCR, resulting in fragments with NgoMIV and NotI sites. A hemagglutinin (HA) epitope tag was fused to the N terminus of tetherin and inserted into retroviral expression vector pLPCX. To construct untagged AGM tetherin, the HA epitope tag was removed by restriction digestion, overhangs were filled in with DNA polymerase I and large Klenow fragment (Invitrogen), and blunt-end ligation was performed with T4 DNA ligase (Roche). The empty pLPCX vector was used as a negative control.

Human, chimpanzee, gorilla, *C. cephus*, and Francois' leaf monkey Tetherins were cloned from the cDNAs of the respective species and were ligated into a pLPCX lentiviral expression vector as untagged constructs, as described above. Codon-optimized HIV-1 Q23-17 Vpu, SIVcpzUS Vpu, SIVcpzUS Nef, SIVcpzTan3.1 Vpu, SIVgor Vpu, and SIVgor Nef were synthesized (GenScript). HIV-1 Lai Nef was cloned from the HIV-1 Lai proviral plasmid (195); HIV-1 Q23-17 Nef was cloned from the HIV-1 Q23-17 provirus, a gift from Julie Overbaugh (210); and SIVcpzTan3.1 Nef was cloned from the SIVcpzTan3.1 proviral plasmid, obtained

from the NIH AIDS Research and Reference Reagent Program (268). The Vpu and Nef constructs were ligated into a pCDNA3.1 expression vector.

Chimeras between HIV-1 Q23-17 Vpu and SIVcpzUS Vpu were constructed with a QuikChange II XL site-directed mutagenesis kit (Stratagene) or by overlapping PCR approaches. For expression studies, a hemagglutinin (HA) epitope tag was fused to the C termini of chimeric Vpu constructs. The ancestral human Tetherin was constructed by overlapping PCR to insert 5 amino acids (aa) in the cytoplasmic tail domain (residues 14 to 18) and to substitute E for K at aa 19.

Human Viperin was cloned from human cDNA derived from 293T cells, and inserted into a retroviral expression vector pLPCX as an untagged construct. The five primate Viperin orthologs were similarly cloned from cDNA into the pLPCX retroviral expression vector as untagged constructs. HIV-1 Lai Nef and HIV-1 Q23-17 Nef was cloned into an expression vector driven by the HIV-1 LTR as described previously (142). Codon-optimized HIV-1 Lai Vpu was a gift from Stephan Bour (178). HIVLai, HIVLai Δ Nef and HIVLai Δ Vpu Δ Nef, SIVagmTAN Δ Env Δ Nef were described previously (140, 142). HIVNL4-3 Δ Nef was obtained from the NIH Aids Research and Reference Reagent Program, 11100. HIVSF62 Δ Nef was generated by fill-on of the XhoI site (nt 8576) resulting in a 2bp frameshift mutation in the Nef open reading frame of the full length HIV-1SF162 provirus (41). HIV-1Q23-17 Δ Nef was constructed by introducing a luciferase gene in place of Nef into the full length HIV-1 Q23-17 provirus (210). SIVcpz Δ Nef was generated by introducing a luciferase gene in place of Nef into the full length SIVcpzTAN3.1 provirus (268) (NIH Aids Research and Reference

Reagent Program, 11100) by overlapping PCR between the NdeI and NheI region and sequence verified. HIV-2Rod9ΔEnvΔNef was a gift from Masahiro Yamashita and SIVmac239ΔEnvΔNef was a gift from David Evans (215). pGIPZ vector-based control shRNA or shRNA targeting Viperin mRNA (hairpin construct: TGCTGTTGACAGTGAGCGCGATGAAAGACTCCTACCTTATTAGTGAAGCCACAGATGTAATAAGGT AGGAGTCTTTTCATCTTGCCTACTGCCTCGGA) were purchased from FHCRC RNAi core facility.

Primate SAMHD1 was cloned from cDNA from the respective species and ligated into pLPCX construct, with a hemagglutinin (HA) epitope tag fused to the C-termini. Vpr and Vpx constructs ligated into a pCDNA3.1 expression vector, with a 3xFLAG epitope tag fused to the N-termini. The following genes were cloned from provirus plasmids: HIVLai Vpr, SIVagmGri677 Vpr, SIVagmVer 9648 Vpr, HIV-2 Rod9 Vpr and Vpx, HIV-2 7312a Vpr and Vpx (as previously described (257)); HIV-1 Q23-17 Vpr (provirus was a gift from Julie Overbaugh (210)); SIVmac239 Vpr and Vpx (provirus plasmid, obtained from NIH AIDS Research and Reference Reagent Program (215)); SIVcpzTan2.69 Vpr and SIVcpzTan3.1 Vpr (proviral plasmid, obtained from the NIH AIDS Research and Reference Reagent Program (268)). The following genes were codon-optimized and synthesized (Genscript): SIVolc 97CI12 Vpr (FM165200), SIVmnd1 GB1 Vpr (M27470), SIVrcm NG411 Vpr and Vpx (AF349680), SIVmnd2 5440 Vpr and Vpx (AY159322), SIVdeb CM5 Vpr (AY523866) and SIVmus1 CM1239 Vpr (EF070330).

TRANSFECTION AND VIRUS PSEUDOTYPING

293T and COS-7 cells were seeded at 1.67×10^5 and 8.33×10^4 cells/ml, respectively. DNA was transfected with Eugene6 reagent (Mirus) according to the manufacturer's recommendations. To measure the tetherin restriction of HIV1VpuFS, 293T cells were transfected with HIV1VpuFS (100 ng), human tetherin (200 ng), ceptus monkey tetherin (400 ng), AGM tetherin (400 ng), HIV-1 Vpu (125 ng), or SIVmus Vpu (100 ng). Transfections involving SIVagm provirus were performed with SIVagmTan (100 ng), SIVagmTan Env⁻ Nef⁻ (100 ng) with vesicular stomatitis virus G protein (VSV-G) (50 ng), and SIVagmSab (100 ng). AGM titration was performed with 0, 3.12, 6.25, 12.5, 25, 50, and 100 ng of native (untagged) AGM tetherin, VSV-G (50 ng), and SIVagmTan (100 ng) or SIVagmTan Env⁻ Nef⁻ (100 ng). For experiments involving Nef, 293T cells were transfected with HIV1VpuFSLuc2 (100 ng), human tetherin (100 ng), chimpanzee tetherin (100 ng), AGM tetherin (100 ng), and SIVmus Vpu (100 ng), SIVagmTan Nef (250 ng), or SIVagmSab Nef (250 ng). In all experiments, the total amount of DNA was maintained constant by adding the respective amounts of empty vectors. Forty-eight hours after transfection, supernatant containing virus was filtered through a 0.22- μ m filter and analyzed by a Western blot or infectivity assay. Cells were washed with Dulbecco's phosphate-buffered saline and removed with 0.05% trypsin for Western blot analysis. VSV-G-pseudotyped viruses for electron microscopy and Western blot experiments were prepared by the cotransfection of a VSV-G expression vector (pLVSV- G) (50 ng) with SIVagmTan Env⁻ Nef⁻ (100 ng) or SIVagmTan (100 ng) in 293T cells, as described previously (304). Forty-eight hours after transfection, the supernatant containing pseudotyped viruses was pooled and filtered through a 0.22- μ m filter. Virus was

concentrated by ultracentrifugation, and titers were determined by infecting reporter TZM-bl cells with serial dilutions of virus stock as described previously (290).

INFECTIVITY ASSAY

An infectivity assay was performed with TZM-bl cells as described previously (21). TZM-bl cells were seeded at 2×10^5 cells/ml in 96-well plates. Serial dilutions of virus supernatant were used to infect TZM-bl cells by spinoculation at 1,200 relative centrifugal force (RCF) for 2 h in the presence of 20 μ g/ml DEAE-dextran. Forty-eight hours postinfection, 200 μ g/ml of 4-methylumbelliferyl- β -D-galactopyranoside was added to cells, and the resulting fluorescence (*lacZ* activity) was measured using a spectrophotometer at 30-s intervals at 360 nm/460 nm. The relative infectivity was determined by the linear rate of increasing *lacZ* activity over time. An HIV1VpuFSLuc2 infectivity assay was performed with SupT1 cells at 2.5×10^5 cells/ml in 96-well plates. Serial dilutions of virus supernatants were used to infect SupT1 cells by spinoculation at 1,200 RCF for 1 h in the presence of 20 μ g/ml DEAE-dextran. Forty-eight hours postinfection, the level of luciferase expression was determined by use of the Bright-Glo luciferase assay system (Promega) according to the manufacturer's instructions.

For the second tetherin study (Chapter Four), 293T cells were cotransfected with 200 ng of an HIV-1 reporter provirus (HIV1VpuFSLuc2), 25 ng of a Vpu or Nef construct, and native Tetherin as indicated in the figures. The total amount of DNA in all transfections was maintained constant with appropriate empty vectors. The HIV-1 double mutant reporter

virus (HIV1VpuFSLuc2) expresses a frameshift mutation in Vpu and a luciferase gene inserted into the Nef open reading frame (24). Forty-eight hours after transfection, an infectivity assay was performed with SupT1 cells at 2.5×10^5 /ml in 96-well plates as described above.

For the Viperin study (Chapter Five), 293T cells were seeded at 1.67×10^5 cells/ml in 12-well plates, and DNA was transfected with TransIT LT-1 (Mirus) according to the manufacturer's recommendations. The total amount of DNA in all transfections was maintained constant with appropriate empty vectors. Forty-eight hours after transfection, supernatant was collected, filtered through a $0.2\mu\text{M}$ filter and serially diluted for the following infectivity assay. SupT1 cells at 2.5×10^5 cells/ml in 96-well plates as described previously (142), or TZM.bl cells at 1.0×10^5 cells/ml in 96-well plate as described above. The β -Galactosidase activity was detected using the Galacto-Star system (Applied Biosystems) according to the manufacturer's recommendations.

SAMHD1 TRANSFECTION

293T cells were transfected with 100 ng of SAMHD1 (in LPCX expression vector, C-terminal HA epitope tag) with or without 100 ng of Vpr/Vpx constructs (in pCDNA3.1 expression vector, N-terminal 3xFLAG epitope tag) using TransIT-LT1 (Mirus Bio). The amount of codon optimized Vpr/Vpx was reduced to normalize for similar levels of protein expression. The total amount of DNA in all transfections was maintained constant with

appropriate empty vectors. Forty-eight hours post-transfection, cells were harvested for western blot analysis.

WESTERN BLOTTING

Forty-eight hours after transfection or infection, cells were analyzed by Western blotting as described previously (38), with the following modifications. Lysis was performed with NTE medium (10 mM Tris [pH 8.0], 1 mM EDTA, 50 mM NaCl) in the presence of protease inhibitor cocktail (Roche) for 5 min, followed by NP40-doc (1%NP-40, 0.2% sodium deoxycholate, 0.12 M NaCl, 20 mM Tris [pH 8.0]) for 10 min. Proteins were separated on a 4 to 12% NuPAGE Novex Bis-Tris precast gel (Invitrogen). The membrane was probed with the following primary antibodies: HA-specific antibody (HA.11 mouse immunoglobulin G; Babco) at a 1:1,000 dilution and anti-actin rabbit antibody (Sigma-Aldrich) at a 1:500 dilution. Primary antibodies were detected with horseradish peroxidase-conjugated goat anti-mouse or anti-rabbit antibodies, respectively. SIVagm was detected with sera from rhesus macaques infected with SIVagmsab92018 (Cristian Apetrei, Tulane National Primate Research Center) and probed with horseradish peroxidase-conjugated goat anti-monkey immunoglobulin G secondary antibody (Cappel).

For the second tetherin study (Chapter Four), forty-eight hours posttransfection, cells were analyzed by Western blotting as described previously above. An HA-specific antibody (HA.11 mouse immunoglobulin G; Babco) at a 1:1,000 dilution and a rabbit anti-actin antibody (Sigma-Aldrich) at a 1:2,000 dilution were used. The primary antibodies were

detected with a horseradish peroxidase-conjugated goat anti-mouse or anti-rabbit antibody, respectively.

In the Viperin study (Chapter Five), western blot analysis was performed with the following antibodies: HA-specific antibody (Babco), anti-Viperin (Enzo Life Sciences), anti-caveolin-1 (Santa Cruz Biotechnologies), anti-transferrin receptor (Abcam), anti-actin (Sigma-Aldrich), anti-tubulin (Sigma-Aldrich), HIV-1 p24 antibody (NIH Aids Research and Reference Reagent Program, 183-H12-5C) (42), SIVmac p27 antibody (NIH Aids Research and Reference Reagent Program, 55-2F12) (97), and HIV-1 Nef antiserum (Aidsreagent, 2121) (179). Primary antibodies were detected with a corresponding horseradish peroxidase-conjugated secondary antibody.

For the SAMHD1 study (Chapter Six), western blot analysis was performed with the following antibodies: HA-specific antibody (Babco), anti-FLAG M2 antibody (Sigma-Aldrich), anti-actin (Sigma-Aldrich). Primary antibodies were detected with a corresponding horseradish peroxidase-conjugated secondary antibody.

INTERFERON STUDIES

Recombinant human IFN- α 2A and IFN- β 1b were obtained from PBL Biomedical Laboratories (catalog numbers 11100-1 and 11420-1). Cells were exposed to 0, 100, or 1,000 units/ml IFN for 24 or 48 h and analyzed for tetherin RNA expression by semiquantitative reverse transcription-PCR (RT-PCR) or fixed for thin-section electron

microscopy, respectively. For the analysis of endogenous tetherin effects, COS-7 cells were infected with VSV-Gpseudotyped SIVagmTan or VSV-G-pseudotyped SIVagmTan Env⁻ Nef⁻ by spinoculation at 1,200 RCF for 2 h in the presence of 20 µg/ml DEAE-dextran. IFN-β1b was added 6 h later, followed by an additional 42 h of incubation before fixing for thin-section electron microscopy or analysis by Western blotting as described above.

SEMIQUANTITATIVE RT-PCR

Cells were removed by use of 0.05% trypsin- EDTA, and RNA was extracted by use of an RNeasy minikit (Invitrogen) according to the manufacturer's protocol. Human tetherin, AGM tetherin, and β-actin were reverse transcribed with a OneStep RT-PCR kit (Qiagen) for 30 min at 50°C, followed by inactivation at 95°C for 15 min. Four microliters of cDNA was amplified by PCR with *Taq* DNA polymerase (Roche), and amplified products were separated on a 1.25% agarose gel. AGM and human β-actin were amplified with the following set of primers: TGACATTAAGGAGAAGCTGTGCTA and ACTCGTCATACTCCTGCTTGCT. AGM tetherin spanning exon 2 to exon 4 was amplified with the following set of primers:

CAAGGACGAAAGAAAGTGGAG and AAGCCCAGCAGCAGAATCAG. Human tetherin spanning exon 1 to exon 4 was amplified with the following set of primers: ATCTCCTGCAACAAGAGCTGAC and GTACTTCTTGCCGCGATTCTC.

THIN-SECTION ELECTRON MICROSCOPY

Cells were fixed with 2% paraformaldehyde– 2.5% glutaraldehyde in 0.1 M cacodylate buffer and removed with a cell scraper. All washes were performed with 0.1 M cacodylate buffer. As a postfixative, 1% OsO₄ was added, followed by 4% aqueous uranyl acetate. Cells were dehydrated in a series of ethanol gradients (50 to 100%), embedded in Epon 812 resin, and cured for 48 h at 60°C. Thin sections (70 to 100 nm) of the samples were obtained and stained with uranyl acetate, followed by lead citrate. Electron micrographs were taken using a Jeol 1230 transmission electron microscope with an Ultrascan 1000 camera.

NUCLEOTIDE SEQUENCE ACCESSION NUMBER

The sequences of the 20 primate *tetherin* genes have been entered into the GenBank database under accession numbers NM_004335, GQ864267, and HM136905 to HM136922.

The sequences of the 18 primate *viperin* genes have been entered into the GenBank database under accession numbers NM_080657, JQ437821 to JQ437837.

The sequences of the 31 *SAMHD1* genes have been entered into the GenBank database under accession numbers NP_056289, and JQ231123-JQ231152.

SEQUENCING OF PRIMATE *TETHERIN* GENES

The *tetherin* genes from the following primates were amplified from RNA isolated from cell lines obtained from Coriell Cell Repositories (Camden, NJ): bonobo (*Pan paniscus*), gorilla (*Gorilla gorilla*), Sumatran orangutan (*Pongo pygmaeus*), white-cheeked gibbon (*Nomascus leucogenys*), agile gibbon (*Hylobates agilis*), rhesus macaque (*Macaca mulatta*), patas monkey (*Erythrocebus patas*), mustached monkey (*Cercopithecus cephus*), kikuyu colobus (*Colobus guereza kikuyuensis*), douc langur (*Pygathrix nemaeus*), Francois' leaf monkey (FLM) (*Trachypithecus francoisi*), tamarin (*Saguinus labiatus*), pygmy marmoset (*Callithrix pygmaea*), white-faced saki (*Pithecia pithecia*), Bolivian red howler (*Alouatta sara*), and woolly monkey (*Lagothrix lagotricha*). African green monkey (*Chlorocebus aethiops*) Tetherin was amplified by reverse transcription-PCR (RT-PCR) from an RNA extract of COS-7 cells. Tetherin was amplified by RT-PCR with a OneStep RT-PCR kit (Qiagen), and the cDNA derived was directly sequenced. Tetherin was amplified with "forward" primer CD317upstreamForward (5'-CCCCTAACTTCAGGCCAGACTC-3') or CD317ATGForward (5'-CAGCTAGAGGGGAGATCTGGATG-3') in combination with "reverse" primer CD317downstreamReverse (5'-CTCACTGACCAGCTTCCTGGG-3').

SEQUENCING OF PRIMATE VIPERIN GENES

The *viperin* genes from the following primates were amplified from RNA isolated from cell lines obtained from Coriell Cell Repositories (Camden, NJ): chimpanzee (*Pan troglodytes*), gorilla (*Gorilla gorilla*), Sumatran orangutan (*Pongo pygmaeus*), Siamang gibbon (*Hylobates syndactylus*), agile gibbon (*Hylobates agilis*), rhesus macaque (*Macaca mulatta*), greater

white-nosed monkey (*Cercopithecus nictitans*), kikuyu colobus (*Colobus guereza kikuyuensis*), Francois' leaf monkey (FLM) (*Trachypithecus francoisi*), spider monkey (*Ateles geoffroyi*), owl monkey (*Aotus trivirgatus*), dusty titi monkey (*Callicebus moloch*) and woolly monkey (*Lagothrix lagotricha*). Human (*Homo sapiens*), African green monkey (*Chlorocebus aethiops*) and Baboon (*Papio anubis*) Viperin was amplified by reverse transcription-PCR (RT-PCR) from an RNA extract of 293T cells, COS-7 cells and B-LCL cells. Viperin was amplified by RT-PCR with a OneStep RT-PCR kit (Qiagen), and the cDNA derived was directly sequenced. Viperin was amplified with "forward" primer (5'-ATGTGGGGTGCTTACACCTGCTGCTTTTGCTG-3') or (5'-ATGTGGGTACTCACGCCTGCTGCTTTTGCTG-3') in combination with "reverse" primer (5'-CTACCAATCCAGCTTCAGATCAGCCTTACTC-3') or (5'-CTACCAATCCAGCTTCAGATCAGCCTTACTC-3'). Sequences for prosimian grey mouse lemur (*Microcebus murinus*) and tarsier (*Tarsius syrichta*) viperin gene were acquired by tblastx search on the NCBI database from cont1.216710 (ABDC01216711.1) and contig1.93320 (ABRT010093321.1) respectively.

SEQUENCING OF PRIMATE *SAMHD1* GENES

The *SAMHD1* genes from the following primates were amplified from RNA isolated from cell lines obtained from Coriell Cell Repositories (Camden, NJ): Chimpanzee (*Pan troglodytes*), Bonobo (*Pan paniscus*), Gorilla (*Gorilla gorilla*), Sumatran orangutan (*Pongo pygmaeus*), White-cheeked gibbon (*Nomascus leucogenys*), Agile gibbon (*Hylobates agilis*),

Siamang gibbon (*Hylobates syndactylus*), Rhesus macaque (*Macaca mulatta*), patas monkey (*Erythrocebus patas*), Talapoin monkey (*Miopithecus talapoin*), Greater white-nosed monkey (*Cercopithecus nictitans*), De Brazza's monkey (*Cercopithecus neglectus*), Wolf's guenon (*Cercopithecus wolfi*), Allen's swamp monkey (*Allenopithecus nigroviridis*), Sooty mangabey (*Cercocebus atys*), Red-capped mangabey (*Cercocebus torquatus*), Mandrill (*Mandrillus sphinx*), Drill (*Mandrillus leucophaeus*), Kikuyu colobus (*Colobus guereza kikuyuensis*), Francois' leaf monkey (FLM) (*Trachypithecus francoisi*), Proboscis monkey (*Nasalis larvatus*), Tamarin (*Saguinus labiatus*), Pygmy marmoset (*Callithrix pygmaea*), White-faced saki (*Pithecia pithecia*), Spider monkey (*Ateles geoffroyi*), Owl monkey (*Aotus trivirgatus*), Dusty titi monkey (*Callicebus moloch*) and Woolly monkey (*Lagothrix lagotricha*). Human, African green monkey (*Chlorocebus aethiops*) and Baboon (*Papio anubis*) SAMHD1 was amplified by reverse transcription-PCR (RT-PCR) from an RNA extract of 293T cells, Vero cell (AGM Vervet subspecies), COS-7 cells (AGM *Sabaeus* subspecies) and B-LCL cells. SAMHD1 was amplified by RT-PCR with SuperScript III One-Step RT-PCR (Qiagen), and the cDNA derived was directly sequenced. SAMHD1 was amplified with "forward" primer SAMHD1-Hominoid-F (5'-ATGCAGCGAGCCGATTCCGAGCAGCC-3'), SAMHD1-OWM-F (5'-ATGCAGCAAGCCGACTCCGACCAGCC-3') or SAMHD1-NWM-F (5'-ATGCAGCAAGCCGACTTCGAGCAGCC-3') in combination with "reverse" primer SAMHD1-Hominoids-r (5'-TCACATTGGGTCATCTTTAAAAAGCTG-3'), SAMHD1-OWM-r (5'-TCACTTTGGGTCATCTTTAAAAAGCTG-3') or SAMHD1-NWM-r (5'-TCACACCGGGTCATCCTTAAAAAGCTG-3').

TETHERIN SEQUENCE ANALYSIS

DNA sequences were aligned by ClustalX (272) and were edited by hand based on amino acid sequences. A phylogeny of *tetherin* genes was constructed from DNA sequences with ClustalX by the neighbor-joining method using the Jukes Cantor method of correction and with MrBayes by the maximumlikelihood method. The two methods yielded trees with identical topologies. Maximum-likelihood analysis was performed with CODEML from the PAML suite of programs (308). To detect selection in Tetherin, we fitted the data to site-specific models (nonsynonymous [NS] sites) that disallowed (NSsites model 7) or permitted (NSsites model 8) positive selection and compared the results by likelihood ratio tests. Consistent results were obtained when M1 (a two-state neutral model) was compared with M2 (a selection model allowing a nonsynonymous/synonymous change [dN/dS] ratio of >1). Sequence alignments were obtained when the data were fitted with an F61 model of codon frequency, and consistent results were obtained when the data were fitted with an F3 x 4 model of codon frequency. We calculated the global ratios of dN to dS by a free-ratio model that allows dN/dS to vary along individual branches.

VPU SEQUENCE ANALYSIS

HIV-1 group M Vpu sequences and SIVcpz Vpu sequences were obtained from the HIV sequence database (<http://www.hiv.lanl.gov>) (148), aligned by ClustalX (272), and edited by hand. A total of 1,271 sequences representing HIV-1 group M Vpu were analyzed

to generate the consensus. Sequence logos of the alignment were plotted using WebLogo (<http://weblogo.berkeley.edu>) (47).

VIPERIN SEQUENCE ANALYSIS

DNA sequences were aligned by ClustalX (272) and were edited manually. The amino acid positions are annotated in reference to the human Viperin sequence. A phylogeny of *viperin* genes was constructed from DNA sequences with ClustalX by the neighbor-joining method using the Jukes Cantor method of correction and with PhyML (86) by the maximum-likelihood method. The two methods yielded trees with identical topologies. Maximum-likelihood analysis was performed with CODEML from the PAML suite of programs (308) as previously described (141, 142). Sequence alignments were obtained when the data were fitted with an F61 model of codon frequency, and consistent results were obtained when the data were fitted with an F3 x 4 model of codon frequency. *Viperin* sequences were fitted to NSsites models that disallowed (NSsites model 1 and 7) or permitted (NSsites model 2 and 8) positive selection. Likelihood ratio tests were performed to evaluate whether permitting codons to evolve under positive selection gave a better fit to the data. A cutoff of posterior probability of $p > 0.95$ was implemented in these analyses (M8) to identify amino acid residues having evolved under positive selection. Analyses were also validated with REL from the HyPhy package (209). Free ratio analysis in PAML was used to calculate the ω (dN/dS) ratios of individual branches. Likelihood ratio test statistics was performed for models of variable selective pressures along branches of primate *viperin* genes between

M0 (same dN/dS ratio for all branches) and M1 (different dN/dS ratio for each branch). The degree of freedom is equal to one less than the total number of branches in the phylogeny.

SAMHD1 SEQUENCE ANALYSIS

SAMHD1 DNA sequences were aligned by ClustalX (272) and were edited by hand based on amino acid sequences or with PhyML (86) by the maximum-likelihood method. The two methods yielded trees with identical topologies. Maximum-likelihood analysis was performed with CODEML from the PAML suite of programs (308) as previously described above. Briefly, *SAMHD1* sequences were fitted to NSsites models that disallowed (NSsites model 1 and 7) or permitted (NSsites model 2 and 8) positive selection. Likelihood ratio tests were performed to evaluate whether permitting codons to evolve under positive selection gave a better fit to the data. Data were fitted with an F61 model of codon frequency, and consistent results were obtained when the data were fitted with an F3 x 4 model of codon frequency. These analyses (M8) identified amino acid residues with high posterior probability ($p > 0.95$) of having evolved under positive selection. Analyses were also validated with PARRIS and REL from the HyPhy package (209). Free ratio analysis in PAML was used to calculate the ω (dN/dS) ratios of individual branches.

VPR AND VPX PHYLOGENETIC ANALYSIS

Phylogenetic trees were constructed from amino acid alignments of *vpr* and *vpx* sequences obtained from the Los Alamos HIV sequence database (148). Alignments were performed using ClustalX (272) and edited by, or fast statistical alignment (FSA) (33) for a more conservative alignment that maximizes on accuracy. Phylogenies were constructed with PhyML (10) by the maximum-likelihood (ML) method; and MrBayes v3.1.2 (102) and BEAST v1.6.2 (57) using a Bayesian MCMC inference. Support for ML trees was assessed by 1000 non-parametric bootstraps. MrBayes analyses were run for 10,000,000 steps with a sample frequency set to 1000 and burn-in length of 1,000,000. BEAST analyses were run until convergence with a minimum of 1,000,000 generations, sampling every 1000 and discarding the initial 10% as burn-in. Convergence and mixing for both MrBayes and BEAST were assessed using Tracer v1.5 (56). Analyses from both Bayesian methods were performed at least twice.

FLOW CYTOMETRY

To analyze the expression of Tetherin on the cell surface, 293T cells were cotransfected with 250 ng native human Tetherin in the presence of 750 ng of the respective Vpu constructs. Twenty-four hours posttransfection, cells were gently rinsed with 1_ Dulbecco's phosphate-buffered saline (DPBS) and were resuspended in DPBS containing 4% calf serum. Cells were incubated first with an anti-human BST-2 (anti-human Tetherin) antibody obtained from the NIH AIDS Research and Reference Reagent Program (169) and subsequently with an anti-rabbit antibody conjugated with fluorescein isothiocyanate (FITC) (BD Pharmingen). Unbound antibodies were washed away, and

labeled cells were resuspended in DPBS containing 4% calf serum. Flow cytometry was performed with a BD FACSCalibur platform and CellQuest software (BD). To analyze the downregulation of Tetherin expression on the cell surface by Vpu, cell events were plotted by the forward scatter (FSC) parameter versus the FL-1 parameter (Tetherin). To analyze the downregulation of CD4 expression by Vpu, 293T cells were cotransfected with 125 ng of the bicistronic pIRES-eGFP2 vector, expressing human CD4 and green fluorescent protein (GFP), and 1 µg of the respective Vpu constructs. Twenty-four hours posttransfection, cells were incubated with an allophycocyanin (APC)-conjugated mouse anti-human CD4 antibody (BD Pharmingen) or an APC-conjugated mouse IgG1(κ) isotype control antibody (BD Pharmingen). For analysis, cell events were plotted by the FL-1 (GFP) parameter versus the FL-4 parameter (APC). To analyze the downregulation of CD4 expression by Vpu, GFP-positive events were gated, and the percentages of CD4-positive event counts in the presence or absence of the various Vpu constructs were compared.

VIRUS PRODUCTION p24 ELISA

Virus were serially diluted and measured by HIV-1 p24 antigen capture assay (Advanced BioScience Lab Inc) and detected with QuantaRed enhanced chemifluorescent HRP substrate (Thermo Scientific) according to the manufacturer's protocol.

PBMC ISOLATION AND SEPARATION

Patient pall filters were obtained from Puget Sound Blood Center. PBMCs were isolated by standard ficoll histopaque gradient methods. Monocytes and CD4⁺ T cells were isolated by Human CD14 selection and CD4⁺ magnetic bead isolation (EasySep), and the isolation purity (>97-99%) was confirmed by flow cytometry staining (BD Pharmingen). Monocytes were maintained in RPMI containing 10% FBS. CD4⁺ T cells were activated with 2.5µg/ml PHA and 20U/ml IL-2 for 3 days before interferon treatment. Monocytes and CD4⁺ T cells were treated with 500 IU/ml human interferon β1b for 20 hours, followed by western blot analysis on total cell lysates.

SPREADING INFECTIVITY ASSAY

U937 cells stably transduced with either a Viperin-targeting shRNA or control shRNA constructs were infected with a wild type HIV-1Lai virus or HIV-1LaiΔNef at an moi of 0.5. Cells were washed with PBS three times and maintained in media containing 500 IU/ml human interferon β1b throughout the course of the experiment. Supernatant was collected at indicated time points and virus was quantified by p24 ELISA.

CO-IMMUNOPRECIPITATIONS

293T cells were transfected by TransIT-LT1 (Mirus Bio) with the appropriate plasmids 36 hours prior to lysis, and were treated with 25µM MG-132 (Calbiochem) for 12 hours. Cells were washed twice with PBS and lysed with IP Lysis Buffer (50mM Tris pH 7.4, 250mM

NaCl, 0.4% (v/v) NP-40, 1mM DTT, plus Protease Inhibitor Cocktail (Roche)). Lysates were cleared at 15,500g for 15 minutes and immunoprecipitations were performed for 1 hour at 4°C with EZview Red anti-HA affinity gel (Sigma-Aldrich). Following immunoprecipitation, affinity gel was washed 4 times with IP Lysis Buffer; proteins were eluted in 2X Lammellie Sample Buffer, and analyzed by Western blotting.

CHAPTER THREE

Simian Immunodeficiency Virus SIV_{agm} from African Green Monkeys Does Not Antagonize Endogenous Levels of African Green Monkey Tetherin/BST-2

SUMMARY

The Vpu accessory gene that originated in the primate lentiviral lineage leading to human immunodeficiency virus type 1 is an antagonist of human tetherin/BST-2 restriction. Most other primate lentivirus lineages, including the lineage represented by simian immunodeficiency virus SIV_{agm} from African green monkeys (AGMs), do not encode Vpu. While some primate lineages encode gene products other than Vpu that overcome tetherin/BST-2, I found that SIV_{agm} does not antagonize physiologically relevant levels of AGM tetherin/BST-2. AGM tetherin/BST-2 can be induced by low levels of type I interferon and can potently restrict two independent strains of SIV_{agm}. Although SIV_{agm} Nef had an effect at low levels of AGM tetherin/BST-2, simian immunodeficiency virus SIV_{mus} Vpu, from a virus that infects the related monkey *Cercopithecus cephus*, is able to antagonize even at high levels of AGM tetherin/BST-2 restriction. We propose that since the replication of SIV_{agm} does not induce interferon production in vivo, tetherin/BST-2 is not induced, and therefore, SIV_{agm} does not need Vpu. This suggests that primate lentiviruses evolve tetherin antagonists such as Vpu or Nef only if they encounter tetherin during the typical course of natural infection.

BACKGROUND

Although human tetherin inhibits the release of SIVagm virus-like particles and HIV-1 virus-like particles, SIVagm does not encode Vpu (116). However, SIVmus, which can be found in naturally infected *Cercopithecus cephus* monkeys, a species closely related to AGMs, does encode a Vpu protein (283). The compelling evidence of an independent acquisition of antitetherin factors in multiple viruses, coupled with the presence of Vpu in a SIV from a closely related host species, led me to the hypothesis that SIVagm might also possess a non-Vpu tetherin counterdefense.

The Vpu accessory gene that originated in the primate lentiviral lineage leading to human immunodeficiency virus type 1 is an antagonist of human tetherin/BST-2 restriction. Most other primate lentivirus lineages, including the lineage represented by simian immunodeficiency virus SIVagm from African green monkeys (AGMs), do not encode Vpu. While some primate lineages encode gene products other than Vpu that overcome tetherin/BST-2, I find that SIVagm does not antagonize physiologically relevant levels of AGM tetherin/BST-2. AGM tetherin/BST-2 can be induced by low levels of type I interferon and can potently restrict two independent strains of SIVagm. Although SIVagm Nef had an effect at low levels of AGM tetherin/BST-2, simian immunodeficiency virus SIVmus Vpu, from a virus that infects the related monkey *Cercopithecus cephus*, is able to antagonize even at high levels of AGM tetherin/BST-2 restriction. I propose that since the replication of SIVagm does not induce interferon production in vivo, tetherin/BST-2 is not induced, and therefore, SIVagm does not need Vpu. This suggests that primate lentiviruses evolve

tetherin antagonists such as Vpu or Nef only if they encounter tetherin during the typical course of natural infection.

SIVagm displays several key differences from pathogenic HIV-1. SIVagm isolates from African green monkeys (AGMs) cluster phylogenetically into four distinct clades, named SIVagmVer, SIVagmGri, SIVagmTan, and SIVagmSab, for their host species, vervet, grivet, tantalus, and sabaues monkeys, respectively (4, 5, 111, 173, 297). Chronic infection in agms (and the non-pathogenic sooty mangabeys) is associated with lower levels of immune activation and less apoptosis of bystander T cells (reviewed in (253)). It has also been proposed that primate natural hosts have a protected pool of central memory CD4⁺ T cells to explain the non-pathogenic outcome of infections in these hosts (30, 191). Importantly, these SIVagm viruses cause a nonpathogenic infection in their natural AGM hosts, in contrast to pathogenic HIV infections of humans (53). Both HIV-1 and SIVagm reach high levels of viral titers in vivo and replicate chronically in infected individuals. However, HIV-1 infection of humans usually results in chronic IFN stimulation (152), whereas there is an absence of chronic stimulation of IFN production in SIVagm infection in naturally infected AGMs despite equivalent high levels of virus titers (54).

Initially, it was proposed that SIVagm infection of AGMs represent an ancient relationship of virus-host coevolution. This was an appealing model as it could explain the observation that the infected AGMs (up to 70% prevalence) do not usually progress to immunodeficiency (113, 204). In support of this, phylogenetic analyses of CD4 and CCR5 genes from the AGM subspecies showed congruence with the SIVagm phylogeny suggesting

a coevolution model (65, 130). However, the ancient coevolution model has since been legitimately questioned. Resolution of the AGM mitochondrial genomes showed the AGM subspecies were significantly different from the SIVagm phylogeny (297). Moreover, preferential host switching of SIVs between genetically-similar host species may account for some of the apparent codivergence observed (40). Thus, SIVagm was likely the result of a west-to-east transmission after the radiation of the AGM subspecies, and not an ancient codivergence.

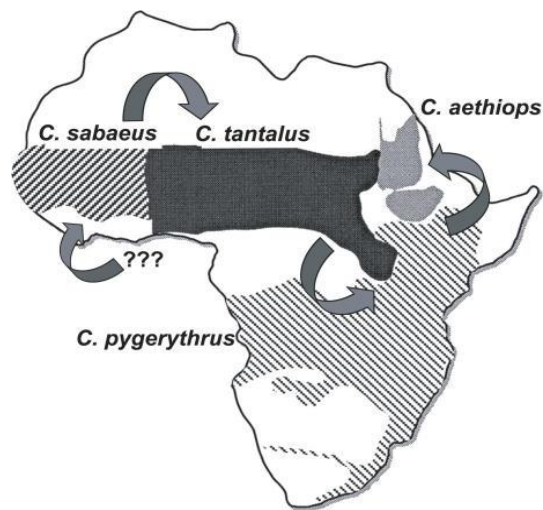


Figure 12

SIVagm Transmission Pattern across sub-Saharan Africa

Phylogenetic relationship (based on the full genome) of the four SIVagm viruses that infect their host-specific AGM subspecies is shown on the left. Distribution of the four AGM subspecies across the African continent is depicted on the right, showing the likely transmission route of SIVagm. *C. sabaenus* was likely the first AGM to be infected with SIV. The arrows depict a possible route of transmission of the virus across already established AGM ranges.

This figure is from (297).

Here, I report that SIVagm is restricted by endogenous AGM tetherin. Surprisingly, AGM tetherin causes a virion retention phenotype against the wild types (WTs) from both tantalus monkeys and sabaesus monkeys. Furthermore, I show that endogenous AGM tetherin expression is induced by type I IFNs, resulting in virion retention phenotypes for WT SIVagm. While I did see an effect of SIVagm on low levels of tetherin, I find that this effect is minor compared to the effects of SIVmus Vpu to overcome AGM tetherin restriction. Thus, SIVagm has not acquired an antagonist of AGM tetherin that is as potent as the antagonists encoded by HIV-1 or SIVmac. I propose that since SIVagm infection occurs in the absence of chronic IFN production (54), SIVagm does not encounter tetherin during the course of infection and does not require Vpu or Nef activity to counteract tetherin.

RESULTS

HIV-1 Vpu and SIVmus Vpu overcome restriction from tetherins from the host and related species.

Cercopithecus cephus (also called mustached monkey), AGM, and human tetherins were tested for antiviral activity. I was interested in tetherin from *C. cephus* because *C. cephus* monkeys are related to AGMs and because SIVmus that infects *C. cephus* encodes a Vpu protein, unlike SIVagm (46, 275). We cloned the gene that encodes tetherin from *C. cephus* and from *Chlorocebus tantalus* (AGM) into a retroviral vector expressing an N-

terminal HA epitope tag. Since HIV-1 Vpu is known to counteract human tetherin (176), I tested the ability of these tetherins to restrict HIV-1 expressing a frameshift mutation in Vpu (HIV1VpuFS). I also complemented these transfections with either HIV-1 Vpu or SIVmus Vpu expression vectors in *trans*. For this, plasmids encoding HIV1VpuFS, tetherin, and/or Vpu were transiently cotransfected into 293T cells (which express low levels of endogenous tetherin (176)), and the activity of tetherin or Vpu was measured by the infectivity of released virus on indicator cells (see Materials and Methods).

I found that human, *Cephus* monkey, and AGM tetherin all restricted the release of infectious HIV-1 virions by equal amounts in the absence of Vpu (Figure 13A). HIV-1 Vpu was able to overcome human tetherin restriction but was unable to overcome restriction by *C. cephus* or AGM tetherin (Figure 13A). Conversely, SIVmus Vpu was able to overcome restriction by *C. cephus* and AGM tetherins but had only a mild effect on human tetherin (Figure 13A). This indicates that while tetherins from all three species are functional, the Vpu proteins of HIV-1 and SIVmus display a species-specific antagonism of tetherin, which corroborates previous findings (78). Furthermore, I found that HIV-1 Vpu resulted in decreased levels of expression of human tetherin but had a minimal effect on *C. cephus* and AGM tetherin levels (Figure 13B). Conversely, SIVmus Vpu decreased the levels of *C. cephus* and AGM tetherins but had little effect on human tetherin (Figure 13B). This result indicates that the mechanism of SIVmus Vpu activity is likely similar to that of HIV-1 Vpu, likely through the degradation of tetherin (78).

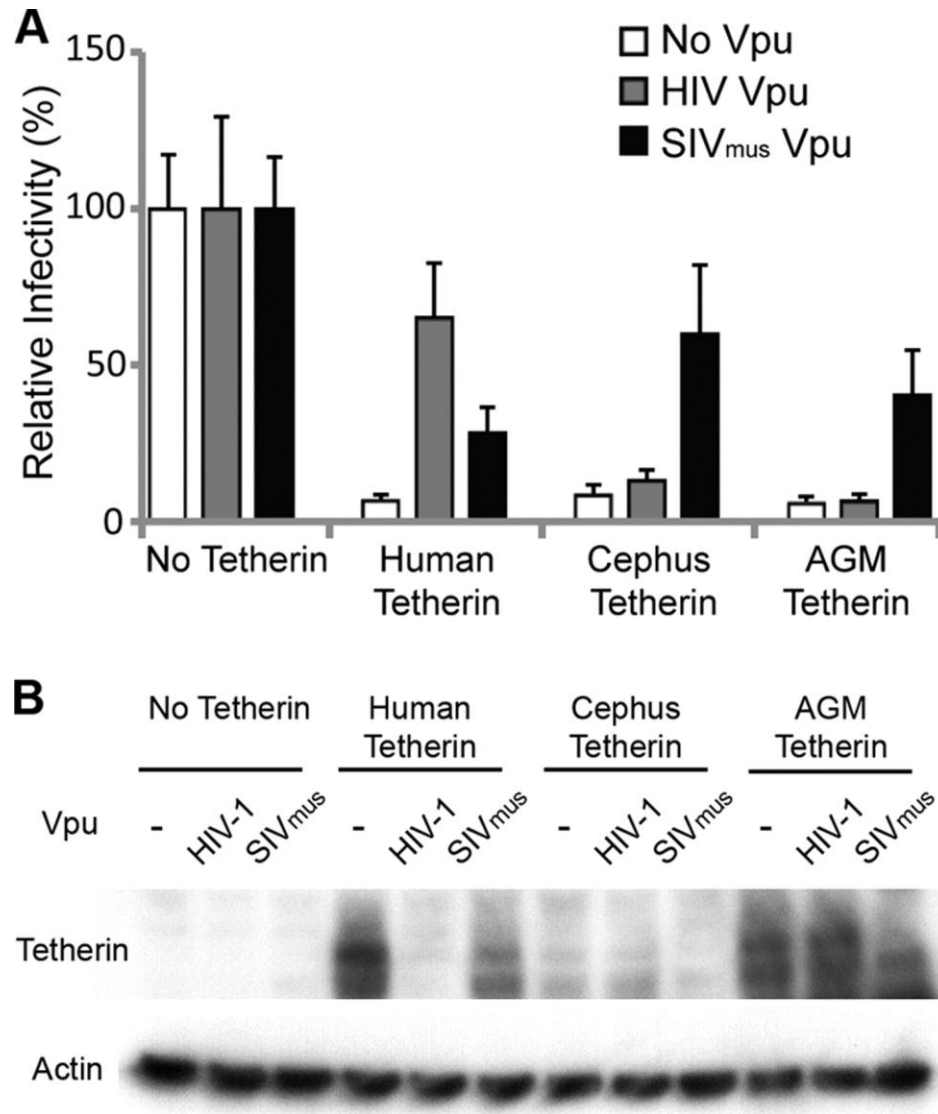


Figure 13

AGM and cephus tetherins restrict HIV1VpuFS and are counteracted by SIV_{mus} Vpu.

(A) 293T cells were cotransfected with HIV1VpuFS (100 ng), human (200 ng), *C. cephus* (Cephus) (400 ng), or AGM tetherin (400 ng); HIV-1 Vpu (125 ng); and SIV_{mus} Vpu (100 ng) for 48 h. The respective empty vectors were used, indicated by no tetherin or no Vpu. Equal amounts of virus-containing supernatant were used to infect TZM-bl reporter cells for 48 h. Relative infectivity was determined by the rate of β -galactosidase activity. Bars represent the average data for eight infections, normalized to the relative infectivity of the respective Vpu proteins in the absence of tetherin. Error bars indicate standard deviations.

(B) 293T cell lysates (A) were collected 48 h after transfection and analyzed by Western blot analysis for HA-tagged tetherin and β -actin expression levels.

SIVagmTan and SIVagmSab are restricted by AGM tetherin and do not encode a tetherin counterdefense.

Since AGM tetherin is able to restrict HIV-1 (Figure 13), I determined whether AGM tetherin could restrict SIVagm. HIV-2, which does not encode a Vpu protein, has Vpu-like activity in its viral envelope (31). Although SIVagm does not encode Vpu, I suspected that the SIVagm envelope protein (Env) or Nef might encode a Vpu-like activity, as seen in HIV-2 and SIVmac/SIVsmm, respectively (31, 109). To test this, I compared the infectivity of SIVagmTan to that of a construct containing a deletion in Env and Nef (SIVagmTan Env⁻ Nef⁻) in the presence of AGM tetherin. SIVagmTan Env⁻ Nef⁻ was pseudotyped by cotransfection with VSV-G to produce infectious virus. Viral constructs and tetherin were cotransfected in 293T cells, and viral production was analyzed in an infectivity assay. As described above, I found that HIV1VpuFS was restricted by both human and AGM tetherins. Surprisingly, I also found that SIVagmTan and SIVagmTan Env⁻ Nef⁻ were restricted by both human and AGM tetherins (Figure 14A, left). This means that unlike HIV-2, SIVagmTan Env does not contain a Vpu-like activity, nor is this activity encoded by the Nef gene. Although both SIVagmTan constructs have a premature stop codon in the Vpr coding region, there was no effect on tetherin restriction when virions were complemented with Vpr from SIVagm or HIV-1 (data not shown).

To verify these findings, I also tested the full-length molecular infectious clone of SIVagmSab against human and AGM tetherins. SIVagmSab is closely related to SIVagmTan and is the most basal taxon of the SIVagm lineage (18, 37). Like SIVagmTan, SIVagmSab does

not encode a Vpu protein (18, 26, 37), and all of the accessory genes of the SIVagmSab clone are intact. I also independently cloned the tetherin gene from primary fibroblasts of *Chlorocebus sabaeus* and found it to be identical to the AGM tetherin that I used previously (data not shown). Strikingly, similar to the findings with SIVagmTan, I also found that a full-length SIVagmSab clone was restricted by both human and AGM tetherins to the same extent as HIV1VpuFS (Figure 14A, right). I also compared the levels of production of cell-free SIVagm virions in the presence of sabaeus monkey tetherin. 293T cells were transfected with SIVagmTan or SIVagmSab in the presence or absence of AGM tetherin. Supernatant fractions containing cell-free virions were filtered and probed with sera obtained from rhesus macaques infected with SIVagmsab92018 (provided by Cristian Apetrei, Tulane National Primate Research Center). There was less cell-free SIVagmTan and SIVagmSab p27 capsid detected in the presence of AGM tetherin (Figure 14B). In contrast, intracellular levels of p55 and p27 were similar regardless of the level of expression of AGM tetherin. Thus, WT SIVagmSab virions are prevented from release in the presence of AGM tetherin. These results indicate that in at least two SIVagm lineages, viral isolates do not encode a viral antagonist against its host tetherin.

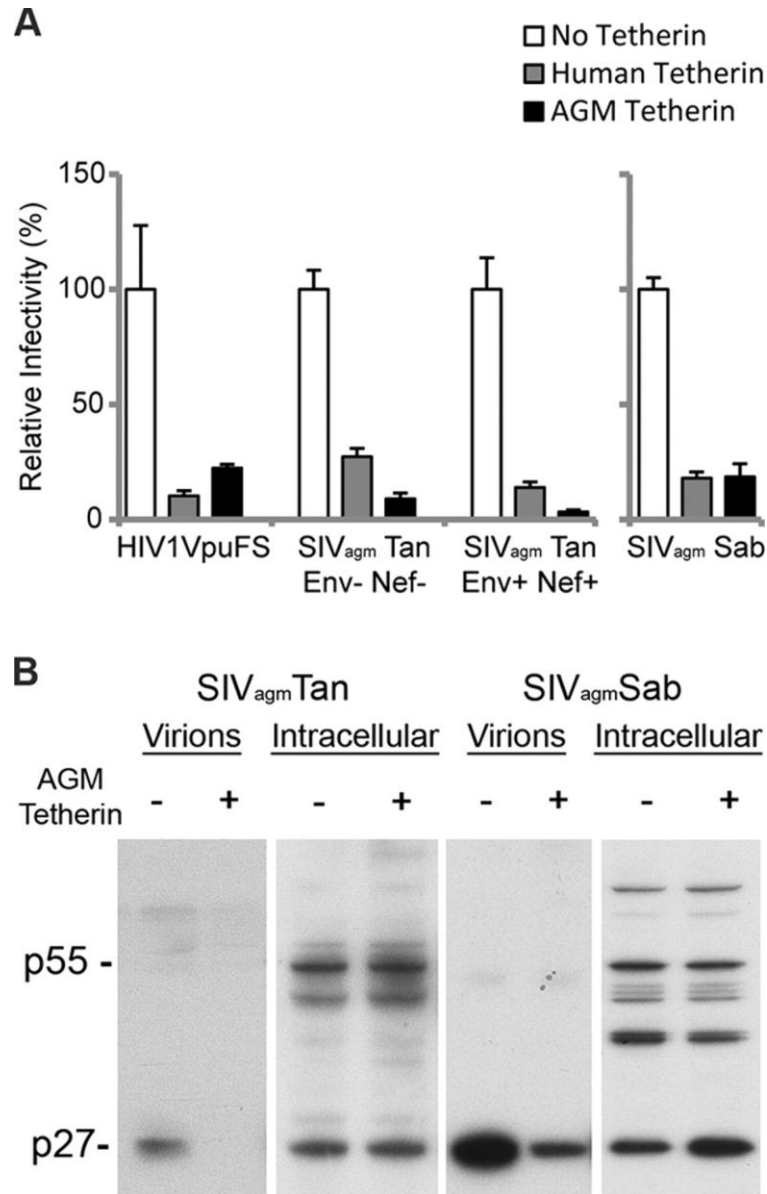


Figure 14

SIV_{agm} does not encode Vpu-like activity.

(A) 293T cells were cotransfected with HIV1VpuFS, SIV_{agm}Tan Env⁻ Nef⁻ (and VSV-G for pseudotyping), SIV_{agm}Tan Env⁺ Nef⁺ (left), or SIV_{agm}Sab (right) and no tetherin (empty vector) or human or AGM tetherin for 48 h. Virus was used to infect TZM-bl reporter cells for 48 h to determine the relative infectivity.

(B) 293T cells were transfected with SIV_{agm}Tan (left) or SIV_{agm}Sab (right) with or without AGM tetherin. Virions from the supernatant were collected and pelleted, while cells were lysed to yield intracellular virions. Western blot analysis was performed to compare the amounts of cell-free virions.

I also examined the fate of SIVagm virions produced in the presence of AGM tetherin by electron microscopy. Human 293T cells were cotransfected with SIVagmSab and AGM tetherins for 48 h and subsequently visualized by thin-section electron microscopy. In the absence of AGM tetherin, SIVagmSab virions were observed to bud from the plasma membrane in a single layer (Figure 15A and B). In the presence of AGM tetherin, we observed that SIVagmSab virions budding from the plasma membrane were markedly tethered together and extended outward in a layered arrangement (Figure 15C and D). Notably, most of the tethered virions were mature, as indicated by the condensed capsid. This indicates that AGM tetherin restricts WT SIVagm virion release by tethering mature virions to the plasma membrane (similar to the effect of human tetherin on Vpu mutant HIV-1 (176)).

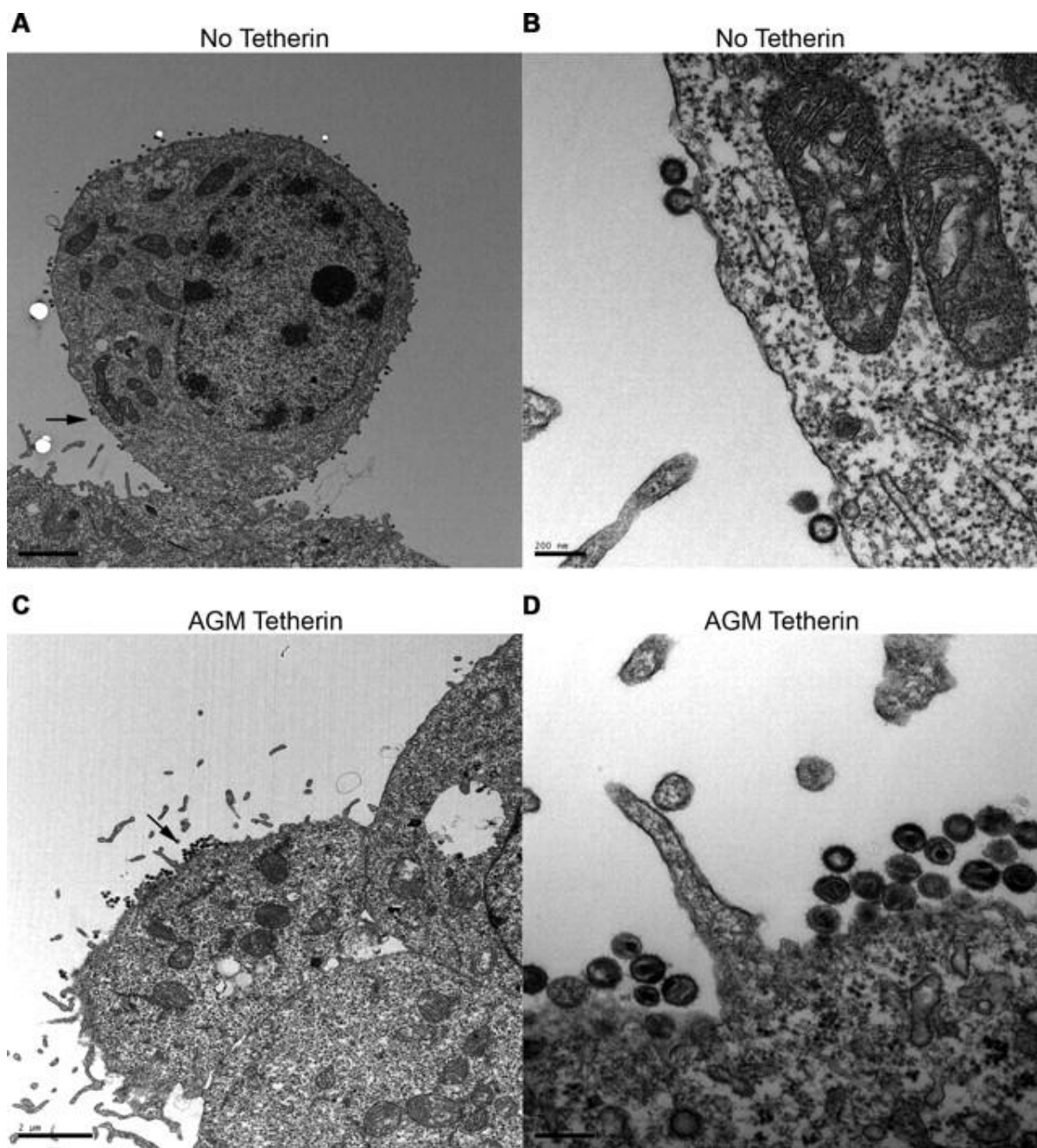


Figure 15

AGM tetherin retains SIV_{agm}Sab on the plasma membrane. Shown is thin-section electron microscopy of 293T cells transfected for 48 h with SIV_{agm}Sab in the absence of AGM tetherin (A and B) or in the presence of AGM tetherin (C and D).

(A) SIV_{agm}Sab budding from the plasma membrane in a single layer in the absence of tetherin. The arrow indicates the location of the magnified image.

(B) Magnified image from A.

(C) Accumulation of budding SIV_{agm}Sab cells on the plasma membrane in the presence of AGM tetherin. Note that mature virions form multiple layers. The arrow indicates the location of the magnified image.

(D) Magnified image of C. Scale bars, 2 μ m (A and C) and 200 nm (B and D).

Since the SIVmac/SIVsmm lineage has evolved Nef to counteract its host and closely related tetherins (109, 315), I directly tested if SIVagmTan Nef had the ability to counteract tetherins from other species. I cloned the Nef gene from SIVagmTan into an expression vector and verified its activity by showing that it could downregulate CD4 levels (data not shown), which is consistent with previously reported findings (234). SIVagmTan Nef was then cotransfected in 293T cells with SIVagmTan Nef; human, chimpanzee, or AGM tetherin; and an HIV-1 construct that had a luciferase gene inserted into the Nef open reading frame and expressed a frameshift mutation in Vpu. The ability of Nef to counteract tetherin was assayed by the infectivity of released virus on SupT1 cells (see Materials and Methods). Consistent with the findings shown in Figure 14, SIVagmTan Nef did not overcome AGM tetherin restriction (Figure 16A). SIVagmTan Nef also did not counteract human tetherin restriction; however, chimpanzee tetherin was antagonized by SIVagmTan Nef. Thus, SIVagmTan Nef has the ability to antagonize other species' tetherin but not its host tetherin.

To verify that the N-terminal HA epitope tag did not interfere with tetherin interactions with viral proteins, we performed a titration of native (untagged) AGM tetherin against WT SIVagmTan and SIVagmTan Env⁻ Nef⁻. Both viruses were pseudotyped with VSV-G, and the relative infectivity was normalized in the absence of tetherin. There was a difference between WT SIVagmTan (Figure 16B) and the mutant virus lacking Env and Nef (Figure 16B) at low levels of AGM tetherin; however, a dramatic restriction was observed at higher levels of tetherin. Importantly, both viruses displayed dose-dependent restriction by AGM tetherin, even at the low levels of tetherin expression (Figure 16B). Since I saw an

effect of WT SIVagm on tetherin only at low levels of tetherin expression, we then directly compared the effects of SIVagmSab Nef, SIVagmTan Nef, and SIVmus Vpu for the ability to counteract AGM tetherin restriction by using the HIV-1 reporter virus lacking Vpu and Nef. Indeed, I found that SIVmus Vpu was able to effectively antagonize AGM tetherin when 100 ng of SIVagm tetherin plasmid was transfected, but the Nef proteins from SIVagmTan and SIVagmSab did not counteract AGM tetherin (Figure 16C). Thus, even if SIVagm Nef genes encode activity against AGM tetherin, the effects are minor compared to those of SIVmus Vpu.

I also complemented HIV1VpuFS and SIVagmTan with SIVmus Vpu. I found that in the presence of SIVmus Vpu, HIV1VpuFS counteracted AGM tetherin restriction. Similarly, SIVagmTan was rescued by SIVmus Vpu to overcome AGM tetherin restriction (Figure 16D). Thus, AGM tetherin retains the ability to be counteracted by SIVmus Vpu, yet the SIVagm lineage does not appear to take advantage of this susceptibility to antagonize tetherin.

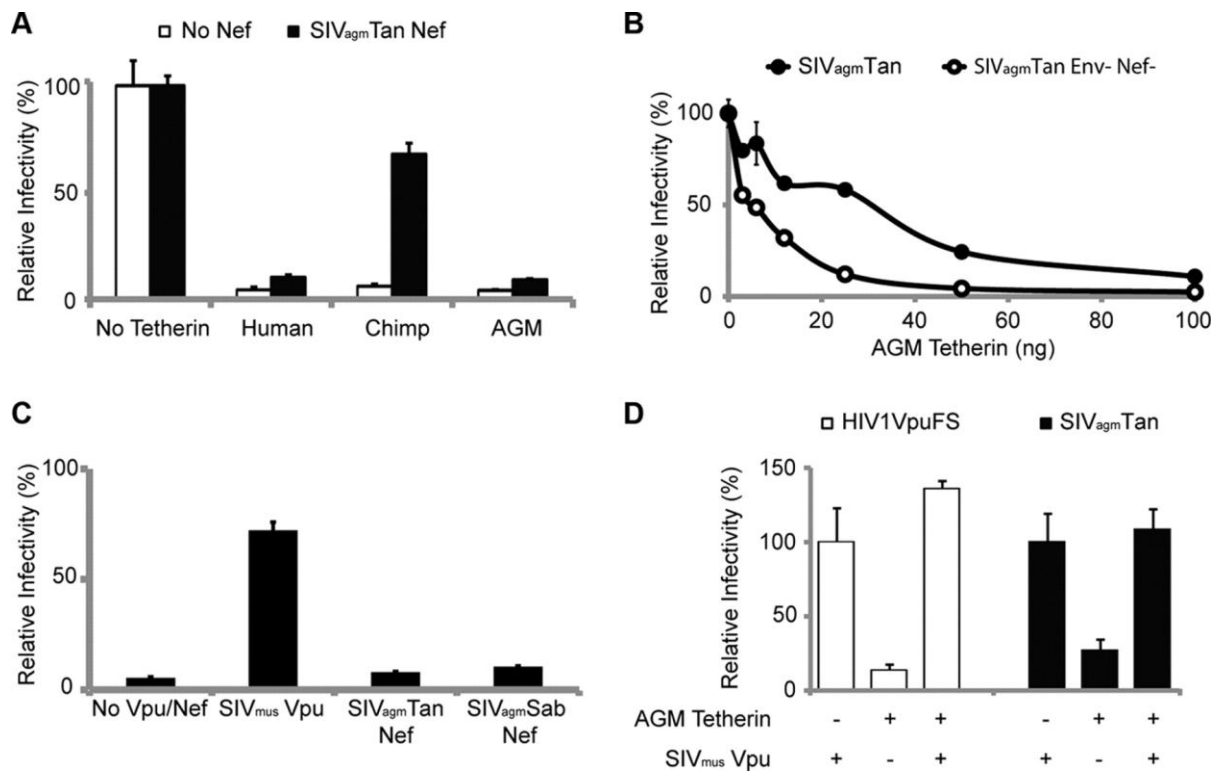


Figure 16

AGM tetherin is not antagonized by SIV_{agm} Nef but retains interface with SIV_{mus} Vpu.

(A) 293T cells were cotransfected with HIV1VpuFSLuc2 (100 ng), SIV_{agm}Tan Nef (250 ng), and human (100 ng), chimpanzee (100 ng), or AGM (100 ng) tetherin. Virus was assayed on SupT1 cells, and relative infectivity was normalized in the absence of tetherin. Bars represent average data for four infections, and error bars indicate standard deviations.

(B) 293T cells were cotransfected with VSV-G and SIV_{agm}Tan (solid circles) or SIV_{agm}Tan Env⁻ Nef⁻ (open circles) with increasing amounts of untagged AGM tetherin (0, 3.12, 6.25, 12.5, 25, 50, and 100 ng). Virus infectivity was assayed on TZM-bl reporter cells, and relative infectivity was normalized in the absence of tetherin. Points represent average data for four infections, and error bars represent standard deviations.

(C) 293T cells were cotransfected with HIV1VpuFSLuc2 (100 ng), AGM tetherin (100 ng), SIV_{mus} Vpu (100 ng), SIV_{agm}Tan Nef (250 ng), or SIV_{agm}Sab Nef (250 ng). Virus was assayed on SupT1 cells, and relative infectivity was normalized in the absence of tetherin. Bars represent average data for four infections, and error bars indicate standard deviations.

(D) 293T cells were cotransfected with HIV1VpuFS or SIV_{agm}Tan, AGM tetherin, and SIV_{mus} Vpu where indicated for 48 h. Virus was added to TZM.bl reporter cells for 48 h, and relative infectivity was determined as described in the legend of Figure 13A, normalized to the respective virus in the absence of tetherin. Bars represent average data for eight readings, and error bars indicate standard deviations.

Type I IFNs induce AGM tetherin.

Human tetherin expression is induced by type I IFN (176, 282). Thus, we considered the possibility that SIVagm has not evolved to inhibit tetherin because tetherin is not induced by IFN in AGM cells. I determined whether endogenous AGM tetherin is induced by IFN and if it is functional and active against SIVagm. Two AGM cell lines, COS-7 (*C. tantalus*) and sabaeus primary fibroblasts (*C. sabaesus*), and human 293T cells were incubated with increasing amounts of type I IFNs: IFN- α 2a or - β 1b (0, 100, and 1,000 IU/ml). Tetherin mRNA expression was measured by RT-PCR of equal amounts of RNA. To ensure that I amplified mRNA and not genomic DNA, primer sets specific to human and AGM tetherins were designed to flank introns. As a control, I measured the expression of β -actin, which is not affected by type I IFNs. Twenty-four hours after exposure to IFN- α 2a or - β 1b, human tetherin mRNA levels were upregulated in 293T cells (Figure 17A, top). Similarly, in both species of AGM cells, AGM tetherin mRNA levels increased 24 h after exposure to IFN- α 2a or - β 1b (Figure 17A, middle and bottom). I conclude that type I IFNs induce AGM tetherin mRNA expression in AGM cells.

Next, I determined if type I IFN induces a tetherin-associated virion retention phenotype in AGM cells. SIVagmTan (pseudotyped with VSV-G) was used to infect AGM COS-7 cells, and 6 h after infection, cells were exposed to 1,000 IU/ml IFN- β 1b for a further 42 h before being fixed for thin-section electron microscopy. Upon exposure to IFN- β 1b, I observed a marked retention of matured SIVagm virions on the plasma membrane of infected AGM cells (Figure 17C), similar to the retention phenotype seen when AGM

tetherin was expressed exogenously (Figure 17C and D). In comparison, virion budding in the absence of type I IFN (Figure 17B) was similar to the phenotype observed in the absence of AGM tetherin (Figure 15A and B). Thus, type I IFN induces a tetherin-associated retention phenotype in AGM cells, which SIVagm is unable to overcome. Although experiments here were not performed using primary peripheral blood mononuclear cells from AGMs, these findings are consistent for primary fibroblasts from AGMs and thus not a result of subspecies specificity or transformed cells.

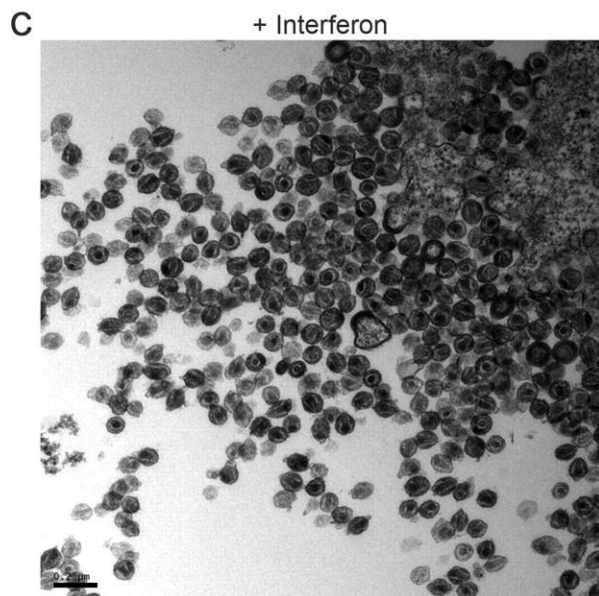
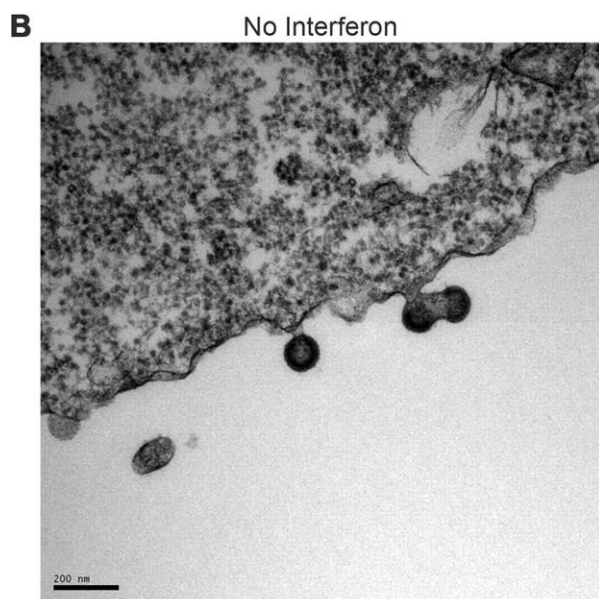
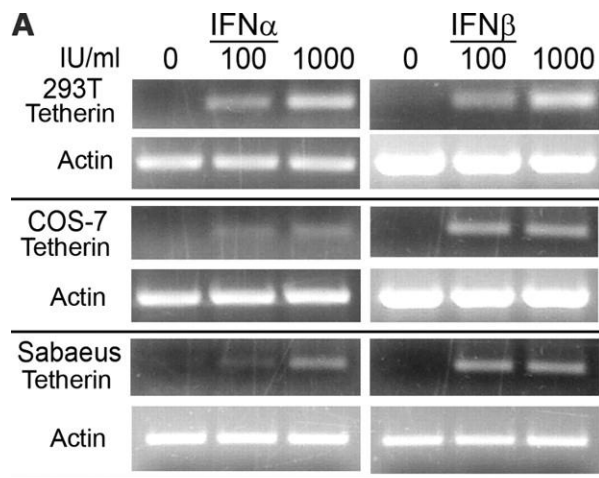


Figure 17

Type I IFNs induce AGM tetherin and the tetherin virion retention phenotype.

(A) 293T (human), COS-7 (AGM), and *C. sabaeus* primary fibroblast (AGM) cells were incubated with 0, 100, or 1,000 IU/ml IFN- α 2a or IFN- β 1b for 24 h. Cells were harvested and lysed for RT-PCR analysis.

(B and C) Thin-section electron microscopy of accumulated SIV_{agm}Tan budding from COS-7 cells exposed to no IFN (B) or 1,000 IU/ml IFN- β 1b

(C). COS-7 cells were infected with VSV-G-pseudotyped SIV_{agm}Tan. Six hours after infection, cells were exposed to 1,000 IU/ml IFN- β 1b and fixed for thin-section electron microscopy after an additional 42 h. Scale bars, 0.2 μ m.

Finally, I verified the restriction of cell-free virus release by endogenous AGM tetherin at lower doses of IFN. The amount of IFN seen in SIVagm-infected AGMs is about 100 to 1,000 IU/ml, peaking at 2,500 IU/ml (54). Therefore, COS-7 cells were infected with equivalent amounts of VSV-G-pseudotyped SIVagmTan or SIVagmTan Env⁻ Nef⁻, and at 6 h postinfection, cells were exposed to increasing amounts of IFN- β 1b (0, 10, and 100 IU/ml). Cell-free virions were compared to cell-associated virions by Western blot analysis. Cell-free SIVagmTan and SIVagmTan Env⁻ Nef⁻ displayed a dose-response decrease upon the addition of 10 and 100 IU/ml IFN regardless of the presence or absence of Env and Nef (Figure 17). Importantly, there was a major effect on viral release at 100 IU/ml. Thus, relatively low levels of IFN are able to induce the tetherin-associated cell-free virus restriction phenotype.

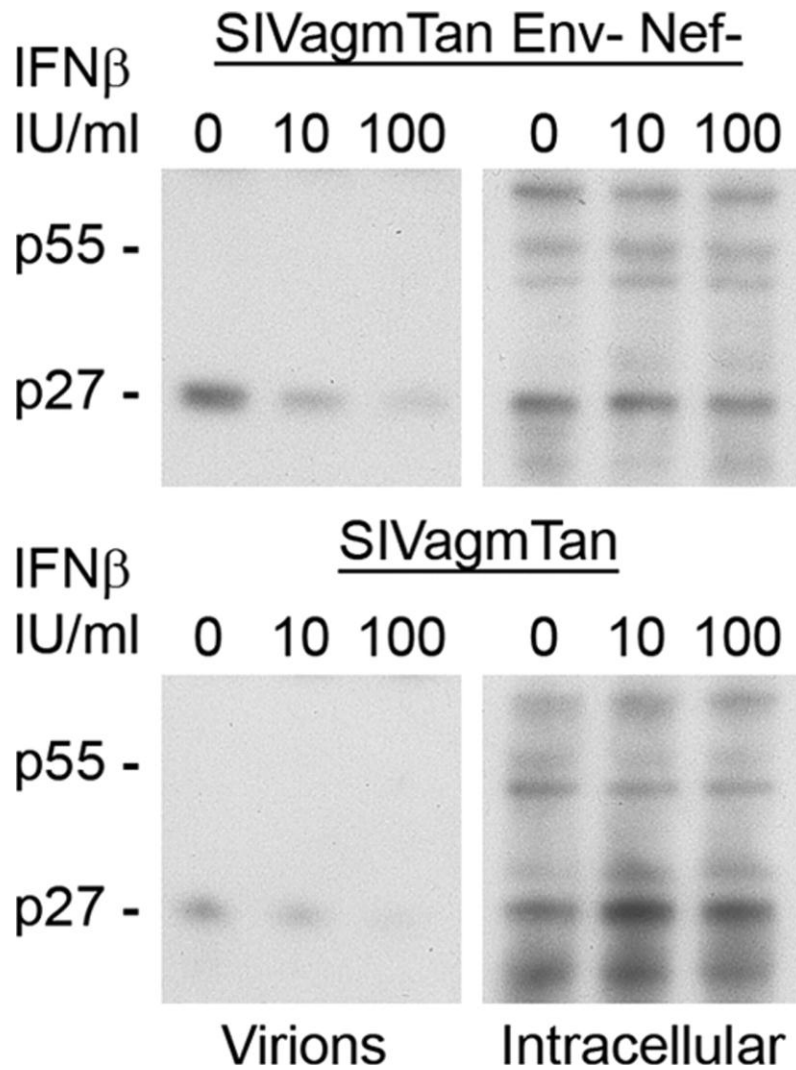


Figure 18

Type I IFNs induce AGM tetherin restriction of virus release.

COS-7 (AGM) cells were infected with VSV-G-pseudotyped SIV_{agm}Tan Env⁻ Nef⁻ (top) or VSV-G-pseudotyped SIV_{agm}Tan (bottom) and exposed to 0, 10, or 100 IU/ml IFN- β 6 h postinfection. Virions from the supernatant were collected and pelleted, while cells were lysed to yield intracellular virions. Western blot analysis was performed to compare the amounts of cell-free virions.

DISCUSSION

Many primate lentiviruses encode a viral antagonist against tetherin, such as Vpu in HIV-1, Env in HIV-2, or Nef in SIVmac/SIVsmm. In contrast, I show here that SIVagm does not encode a major viral antagonist against its AGM host tetherin despite AGM tetherin being functionally active, able to be inhibited by Vpu from SIVmus, and induced by type I IFN. Since tetherin is an IFN-regulated gene (even in AGM cells), we propose that SIVagm has evolved to replicate without inducing an IFN response, thus obviating its need for a virally encoded activity to counteract the antiviral effects of tetherin.

Primates naturally infected with their own species of lentiviruses can have a nonpathogenic outcome. In AGMs and other primates naturally infected with SIV, such as sooty mangabeys (SIVsmm), viral replication can reach high titers in the blood (54, 85, 152). However, these primates do not develop AIDS-like symptoms and often have nonpathogenic outcomes. A hallmark of these nonpathogenic SIV infections is the lack of chronic immune activation. In SIVagm-infected AGMs, IFN- α levels in plasma peak 8 days postinfection and quickly recede to undetectable levels by 35 days postinfection (54). The transient immune response correlates with the peak and decrease in plasma viral loads, after which the viral load stabilizes at a set level. The decrease in plasma viral loads observed after the production of type I IFN is consistent with evidence that antiviral factors such as tetherin are induced. Needless to say, the effects of other concurrent cellular responses, such as cytotoxic T lymphocytes, on the decrease in viral titer cannot be discounted.

While the manuscript was under review, Zhang et al. showed that SIVagm Nef had an effect against AGM tetherin (315). I observed that at low levels of AGM tetherin, WT SIVagmTan was more infectious than SIVagmTan Env⁻ Nef⁻ (Figure 16B). However, the effect of SIVagm Nef is minor compared to that of SIVmus Vpu (Figure 16C). For example, SIVmus Vpu counteracts even high levels of tetherin, whereas SIVagm Nef and/or Env had only a two- to threefold effect at low levels of AGM tetherin. When I looked at endogenous levels of AGM tetherin induced by IFN, I observed a restriction of WT SIVagmTan even at low levels of IFN (Figure 17C and Figure 18). Since SIVagmTan Nef can counteract chimpanzee tetherin, SIVagm Tan Nef has the ability to antagonize other species' tetherins but not its host tetherin (Figure 16A). Sequence differences between chimpanzee tetherin and AGM tetherin point to an evolution of AGM tetherin that has resulted in the inability of SIVagmTan Nef to recognize target sequences within AGM tetherin. Therefore, although SIVagm Nef has an effect at low levels of AGM tetherin, we believe that the activity is insufficient to overcome endogenous levels during the course of acute infection.

Host cellular environment determines the role of viral antagonists

The host cellular immune environment directly impacts virus replication. Likewise, IFN modulation can alter the outcome of viral infections. First, viruses can be capable of actively inhibiting the production of type I IFN. An example is the Ebola virus IFN antagonist VP35. VP35 inhibits the transcriptional activation of the IFN regulatory factor 3 promoter, essentially blocking the host from initiating an IFN response (20). Second, hosts can evolve

to decrease their immune response to specific viral agonists, such as the polymorphisms of IFN regulatory factor 7 in sooty mangabeys, which result in attenuated type I IFN production when SIVsmm engages Toll-like receptor 7 or Toll-like receptor 9 (152). To date, there is no evidence that the lack of chronic IFN production during SIVagm infection of AGMs is due to either a virally directed or host-adapted response. Nonetheless, given that the stealth replication of SIVagm does not induce chronic immune activation, we expect that tetherin would not be constantly induced. Thus, SIVagm would not need Vpu activity to counteract tetherin (, left). Collectively, retroviruses that do not encounter tetherin during their replication lack the selective pressure to maintain “Vpu” activity

Conversely, the host cellular immune status allows us to predict whether viruses encode a viral antagonist of tetherin. SIVmac-infected rhesus macaques and HIV-1-infected humans often display AIDS-like symptoms. These hosts maintain chronically elevated IFN production levels throughout infection (152). As a result, overt viral replication occurs in an environment of chronic tetherin induction. This creates a need for these lentiviruses to acquire and maintain the ability to counteract tetherin restriction, as depicted by Vpu of HIV-1 (, right). In the same manner, SIVmac/SIVsmm has adapted Nef to act as a viral counterdefense against tetherin (109, 315). In conclusion, lentiviral replication in an environment of chronic innate immune responses may distinguish pathogenic from nonpathogenic infections (152), and this may subsequently play an important role in determining the viral factors that arose evolutionarily to counteract factors such as tetherin that are induced by such responses.

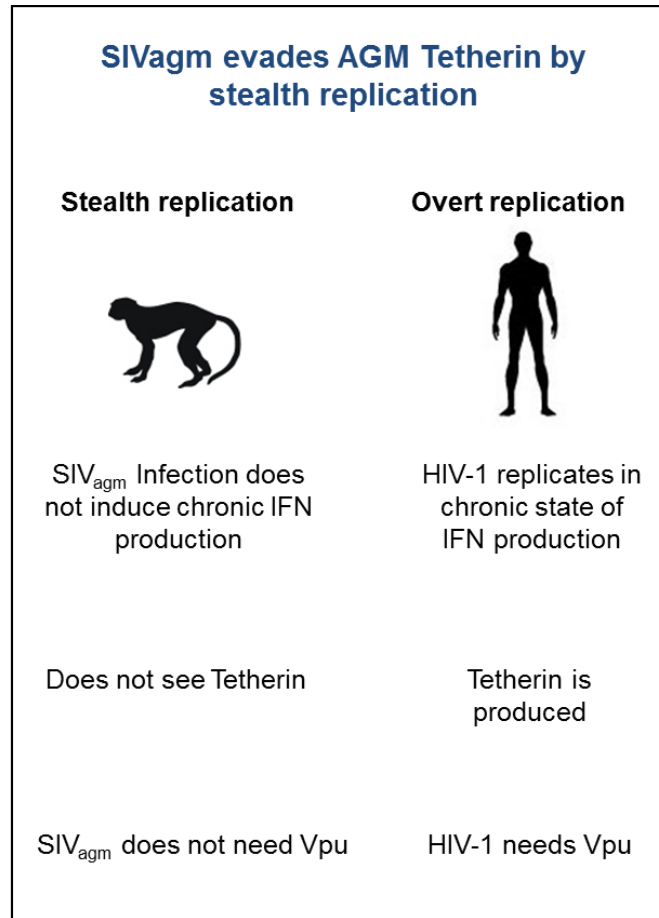


Figure 19

Schematic summary of host-virus consequences in non-pathogenic (left) and pathogenic (right) infections of HIV/SIV.

CHAPTER FOUR

Ancient Adaptive Evolution of Tetherin Shaped the Functions of Vpu and Nef in Human Immunodeficiency Virus and Primate Lentiviruses

SUMMARY

Tetherin/BST-2 is a host-encoded protein that restricts a wide diversity of viruses at the stage of virion release. However, viruses have evolved antagonists of Tetherin, including the Vpu and Nef proteins of primate lentiviruses. Like other host genes subject to viral antagonism, primate Tetherin genes have evolved under positive selection. I show here that viral antagonists acting at three independent sites of selection have driven the evolution of Tetherin, with the strongest selective pressure on the cytoplasmic tail domain. Human Tetherin is unique among the Tetherins of simian primates in that it has a 5-amino-acid deletion that results in the loss of the residue under the strongest positive selection. I show that this residue at amino acid 17 is the site of the functional interaction of Tetherin with Nef, since single amino acid substitutions at this single position can determine the susceptibility of Tetherin to Nef antagonism. While the simian immunodeficiency viruses SIVcpz and SIVgor are able to antagonize their hosts' Tetherin with Nef, human immunodeficiency virus type 1 (HIV-1) Vpu has evolved to counteract Tetherin in humans. I mapped the adaptations in the N-terminal transmembrane domain of Vpu that allow it to counteract human Tetherin. Our combined evolutionary and functional studies have

allowed us to reconstruct the host-pathogen interactions that have shaped Tetherin and its lentivirus-encoded antagonists.

BACKGROUND

Humans and other primates encode a wide repertoire of proteins that intrinsically inhibit retroviral infections (300). Tetherin, also known as BST-2 or CD317, is an example of such an intrinsic antiviral protein that inhibits virus release by anchoring in the envelope of budding virions and directly tethering virions to the plasma membrane (199). This relatively nonspecific antiviral mechanism allows Tetherin to potentially restrict a wide array of viruses, including HIV and other primate lentiviruses (116, 119, 144, 176, 222, 282).

A characteristic of host antiviral factors is that they often result in viruses evolving antagonists to counteract restriction. Indeed, viruses have evolved multiple independent antagonists to counteract Tetherin (reviewed in reference (273)). For example, HIV-1 encodes a Vpu protein that potentially antagonizes human Tetherin (176, 282) through interactions with the transmembrane domain of Tetherin, leading to its degradation via β -TrCP (55, 79, 88, 153, 163, 168, 220). However, Vpu is exclusive to HIV-1 and a specific lineage of primate lentiviruses including the simian immunodeficiency virus SIVcpz, the precursor of HIV-1, and the closely related SIVgor (46, 151, 267, 284). Primate lentiviruses that do not encode Vpu, such as SIVmac and SIVsm, instead use Nef to antagonize Tetherin (109, 315). HIV-2, which does not encode Vpu, encodes an antagonist of Tetherin in its envelope (31, 134). Viruses other than primate lentiviruses have also evolved antagonists of

Tetherin. These include Ebola virus, which antagonizes Tetherin through its glycoprotein (GP) (119), and Kaposi's sarcoma-associated herpesvirus (KSHV), which is able to counteract Tetherin with its K5 protein (156).

While the consensus is that tetherin potently restricts the release of cell-free nascent virus particles, there is debate over its implication for cell-transmission. Several studies suggest that cell-to-cell transmission of HIV-1 is unaffected by tetherin or even enhanced in some instances (45, 112). On the other hand, there is evidence that the aggregation of virion particles at virological synapses by tetherin are unable to transfer efficiently and thus inhibits cell-to-cell transmission (37, 129). Nonetheless, the independent acquisitions of a viral tetherin antagonist by multiple viruses emphasize the role of tetherin and the strong selective pressure imposed by its potent restriction.

Two previous studies using a set of primate sequences primarily from Old World monkeys (OWM) and hominoids found that *tetherin* has evolved under positive selection (88, 163). Here I examine all three lineages of simian primates (including the New World monkeys [NWM]) with a larger data set that allows us to determine which part of *tetherin* has been under the strongest positive selection during specific periods in primate evolution. I find that during simian primate evolution, three separate types of antagonists have shaped *tetherin*, specifically the cytoplasmic tail of Tetherin, with distinct amino acid residues evolving rapidly in New World monkeys versus Old World monkeys and hominoids. Changes in the amino acid under the strongest positive selection correspond exactly to the specificity of Nef.

Consistent with ongoing selective pressure on *tetherin* genes, I show that both SIVcpz Nef and SIVgor Nef are potent antagonists of chimpanzee and gorilla Tetherins but are unable to antagonize human Tetherin. Conversely, the Vpu proteins of SIVcpz and SIVgor are unable to antagonize Tetherin, while this function has been gained by HIV-1 type M strains. While this article was in preparation, similar results were published by Sauter et al. (229) and Yang et al. (307). I demonstrate that the site of Nef interaction in the cytoplasmic domain of Tetherin is under the strongest selective pressure in hominoids and Old World monkeys. However, a deletion covering this site is fixed in human *tetherin*. Therefore, cross-species transmission of HIV-1 to humans necessitated a gain of function by Vpu through adaptations in two regions within the N-terminal transmembrane domain of Vpu in order for the virus to downregulate Tetherin and escape its antiviral effects.

Our combined evolutionary and functional studies allow us to reconstruct the host-pathogen interactions that have shaped Tetherin as well as two antagonists encoded by lentiviruses. We propose that the Nef interaction interface of Tetherin was subject to strong positive selection in primates but that this interaction domain was completely lost in the human lineage, potentially to escape antagonism by an ancient Nef-like factor. Subsequently, a modern lentivirus adapted to grow in humans by neofunctionalization of Vpu through evolving changes in the N terminus of Vpu.

RESULTS

SIVcpz and SIVgor use a Tetherin antagonist different from that of HIV-1 type M strains.

HIV-1 Vpu potentially antagonizes Tetherin, whereas SIVmac or SIVsm does not encode a Vpu protein and instead uses Nef to antagonize Tetherin (109, 176). In order to understand the evolutionary pressures on both viral antagonists and on hominoid Tetherin, I tested the capabilities of Vpu and Nef from multiple strains of HIV-1, SIVcpz (the precursor virus of HIV-1), and the closely related SIVgor for antagonistic activity against Tetherin from their own host species. 293T cells were used for my experiments, because they express very small endogenous amounts of human Tetherin (176). 293T cells were cotransfected with an HIV-1 reporter virus lacking Vpu and Nef, along with constant amounts of different Vpu or Nef constructs, and increasing amounts of plasmids encoding different *tetherin* genes. The release of the infectious HIV-1 reporter virus was assayed by infecting SupT1 cells as previously described (144).

Consistent with previous observations, I found that human Tetherin potentially inhibits virus release and that this restriction is effectively antagonized by Vpu but not by Nef proteins from either the Lai (clade B) or the Q23-17 (clade A) strain of HIV-1, even at high levels of Tetherin (Figure 20A, compare filled circles with open circles). In contrast, chimpanzee Tetherin is antagonized by Nef, but not at all by Vpu, from SIVcpzTan3.1 and only very slightly by Vpu from SIVcpzUS (Figure 20B). The potency of Nef antagonism differs between SIVcpz strains; SIVcpzTan3.1 Nef did not antagonize chimpanzee Tetherin as efficiently as did SIVcpzUS Nef. Nonetheless, Nef is the primary antagonist in SIVcpz (Figure 20B, compare open circles with filled circles). As with SIVcpz, SIVgor Nef, but not SIVgor Vpu, is a potent antagonist of gorilla Tetherin (Figure 20C, compare open circles with filled circles). Although SIVcpz and SIVgor Vpu proteins were poorly active against their respective

hosts' Tetherins, they were still able to downregulate the levels of human CD4 expression efficiently (Figure 20D). These results demonstrate that primate lentiviruses have selectively evolved antagonists against their hosts' Tetherins. SIVcpz and SIVgor use Nef as a potent antagonist against Tetherin, whereas HIV-1 accomplishes that task with Vpu. Similar results have recently been reported by others (229, 307).

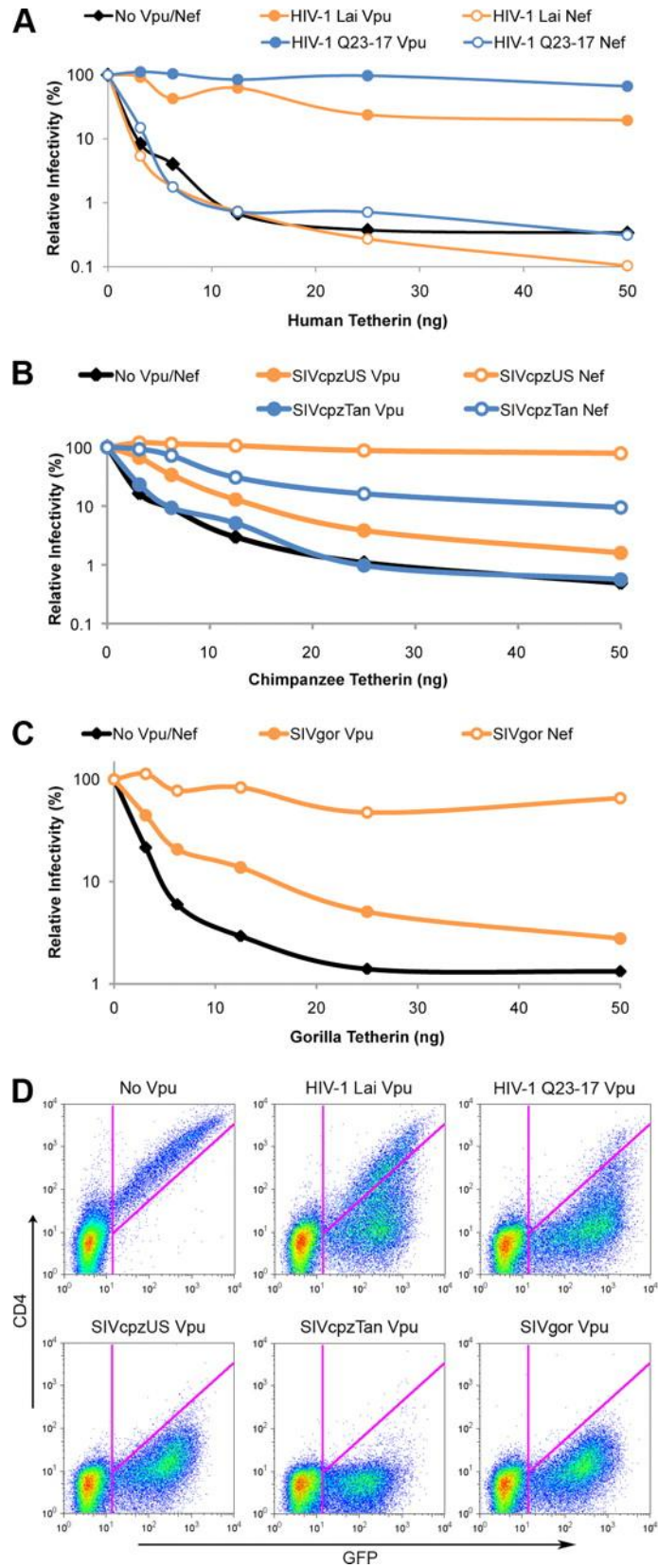


Figure 20

HIV-1 Vpu, SIVcpz Nef, and SIVgor Nef are potent antagonists of their hosts' Tetherins.

(A) Viral infectivity assay of an HIV-1 Δ Vpu Δ Nef reporter virus (HIV1VpuFSLuc2) released into the supernatant, with increasing amounts of untagged human Tetherin (0, 3.125, 6.25, 12.5, 25, and 50 ng) in the presence of either 25 ng Vpu (filled circles) or 25 ng Nef (open circles) from HIV-1 strain Lai (orange) or Q23-17 (blue). The relative infectivity was normalized to the viral infectivity when the respective Vpu/Nef was expressed in the absence of Tetherin.

(B) Native chimpanzee Tetherin was titrated in the presence of either 25 ng Vpu (filled circles) or 25 ng Nef (open circles) from strain SIVcpzUS (orange) or SIVcpzTan3.1 (blue).

(C) Native gorilla Tetherin was titrated in the presence of either 25 ng Vpu (filled circles) or 25 ng Nef (open circles) from SIVgor.


(D) 293T cells were cotransfected with a bicistronic vector expressing human CD4 and enhanced GFP (eGFP) and the indicated Vpu constructs. Cells were stained (with APC) for CD4 expression and were analyzed by flow cytometry. GFP-positive events were gated, and the percentages of CD4-positive event counts in the presence versus the absence of the indicated Vpu constructs were compared.

Species-specific antagonism of SIVcpz and SIVgor Nef.

To determine the specificity of Tetherin antagonists in the event of cross-species transmission, I tested a panel of Vpu and Nef proteins from HIV-1, SIVcpz, and SIVgor against human, chimpanzee, and gorilla Tetherins by using an infectivity assay as a measure of viral release (Figure 21A). The relative infectivity of the released virus was also plotted on a radar chart in order to visualize the ability of Vpu (Figure 21B) or Nef (Figure 21C) to counteract each species' Tetherin. HIV-1 Vpu potently antagonized human, chimpanzee, and gorilla Tetherins (Figure 21A, blue) while HIV-1 Nef was inactive (Figure 21B, blue). However, Vpu encoded by SIVcpz or SIVgor could not antagonize the Tetherins of closely related species (Figure 21A, red and green). Nef encoded by SIVcpz or SIVgor was able to counteract both chimpanzee and gorilla Tetherins but not human Tetherin (Figure 21B, red and green). These results show that differences between human Tetherin, on the one hand, and chimpanzee and gorilla Tetherins, on the other, have determined the landscape of species-specific antagonism by SIVcpz and SIVgor Nef proteins.

A

Relative Infectivity (%): 0 100



	No Tetherin	Human	Chimp	Gorilla
No Vpu/Nef	100	2.8	3.2	5.1
HIV-1 Lai Vpu	100	170.4	139.8	126.4
HIV-1 Q23-17 Vpu	100	87.2	102.5	111.9
HIV-1 Lai Nef	100	2.7	4.0	2.4
HIV-1 Q23-17 Nef	100	5.2	8.6	5.9
SIVcpzUS Vpu	100	3.6	4.7	3.5
SIVcpzTan Vpu	100	1.9	1.8	7.5
SIVcpzUS Nef	100	1.1	115.9	74.0
SIVcpzTan Nef	100	4.1	77.3	44.5
SIVgor Vpu	100	2.7	5.4	9.4
SIVgor Nef	100	2.1	129.3	118.2

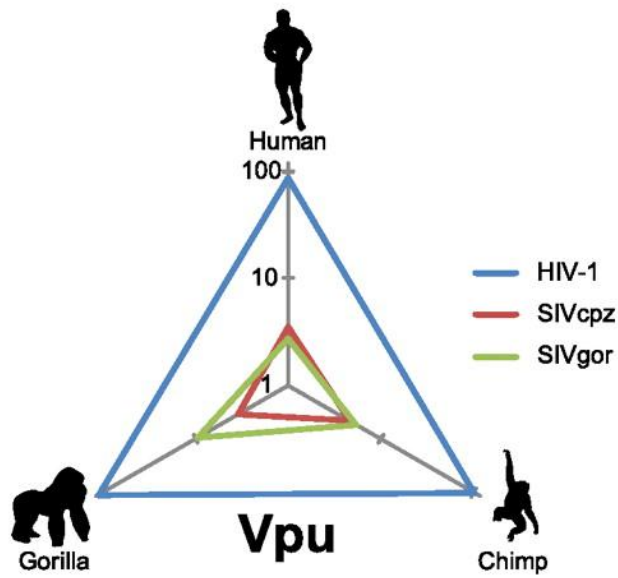
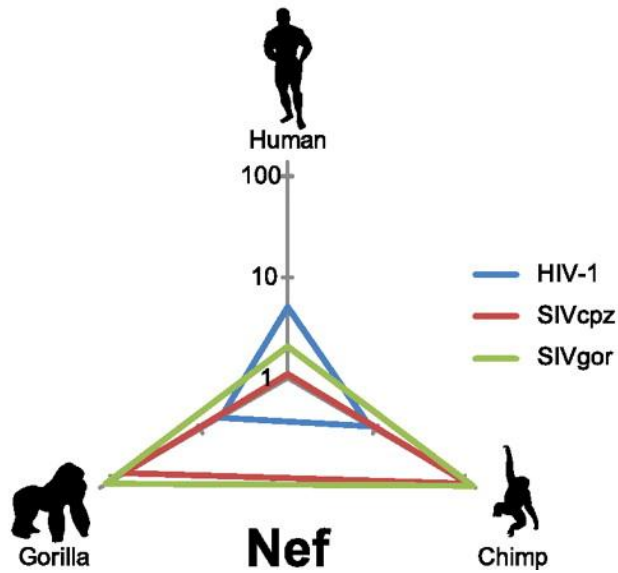
B**C**

Figure 21

Species-specific antagonism by HIV-1, SIVcpz, and SIVgor viral antagonists.

(A) Heat map of Vpu/Nef antagonism of human, chimpanzee, and gorilla Tetherins. The infectivity of an HIV-1 Δ Vpu Δ Nef reporter virus released into the supernatant (normalized to that in the absence of Tetherin) was assayed in the presence of human (25 ng), chimpanzee (25 ng), or gorilla (25 ng) Tetherin (columns) and of the indicated Vpu/Nef construct (rows). The percentages in each column indicate the infectivity of the virus relative to that in the absence of exogenous Tetherin (first column). (B and C) The results for HIV-1 Q23-17, SIVcpzUS, and SIVgor are plotted on radar charts.

(B) Relative infectivity (expressed as a percentage) of an HIV-1 Δ Vpu Δ Nef reporter virus released into the supernatant in the presence of human, chimpanzee, or gorilla Tetherin, as indicated, and of Vpu from HIV-1 Lai (blue), SIVcpzUS (red), or SIVgor (green).

(C) Relative infectivity (expressed as a percentage) of an HIV-1 Δ Vpu Δ Nef reporter virus released into the supernatant in the presence of human, chimpanzee, or gorilla Tetherin, as indicated, and of Nef from HIV-1 Lai (blue), SIVcpzUS (red), or SIVgor (green).

Positive selection in primate Tetherin.

Tetherin has a unique topology consisting of an N-terminal cytoplasmic tail, a transmembrane domain, and a coiled-coil domain followed by a C-terminal glycosylphosphatidylinositol (GPI) anchor (131, 199). Previous findings have demonstrated that the cytoplasmic tail domain of Tetherin harbors the sites of interaction with SIVsm Nef, while HIV-1 Vpu interacts with the transmembrane domain of Tetherin (88, 109, 163). Although recent studies have shown that *tetherin* has evolved under positive selection among primates (88, 163), both of these studies had a limited diversity of sequences in their data sets; hence, they lacked the power to detect which part of *tetherin* was under the strongest positive selection and, therefore, which viral antagonist has exerted the most selective pressure during primate evolution. Thus, I sequenced the *tetherin* coding sequence (approximately 555 bp) from 20 primate genomes representing 33 million years of evolution, including 7 hominoids, 8 Old World monkeys (OWM), and 5 New World monkeys (NWM). The phylogeny constructed from the primate *tetherin* sequences was congruent with the generally accepted primate phylogeny (213), confirming that the sequences are orthologous (Figure 23). There was no evidence of recombination as ascertained by a GARD analysis (127). Using a maximum-likelihood approach with CODEML from the PAML suite of programs (308), I compared the likelihood of *tetherin* evolution under models that disallowed (NSsites model 7) or permitted (NSsites model 8) positive selection. In agreement with previous studies, I found that *tetherin* had evolved under positive selection (Figure 22A). To determine the selective pressures across the different primate lineages, I performed a free ratio analysis of primate *tetherin* that allows for

variation in the ω (dN/dS) ratios for each lineage. Several branches of the phylogeny, mainly the branches leading up to the New World monkeys, Old World monkeys, and hominoids, showed dN/dS ratios of >1 (Figure 23), suggesting an ancient positive selection in primate lineages.

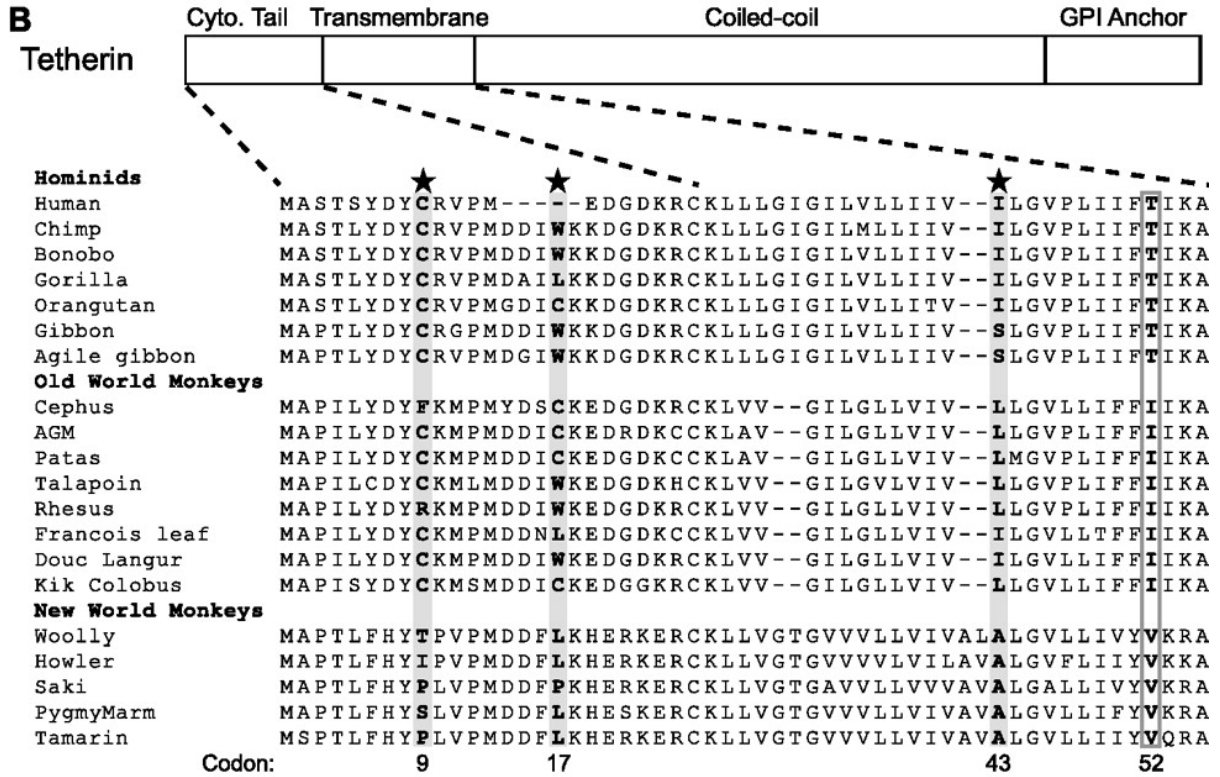
To determine which domains are responsible for the signatures of positive selection, I performed PAML analyses on the separate domains of *tetherin*: the cytoplasmic tail domain (aa 1 to 25), the transmembrane domain (aa 26 to 53), and the remaining extracellular domains, consisting of the coiled-coil domain and the GPI anchor (aa 54 to 185). I found that the cytoplasmic tail and transmembrane domains have evolved under positive selection, whereas the extracellular domains have not (Figure 22A).

Next, I sought to identify the specific residues that have been subjected to positive selection. Three amino acid residues (codons 9, 17, and 43) were found to evolve under positive selection with strong confidence (posterior probability, >0.95) as determined by PAML (Figure 22B and C). This was confirmed by random-effect likelihood (REL) analyses (Figure 22D) (126). Previous analyses have suggested that a number of additional residues within Tetherin's cytoplasmic tail and transmembrane domain have evolved under positive selection, although the statistical power of those studies was hampered by a small data set (88, 163). However, we find no detectable signal for positive selection when we omit residues 9, 17, and 43 of primate Tetherin (Figure 22E). Therefore, the use of the more-extensive sequence divergence in our data set allows us to conclude that only three codons (residues 9, 17, and 43) of Tetherin display evidence of recurrent positive selection in the

primates. Residue 9 evolved rapidly primarily in the NWM lineage (although some OWM also are divergent at this position) but is highly conserved in hominoids. Indeed, NWM Tetherins primarily display a signature of positive selection at residue 9, whereas OWM and hominoid Tetherins display a signature of positive selection at residues 17 and 43 instead. Importantly, we find that residue 52 (the boxed isoleucine in boldface in Figure 22B), which is critical for resistance against HIV-1 Vpu (88), has not evolved under positive selection (Bayes factor, 17.3).

A Likelihood ratio test statistics for models of variable selective pressure among sites

Tetherin Region Analyzed	2lnλ	df	p-Value
Full gene (aa 1-185)	7.0	2	<0.05
Cytoplasmic tail (aa 1-25)	12.5	2	<0.002
Transmembrane (aa 26-53)	14.5	2	<0.001
Extracellular domains (aa 54-185)	0.01	2	>0.99(NS)



C Codons under positive selection in PAML analysis of Tetherin from all primates (excluding humans)

Codon	dN/dS	p-Value
9	5.06	>0.99
17	5.07	>0.99
43	4.96	>0.97

D REL analysis of Tetherin whole gene

Codon	dN/dS	Bayes Factor
9	3.48	185.7
17	3.70	2426.2
43	1.17	90.3
52	0.20	17.3

E Analysis of sites under positive selection in Tetherin

Tetherin	2lnλ	df	p-Value
All primates	7.0	2	<0.05
All primates (- human)	18.0	2	<0.001
All primates (- human) Δ 17, 43	3.3	2	>0.19 (NS)
All primates (- human) Δ 9, 17, 43	0.02	2	>0.88 (NS)

Figure 22

Tetherin was under strong positive selection in the cytoplasmic tail domain.

(A) Likelihood ratio tests were used to determine if any codons were associated with dN/dS ratios significantly greater than 1 (hence under positive selection). Neutral models (M7) were compared to selection models (M8) under the F61 model of codon substitution. Similar results were obtained in a comparison of M1 (neutral) versus M2 (selection) (data not shown).

(B) An alignment of the cytoplasmic tail and transmembrane domains of Tetherins from the 20 primates used in the analyses is shown, with three positively selected codons (codons 9, 17, and 43) shaded (indicated by stars); these were identified by PAML and REL as being subjected to positive selection with high posterior probabilities ($P, >0.95$). Codon 52, which is critical for resistance against HIV-1 Vpu but was not identified as evolving under positive selection, is boxed.

(C) PAML omits regions that have deletions in the alignment from the analysis. Therefore, PAML analyses were repeated without human *tetherin*. Codons with a posterior probability of >95% were highlighted in a PAML analysis of *tetherin* genes from all primates, excluding humans.

(D) Summary of the REL analysis of whole *tetherin* genes from 20 primates. Sites displaying positive selection signals with a significance (Bayes factor) greater than 50 (codons 9, 17, and 43) are shown in boldface. Codon 52, which did not meet the cutoff, is included for reference.

(E) Likelihood ratio tests were performed between the M7 (neutral) and M8 (selection) models for the full *tetherin* gene, without human *tetherin*, or without human *tetherin* and with amino acids 9, 17, and 43 omitted from the alignment.

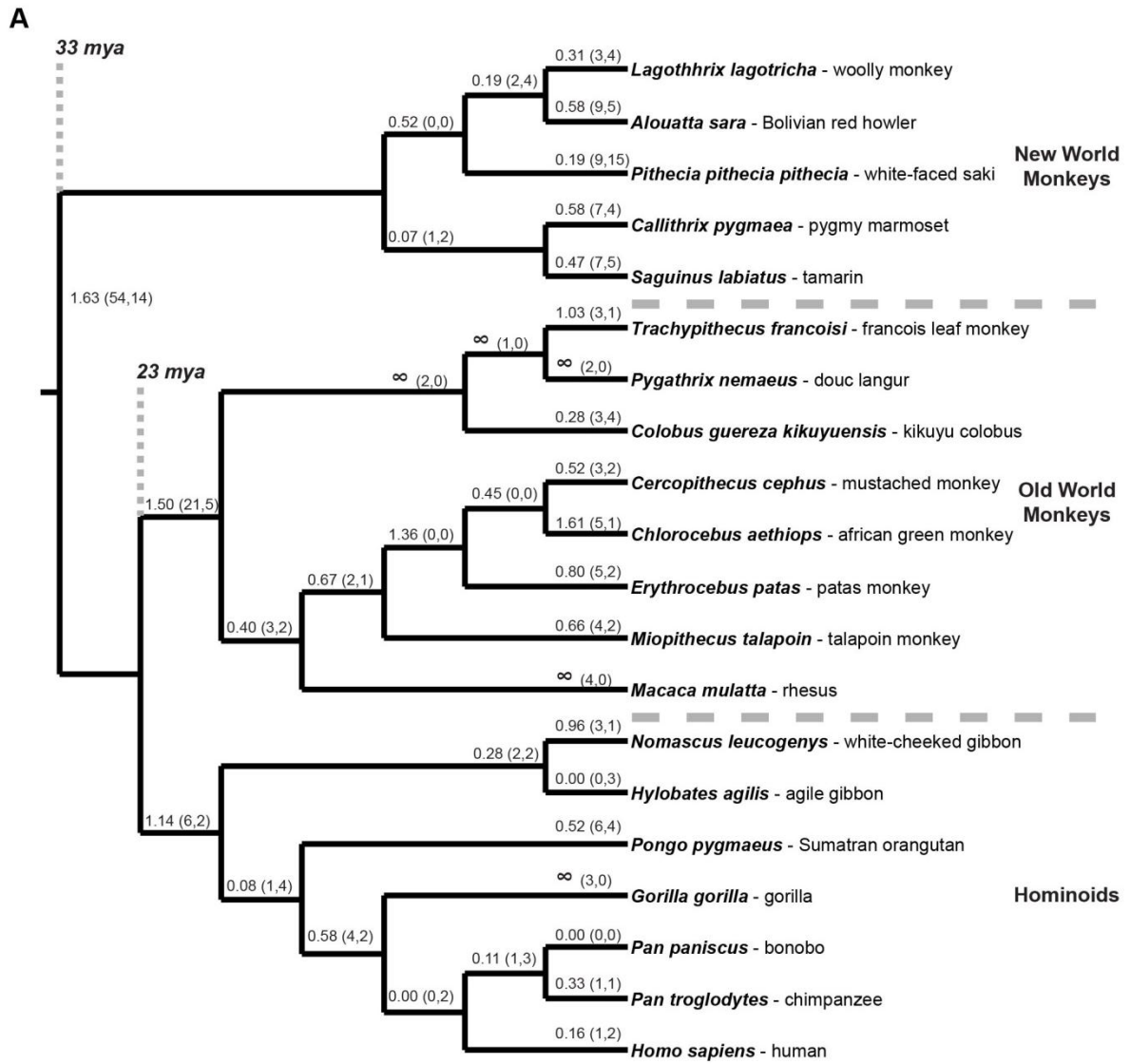


Figure 23

Ancient positive selection of primate *tetherins*.

(A) *Tetherin* from 20 primates were sequenced, representing 33 million years of evolutionary divergence. The global ratios of non-synonymous changes (dN) / synonymous changes (dS) by a free-ratio model that allows dN/dS to vary along individual branches. The dN/dS ratios are indicated at the nodes, the number of non-synonymous changes and synonymous changes are indicated in parenthesis, respectively.

Positive selection of *tetherin* was driven by Nef-like antagonism.

Residue 17, which lies within the cytoplasmic tail domain, shows the strongest recurrent signature of positive selection during primate evolution (Figure 22D). Previous work has shown that amino acids in this part of Tetherin are important for the ability of Nef to antagonize Tetherin (109, 315). Thus, I wanted to determine if changes at this single position, amino acid 17, are responsible for the species specificity of Nef. To do this, I analyzed the specificity of Nef against Tetherins from different species that differ at amino acid 17.

I have shown previously that although SIVagm is unable to effectively antagonize endogenous levels of African green monkey (AGM) Tetherin, SIVagm Nef can potentially antagonize chimpanzee Tetherin (Chapter four, (144)). Importantly, chimpanzee and AGM Tetherins differ at residue 17, which is a cysteine in AGM and a tryptophan in chimpanzees. I altered residue 17 in AGM Tetherin from cysteine (as encoded in AGMs) to tryptophan (as encoded in chimpanzees) and tested it against SIVagm Nef (Figure 24A). Both AGM Tetherin constructs were able to inhibit virus release and were potentially antagonized by SIVmus Vpu, as previously shown (Chapter four, (144)). Although SIVagm Nef had a minor effect against AGM Tetherin, a single substitution at residue 17 (AGM C17W) conferred a dramatic susceptibility to SIVagm Nef antagonism (Figure 24A, right).

Next, to determine if changes in residue 17 could confer resistance against current SIV Nef antagonists, I performed a reciprocal mutation of residue 17 in chimpanzee Tetherin from tryptophan (as encoded in chimpanzees) to cysteine (as encoded in AGMs) and tested

it against SIVcpz Nef. Both chimpanzee Tetherin constructs potentially inhibited virus release and were potentially antagonized by HIV Vpu. However, although SIVcpz Nef potentially antagonized chimpanzee Tetherin, the construct with the single substitution at residue 17 (Chimp W17C) displayed markedly increased resistance to SIVcpz Nef antagonism (B, right). These results demonstrate that the exact amino acid under positive selection in Tetherin is the determinant for Nef antagonism.

The congruence of the 5-amino-acid deletion in human Tetherin with the site that displayed the highest degree of adaptation in other primates suggests that the deletion was itself driven by the need to escape antagonism by a Nef-like factor early in the human lineage. To test this hypothesis, I reconstructed human Tetherin as it likely existed prior to the deletion event (Figure 24C, Anc. Human) (the DDIWK deletion was restored, and the glutamine, the amino acid following the deletion, was replaced with a lysine) and tested a panel of primate lentiviral Vpu and Nef proteins against it. The ancestral human Tetherin effectively restricted virus release but was antagonized by HIV-1 Vpu. However, the ancestral human Tetherin was antagonized by Nef proteins from SIVcpz and SIVgor, whereas the extant human Tetherin (after the deletion) was resistant to both Nef proteins (Figure 24C). I also introduced the same 5-amino-acid deletion into chimpanzee Tetherin (Chimp Δ DDIWK) and found that the deletion conferred resistance against SIVcpz Nef (Figure 24B). Therefore, I conclude that an ancient Nef-like factor likely drove both the positive selection of residue 17 in the cytoplasmic tail domain of Tetherin in simian primates and the deletion of this residue in humans.

Amino acid 43 in the transmembrane region is also under positive selection, albeit the signal is much weaker than that for amino acid 17 (Figure 22D). Because the determinants for the action of HIV-1 Vpu on Tetherin lie in the transmembrane region of Tetherin (88, 163, 220), we wanted to determine whether amino acid 43 was driven to positive selection by Vpu. To do this, we chose to examine *C. cephus* and Francois' leaf monkey (FLM) Tetherins, which differ at amino acid 43 by an isoleucine-to-leucine change (Figure 24B). Human, *C. cephus*, and FLM Tetherins were able to potently restrict virus release (Figure 24D, left). HIV-1 Vpu was not able to antagonize either *C. cephus* (Chapter four, (144)) or FLM (data not shown) Tetherin, consistent with an inability of HIV-1 Vpu to antagonize Tetherin from other Old World monkeys (144, 229, 307). Likewise, the Vpu from SIVmus was unable to antagonize human Tetherin (Figure 24D, right). However, SIVmus Vpu could antagonize both *C. cephus* and FLM Tetherins equally well (Figure 24D, right). This indicates that, in contrast to my findings for Nef (or a Nef-like factor), Vpu has not driven positive selection either in hominoids or in Old World monkeys.

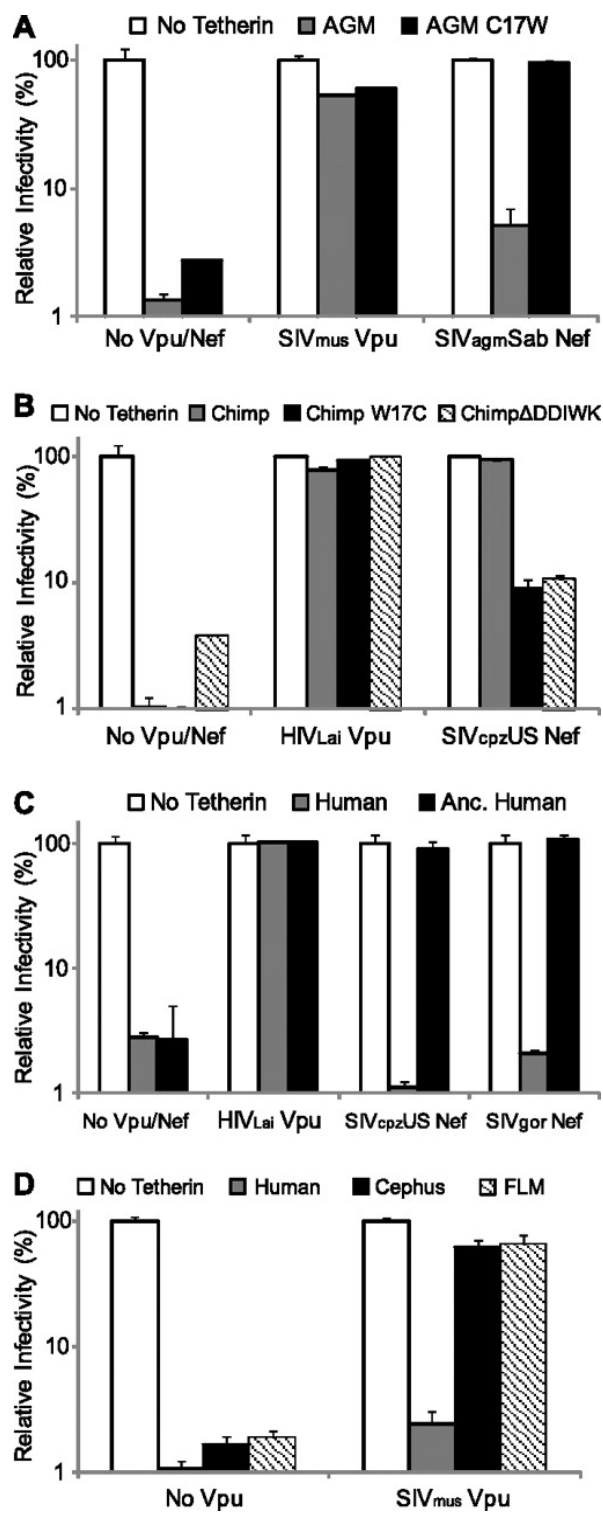


Figure 24

An amino acid under selection in the cytoplasmic tail of Tetherin explains the specificity of Nef.

Shown are results of assays to determine the infectivity of an HIV-1 Δ Vpu Δ Nef reporter virus released into the supernatant. The relative infectivity was normalized to the viral infectivity obtained when the indicated Vpu/Nef protein was expressed in the absence of Tetherin. Error bars indicate standard deviations.

(A) Infectivity was assayed either in the absence of Tetherin (open bars) or in the presence of AGM (shaded bars) or AGM C17W (filled bars) Tetherin and in the presence of the indicated Vpu or Nef construct.

(B) Infectivity was assayed either in the absence of Tetherin (open bars) or in the presence of chimpanzee Tetherin (shaded bars), chimpanzee W17C Tetherin (filled bars), or Chimp Δ DDIWK Tetherin (hatched bars).

(C) Infectivity was assayed either in the absence of Tetherin (open bars) or in the presence of human Tetherin (shaded bars) or ancestral human Tetherin (filled bars) and in the presence of the indicated Vpu or Nef construct.

(D) Infectivity was assayed either in the absence of Tetherin (open bars) or in the presence of human Tetherin (shaded bars), *C. cephus* Tetherin (filled bars), or Francois' leaf monkey (FLM) Tetherin (hatched bars) and either without Vpu or with SIVmus Vpu. The “ancestral” human Tetherin is the human Tetherin with the amino acids DDIWK restored in place of the deletion, and with the E following this deletion replaced with a K (Figure 22).

The transmembrane domain of Vpu determines Tetherin antagonism activity.

Since HIV-1 Vpu, but not SIVcpz Vpu, is a potent antagonist against Tetherin (Figure 21A), I sought to determine how the Vpu protein of HIV-1 type M might have evolved in order to antagonize human Tetherin. I constructed a panel of chimeric proteins between HIV-1 and SIVcpz Vpu (Figure 25A, left). The chimeric Vpu proteins were all expressed at similar levels in transfected cells (Figure 25A, right).

I found that although full-length SIVcpz Vpu was unable to counteract human Tetherin, substitution of the N-terminal transmembrane domain from HIV-1 Vpu for that of SIVcpz Vpu conferred the ability to counteract Tetherin (Figure 25B). This was specific to the transmembrane domain of Vpu, since substitution of the cytoplasmic domain (α -helix) leading up to the β -TrCP binding motif (DSGxxS) was insufficient to rescue the restriction phenotype (data not shown). Two regions in the transmembrane domain of Vpu were necessary for Tetherin antagonism activity: amino acids 1 to 8 and amino acids 14 to 22. Replacement of either region alone was insufficient to counteract Tetherin [Figure 25B, HIV(1-8) and HIV(14-22)]. Further chimeras within each region yielded intermediate phenotypes, suggesting that these regions harbored several minor determinants (data not shown). More importantly, SIVcpz Vpu was able to completely rescue the Tetherin restriction phenotype when it encoded both regions 1-8 and 14-22 from HIV (Figure 25B).

The ability of each Vpu to antagonize Tetherin function correlated with an effect on Tetherin expression on the cell surface (282) in a cotransfection experiment (Figure 25C). However, here, it is clear that there is a threshold effect, since each of the Vpu proteins has

some effect on cell surface Tetherin levels, but those that rescue virus infectivity (Figure 25B) are more effective than those that do not (Figure 25C). As a control, I examined each of the chimeric proteins for its ability to downregulate the expression of human CD4 on the cell surface (Figure 25D). All the chimeric Vpu proteins (including the singly substituted 1-8 or 14-22 region of HIV-1 in SIVcpz [Figure 25D]) effectively downregulated CD4 expression, consistent with the evidence that the ability of Vpu to modulate CD4 levels is separable from its viral release activity (238). Thus, adaptations in two regions within the N-terminal transmembrane domain conferred on HIV-1 Vpu the specific ability to antagonize Tetherin.

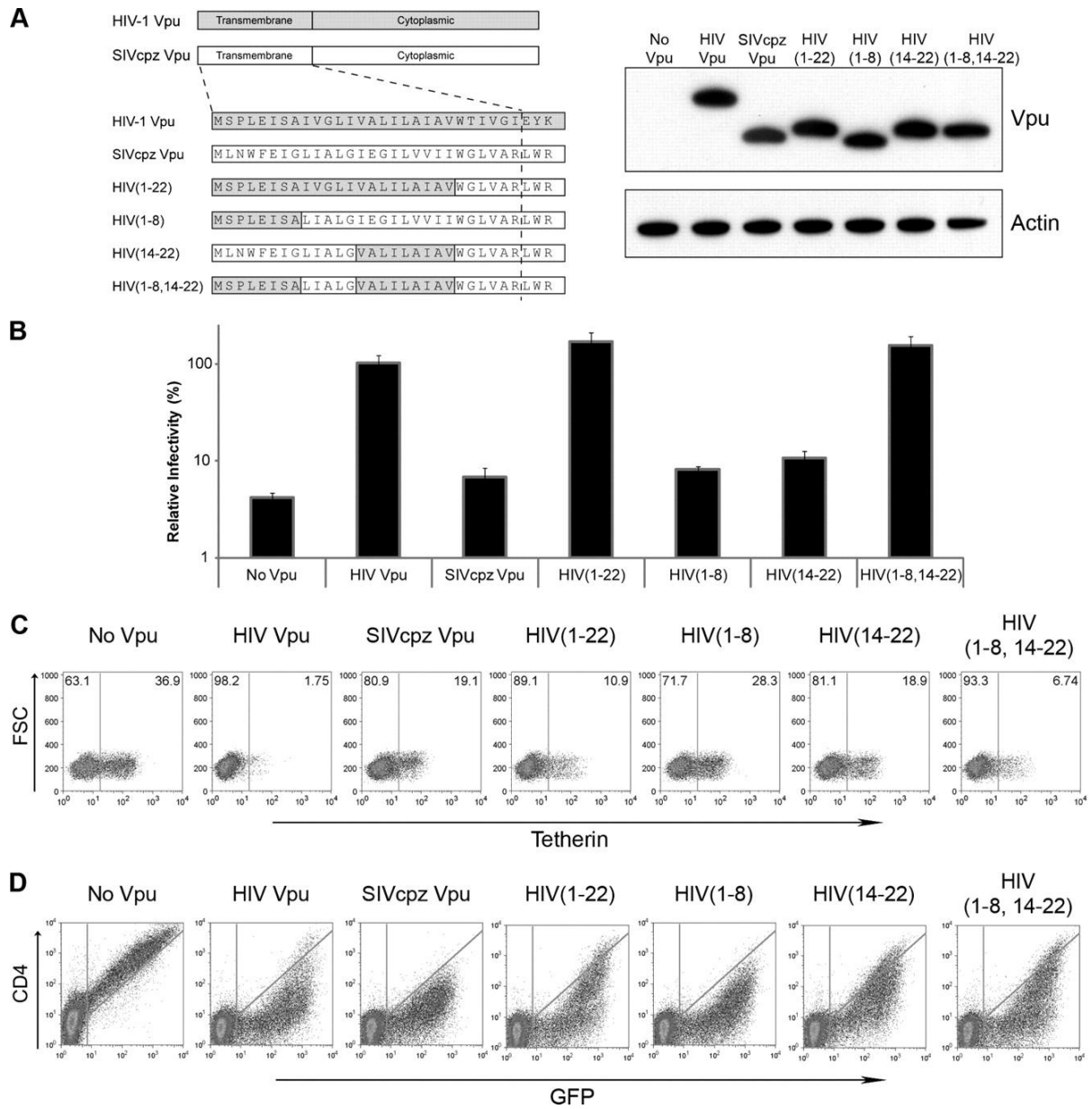


Figure 25

The N-terminal transmembrane domain of Vpu confers Tetherin antagonism activity.

(A) (Left) Alignment of the N-terminal transmembrane domains of the chimeric Vpu constructs between HIV-1 strain Q23-17 (shaded areas) and strain SIVcpzUS (open areas). (Right) Expression of chimeric Vpu constructs. Western blot analysis was performed to determine the expression levels of C-terminally HA epitope-tagged Vpu and β -actin.

(B) Assay of the infectivity of an HIV-1 Δ Vpu Δ Nef reporter virus (HIV1VpuFSLuc2) in the presence of human Tetherin (25 ng) and native Vpu proteins (untagged) as indicated.

(C) Expression of Tetherin on the cell surface as determined by flow cytometry in the presence or absence of different native Vpu proteins (untagged). Forward scatter is shown along the y axis, and Tetherin (detected with an FITC-labeled secondary antibody) is shown along the x axis. The solid line represents gating, determined by using untransfected 293T cells as controls, and the percentage of cells expressing cell surface Tetherin is given on the upper right.

(D) Flow cytometric analysis of 293T cells cotransfected with a bicistronic vector (expressing human CD4 and eGFP) and the indicated native Vpu constructs (untagged). GFP-positive events were gated, and the percentages of CD4-positive (APC-labeled) event counts in the presence or absence of the indicated Vpu constructs were compared.

Since the difference between the abilities of HIV-1 Vpu and one strain of SIVcpz Vpu to antagonize human Tetherin mapped to two regions of the transmembrane domain, I next examined how likely it was that other strains of SIVcpz Vpu might also encode HIV-1-like activity. Thus, I compared an alignment of Vpu proteins from multiple strains of SIVcpz against the Vpu from HIV-1 group M strains. In contrast to the highly conserved transmembrane domain of HIV-1 group M Vpu, the N-terminal transmembrane domain was divergent across SIVcpz strains, as might be expected based on their more ancient divergence (Figure 26). Although none of the Vpu proteins of SIVcpz strains were identical to the consensus Vpu of HIV-1 group M, among several strains of SIVcpz (LB7, CAM5, EK505, and MB66) that include the closest relatives of HIV-1 group M (120), the SIVcpz strain LB7 would be predicted to require seven minimal adaptations within the two critical regions of Vpu (amino acids 1 to 8 and 14 to 22) in order to gain the ability to antagonize human Tetherin.

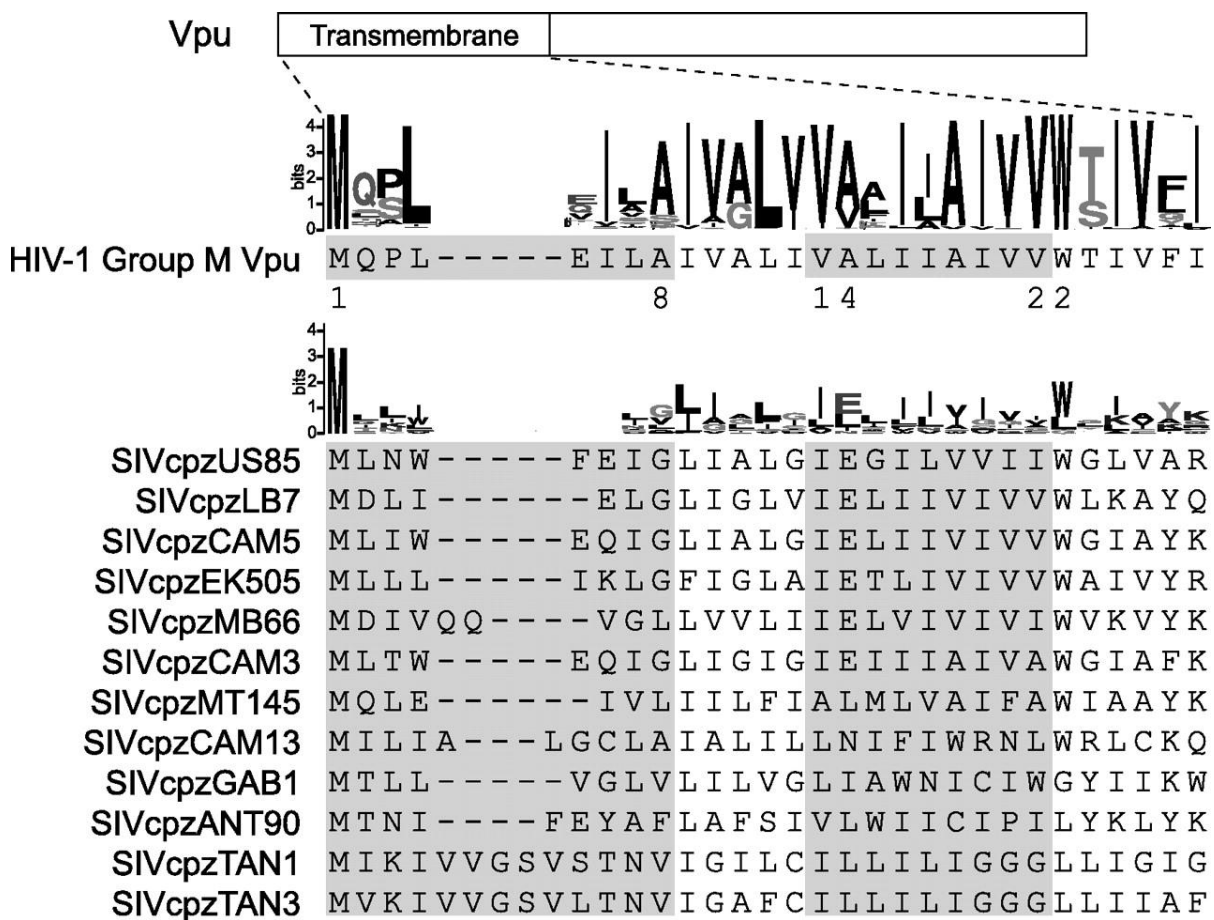


Figure 26

The N-terminal transmembrane domain of SIVcpz Vpu is divergent from that of the highly conserved HIV-1 Vpu.

Shown is an alignment of the consensus sequence for the N-terminal transmembrane domain (aa 1 to 28) of HIV-1 group M Vpu with the transmembrane domains of Vpu proteins from SIVcpz strains. Sequence logos were plotted from 1,271 sequences of HIV-1 group M Vpu (top) and from the indicated SIVcpz strains (bottom). The two regions important for Tetherin antagonism activity (aa 1 to 8 and aa 14 to 22) are shaded.

DISCUSSION

Host proteins locked in genetic conflict often display signatures of positive selection. Here, we find that *tetherin* has been evolving under positive selection in primates, and the highest recurrent signal of positive selection during primate evolution corresponds to the amino acid that is a determinant for Nef, but not Vpu, antagonism of Tetherin. Chimpanzee and gorilla Tetherins are antagonized by SIVcpz Nef and SIVgor Nef but not by the Vpu proteins encoded by these two viruses. However, because of a unique 5-amino-acid deletion in the cytoplasmic tail domain of human Tetherin that eliminates the site under the greatest positive selection in *tetherin*, the cross-species transmission of SIVcpz to humans involved the evolution of Vpu to counteract human Tetherin through adaptations in two regions of the N-terminal transmembrane region of HIV-1 Vpu.

Our study differed from previous analyses of positive selection on Tetherin (88, 163, 188) in having less intraspecies sampling but more sampling of deeper, interspecies divergences. Our conclusions differ qualitatively from those reached previously. In particular, because of the increased statistical power of our data set, we can rule out any significant contribution to the positive selection of Tetherin outside of residues 9, 17, and 43. Intriguingly, this signal has not remained uniform among simian primates. New World monkey Tetherin appears to have recurrently evolved at residue 9, which shows some variability among Old World monkeys but is fixed in hominoids. In contrast, residues 17 and 43 appear to be rapidly evolving in Old World monkeys and hominoids but not in New World monkeys. This makes a strong case that mutually exclusive types of antagonists have

shaped Tetherin in the 3 lineages of simian primates. This suggests that an unknown antagonist with a specificity unlike that of Nef or Vpu was the primary driver of Tetherin evolution in New World monkeys. It is somewhat surprising that only three residues have been under positive selection, considering that Tetherin restricts a broad diversity of viruses (116, 119, 144, 176, 222) and that recent work shows that a Tetherin with substantial changes in the transmembrane and coiled-coiled domains can still act to block virus release (199). However, there may be additional constraints on *tetherin* evolution due to some other function of Tetherin (36). In addition, many viruses may have evolved alternative strategies that circumvent Tetherin without necessitating a direct antagonistic interaction. For example, viruses that target induction of the interferon (IFN) pathway (19) might not need to antagonize Tetherin directly if they can prevent its induction following infection.

A single substitution at residue 17 of AGM Tetherin conferred susceptibility to SIVagm Nef, whereas the reciprocal substitution at residue 17 of chimpanzee Tetherin conferred resistance to SIVcpz Nef. Thus, the amino acid under the most intense selective pressure is responsible for both the gain and the loss of antagonism by Nef. These results argue strongly that a Nef-like factor is responsible for the recurrent viral escape from Tetherin during simian primate evolution. By “Nef-like” factor, we mean a viral antagonist with exactly the same specificity toward Tetherin as that of Nef, if not Nef itself. This line of reasoning suggests that more ancient lentiviruses have been in primate populations before the currently known primate lentiviruses (245). This hypothesis is supported by the recent discovery of much older endogenous lentiviruses (75, 76). We cannot, however, rule out the

possibility that unrelated viruses encode a Tetherin antagonist with exactly the same specificity as the Nef from primate lentiviruses.

In contrast to the positive selection observed on amino acid 17 that correlates with Nef function, amino acid 52 in the transmembrane domain, which encodes much of the susceptibility of primate Tetherin to Vpu antagonism (88), is not subject to positive selection (Figure 22B) and indeed is conserved as a isoleucine (in all Old World monkeys) or a threonine (in all hominoids). This is highly reminiscent of residue 128 in APOBEC3G, which encodes its susceptibility to Vif antagonism (28, 236) but was not found to be evolving under positive selection in primates (230). Thus, as with the APOBEC3G-Vif interactions, we argue that Vpu antagonism by recent lentivirus proteins did not drive *tetherin* evolution. We also found no evidence that the single residue under positive selection in the transmembrane domain (amino acid 43) was driven by a factor similar to SIVmus Vpu. These results argue that, unlike the Nef-like factor that drove selection on amino acid 17, Vpu and Vpu-like factors (i.e., factors with the same specificity as modern Vpu proteins) are too recent to have had an effect on *tetherin* evolution.

Human Tetherin is unique among primates due to a 5-amino-acid deletion (including residue 17) in the cytoplasmic tail domain of Tetherin that has been fixed in the human population (NCBI single-nucleotide polymorphism [SNP] database). This deletion was most likely adaptive, since it includes the amino acid under the strongest selective pressure in Old World monkeys and hominoids. It is not clear why a deletion event to escape Nef-like antagonism would occur exclusively in human Tetherin, whereas other primates instead

show adaptive evolution at residue 17. It is possible that this domain also encodes another function in addition to viral restriction, pressure for which was relaxed in the human lineage, or that there was a lack of preexisting SNPs in the human population at the time of selection. Alternatively, simultaneous selective pressure by multiple Nef-like proteins may have driven a deletion instead of an amino acid substitution in human Tetherin.

Due to the unique deletion in the cytoplasmic tail domain of human Tetherin, the Nef protein of the HIV-1 precursor SIVcpz was ineffective as a Tetherin antagonist following cross-species transmission to humans. We propose that as a result of the selective pressure exerted by Tetherin, the precursor virus evolved Vpu to counteract human Tetherin through adaptations in two regions of the N-terminal transmembrane domain of Vpu (Figure 25B). Therefore, the most parsimonious explanation points to sequence variations of Vpu (Figure 26) in SIVcpz that predisposed certain strains to be more adaptable, in particular the strain that gave rise to the pandemic HIV-1 group M. Our findings support and extend the conclusions of Sauter et al., who performed an extensive study of HIV-1 Vpu proteins from groups M, N, and O, and proposed that the ability both to antagonize Tetherin and to degrade CD4 facilitated the pandemic spread of group M HIV-1 (229). I show that gain-of-function antagonism of human Tetherin occurred through adaptations in the N-terminal transmembrane domain of Vpu (Figure 26B). In my characterization, I found that the determinants were situated in two regions. An alignment of Vpu from multiple strains of SIVcpz shows that several strains of SIVcpz (LB7, CAM5, and EK505) would require fewer changes. Furthermore, based on the highly divergent sequences currently available, it is

highly possible that a strain(s) of SIVcpz responsible for the cross-species transmission has yet to be sequenced.

CHAPTER FIVE

The function and evolution of the restriction factor Viperin in primates
was not driven by lentiviruses

SUMMARY

Viperin, also known as *RSAD2*, is an interferon-inducible protein that potently restricts viruses such as influenza, hepatitis C virus, human cytomegalovirus and West Nile virus. Like other host restriction factors that have a broad antiviral range, we find that *viperin* has also been evolving under positive selection in primates. The pattern of positive selection is indicative of Viperin's escape from multiple viral antagonists over the course of primate evolution. Here, we investigate the possibility that Viperin also restricts human immunodeficiency virus and other retroviruses. We find that Viperin is interferon-induced in HIV primary target cells. We show that exogenous expression of Viperin restricts the LAI strain of HIV-1 at the stage of virus release from the cell, and can be partially counteracted by the HIV-encoded Nef protein. However, the effect of Viperin restriction is highly strain-specific and does not affect most HIV-1 strains or other retroviruses tested. Moreover, knockdown of endogenous Viperin in a lymphocytic cell line did not significantly affect the spreading infection of HIV-1. Taken together, these findings indicate that Viperin is not a major restriction factor against HIV-1 and other retroviruses. Therefore, other viral lineages are likely responsible for the evolutionary signatures of positive selection in *viperin* among primates.

INTRODUCTION

Antiviral proteins engaged in virus-host interactions are often locked in evolutionary "arms-races", which have been referred to as "Red Queen" conflicts (286). Viral infections continuously exert immense selective pressures on the host antiviral proteins to evolve adaptively. The signatures of these evolutionary conflicts can be inferred by observing signals of adaptive evolution (also called positive selection) in antiviral genes that result from repeated episodes of Darwinian selection due to past viral infections (59). Often, the exact amino acids under positive selection can describe the sites and domains involved in host-virus interaction (141, 142, 231). Thus, a detailed look at the evolutionary trajectory of an antiviral gene can provide valuable information about the viral pressures that shaped host evolution

Viperin (Virus inhibitory protein, endoplasmic reticulum-associated, interferon-inducible, also known as *RSAD2*) is a host protein with broad antiviral activity (reviewed in (64, 161, 240)). Viperin inhibits the release of a wide range of viruses in cell culture including Influenza A virus (293), Hepatitis C virus (96, 110), and Japanese Encephalitis virus (39). Moreover, *viperin* knockout mice demonstrate the importance of this protein in controlling West Nile Virus pathogenesis in vivo (265). In the case of human cytomegalovirus (HCMV), Viperin has been reported not only to inhibit the expression of late viral gene products (43) but also to enhance HCMV infectivity by remodeling the cellular actin cytoskeleton (241).

The precise mechanism of the broad spectrum antiviral function of Viperin remains unclear. However, one model for Viperin antiviral activity links lipid rafts disruption to the restriction of Influenza virus release (293). Lipid rafts are sphingolipid- and cholesterol-enriched microdomains on the plasma membrane that have also been implicated in a number of processes including membrane signaling, polarization, and immunological synapse function (186, 250). Additionally, lipid rafts also play an important role in the entry and assembly stages of viral replication (162, 186) and the host sterol biosynthesis pathway is downregulated in response to viral infections as part of the innate immune response via type I interferon signaling (27). Viperin has also been shown to directly inhibit farnesyl diphosphate synthetase (FPPS), a cellular enzyme critically involved in the biosynthesis of isoprenoid-derived lipids (293). This suggests that the disruption of cellular lipid raft formation may represent a generalized host defense against viruses.

We find that *viperin*, like other host restriction factors against viruses, has evolved under positive selection in primates. As lipid rafts are thought to be sites of assembly and budding for HIV and other retroviruses (181, 185, 186, 206), we investigated whether Viperin restricts HIV-1 and other retroviruses. We find that Viperin inhibits the release of the LAI strain of HIV-1 and is partially counteracted by Nef. However, we show that HIV-1 and SIV strains have intrinsic differences in their sensitivity to Viperin and most are unaffected by over-expression of Viperin. Furthermore, we did not see an effect of Viperin knockdown on HIV-1 growth. Collectively, our findings suggest that Viperin is not a major restriction factor against HIV-1 and retroviruses, and thus its positive selection must have been driven by other viral pathogens.

RESULTS

Viperin has been evolving under positive selection in primates

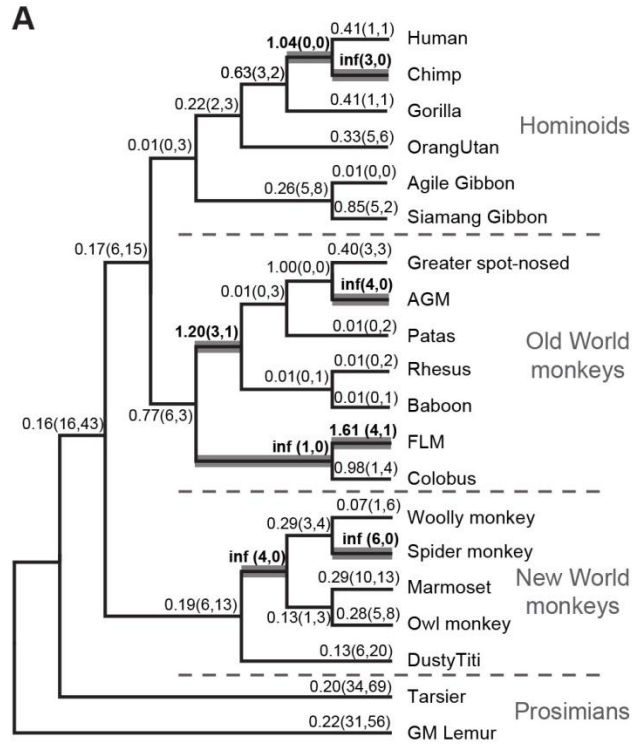
A recurring theme of host restriction factors is that they exhibit a strong signature of positive selection (166). Given the remarkable breadth of viruses restricted by Viperin (43, 110, 161, 240, 293), we hypothesized that *viperin* might also be evolving under positive selection. To investigate this possibility, we sequenced the *viperin* gene from 18 species of primates and obtained 2 sequences of prosimian *viperin* from Genbank (Figure 27A). Together, these primate species span around 60 million years of divergence. The phylogeny constructed from the primate *viperin* sequences was congruent with the generally accepted primate phylogeny (198), confirming that the sequences are orthologous. There was no evidence of recombination as ascertained by a GARD analysis (127).

In order to determine the lineage-specific pressures on the primate *viperin* gene, we performed a free-ratio analysis using the PAML program suite (308), which allows an independent assignment of omega (dN/dS) ratios to each evolutionary branch of the primate phylogeny, where dN/dS ratios > 1 are indicative of positive selection. Several branches of the phylogeny within the New World monkeys, Old World monkeys, and hominoids showed dN/dS ratios > 1 (Figure 27A, bold branches). For instance, the branches leading up to human-chimpanzee common ancestor and African green monkey have dN/dS ratios > 1 , indicative of positive selection. To test whether Viperin was subject to episodic or constant selective pressures over primate evolution, we compared the likelihood ratios of

the free-ratio model (Figure 27B, Model 1) where all branches were allowed to have their own independent dN/dS, versus a model where the entire phylogeny had the same dN/dS value (Figure 27B, Model 0). We found that the free-ratio model fit the data better although this was marginally significant ($p=0.08$). We therefore conclude that primate *viperin* has been ancient, episodic positive selection.

We also performed a maximum likelihood analysis using codeml from the PAML program suite (308) that allows for different dN/dS ratios across individual codons, and found strong evidence that the *viperin* gene has been evolving under positive selection in primates (Figure 27C). In order to determine which domain(s) in Viperin are responsible for the signal of positive selection we examined each domain separately (the N-terminal alpha helix domain, a short middle region, the Radical S-adenosylmethionine (SAM) domain and a flexible C-terminal domain (Figure 27D)). While the N-terminal alpha helix was not under positive selection, the middle region, Radical SAM domain and C-terminal flexible domain showed signs of positive selection with high confidence (Figure 27D). In particular, five amino acid positions stood out with strong signals of positive selection (corresponding to residues 42, 51, 142, 145, 352 in human Viperin). These five amino acid residues were independently confirmed to be under positive selection with strong significance by random-effect likelihood (REL) analyses (data not shown) (126). Importantly, removal of these five amino acids from the analyses resulted in a loss of any statistically significant signals of adaptive evolution (Figure 27C), validating that the majority of the positive selection was acting on these sites. The dispersed nature of these positively selected residues are reminiscent of other broadly acting antiviral genes like Protein Kinase R (PKR), wherein

escape from viral antagonism drives the positive selection of PKR (58). This is in contrast to other rather than restriction factors like TRIM5alpha, where a cluster of positive selectively selected residues identifies the viral specificity domains (231). Therefore, we conclude that *viperin* has evolved under positive selection, likely to escape viral antagonism by a variety of viral lineages over the course of primate evolution.

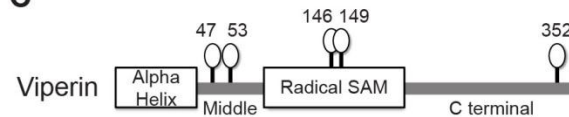


B

Likelihood ratio test statistics for models of variable selective pressure along branches

Viperin	lnl	2lnλ	df	p-value
Model 0 (Same dN/dS ratio for all branches)	-3602.55			
Model 1 (Different dN/dS ratio for each branch)	-3577.75	49.61	37	< 0.081

C



Likelihood ratio test statistics for models of variable selective pressure among sites of Viperin

Viperin	2lnλ	df	p-value
Full gene (aa 1-361)	26.65	2	< 0.001
Full gene (Δ47, 53, 146, 149, 352)	0.56	2	> 0.755 (NS)

D

Viperin region analyzed	2lnλ	df	p-value
Alpha helix (aa 1-43)	0	2	1 (NS)
Middle domain (aa 44-77)	16.34	2	< 0.003
Radical SAM domain (aa 78-262)	7.22	2	< 0.028
C terminal (aa 263-361)	12.07	2	< 0.003

Figure 27

(A) Cladogram of 20 primate *viperin* genes sequenced for the evolutionary analyses. Free ratio analysis in PAML was used to calculate the ω (dN/dS) ratios of individual branches. The corresponding ω ratios are shown above each branch, and the number of non-synonymous changes and synonymous changes are indicated in parentheses. Branches with $\omega > 1$ are highlighted in bold. In the case of no observed synonymous changes, the ω ratio (inf) could not be calculated.

(B) Likelihood ratio test statistics for models of variable selective pressures along branches of primate *viperin* genes are shown, in comparison between M0 (same dN/dS ratio for all branches) and M1 (different dN/dS ratio for each branch).

(C) A schematic of Viperin protein domain structure is shown. Residues under positive selection with high confidence ($P > 0.95$) are indicated in symbols above the protein. The table summarizes the likelihood ratio test statistics for models of variable selective pressure among *viperin* sites (M7 vs M8). Similar results were obtained in a comparison of M1 (neutral) versus M2 (selection) (data not shown). The amino acid positions are annotated in reference to the human Viperin sequence.

(D) The table summarizes likelihood ratio test statistics performed between the M7 (neutral) and M8 (selection) models for the individual protein domains of *viperin* gene from 20 primate species.

Viperin inhibits HIV-1 Lai virus release and is partially counteracted by Nef

Given the broad antiviral range of Viperin, we wished to investigate whether Viperin might also be relevant to restricting HIV-1 infection. We first studied whether Viperin is expressed at the protein level in HIV-1 target cells. Primary CD4⁺ T cells and monocytes were isolated from peripheral blood mononuclear cells of two donors and treated with interferon β for twenty hours. We found that both primary CD4⁺ T cells and monocytes express endogenous Viperin after induction with interferon (Figure 28A), but expression levels were undetectable in the absence of interferon.

Given that Viperin is under positive selection and expressed in HIV-1 primary target cells after interferon induction, we investigated whether Viperin restricts HIV-1. To begin these studies, we first compared levels of endogenous Viperin expression with levels achieved by transfection of the cloned human *viperin* gene into 293T cells. We found that untransfected 293T cells express undetectable levels of endogenous Viperin. However, the transient expression of Viperin in 293T cells transfected with between 0.3 and 1 μ g of DNA bracketed the amount of endogenous Viperin expression in primary CD4⁺ T cells and U937 cells when induced with interferon (Figure 28B). Therefore, in subsequent studies, we used amounts of the plasmid encoding the human *viperin* gene that gave levels of Viperin expression just below and just above the levels expressed in primary cells.

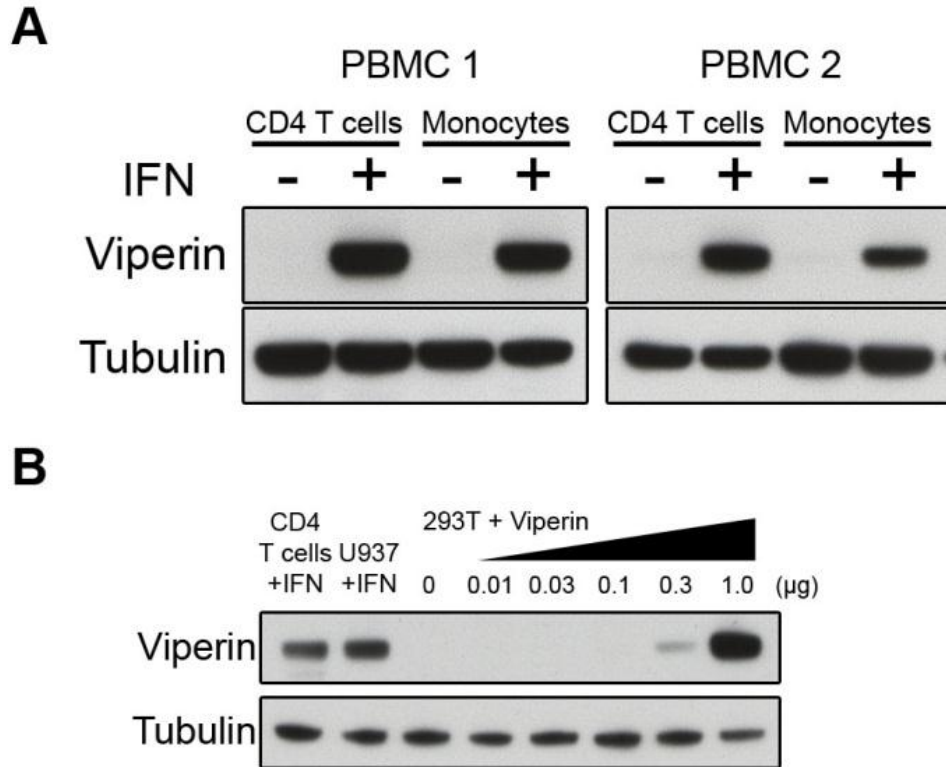


Figure 28

(A) Viperin expression in HIV-1 primary target cells was determined by western blot analysis. CD4+ T cells and monocytes isolated from two donor-derived peripheral blood mononuclear cells were treated with or without interferon β 1b induction (500 IU/ml) for twenty hours.

(B) Western blot analysis of endogenous Viperin expression in primary CD4+ T cells and U937 cells treated with interferon β 1b (500 IU/ml) was compared to the transient expression of Viperin (3-fold serial dilutions: 0, 0.01, 0.03, 0.1, 0.3, 1.0 μ g) transfected in 293T cells.

We tested whether exogenous Viperin expression could restrict HIV-1 by co-transfecting 293T cells with a full-length HIV-1 Lai strain with increasing amounts of the human *viperin* gene. Additionally, we tested HIV-1 Lai lacking a *nef* gene, since Nef has been

implicated in modulating cellular cholesterol levels (281, 318). We measured the antiviral activity of Viperin was by infecting TZM.BL indicator cells with released virus, and assaying for β -galactosidase reporter activity (See Materials and Methods). We found that wild-type HIV-1 virus was marginally affected at low amounts of Viperin, but was inhibited at the highest dose of Viperin (Figure 29A, closed circles). Consistent with the known defect on virion infectivity in the absence of Nef (11), the HIV Δ Nef virus had a lower infectivity even in the absence of Viperin as measured by the β -galactosidase activity (Figure 29A left, compare closed circles and open circles at 0 μ g viperin). Despite that initial observation, the HIV Δ Nef virus was restricted further by viperin in a dose-dependent manner (Figure 29A, open circles). To compare the degree of restriction between the two viruses, we normalized the β -galactosidase reporter activity of each virus to their measurements in the absence of Viperin (Figure 29A right). We observed that the wildtype HIV virus was only restricted at the highest levels of Viperin expression, whereas the HIV Δ Nef virus was more sensitive to Viperin restriction than wildtype HIV, even at the lower levels of Viperin expression.

Because Viperin restricts influenza virus at the step of virus release (293) and HCMV by inhibiting the production of viral structural proteins (43), we investigated whether HIV-1 production and/or release is affected by Viperin by western blotting for cell-associated and cell-free Gag proteins. We hypothesized that if Viperin affects HIV production, we expected to see a decrease in intracellular p55gag expression that correlates with a decrease in cell-free p24gag. Conversely, if Viperin affects virus release, we would see lower levels of cell-free p24gag while levels of p55gag would remain unchanged.

We found that cell-associated HIV-1 p55gag for both WT and Δ Nef virus was only marginally affected by the expression of Viperin (Figure 29B). Moreover, cell-free levels of p24gag from wild type HIV-1 were modestly affected by the expression of Viperin (Figure 29B) in a manner consistent with a slight decrease in the amount of supernatant HIV p24gag when measured with an enzyme linked immunosorbent assay (ELISA) assay (Figure 29C, middle). However, Viperin expression showed a drastic reduction in cell-free HIV Δ Nef p24gag (Figure 29B, right), with only a small effect on intracellular p55gag levels (Figure 29B, left). This suggests that Viperin affects release of HIV Δ Nef virus.

Since Viperin might also be affecting the quality of the virus particles, we quantified the specific infectivity of virus particles by measuring the ratio of infectious titer to relative particle production (by p24 ELISA). Consistent with other studies, we find that wildtype HIV virus was more infectious than HIV Δ Nef virus (Figure 29C). However, viperin expression did not affect the specific infectivity (infectivity divided by p24gag) of either wildtype HIV virus or HIV Δ Nef virus particles (Figure 29C, right), indicating that the Viperin-mediated restriction of HIV-1 is not due to a reduction in viral infectivity.

Since Viperin seemed to affect virus release, we compared Viperin restriction to that of Tetherin, a well-characterized host restriction factor that inhibits virus release (176, 282). Virus restriction by a combination of Viperin and Tetherin expression was roughly additive (Figure 29D). Furthermore, the response of Viperin and Tetherin is different since HIV-1 Vpu abrogates Tetherin restriction but has no effect on Viperin restriction, whereas HIV-1 Nef

abrogates Viperin restriction (Fig. 3D). These results suggest that Viperin restricts HIV-1 release by a mechanism that is distinct from the pathway used by Tetherin.

Because HIV Δ Nef was more sensitive to Viperin restriction compared to wildtype HIV, we examined whether Nef expressed *in trans* could rescue the restriction Viperin imposed on a Δ Nef mutant. Nef expression from either the HIV-1 Lai and Q23-17 strains modestly rescued HIV-1 Δ Nef virus release in the presence of Viperin (Figure 30A), indicating that the partial Nef rescue of Viperin restriction is consistent with an increase in HIV-1 release. The partial Nef counteraction of Viperin restriction is consistent with the observed reduction in wildtype HIV-1 release at high levels of Viperin overexpression (Fig. 3). One step by which accessory proteins from HIV-1 alleviate restriction is by causing degradation of the restriction factors (151). However, we found that the expression of Nef did not affect the levels of Viperin expression (Figure 30B), suggesting that Nef abrogation of Viperin was via a distinct mechanism from direct protein degradation. Thus, Viperin restriction of HIV-1 release can be partially counteracted by Nef in a manner that does not directly affect Viperin protein expression.

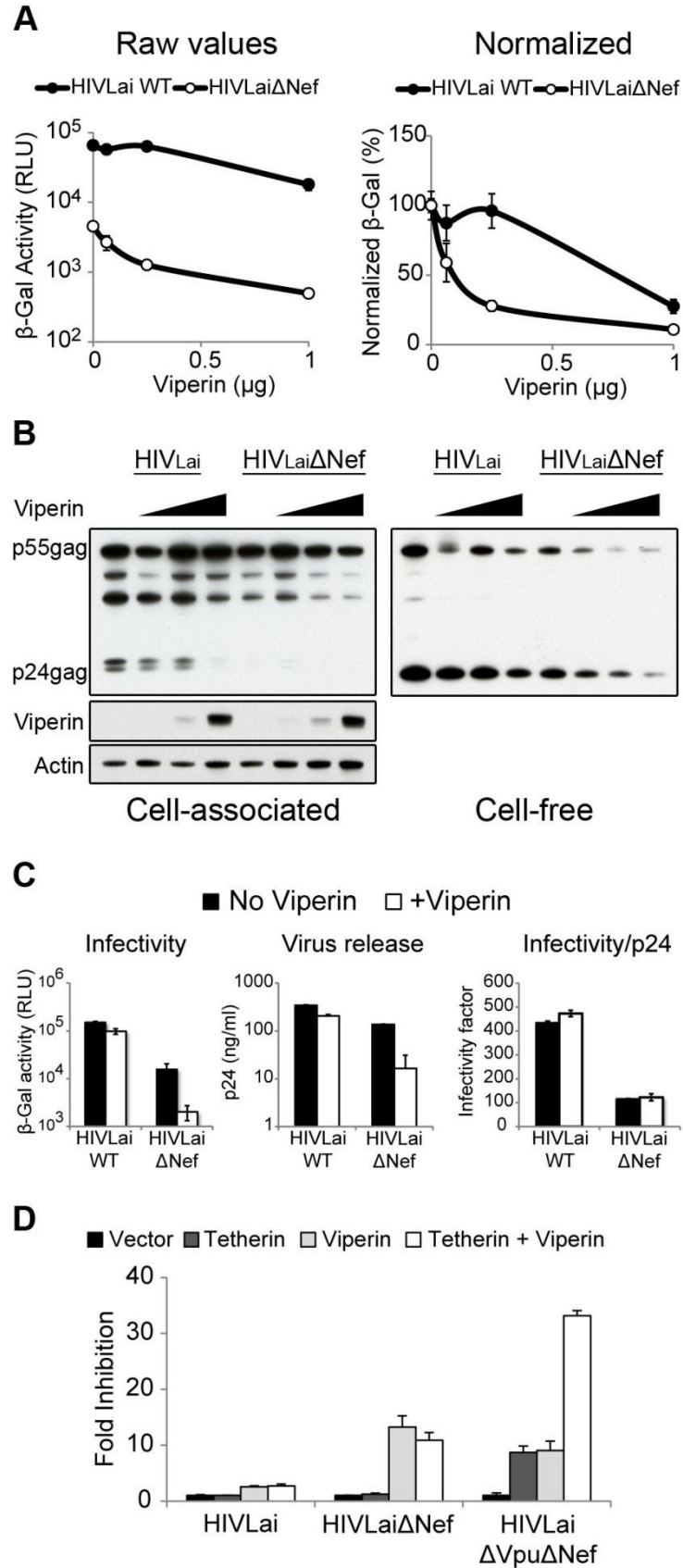


Figure 29

(A) The effect of viperin was measured by the infectious virus yield. 293T cells co-transfected with 200 ng of HIVLai or HIVLai Δ Nef with serial dilutions of human viperin was titrated by infecting TZM.BL indicator cells. The infectivity readout by β -galactosidase activity measured in relative light units (RLU) is shown on the left, and the respective viruses were normalized to β -galactosidase activity in the absence of viperin as shown on the right. Error bars indicate standard deviations from three infection replicates; this data is representative of five independent experiments.

(B) Western blot analysis was performed on the cell-free virus and cellular extracts, and probed with α -p24 antibody. Viperin expression in the cellular extracts is shown, and actin was probed as a loading control. This blot is representative of four independent experiments.

(C) The effect of Viperin on the specific infectivity of virus particles was calculated. HIVLai or HIVLai Δ Nef virus from 293T cells co-transfected with or without Viperin (700 ng) was titrated by infecting TZM.BL indicator cells as shown on the left. Virus release in the cell-free supernatant was quantified by p24 ELISA as shown in the middle. The specific infectivity was calculated as ratio of β -galactosidase activity (RLU) over the amount of p24 (ng/ml), as shown on the right. Error bars indicate standard deviations of triplicate infections, this data is representative of at least three independent experiments.

(D) Virus yield from 293T cells co-transfected with a combination of Tetherin (50 ng) or Viperin (700 ng) was titrated on TZM.BL cells. Fold inhibition was calculated in comparison to virus yield in absence of Tetherin/Viperin. Error bars indicate standard deviations of triplicate infections, this data is representative of three independent experiments.

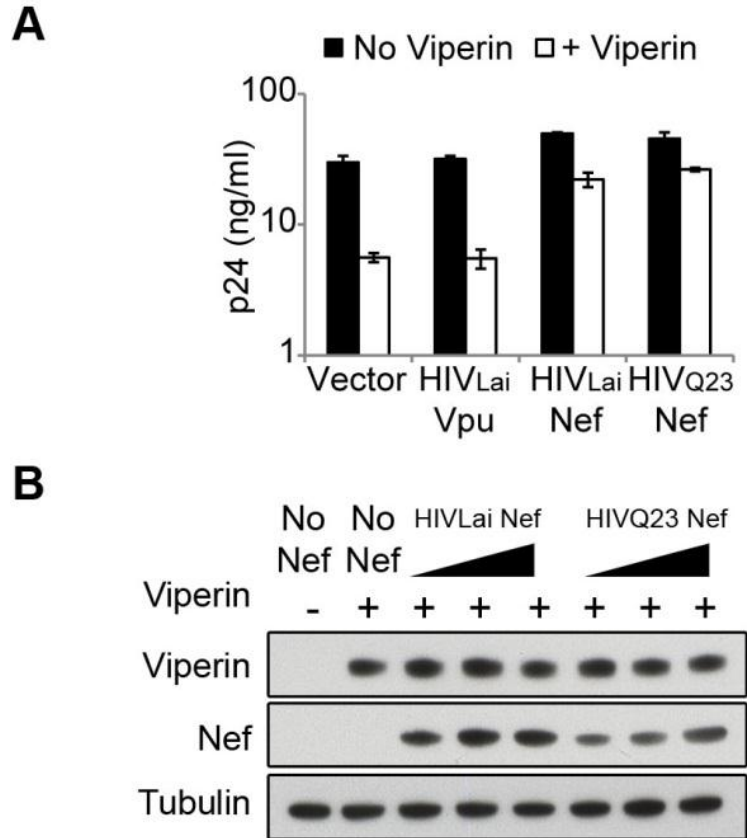


Figure 30

(A) HIVLai Δ Vpu Δ Nef (200 ng) was complemented *in trans* with 200 ng of HIV-1 Lai Vpu, HIV Lai Nef or HIV Q23-17 Nef, in the presence or absence of Viperin (700 ng). Virus release was measured from the cell-free supernatant by p24 ELISA quantification. Error bars indicate standard deviations of three replicates, and is representative of three independent experiments.

(B) Viperin protein expression was analyzed by western blot twenty-four hours after co-transfection of 293T cells with human Viperin (700 ng) and 5-fold serial dilutions of native HIVLai Nef or HIVQ23-37 Nef (10, 50, 250 ng). Native untagged Nef expression is shown, and Tubulin was probed as a loading control.

Most HIV strains, SIVs and retroviruses are resistant to Viperin restriction

To examine the breadth of Viperin restriction on HIV-1, we tested several strains of HIV-1 for their susceptibility to Viperin restriction on virus release. The proviruses were deleted of their *nef* gene to exclude the possible confounding effects of Nef specificity. Consistent with the earlier experiments (Figure 28C), HIVLaiΔNef virus release was inhibited by human Viperin. However, virus release of the HIVΔNef NL4-3, SF162 (both HIV-1 subtype B) and Q23-17 strains (HIV-1 subtype A) were unaffected by Viperin expression (Figure 31A). To verify these observations, we performed a western blot analysis comparing the cell-associated and cell-free HIV-1 Gag protein levels. In contrast to the dose-dependent inhibition of HIVLaiΔNef virus release, cell-free HIVNL4-3ΔNef virus release remained unaffected (Figure 31B). While there was an observable effect on intracellular HIVNL4-3ΔNef virus p55 levels, this difference was not reflected in the cell-free Gag p24 levels or the ELISA assay. In addition, we tested a widely used HIV-1 vector encoded from a codon-optimized Gag-pol sequence called pCNC-SynGP (103). We observed that the cell-free HIV-1 pCNC-SynGP Gag was unaffected by Viperin expression. Instead, cell-associated p55gag protein production was slightly increased in the presence of Viperin expression. As for the HIVΔNef SF162 and Q23-17 strains, there were no significant effects on cell-free p24gag or cell-associated p55gag expression levels. One exception is a noticeable decrease in the partially processed, cell-associated, HIVΔNef SF162 p40gag levels. However, while Viperin might have a subtle effect on the intracellular Gag levels of certain HIVΔNef strains, the difference was not reflected in the cell-free virus or measured in the ELISA assay. Thus, it

appears that Viperin does not significantly impact the virus release of most HIV Δ Nef strains tested except for the HIV-1 Lai strain.

We next investigated the ability of Viperin to restrict related simian immunodeficiency virus (SIV). In addition to their *nef* gene deletion, the proviruses were also pseudotyped with VSV-G so that the entry of all viruses would be equal. Using an infectivity assay, we found that SIVmac239 Δ Nef was as sensitive to Viperin as HIV-1Lai Δ Nef (Figure 31C, open squares). However, SIVagmTAN1 Δ Nef, SIVcpzTAN3.1 Δ Nef and HIV-2ROD9 Δ Nef were resistant to Viperin restriction. Since Viperin did not appear to restrict the majority of primate lentiviruses we tested, we also examined two additional divergent retroviruses – murine leukemia virus (MLV) and feline immunodeficiency virus (FIV). In contrast to the control HIV Δ Nef Lai virus, MLV and FIV were unaffected by Viperin expression (Figure 31D), indicating that Viperin does not generally restrict retroviruses. Thus, while Viperin may inhibit a limited subset of primate lentivirus strains (HIV-1Lai and SIVmac239, for example), the majority of HIV-1 strains, SIVs and retroviruses that we tested are not affected by Viperin expression.

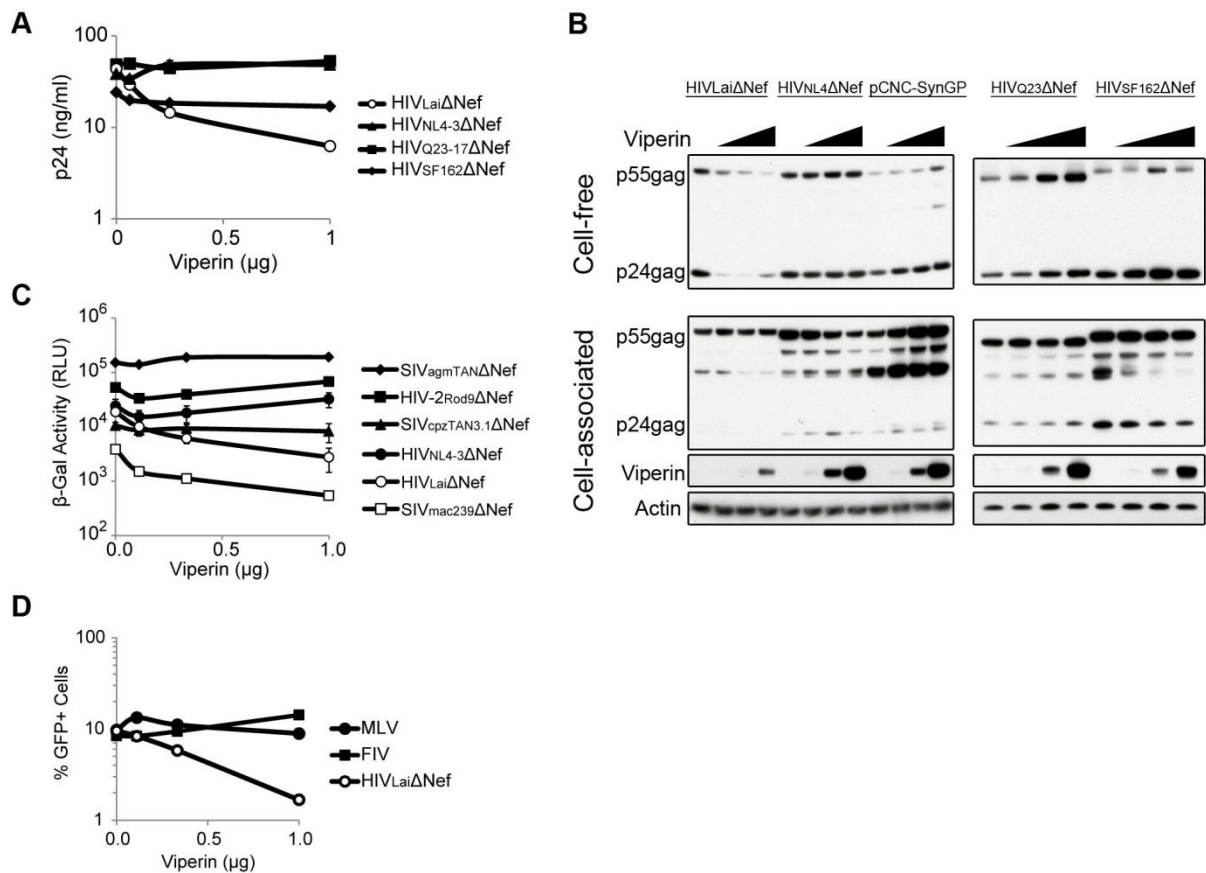


Figure 31

(A) A panel of HIV-1ΔNef strains were tested for their sensitivity to Viperin overexpression. Virus release was assayed by p24 ELISA quantification of cell-free supernatant forty-eight hours after co-transfection of 293T cells. Error bars indicate standard deviations of three replicates, and is representative of three independent experiments.

(B) Western blot analysis was performed on the cell-free virus and cellular extracts of (A). HIV-1 Gag expression was accessed by α -p24 antibody. Viperin expression in the cellular extracts is shown, and Actin was probed as a loading control. This blot is representative of at least three independent experiments.

(C) Single-cycle infectious virus yield of VSV-G pseudotyped primate lentiviruses from 293T cells co-transfected with and serial titration of Viperin was titrated on TZM.BL indicator cells. Proviruses were deleted of the *nef* gene. The infectivity readout by β -galactosidase activity was measured in relative light units (RLU).

(D) The effect of Viperin on retroviruses was measured by co-transfecting 293T cells with MLV, FIV or HIV_{Lai}ΔNef with serial titrations of viperin. Viruses were pseudotyped with VSV-G and titrated by infecting HeLa cells. The expression of virus-encoded GFP was quantified by flow cytometry. This analysis is representative of at three independent experiments.

Endogenous Viperin does not inhibit HIV-1 Lai

To determine the effect of endogenous Viperin on HIV-1, we sought to knock-down Viperin expression with shRNAs. We were unable to obtain suitable stable or transient knockdown in primary T cells (data not shown). Many T cell lines such as SupT1 cells also do not express Viperin after interferon induction (data not shown). However, CD4+ U937 monocytic cells do express Viperin after interferon induction (Figure 28B). Using a stably transduced shRNA construct, we were able to partially knockdown expression of Viperin in U937 cells (Figure 32A). U937 cells that were either knocked-down for Viperin (shRNA_{Vip}) or transduced with a control shRNA (shCON) were infected with HIV-1LAI and HIV-1LAI Δ Nef at a multiplicity of infection of 0.5. Infections were done in the presence of interferon to induce Viperin expression. Viral supernatant was collected periodically over 11 days and spreading infection was monitored by p24 ELISA. We found that there was no significant difference between WT and Δ Nef virus growth in the cells knocked-down for Viperin expression (Figure 32B). Considering that the HIV_{LAI} Δ Nef is the most sensitive strain in Viperin overexpression experiments (Figure 28 and Figure 30), these results suggest that endogenous levels of Viperin do not affect spreading infection by HIV-1.

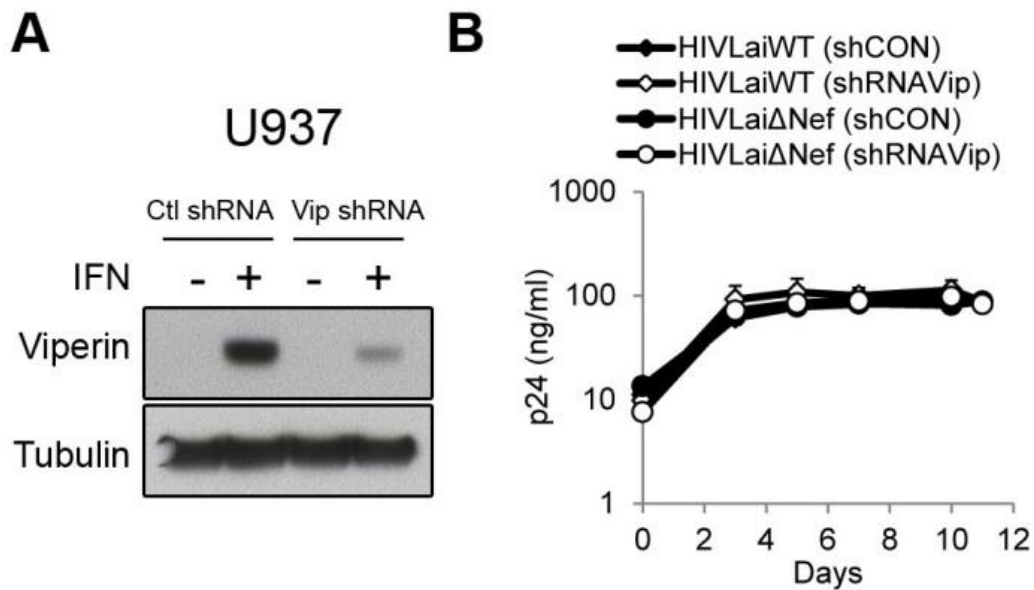


Figure 32

(A) Viperin expression in U937 cells stably transduced with empty pGIPZ shRNA vector (Ctl) or viperin targeting shRNA (Vip) was analyzed by western blot twenty hours after interferon β 1b treatment (500 IU/ml).

(B) Spreading infection of wildtype HIVLai or HIVLai Δ Nef was quantified by p24 ELISA at indicated time points after infecting shRNA-transduced U937 cells at an moi of 0.5. Cells were maintained in interferon β 1b (500 IU/ml) for the duration of the experiment.

No functional divergence in lentiviral restriction among primate Viperin orthologs

Most of the experiments that we have carried out were using the human *viperin* allele. However, since *viperin* evolves rapidly under positive selection, we might not be accurately capturing the potential ability of Viperin proteins to restrict lentiviruses. The species-specificity of action is one of the key features that have emerged from the study of rapidly evolving restriction factors. To address the possibility that the human Viperin might not accurately capture the restrictive potential of Viperin, we carried out two experiments to measure any functional divergence between primate Viperin orthologs that may have arisen from the positive selection.

First, we tested 5 additional Viperin orthologs against the HIVLai Δ Nef (Figure 33A). We found that all six Viperin orthologs are able to restrict this virus to approximately the same extent, despite some variation in the degree of restriction. This means that the positive selection of *viperin* does not manifest a functional difference in the degree of restriction of HIVLai Δ Nef. Second, we compared the human and rhesus orthologs against a panel of viruses to assess whether we could discern any key restriction differences between these two Viperin orthologs (Figure 33B). It is notable that human versus rhesus differences have been found in the majority of positively selected restriction factors that have been tested so far (58, 62, 231). However, in the case of Viperin, we found no significant differences between the restriction profiles of human and rhesus Viperin.

These results imply that Viperin's lack of restriction of the majority of lentiviruses and retroviruses tested is not a consequence of testing only one Viperin allele. Moreover, this

strongly implies that gain or loss of lentivirus restriction is not correlated with the dramatic evolutionary changes we observed in the *viperin* gene in primates.

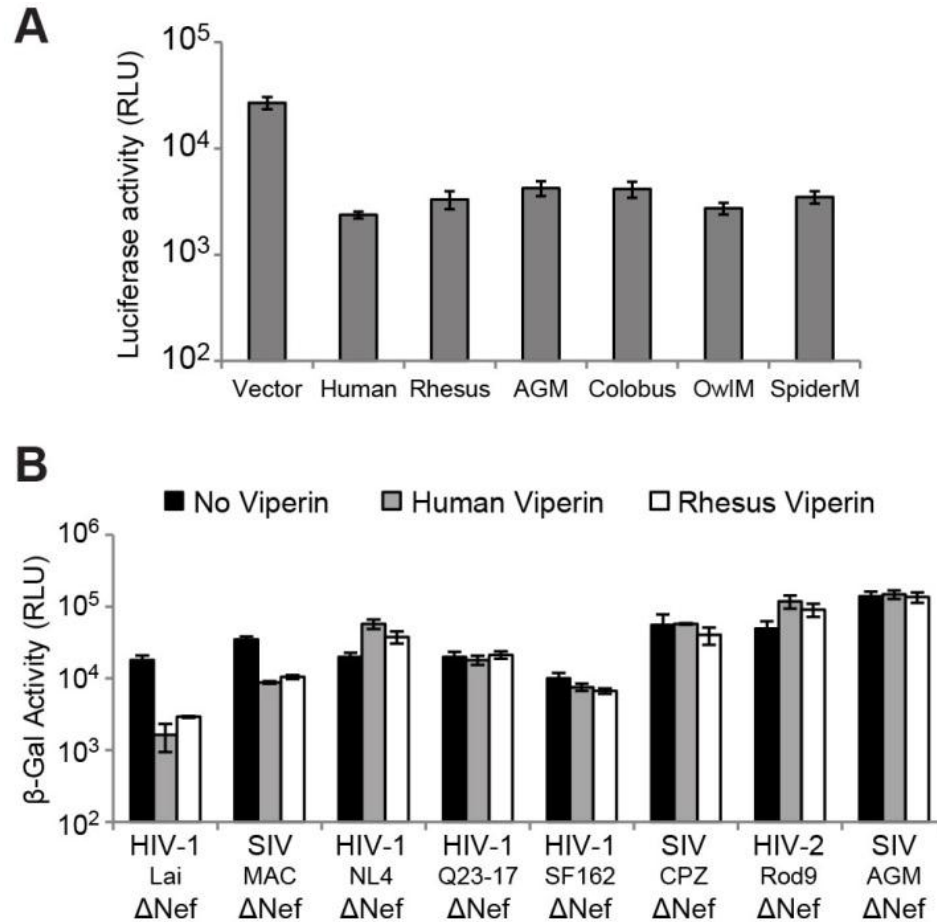


Figure 33

(A) The antiviral activity of primate Viperin orthologs was assayed. 293T cells were co-transfected with HIVLaiΔNef that encodes a luciferase reporter gene (200 ng) and indicated primate Viperin (700 ng). Virus yield was measured by infecting SupT1 cells and assayed for luciferase expression. Error bars represent standard deviations of four infection replicates, and is representative of three independent experiments.

(B) Single-cycle infectious virus yield of VSV-G pseudotyped primate lentiviruses from 293T cells co-transfected with 700 ng of human Viperin, rhesus Viperin or empty vector was titrated on TZM.BL indicator cells. The infectivity readout by β-galactosidase activity was measured in relative light units (RLU). Error bars indicate standard deviations of four infection replicates, and is representative of at least three independent experiments.

DISCUSSION

Primate Viperins are not lentiviral restriction factors

The restriction factor Viperin recognizes and restricts a wide diversity of viruses, including both single-stranded RNA and double-stranded DNA viruses (64, 161, 240). This broad repertoire of antiviral activity prompted us to investigate Viperin's restrictive activity against retroviruses, specifically the primate lentivirus lineage. We found that Viperin is highly interferon-induced in primary target cells of HIV. Viperin overexpression is able to inhibit HIV-1 Lai replication by affecting virus release and this restriction is partially counteracted by the Nef protein. However, most other strains of HIV-1, SIV and other retroviruses are unaffected by primate Viperin orthologs. Finally, endogenous Viperin does not inhibit the spreading infection of HIV-1 Lai. Therefore, we conclude that Viperin is not a major restriction factor against HIV-1 and other primate lentiviruses.

Our overall findings are consistent with a previous study that showed that poly I:C-induced Viperin only had a subtle effect on HIV-1 infection in astrocytes (218). Our findings of Viperin restriction of the Lai strain of HIV-1 but not the NL4-3 strains is unexpected since NL4-3 is a recombinant virus of NY5 and Lai strains (2). At present, we do not have an explanation for why only the HIV-1 Lai strain is Viperin sensitive, but we have mapped the genetic basis of the susceptibility difference to a non-coding region of the virus (data not shown). One possible explanation is that LTR promoter efficiency may affect viral Gag production in a manner that renders it sensitive to Viperin. Nonetheless, considering that most strains of HIV-1, SIVs (excluding SIVmac239), tested are resistant to Viperin, we favor

the most parsimonious conclusion is that Viperin is not a significant player in the immune defense against lentiviruses.

Insight into Viperin function from its positive selection

Antagonistic genetic conflict between hosts and viruses have driven rapid adaptive evolution of antiviral proteins (59, 99), which is characteristic of many retroviral restriction factors (166) as well as other antiviral factors that target a broad range of viruses (58, 194). Like many host restriction factors, we find that *viperin* has been evolving under positive selection in primates. The signatures of rapid evolution in *viperin* may provide valuable information about the mechanism by which it restricts this broad repertoire of viruses, and likely avoids viral antagonism. This is analogous to the dynamics of the host restriction factor Tetherin, where the highest recurrent signal of positive selection corresponds to the amino acid that is a determinant for antagonism by Nef (142). In the antagonist-driven scenario, we speculate that the amino acid residues under positive selection on Viperin might have been driven by pressures to evade viral antagonists and would be indicative of sites directly involved in viral protein interactions. A promising candidate would be Japanese encephalitis virus which encodes an unidentified viral antagonist that degrades Viperin in a proteasome-dependent mechanism (39).

Thus, although Viperin does not encode a restriction factor for lentiviruses, our study documents an ancient, episodic and recurrent history of adaptive evolution in Viperin

over primate evolution, which was likely driven by selective pressures imposed by virus families other than the lentiviruses.

CHAPTER SIX

The Ability of Primate Lentiviruses to Degrade the Monocyte Restriction Factor SAMHD1

Preceded the Birth of the Viral Accessory Protein

SUMMARY

The SAMHD1 protein potently restricts lentiviral infection in dendritic cells and monocytes, but is antagonized by the primate lentiviral protein Vpx. SAMHD1 which targets it for degradation. However, Vpx is only encoded by some lineages of primate lentiviruses whereas its paralog, Vpr, is conserved across extant primate lentiviruses. Nonetheless, I find that not only multiple Vpx but also some Vpr proteins are able to degrade SAMHD1. I show that such antagonism led to dramatic positive selection of SAMHD1 in the primate subfamily *Cercopithecoinae*. Residues evolving under positive selection precisely determine sensitivity to Vpx/Vpr degradation by altering binding specificities. By overlaying these functional analyses on a phylogenetic framework of Vpr and Vpx evolution, we can decipher the chronology of acquisition of SAMHD1-degrading abilities in lentiviruses. We conclude that *vpr* neofunctionalized to degrade SAMHD1 even prior to the birth of a separate *vpx* gene, thereby initiating an evolutionary arms race with SAMHD1.

INTRODUCTION

The evolutionary analysis of both host and viral proteins combined with functional analysis can reveal the evolutionary dynamics of this arms race, both in terms of its birth and its more recent adaptations. Host defense genes like *SAMHD1* involved in antagonistic virus-host interactions often display strong signatures of diversifying selection as a result of repeated episodes of selection by viral antagonists (59, 166). This methodology can be used to pinpoint the exact amino acid residues involved in the viral-host interaction (142, 163, 231), and when applied to a phylogenetic tree, can provide a temporal context for when these interactions have taken place (59).

The recent identification of *SAMHD1* as the target of Vpx allows us to characterize Vpx function from diverse lentiviruses with *SAMHD1* from different hosts. Such an analysis can distinguish between the possibility that *SAMHD1* degradation had an ancient origin and was subsequently lost in some lineages due to lack of selective pressure from *SAMHD1*, or that it was a recent adaptation of some viruses.

Our functional analyses reveal that multiple Vpx proteins share the ability to degrade *SAMHD1* but that this ability is often host-specific. Furthermore, we find that some Vpr proteins from Vpx-lacking lentiviruses also can potentially degrade *SAMHD1*. Moreover, our evolutionary analyses reveal a burst of diversifying selection that shaped *SAMHD1* in the *Cercopithecinae* subfamily of old world monkeys which was driven by its antagonism with Vpr/Vpx proteins. By tracing the evolution of Vpr and Vpx function on a phylogenetic framework, we show that the ability to degrade *SAMHD1* is the result of

neofunctionalization of Vpr that preceded the acquisition of Vpx in primate lentiviruses. We conclude that *vpr* gained a new function to degrade SAMHD1 once during viral evolution, thereby initiating an evolutionary arms race with SAMHD1. However, many lentiviral lineages, including those leading to HIV-1, never acquired this function.

RESULTS

Species-specific antagonism of SAMHD1 by diverse Vpx proteins

A recent study found that SIVrcm Vpx could not degrade human SAMHD1 (133), suggesting that this function might be very limited among primate lentiviruses. I first wished to test if the ability of Vpx to degrade SAMHD1 is conserved, and if there is species-specificity to the interaction. Thus, I cloned SAMHD1 from a panel of primates and assayed for Vpx-mediated SAMHD1 degradation by western blot analysis after transient co-transfection of epitope-tagged SAMHD1 proteins with *vpr* or *vpx* from different lentiviruses.

Consistent with previous reports, I found that HIV-2 (Rod9) Vpx degraded human SAMHD1 and SIVmac Vpx degraded rhesus SAMHD1 (101, 133), (Figure 34A and Figure 34B). I also found that Vpx from a primary strain of HIV-2 7312a degraded SAMHD1 (Figure 34A). Surprisingly, I found that while the HIV-2 (Rod9) had a relatively narrow specificity, only degrading SAMHD1 from human and De Brazza's monkeys among a broader panel of primate SAMHD1 proteins (Table I), HIV-2 (7312a) Vpx could degrade SAMHD1 from humans and all of the Old World monkeys tested (Table I). The corresponding Vpr proteins

of both viruses were unable to degrade human SAMHD1 (Figure 34A), similar to Vpr proteins from HIV-1 and SIVcpz strains (Figure 34A).

SIVrcm also encodes both Vpx and Vpr. However, SIVrcm Vpx is only 42% identical to HIV-2/SIVsmm Vpx at the amino acid level. Nonetheless, I found that SIVrcm Vpx potently degraded SAMHD1 from the host species it naturally infects – the red-capped mangabey (RCM) (Figure 34B). Furthermore, I found that SIVrcm Vpx can degrade SAMHD1 from other Old World monkeys, but not from sooty mangabeys or humans (Table 1). The corresponding Vpr protein of SIVrcm did not have this activity (Figure 34B). Thus, my findings not only suggest that the ability to degrade SAMHD1 is conserved in other clades of Vpx, but also shows species-specificity (Table I).

HIV-1 encodes only *vpr*, while HIV-2 encodes both *vpr* and *vpx*, yet both infect humans. There is an analogous situation in mandrills which are naturally infected by two highly divergent lentiviruses, SIVmnd1 which encodes only *vpr*, and SIVmnd2 which encodes both *vpr* and *vpx* (254, 269, 279). I found that the Vpx protein from SIVmnd2 was able to degrade mandrill SAMHD1, but neither SIVmnd2 Vpr nor SIVmnd1 Vpr could degrade mandrill SAMHD1 (Figure 34C). Thus, even within a given host, some lentiviruses have a protein with the ability to degrade SAMHD1, while others do not.

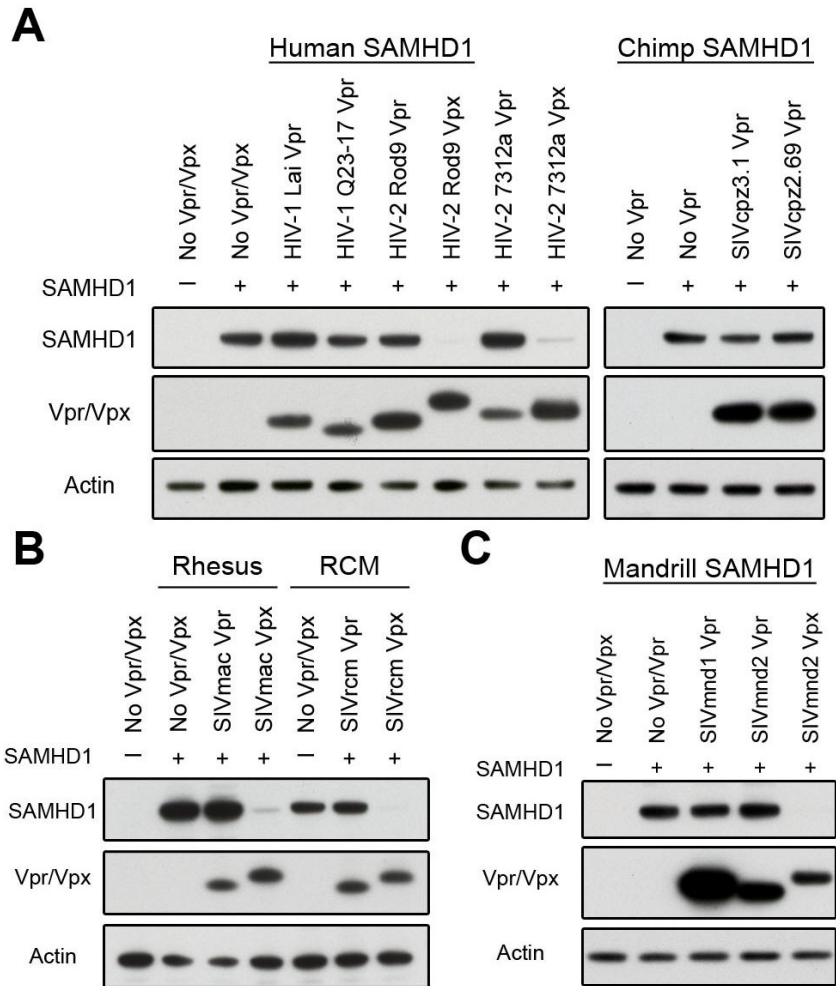


Figure 34

Vpx from diverse primate lentiviruses degrade SAMHD1.

(A) The ability of Vpx and Vpr to degrade SAMHD1 was assayed by western blot analysis of HA-epitope tagged SAMHD1 from respective primate species co-transfected with 3xFLAG-epitope tagged Vpr or Vpx constructs as indicated. Actin was probed as a loading control. Indicated Vpr and Vpx constructs were expressed in the presence of human SAMHD1 (left) or chimpanzee SAMHD1 (right).

(B) Similar western blots as in (A) are shown, analyzing rhesus macaque SAMHD1 (left) and red-capped mangabey (RCM) SAMHD1 (right) expression in the presence of indicated Vpr and Vpx constructs.

(C) Similar western blots as in (A) are shown, analyzing mandrill SAMHD1 expression in the presence of indicated Vpr and Vpx from SIVmnd1 or SIVmnd2.

Some Vpr proteins also antagonize SAMHD1

Thus far, analyses suggest a clear separation of function between the *vpr* and *vpx* genes examined (14) implying that *vpx* alone evolved the ability to degrade SAMHD1. However, the evolutionary history of these genes is far from clear, in part due to the high diversity of sequences (246, 277, 278). This raises the possibility that at least some divergent lentiviral *vpr* genes might share the property of degrading SAMHD1. We used 115 *vpr* and *vpx* gene sequences from diverse HIV and SIV isolates to construct phylogenies using both maximum likelihood (ML) and Bayesian (BI) methods; both methods yielded congruent unrooted topologies (Figure 35A, Figure 36A). The primate lentivirus *vpr* and *vpx* sequences grouped into seven phylogenetic clusters (cutoff at ML bootstrap >75, BI posterior probability > 0.8; shaded by colors in Figure 35A). Phylogenies obtained from an application of the Fast Statistical Alignment (FSA) algorithm that is more conservative in terms of homology assignment (33), or trimmed to the minimal 44 shared amino acid positions from the FSA alignment yielded the similar seven phylogenetic clades (Figure 35B). In all cases, a subset of the *vpr* genes clustered closer to the *vpx* genes than they did to other *vpr* genes (for example, the yellow and green groups in Figure 35A). Thus, we tested the *vpr* genes from each of the diverse primate lineages against their own host SAMHD1 as well as other primate SAMHD1 genes.

The Vpr protein from SIVolc (from the grey color group in Figure 35A), which infects olive colobus monkeys and does not carry Vpx, cannot degrade colobus SAMHD1, similar to HIV-1/SIVcpz Vpr and SIVmnd1 Vpr. On the other hand, however, I found that Vpr from

SIVdeb that infects De Brazza's monkeys (from the green color group in Figure 35A) not only degraded De Brazza's monkey SAMHD1 (Figure 35B) but it also potentially degraded SAMHD1 from all primate species including humans (Table I). Vpr from SIVmus, in the same group as SIVdeb, also had a broad specificity against primate SAMHD1 proteins (Table I). Extending these analyses further, we found that Vpr proteins from both SIVagm Grivet (677 strain) and SIVagm Vervet (9648 strain) (yellow group in Figure 35A) also degraded SAMHD1 from their African green monkey (AGM) host (Figure 35B). SIVagmGri Vpr had a narrow specificity only capable of degrading AGM SAMHD1, whereas SIVagmVer Vpr had a broader specificity (Table I). These data reveal that phylogenetically distinct Vpr proteins functionally degrade SAMHD1, at times with striking species-specificity.

Table 1. Species-Specific SAMHD1 Degradation by Vpr and Vpx									
SAMHD1	HIV-2 Rod9 Vpx	HIV-2 7312a Vpx	SIVmac Vpx	SIVdeb Vpr	SIVmus Vpr	SIVagm.Gri Vpr	SIVagm.Ver Vpr	SIVrcm Vpx	SIVmnd2 Vpx
Human	+	+	+	+	+	–	–	–	–
Rhesus	–	+	+	+	+	–	+	+	+
Red-capped mangabey	–	+	+	+	+	–	+	+	+
Mandrill	–	+	+	+	+	–	+	+	+
African green monkey	–	+	+	+	+	+	+	+	–
De Brazza's	+	+	+	+	+	–	+	+	+
Sooty mangabey	–	+	+	+	+	–	+	–	+

Table 1

Species-specific SAMHD1 degradation by Vpr and Vpx.

The table summarizes results of western blot analyses of SAMHD1 degradation phenotype by indicated Vpr and Vpx across a panel of primate SAMHD1. The host species SAMHD1 is listed in the left column, and the Vpx/Vpr proteins tested against SAMHD1 are listed in the top row. “+” indicates combinations that resulted in a greater than 90% decrease in SAMHD1 levels. “–” indicates combinations that had no significant changes in SAMHD1 levels. The following Vpr proteins from HIV-1 Lai, HIV-1 Q23-17, HIV-2 Rod9, HIV-2 7312a, SIVcpz 3.1, SIVcpz 2.69, SIVmac239, SIVrcm, SIVmnd1, SIVmnd2, and SIVolc—which are inactive against their host species (Figure 34 and Figure 35)—were also unable to degrade the panel of primate species’ SAMHD1 (data not shown). The AGM SAMHD1 tested is from the Vervet subspecies matching the SIVagmVer 9648 host strain; SAMHD1 from the Tantalus subspecies was found to be heterozygous for a second allele that was resistant to all HIV/SIV Vpr and Vpx tested (data not shown).

We overlaid the functional analysis of Vpr and Vpx proteins that do and do not degrade SAMHD1 on the unrooted phylogenetic tree. Notably, all of the Vpr/Vpx proteins that do degrade SAMHD1 are found on one side of the tree (Figure 35A, blue stars), while all of the Vpr proteins that do not degrade SAMHD1 are found on the other side (Figure 35A, red stars). There is strong bootstrap support for the separation of these two subtrees (Bootstrap support (BS) = 90.3, Posterior Probability (PP) = 1) which argues that there was a single gain/loss event for the function of degrading SAMHD1 in Vpr/Vpx evolution, and this function is not only confined to the previously classified “*vpx*” genes, but is also observed in “*vpr*” genes from diverse lentiviral lineages.

Binding of diverse Vprs to SAMHD1 correlates with degradation

Previous studies have shown that Vpx from SIVsm and HIV-2 are able to bind SAMHD1 directly in order to promote its degradation (101, 133). To determine if the diverse Vpr proteins that degrade SAMHD1 also antagonize through protein-protein interactions, we performed co-immunoprecipitations. As the immunoprecipitation was directed against SAMHD1, the proteasome inhibitor MG132 was added to the cells in an attempt to prevent degradation of SAMHD1. Consistent with our degradation results, we found that SIVdeb Vpr co-immunoprecipitates with SAMHD1 from De Brazza’s monkeys (Figure 35C). Similarly, we found that SIVagm Vpr binds AGM SAMHD1. The AGM-SAMHD-1 Vpr complexes, but not the SIVdeb Vpr, also interacted with the Cul4 ubiquitin ligase complex protein, DDB1 (Figure 35C), which is consistent with the mechanism previously shown for degradation of human

SAMHHD1 by HIV-2 Vpx (21, 244). In contrast, SIVmnd1 Vpr did not bind to Mandrill SAMHD1 (Figure 35C), indicating that only Vprs that degrade SAMHD1 are able to bind SAMHD1. Thus, the ability of Vpr to cause degradation of SAMHD1 correlates with its ability to bind SAMHD1, and is at least partially conserved with the known mechanism of Vpx interaction with SAMHD1.

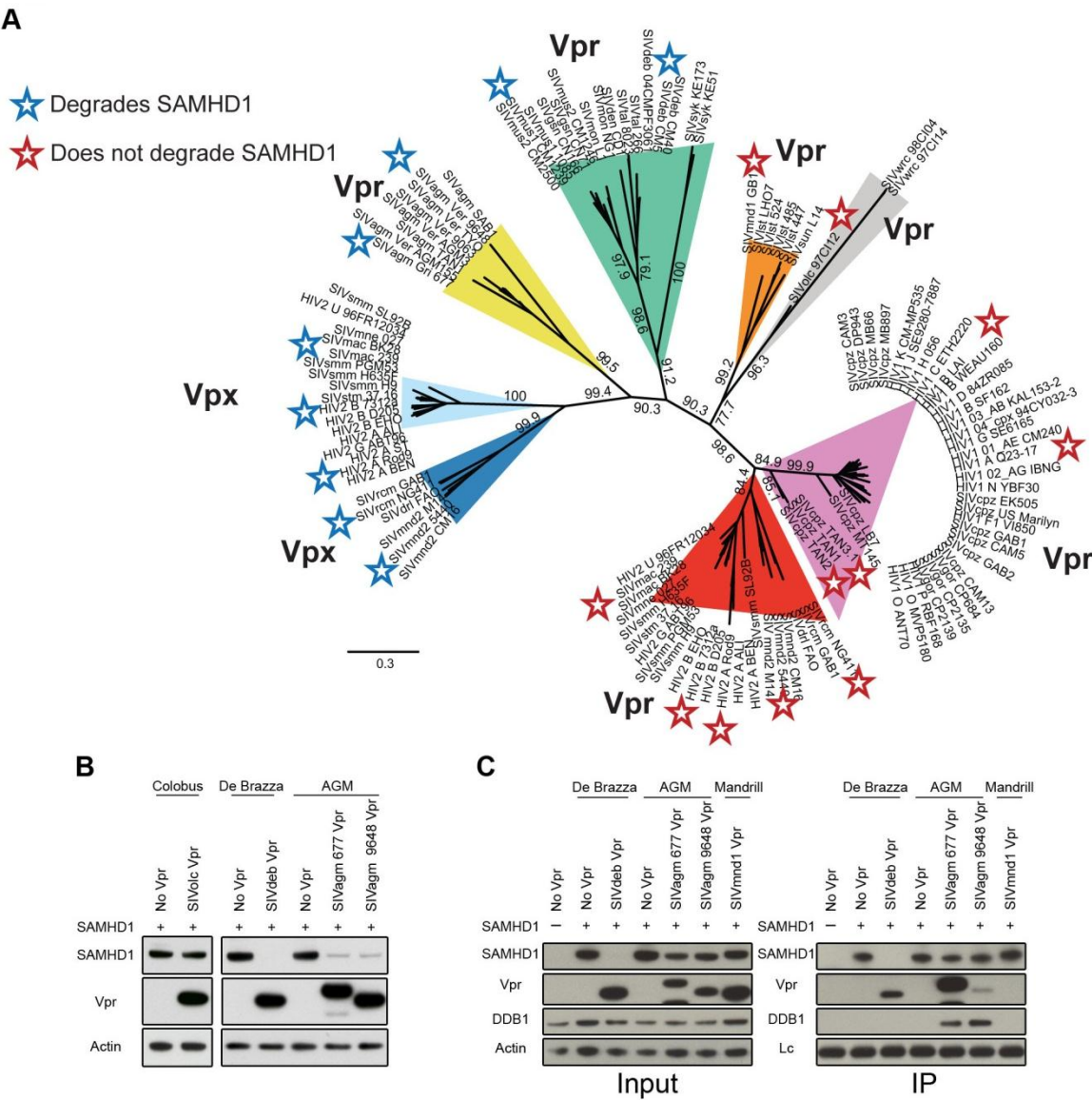


Figure 35

Some Vpr proteins degrade SAMHD1.

(A) Unrooted phylogeny of 115 *vpr* and *vpx* sequences among diverse primate lentiviruses. Bootstrap values indicates maximum likelihood proportions that are highly supported by Bayesian inference (Figure S1A). Seven phylogenetic clusters are shaded in colors (cutoff at ML bootstrap >75, Bayesian posterior probability > 0.87). *Vpx* sequences form 2 clades (Light blue and dark blue shaded) that have strong support of monophyly from all other *vpr* sequences. Functional phenotype of Vpr and Vpx (Table I) that degrade SAMHD1 (Blue stars) or do not degrade SAMHD1 (Red stars) are overlaid on the phylogeny. See also Figure S1B.

(B) Western blot analysis of Colobus monkey, De Brazza's monkey, and African green monkey (AGM) SAMHD1 in the presence of indicated Vpr constructs. The AGM SAMHD1 tested is from the Vervet subspecies matching the SIVagmVer 9648 host strain, the Colobus SAMHD1 tested is from the Colobus guereza subspecies.

(C) Association of SAMHD1 with Vpr and DDB1 by co-immunoprecipitation was detected by western blot analysis of HA-immunoprecipitated SAMHD1 for FLAG-epitope tagged Vpr and DDB1 association (IP), or input expression (Input). After transfection, cells were treated with 25 μ M MG-132 for 12 hours prior to immunoprecipitation. SIVdeb Vpr interacts with De Brazza's monkey SAMHD1 (IP), but SAMHD1 expression was not rescued by MG132 treatment (Input). SIVmnd1 Vpr, which fails to degrade mandrill SAMHD1, was assayed as a negative control. Actin and the antibody light chain (Lc) are shown as loading controls.

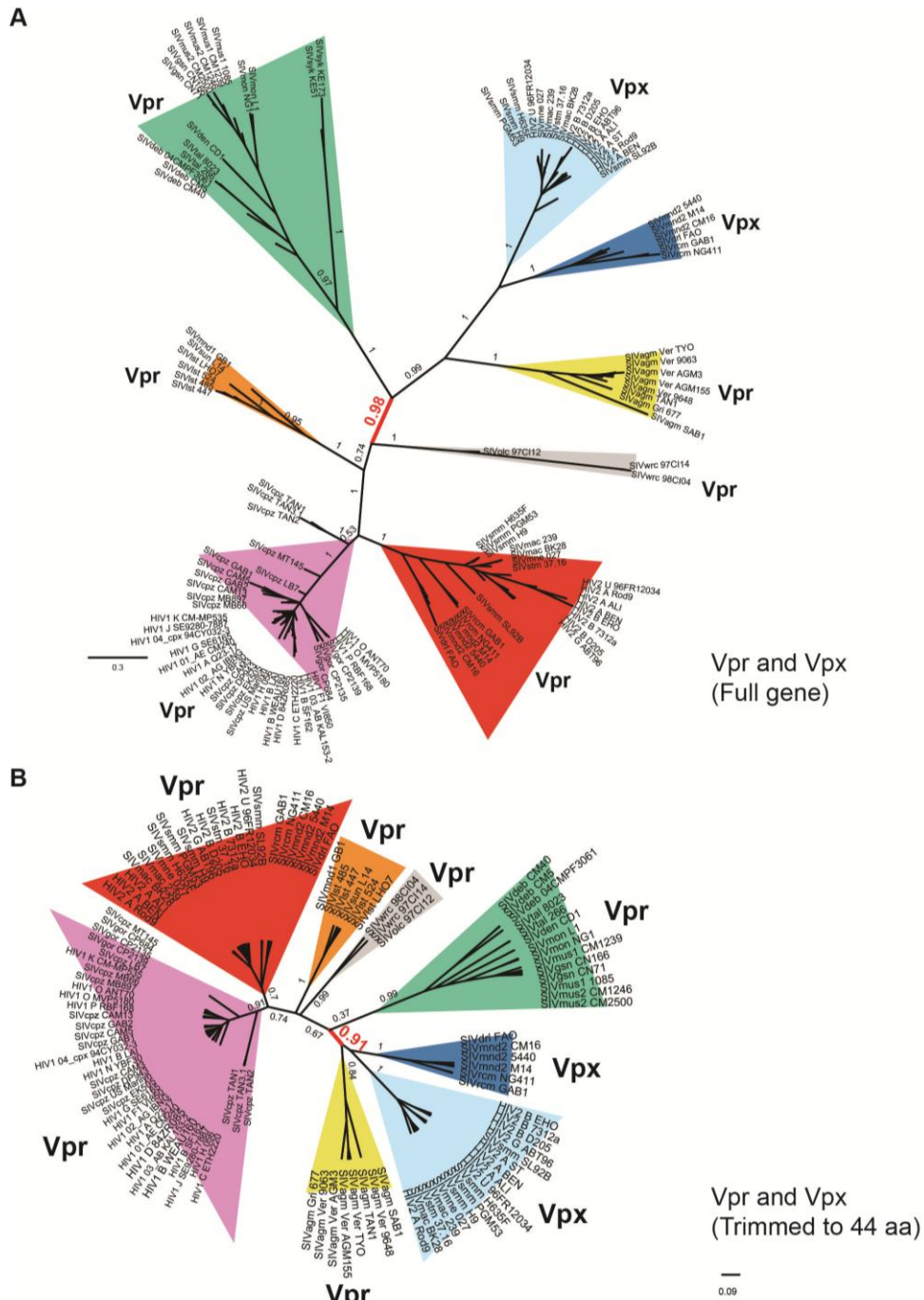


Figure 36

(A) Unrooted phylogeny of 115 *vpr* and *vpx* sequences (Figure 2A) among diverse primate lentiviruses using Bayesian inference. Seven monophyletic clusters shaded in colors.

(B) Unrooted phylogeny of *vpr* and *vpx* sequences from the FSA alignment trimmed to the minimal 44 shared amino acid positions, using Bayesian MCMC inference. A similar topology was obtained with the maximum likelihood method, with lower bootstrap support.

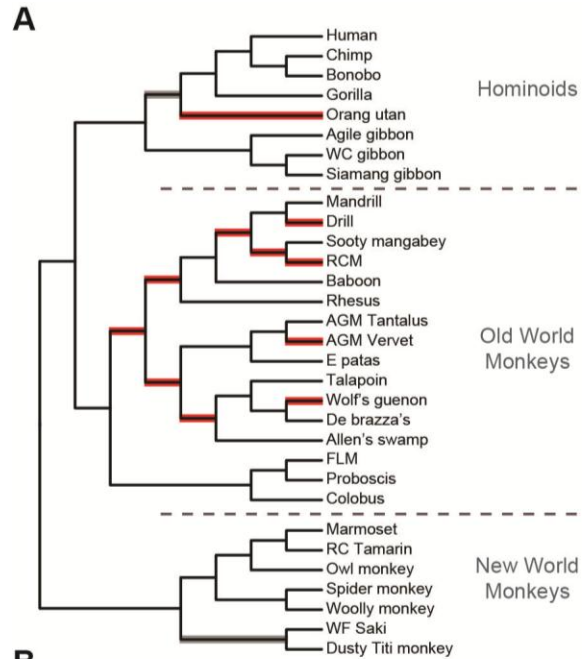
Vpr/Vpx antagonism drove positive selection of *SAMHD1* in Old World monkeys

One key to the question of whether antagonism of a host protein by a viral protein is ancient or recent is to determine the selective pressures that have shaped the host protein evolution. Therefore, I looked if *SAMHD1* is under positive selection by sequencing the coding region of *SAMHD1* from 31 primate species representing approximately 40 million years of evolutionary divergence (Figure 37A). The phylogeny constructed from the primate *SAMHD1* sequences was congruent with the generally accepted primate species phylogeny (198), confirming that the sequences are orthologous. I found that there was strong evidence of recurrent positive selection on *SAMHD1* during primate evolution (Figure 37B, $P < 0.001$), and this conclusion was corroborated with other methods (Figure 38). This signature of positive selection clearly stemmed from the Old World monkeys (OWM) clade ($p < 0.001$), as neither New World monkeys (NWM) ($p > 0.19$) or hominoids ($p > 0.35$) clades showed significant evidence of positive selection. The lack of positive selection in NWM or hominoids was not a result of low statistical power from limited evolutionary depth as the tree length (number of substitutions per codon) of the NWM clade (0.20) and hominoid clade (0.15) was greater than that of the OWM clade (0.13).

In order to investigate the selective pressures across the different primate lineages, I calculated the omega ratio (dN/dS) along each branch by performing a free ratio analysis using PAML, where omega (dN/dS) ratios > 1 are indicative of positive selection (Figure 37A and Figure 38B). Aside from OWM, only the branch leading to orangutans had statistically significant $dN/dS > 1$ (Figure 38C). Strikingly, *SAMHD1* has evolved by positive selection in

multiple branches of the OWM subfamily *Cercopithecinae* (Figure 37A, Figure 37D). This suggests that the most dramatic signatures of recurrent positive selection are exhibited by members of the *Cercopithecinae* primate subfamily, and occurred after this lineage split from the *Colobinae* subfamily.

Positive selection analysis identified six amino acid residues (aa 32 and 36 in the N-terminal domain, aa 46, 69 and 107 in the SAM domain and aa 486 in the C-terminal domain) as having evolved under recurrent positive selection with strong confidence (posterior probability > 0.95) (Figure 37C, Figure 40). Furthermore, if I removed all 6 residue positions from the primate SAMHD1 alignment, the bulk of the gene-wide signature of positive selection was lost ($p > 0.11$), indicating that these amino acids are largely responsible for the signal across the entire gene (Figure 37C).



B
Evolutionary analysis for signatures of positive selection in primate SAMHD1

	2lnλ	df	P-value
All primates	52.18	2	< 0.001
New world monkeys (NWM)	3.25	2	> 0.19 (NS)
Old world monkeys (OWM)	22.28	2	< 0.001
Hominoids (HOM)	2.04	2	> 0.35 (NS)

C
Analysis of sites under positive selection in Old World monkeys' SAMHD1

	2lnλ	df	P-value
Full gene	22.28	2	< 0.001
Full gene (- SAM domain)	9.21	2	< 0.01
Full gene Δ32, 36, 46, 69, 107, 486	5.22	2	> 0.11 (NS)
N Term domain (aa 1 - 43)	3.20	2	> 0.20 (NS)
SAM domain (aa 44 - 110)	14.75	2	< 0.001
Middle domain (aa 111 - 163)	2.47	2	> 0.29 (NS)
HD domain (aa 164 - 319)	1.11	2	> 0.57(NS)
C Term domain (aa 320 - 627)	3.08	2	> 0.21 (NS)

Figure 37

Primate SAMHD1 has been evolving under positive selection.

(A) Cladogram of 31 primate *SAMHD1* genes sequenced for the evolutionary analyses. The panel of primates comprised of 8 hominoids, 16 Old World monkeys and 7 New World monkeys. No evidence of recombination was detected by a GARD analysis (127). Values of ω (dN/dS) along each branch were calculated by a free ratio analysis using PAML (Figure 38B). Branches with statistically significant ω values > 1 are highlighted in red, branches

highlighted in grey indicate lineages that show ω values > 1 , but are not statistically significant based on two-ratio likelihood tests (Figure 38).

(B) Likelihood ratio test statistics were used to determine if *SAMHD1* evolution across various primate lineages was associated with dN/dS ratios significantly greater than 1 (hence under positive selection). Neutral models (M7) were compared to selection models (M8) under the F61 model of codon substitution. Similar results were obtained in a comparison of M1 (neutral) versus M2 (selection) (data not shown). See also Figure 38.

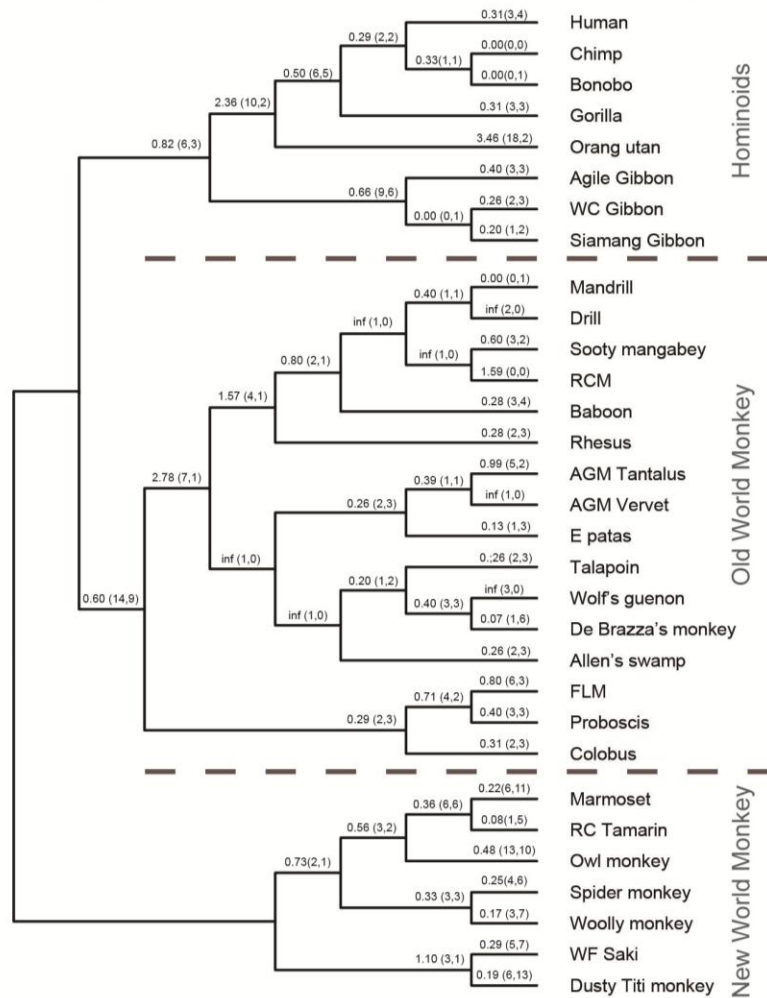
(C) Six positively selected codons were identified (32, 36, 46, 69, 107, 486) with significant posterior probability (Figure 38A) using PAML. The analysis was performed on *SAMHD1* sequences from the panel of 16 Old World monkeys, which showed the strongest burst of positive selection in primates (Figure 37B). Likelihood ratio tests were performed between the M7 (neutral) and M8 (selection) models for the full *SAMHD1* gene, without the SAM domain or with amino acids 32, 36, 46, 67, 107, 486 omitted from the alignment. Domains were analyzed for signatures of positive selection, with the strongest signals located in the SAM domain. See also Figure 38.

A

Likelihood ratio test statistics for PARRIS analysis of SAMHD1 gene

	<i>l</i>	2 <i>l</i>	P-value	Parameter estimates
Null model (M1): no selection	-5483.1			
Alternative model (M2): selection	-5477.7	10.8	< 0.005	$\omega_0 = 0.12$ ($\Gamma_0 = 0.776$) $\omega_1 = 1.00$ ($\Gamma_0 = 0.000$) $\omega_2 = 1.96$ ($\Gamma_0 = 0.227$)

B



C Likelihood Ratio Test Statistics for Models of Selection

	<i>l</i>	2 <i>l</i>	df	P-value
Hominoids				
Orang utan $\omega = 1.0$	-3082.08			
Orang utan $\omega = 3.4672$	-3080.21	3.75	1	< 0.05
Hominoids				
Hominids common ancestor $\omega = 1.0$	-3084.26			
Hominids common ancestor $\omega = 2.3602$	-3084.12	0.29	1	0.59 (NS)
New world monkeys				
WFSaki/Dusty Titi common ancestor $\omega = 1.0$	-3289.54			
WFSaki/Dusty Titi common ancestor $\omega = 1.0982$	-3289.55	0.03	1	0.87 (NS)

D

Evolutionary analysis for signatures of positive selection in SAMHD1 (*Cercopithecinae*)

	2ln λ	df	P-value
<i>Cercopithecinae</i> (old world monkeys)	24.96	2	< 0.001

Figure 38

(A) Likelihood ratio test statistics to determine if the *SAMHD1* gene from 31 primates is evolving under positive selection, using PARRIS from the HyPhy package.

(B) Values for ω (dN/dS) along each branch for *SAMHD1* were calculated by using the free ratio analysis from PAML. ω values are shown on branches, with the number of non-synonymous to synonymous changes indicated in parentheses.

(C) Likelihood ratio statistics were used to determine if *SAMHD1* evolution across the specific primate lineage was associated with dN/dS ratios significantly greater than 1 (hence under positive selection) compared to neutral, dN/dS = 1. Outside of OWM, only the branch leading to orangutans had statistically significant dN/dS > 1.

(D) Likelihood ratio tests were performed between the M7 (neutral) and M8 (selection) models for the full *SAMHD1* gene within the *Cercopithecinae* subfamily of primates in OWM.

If amino acid residues under positive selection determine sensitivity to Vpx antagonism, this would strongly argue that a Vpx-like factor was responsible for the signature of positive selection acting on SAMHD1. Alternatively, if the sites under recurrent positive selection did not affect SAMHD1's susceptibility to Vpx antagonism, this would strongly suggest that Vpx and Vpx-like factors are too recent to significantly affected SAMHD1 evolution. Of the 6 sites identified under strong positive selection, residues 46 and 69 in the SAM domain showed unmistakably strong signals of recurrent positive selection (Figure 39A and Figure 40). These residues also differ in certain primate species' SAMHD1 that show opposite susceptibility to Vpx. In particular, AGM and mandrill SAMHD1 differ at positions 46 and 69, with mandrill encoding the 'ancestral state' at both sites while AGM encodes the 'derived' state (Figure 39A).

To determine if the changes at position 46 and 69 are responsible for the species-specificity of SAMHD1 antagonism by Vpx, we investigated SAMHD1 degradation by SIVmnd2 Vpx, which can degrade mandrill but not AGM SAMHD1 (Table I). I made D46G and Q69R mutations in the AGM 'resistant' SAMHD1 backbone, reverting these two positions to their 'ancestral' state. I found that the introduction of either mutation resulted in increased susceptibility to degradation by SIVmnd2 Vpx (Figure 39B, see AGM D46G, AGM Q69R). This increased sensitivity of SAMHD1 correlated with increased binding to SIVmnd2 Vpx since SIVmnd2 Vpx strongly co-immunoprecipitated with mandrill SAMHD1, but its interaction with AGM SAMHD1 was much weaker (Figure 39C). However, either single reversion point mutation (AGM D46G, AGM Q69R) resulted in a stronger interaction

with SIVmnd2 Vpx (Figure 39C; compare last three lanes). Thus, changes at the positively selected residues 46 and 69 in SAMHD1 determine both binding and susceptibility to Vpx.

I also tested the reciprocal G46D and R69Q mutations in the 'sensitive' Mandrill SAMHD1. I found that while neither mutation alone was sufficient to confer resistance to SIVmnd2 Vpx degradation (Figure 39D, Mnd R69Q and Mnd G46D), a combination of both mutations together resulted in the gain of resistance against degradation by SIVmnd2 Vpx. Thus, these results demonstrate that changes in amino acids evolving under positive selection in SAMHD1 are necessary and sufficient to determine specificity of Vpx antagonism. This strongly suggests that a Vpx-like factor was responsible for the recurrent positive selection on SAMHD1 during primate evolution.

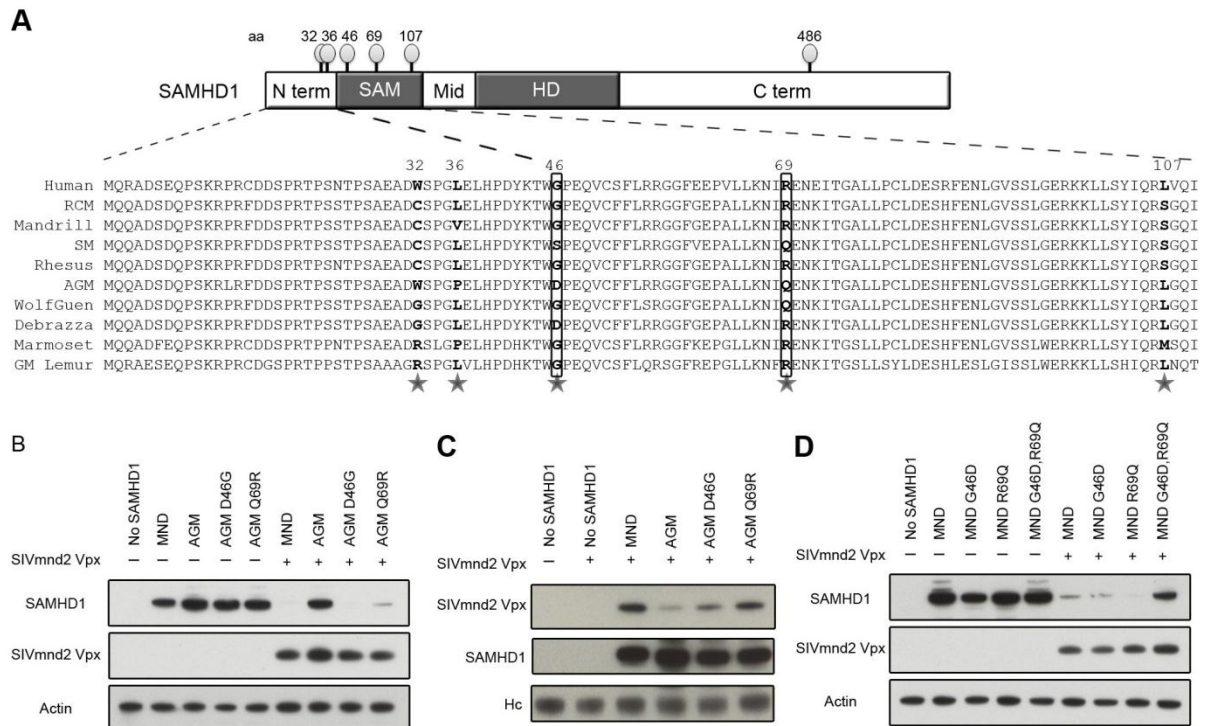


Figure 39

SAMHD1 positive selection residues map to Vpx sensitivity.

(A) Alignment of N-terminal and SAM domain regions from indicated primates. Symbols (circle on a stick) represent the positively selected residues marked on the SAMHD1 domains. Sites 46 and 69 which displayed highly significant signals of positive selection are boxed in the alignment. Stars represent the codons under positive selection with strong support (Figure S3A, S3B and S3C). The N terminal region of SAMHD1 from grey mouse lemur is included to represent amino acid residues encoded by a distantly related prosimian primate.

(B) Expression of mandrill, AGM and AGM point mutants (AGM D46G and AGM Q69R) were analyzed by western blot, in the presence or absence of SIVmnd2 Vpx expression.

(C) Western blot analysis of HA-immunoprecipitated SAMHD1 for FLAG-epitope tagged SIVmnd2 Vpx association. Cells were treated with 25 μ M MG-132 for 12 hours prior to immunoprecipitation. Heavy chain (Hc) is shown as a loading control.

(D) Western blot shows expression of SAMHD1 from mandrill and mandrill-derived mutations (Mnd G46D, Mnd R69Q, and Mnd G46D, R69Q) in the presence or absence of SIVmnd2 Vpx.

A
PAML analysis of codons under positive selection in SAMHD1 full gene (Old World monkeys)

Codon	dN/dS	P-value
32	7.68	0.995
36	7.40	0.955
46	7.63	0.988
69	7.67	0.994
107	7.41	0.955
486	7.61	0.986

B
REL analysis codons under positive selection in SAMHD1 full gene (Old World monkeys)

Codon	dN/dS	Bayes Factor
32	4.06	161.9
36	4.22	311.8
46	4.16	238.2
69	4.17	259.4
107	4.12	191.9
486	4.11	196.5

C
REL analysis codons under positive selection in SAM domain (Old World monkeys)

Codon	dN/dS	Bayes Factor
46	5.37	31736.8
69	5.37	55554.4
107	4.39	24.6

Figure 40

(A) Codons with a posterior probability of >95% were highlighted in a PAML analysis of *SAMHD1* genes from Old World monkeys (16 species) which showed the strongest burst of positive selection in primates (Figure 37B).

(B) Summary of the REL analysis of whole *SAMHD1* gene from 16 Old World monkeys.

(C) The SAM domain showed the strongest signatures of positive selection within Old World monkeys using PAML (Figure 37C). Therefore, REL analysis was repeated using only the SAM domain from Old World monkeys.

The ability to degrade SAMHD1 preceded the birth of Vpx in primate lentiviruses

I wished to determine whether the ability to degrade SAMHD1 was an ancestral trait common to all Vpr/Vpx proteins, and that function was subsequently lost by some Vpr lineages across evolution; or alternatively, whether the ancestral Vpr/Vpx lacked the ability to degrade SAMHD1, but the trait was gained (neofunctionalized) over the course of primate lentivirus evolution. However, in order to interpret whether there was a gain or a loss of the ability of Vpr/Vpx to degrade SAMHD1, it was necessary to root the *vpr/vpx* phylogenetic tree from Figure 35A. Previous studies demonstrated that the endogenous lentivirus in the genomes of lemurs, pSIVgml, is 2 to 6 million years old and unambiguously forms an outgroup to all extant primate lentiviruses (75, 76, 145). However, pSIVgml does not encode a *vpr* or *vpx* gene. Therefore, we performed a phylogenetic analysis of *pol* sequences and found that SIVolc and SIVwrc, which infect the primate species of the *Colobinae* subfamily of OWM, are the closest relative to SIVgml that contain an existing *vpr/vpx* gene (Figure 42A), consistent previous studies (75, 76)). Analysis of *env* sequences (which are 3' of *vpr* and *pol*) showed that the pSIVgml nests with the similar cluster of sequences (Figure 42B). Therefore, we used SIVolc/SIVwrc *vpr* sequences to root the *vpr/vpx* tree, reflecting the high likelihood that this clade represented the earliest branching event of extant primate lentiviruses.

Using this rooted tree, I overlaid the SAMHD1 degradation phenotype onto the phylogeny and found that the *vpr* genes that lacked SAMHD1 degrading ability (Figure 41, red stars) were clearly separable from the SAMHD1 degrading *vpr* and *vpx* genes (Figure 41,

blue stars). Strikingly, all *vpr* and *vpx* genes that shared the ability to degrade SAMHD1 nest within the same monophyletic clade with high confidence (Figure 41, BS = 90.3; Figure 36A, PP = 0.97). Since Vpr from HIV-1, HIV-2, SIVmac, SIVrcm, and SIVmnd2 were unable to degrade SAMHD1 (Figure 41, red stars), the most parsimonious explanation is that the Vpr of their common ancestor (Figure 41, Node 3) lacked the SAMHD1 degradation capability. Given that the outgrouping SIVmnd1 Vpr and SIVolc Vpr proteins were incapable of degrading SAMHD1 (Figure 34 and Figure 35), this strongly supports the hypothesis that the ancestral Vpr was “inactive” against SAMHD1 (Figure 41, Node 1) and the ability to degrade SAMHD1 subsequently arose only once during *vpr* and *vpx* evolution.

Based on the phylogeny, I can clearly pinpoint that the neofunctionalization of Vpr to degrade SAMHD1 occurred on the branch leading up to the split of SIVagm, SIVdeb/mus/mon lineages (Figure 41, Node 2). Importantly, based on phylogeny, our results suggest that the birth of the *vpx* recombination/duplication dated after the neofunctionalization occurred (Figure 41, Node 4). Thus, the combined phylogenetic and functional study presented here strongly supports a scenario in which the degradation of SAMHD1 by Vpx was preceded by the neofunctionalization of Vpr in a transitional SIV lineage. Furthermore, this phylogenetic framework argues against a subsequent loss of SAMHD1-degrading ability in any lentiviral Vpr protein; that is, those Vpr proteins that currently lack this ability including HIV-1 Vpr likely never possessed it.

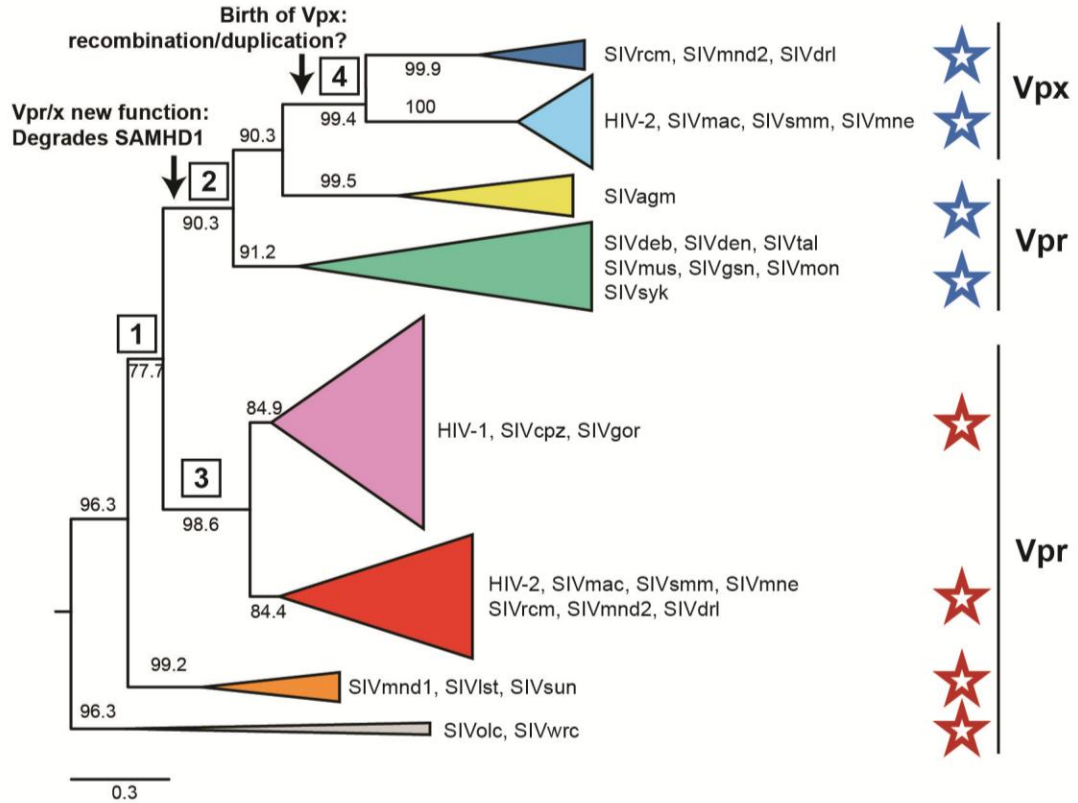


Figure 41

SAMHD1 degradation by some Vpr proteins preceded the birth of Vpx.

(A) The phylogeny shown in Figure 35 was rooted to common ancestor of SIVolc/SIVwrc, as determined by the phylogenetic positioning of the flanking *pol* and *env* genes in relation to pSIVgml (Figure 42), and is consistent with previous reports that the *Colobinae* SIVs are outgroup to the *Cercopithecinae* SIVs (75, 76, 145). Important nodes that infer ancestral traits are boxed in numbers.

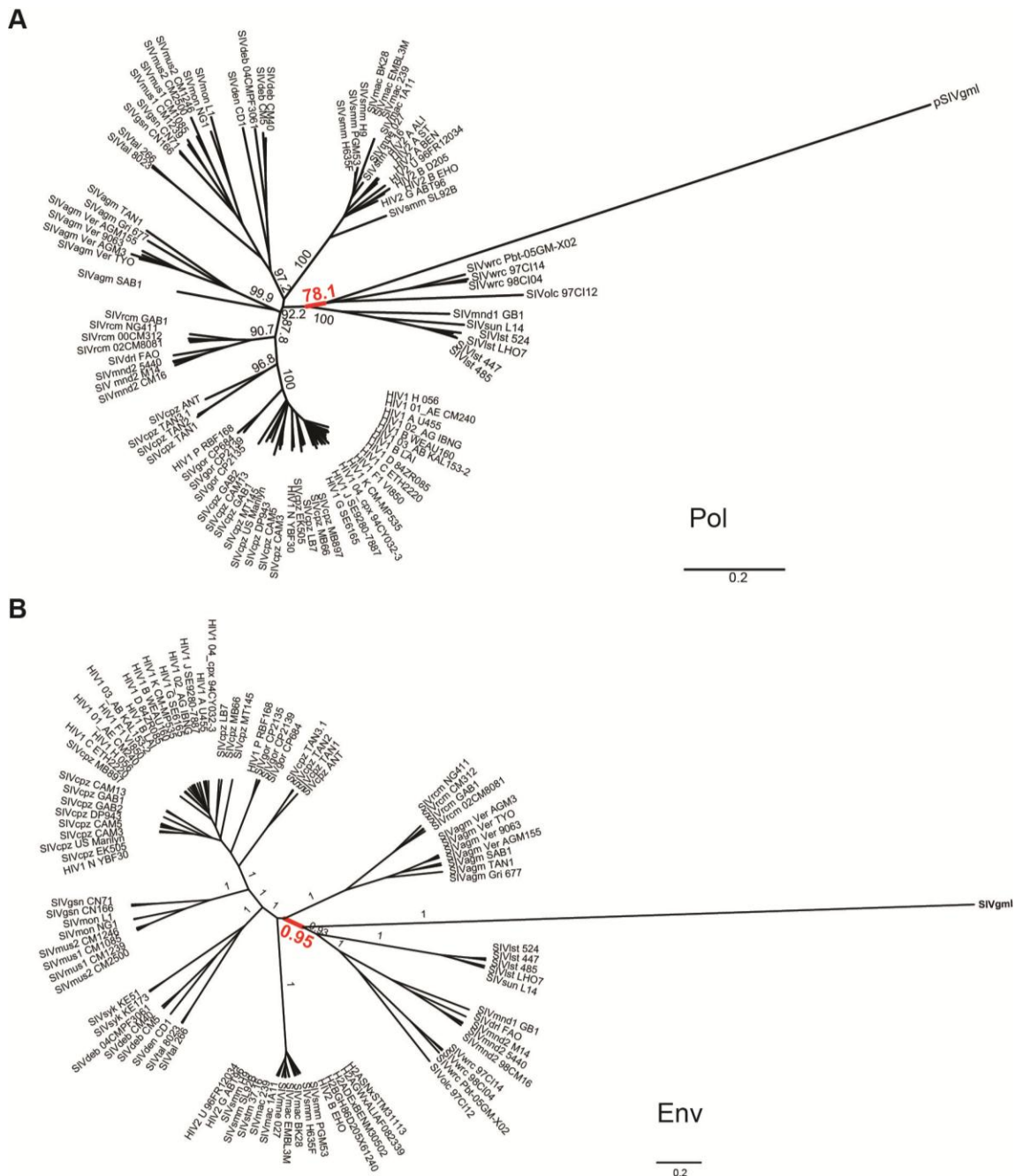


Figure 42

(A) Unrooted phylogeny of 92 *pol* sequences (1,103 aa region) from diverse primate lentiviruses using maximum likelihood method to determine the earliest branching event of extant primate lentiviruses.

(B) Similar branching order of pSIVgml was observed from the *env* sequences using a maximum likelihood method; however, there was low bootstrap support due to the short sequence alignment (55 aa region). Therefore, the phylogeny was constructed using a Bayesian MCMC inference.

DISCUSSION

Here I show that diverse Vpx proteins as well as some Vpr proteins have the ability to target their host species' SAMHD1 for degradation. Both Vpx and Vpr antagonists display species-specific degradation of SAMHD1 which are in some cases quite specific to the virus's extant host. Such species specificity is a hallmark of an antagonistic 'arms race' between host and virus, in which both sides rapidly evolve to gain an advantage. Indeed, I show that SAMHD1 has been evolving under positive selection in primates. I demonstrate that the residues under positive selection in the SAM domain of SAMHD1 determine the specificity of degradation by Vpx, directly implicating Vpr/Vpx antagonism as the source of the remarkable signature of positive selection detected in SAMHD1, which is most pronounced in the Cercopithecina subfamily of Old World monkeys. By combining our functional results with phylogenetic analyses, we show that the ability to degrade SAMHD1 is a neofunctionalization of Vpr which preceded the birth of Vpx by recombination/duplication.

Based on our combined phylogenetic and functional analyses, the common ancestor of SIV viruses most likely encoded a single Vpr that was “inactive” against SAMHD1. The ability to recruit a protein degradation complex is important for Vpr-mediated cell cycle arrest (reviewed in (51)) and thus may represent the ancestral function of Vpr/Vpx. Interestingly, although cell cycle arrest and SAMHD1 degradation functions are segregated into two separate proteins in those viruses that encode Vpr and a Vpx (14), SIVagm Vpr is able to cause both cell cycle arrest (207, 257) and SAMHD1 degradation (Figure 35A). This indicates that the two functions are not mutually exclusive. Furthermore, since cell cycle

arrest by Vpr has species-specificity (257), it is likely that the substrate used by Vpr to cause cell cycle arrest will, like SAMHD1, have evolved under positive selection.

While the cellular protein targeted by Vpr to cause cell cycle arrest is not yet known, the adaptive evolution of SAMHD1 might provide a clue as to why some viruses evolved to encode a separate Vpx and Vpr gene. One scenario we propose is that the neofunctionalization of the ancestral Vpr/x to target SAMHD1 exerted a strong selective pressure on old world monkeys' SAMHD1. As a result, variants of SAMHD1 that conferred protection from Vpr/x antagonism were selected for, leading to the signatures of rapid evolution in SAMHD1, especially localized within the SAM domain. This posed a unique challenge to the ancestral Vpr/x that had to recognize both the cell cycle arrest-factor and multiple rapidly evolving variants of SAMHD1. In order to maintain both functional capabilities, a recombination/duplication of Vpr might have given rise to Vpx. This subsequently allowed the subfunctionalization of Vpx to maximize its SAMHD1-targeting capability, while preserving the cell cycle arrest phenotype in Vpr. This model might explain the complicated evolutionary history of *vpr* and *vpx* (246, 277, 278). Thus, we speculate that the “birth” of a new gene in some lineages leading to both *vpr* and *vpx* in the same viral genome, was a more modern event compared to the neofunctionalization of Vpr, may have been directly driven by the rapid evolution of the SAMHD1 protein.

Why HIV-1 does not encode Vpx

HIV-1 lacks the capability of degrading SAMHD1 since its Vpr protein is unable to degrade SAMHD1 and it does not encode Vpx. Since SIVcpz Vpr also lacks SAMHD1-

degrading ability (Figure 35A), this function was missing in HIV-1 even prior to its cross-species transmission from chimpanzees into humans (). Moreover, human SAMHD1 is not special in terms of its resistance to Vpr antagonism as it is readily degraded by HIV-2 Vpx. This situation is directly analogous to the two lentiviruses that infect mandrills. SIVmnd1 contains only a Vpr gene that has no activity against mandrill SAMHD1 (Figure 34C), whereas SIVmnd2 has both Vpr and Vpx, the latter of which is capable of degrading mandrill SAMHD1 (Figure 34C). Intriguingly, SIVmnd1 appears more pathogenic than SIVmnd2 similar to the higher pathogenicity of HIV-1 relative to HIV-2 (255). One possible explanation is that both HIV-1 and viruses like SIVmnd1 evolved unique antagonistic functions (or more effective countermeasures) that collectively allow HIV-1 to achieve sufficient replicative potential in target cells (including SAMHD1-expressing monocytes) even in the absence of SAMHD1-degrading abilities. On the other hand, Vpx-encoding viruses may have become more dependent on the ability to counteract SAMHD1 to achieve successful replication in target cells and have relaxed selection on alternate measures used by viruses like HIV-1.

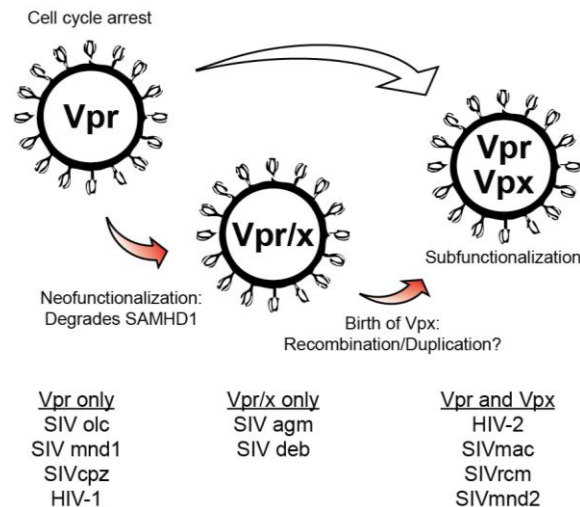


Figure 43

Vpr and Vpx functions and evolution in primate lentiviruses. The ancestral trait of Vpr in primate lentiviruses is likely to cause cell cycle arrest. During its course of evolution, Vpr from some lineages gained the ability to degrade SAMHD1. Subsequently, through recombination or duplication, certain lineages acquired and subfunctionalized Vpx and Vpr.

What the confined signatures of positive selection mean

Most of the signatures of positive selection in primate *SAMHD1* appear to originate from the old world monkey lineages, specifically the subfamily *Cercopithecinae* after its split from *Colobinae*. This highly localized positive selection on the primate phylogeny is unusual. Most previously analyzed host immune genes, such as TRIM5alpha, Tetherin, PKR and APOBEC3G, display signatures of positive selection throughout many primate lineages including hominoids and new world monkeys (58, 142, 163, 166, 230, 231) while others have been restricted to hominoids and old world monkeys alone (TRIM22). Such a localized signature of positive selection might signal the advent of a highly specialized and unique

antagonist. Intriguingly, our phylogenetic framework (Figure 41) strongly argues that the Vpr/Vpx proteins' ability to degrade SAMHD1 arose within the primate lentiviruses, and specifically among lentiviruses that infect *Cercopithecinae* and jumped into *Hominidae*, but not viruses that infect *Colobinae*.

An interesting observation is that SAMHD1 in orang utans are the only primate species outside of the *Cercopithecinae* subfamily that also has a strong signature of positive selection. Yet, to date, there is no evidence of SIVs in orang utans. However, the caveat is that most studies have focused on looking for foamy virus and herpesviruses (122, 287), and lentiviruses might not have been assayed for. Given their unique geographical isolation in south eastern Asia, discovering a primate lentivirus from orang utans or species in that geographical location would be very informative. Alternatively, there are also reports of simian T-lymphotropic virus (STLV) and simian type D retrovirus (SRV) infections in orang utans (287, 294). It might be worth investigating if these viruses encode an antagonist against SAMHD1.

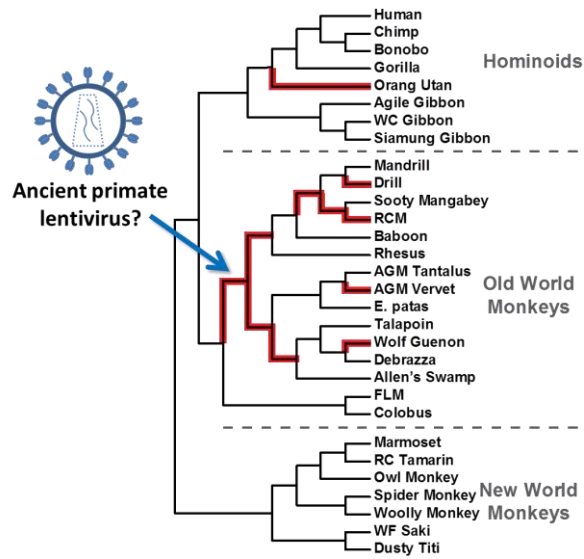


Figure 44

SAMHD1 from multiple primate lineages in *Cercopithecinae* subfamily species have been evolving under positive selection. Since the adaptive evolution of *SAMHD1* was driven by Vpr/Vpx, this infers the presence of ancient primate lentiviruses since antiquity.

CHAPTER SEVEN

SUMMARY AND DISCUSSION

In summary, my research has provided a detailed interdisciplinary perspective of host-virus arms races. By integrating evolutionary biology with virology, I have reconstructed the chronological context of how hosts evolve around viral pressures and ways viruses counter-evolve. First, lentiviruses are able to evolve new functions within existing gene repertoires to counteract rapidly host antiviral genes. Secondly, hosts escape from viral pressure either by single amino acid changes or by deletions of a 'susceptibility domain'. Finally, this work has allowed us to pinpoint the origin of the evolutionary “arms race” between primates and lentiviruses. Thus, my thesis research has helped define the rules by which host-virus arms races ensue.

The astronomical viral diversity that challenges the immune system poses a problem of recognition and specificity. An interesting challenge is that, unlike adaptive immunity which involves somatic learning and memory, host restriction factors are germline-encoded. Therefore, how do germline host restriction factors evolve to escape from viral pressures? And how do antiviral proteins maintain the ability to target the wide spectrum diversity and short time-scale evolution of viruses? In turn, what strategies do viruses employ to counter-evolve to their hosts? Thus, **host antiviral restriction is fundamentally an evolutionary problem**. That is why this combined approach is very effective and yields significant insights.

In this chapter, I will:

- Describe implications of 2 specific host-virus “arms race”
- Detail future research directions that address these implications
- Define features of host restriction factors

Modern consequences for HIV in the Tetherin “arms race”

The Tetherin “arms race” is the best example to date of how past viral pressures have real consequences for modern infections. HIV-1 uses its Vpu accessory protein to counteract Tetherin, but the immediate precursor SIVcpz uses a different accessory protein, Nef, to antagonize its host chimpanzee Tetherin instead. This means that HIV-1 adapted to humans by switching from using Nef to antagonize Tetherin to using another protein, Vpu to do this job. I resolved the mystery of how and why this occurred.

I have found that *tetherin* has been evolving under positive selection in primates. The residue under the strongest recurrent positive selection is the site of functional interaction of Tetherin with Nef. In fact, an amino acid substitution at this single position can determine the susceptibility of Tetherin to Nef antagonism. However, human Tetherin has a unique 5-amino-acid deletion that lost this residue, rendering it immune to Nef. These are significant findings because it demonstrates that hosts escape from viral pressure either by single amino acid changes or by deletions of a 'susceptibility domain'.

As a result of the unique deletion, SIVcpz Nef could not antagonize human Tetherin, and I showed that HIV-1 Vpu evolved to counteract Tetherin upon its transmission to humans through changes at its N-terminus. Thus, we can infer that **positive selection to resist a Nef-like antagonist resulted in the unique deletion in human Tetherin, which in turn drove HIV-1 to switch from Nef to Vpu as its Tetherin-antagonist**. This has two important implications. First, HIV-1's adaptation was a direct consequence of an adaptive escape (5aa deletion) from a past antagonist. This means that the evolutionary history and trajectory of host genes directly influence contemporary host-virus interactions. Second, viruses evolve new functions within existing gene repertoires to counteract rapidly host antiviral genes. The Nef to Vpu "switch" goes against the norms and expectation that adaptation would occur within the precursor Nef antagonist, instead HIV-1 neofunctionalized a separate and distinct Vpu accessory protein. This is the strongest evidence of the remarkable genetic flexibility that HIV and lentiviruses possess. The significance of this is further emphasized by the observation that SIVmus Vpu also has this capacity to antagonize Tetherin (Chapter Three, (144)), indicating that this adaptation has occurred at least twice in different viral lineages.

HIV-1 Nef has unlocked a new and unknown function?

The immediate health relevance of the Nef to Vpu "switch" applies to the pandemic HIV-1. While the evolution of SIVcpz Nef was originally constrained in its role as an antagonist of Tetherin, the evolution of HIV-1 Vpu to antagonize Tetherin may have allowed

HIV-1 Nef to evolve novel functions in humans and to contribute to the pathogenicity of the virus (229). For example, Nef has been implicated in the enhancement of viral infectivity, the downregulation of CD4, major histocompatibility complex class I (MHC-I), and other cell surface receptors, and the remodeling of the actin cytoskeleton (12, 50, 124, 151, 258). It will be informative to observe if some of these functions have evolved in the transition of SIVcpz to humans in ways that increase HIV-1 pathogenicity (124). Importantly, only the pandemic Group M precursor virus made this Vpu switch (229), suggesting that this could be a critical adaptation to the pandemicity of HIV-1 Group M.

To address this, we would first have to identify the determinants for Nef's Tetherin-antagonist activity. That is, what allows SIVcpz Nef to antagonize Tetherin? The expectation is that this phenotype can be conferred onto the inactive HIV-1 Nef by constructing chimeric proteins. One study has since implicated the C-terminal of SIVcpz Nef in this function (314). Furthermore, sequence prediction will be very effective since this motif should be highly conserved in SIVcpz strains. The identity of the Nef determinant might have known functions associated with it and thus inform us of concrete phenotypes to test for. In this model, we would predict that HIV-1 Nef has adapted becoming more effective at an existing function than the precursor SIVcpz Nef. This should be a significant difference that can be quantified.

However, the evidence that HIV-1 Nef has lost its precursor antagonistic activity against Tetherin (Figure 21) strongly suggests that it has neofunctionalized. In this model, we predict that the relaxation of selective constraint allowed HIV-1 Nef to adapt a new

function that the precursor SIVcpz Nef does not possess. Nef is characteristic for its adaptor role in which it directly binds a cellular protein (CD4 or MHC I) and recruits a trafficking complex (AP2 or AP1). Likewise, the hypothesis is that HIV-1 Nef is binding a novel substrate. Therefore, the best method for this problem will be a mass spectrometry analysis of affinity purified proteins that interact with HIV-1 Nef. The key to the success of this approach lies in the specificity of the Nef chimeric proteins. We will capitalize on the profile from their other conserved functions to render background sensitivity irrelevant. Furthermore, we will have a strict definition to identify the candidate proteins since the anti-Tetherin activity of Nef chimeras will be a directly inverse surrogate for the novel function. Ultimately, the single immediate focus is to identify the novel Nef function behind the pathogenicity of HIV-1.

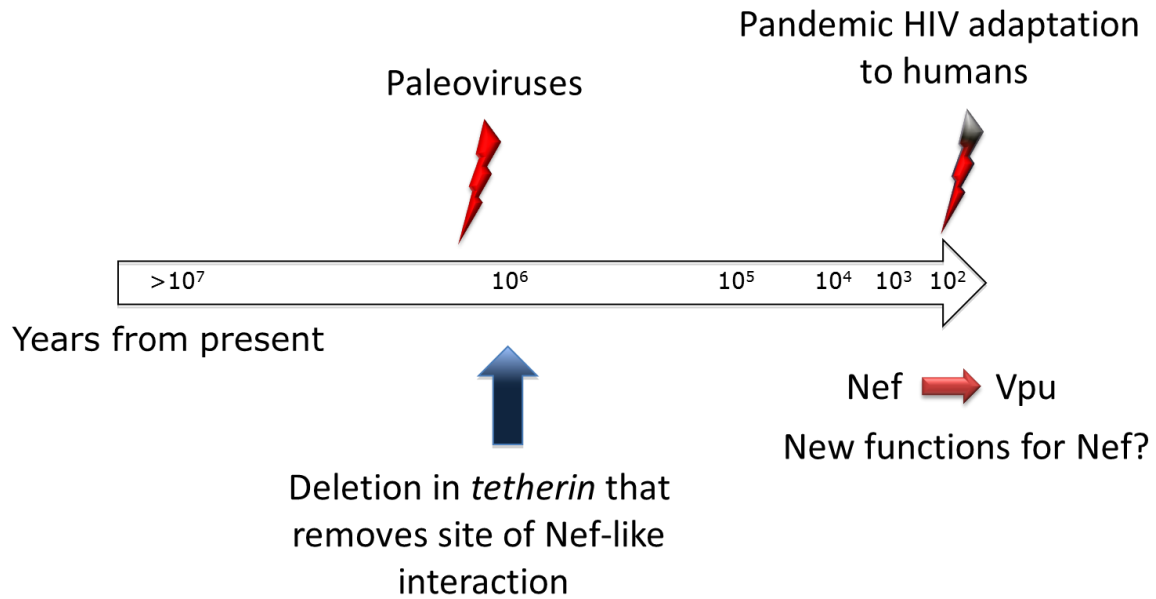


Figure 45

Summary of evolutionary events leading up to HIV-1 neofunctionalization of Vpu to counteract human Tetherin.

Primate *tetherin* gene has been evolving under positive selection due to selective pressures from viral antagonists. To evade an ancient Nef-like antagonist, a 5 amino acid deletion in human tetherin was selected for. As a result, upon the cross-species transmission of HIV-1, the precursor Nef protein was unable to antagonize human tetherin and had to evolve Vpu to counteract tetherin. Since then, HIV-1 Nef has lost the ability to recognize tetherin and I speculate that it might have adapted a new function.

On the Origin of the SAMHD1 “arms race”

The SAMHD1 arms race reinforces the novel findings that neofunctionalization is a viral strategy of host adaptation. The most important question that was answered through the SAMHD1 study is whether SAMHD1 antagonism was an ancestral trait that was lost in some lineages or a newly acquired function. While Vpx is only encoded by some lineages of

primate lentiviruses, its paralog, Vpr, is conserved across all. I have found that while the ability to degrade SAMHD1 is conserved across multiple lineages' Vpx, some Vpr proteins can also degrade SAMHD1. The discovery of these Vpr SAMHD1-antagonists is very significant because it allowed me to conclusively pinpoint when this transitional state arose along the evolution of Vpr and Vpx. By overlaying their functions on a phylogenetic framework of Vpr and Vpx evolution, we can conclude that **Vpr neofunctionalized to degrade SAMHD1 even prior to the birth of a separate Vpx.**

I have also shown that residues in SAMHD1 under positive selection directly determine Vpx sensitivity. This suggests that the **birth of the SAMHD1-degrading ability within primate lentiviruses initiated the evolutionary arms-race** that led to such a highly localized signature of positive selection within *Cercopithecinae* (Figure 37). Taken together, this means that both the positive selection of SAMHD1 and consequently the birth of Vpx may have been driven by the neofunctionalization of Vpr to antagonize SAMHD1. This subsequently allowed the subfunctionalization of Vpx to target rapidly evolving variants of SAMHD1. Thus, the reconstruction of the SAMHD1 and Vpr/Vpx genetic conflict is very exciting because it has given us an unprecedented view into how evolutionary “arms races” are initiated.

Implications for the recombinant origin of HIV-1/SIVcpz ancestor

The findings of the SAMHD1 study also raise important questions about the origin of the hybrid recombinant common ancestor of HIV-1/SIVcpz. Move up one paragraph so that

it follows the other SAMHD1 discussion. The common ancestor HIV-1/SIVcpz lineage is the result of a double recombination between SIVrcm (5' coding region) and (3' end), and SIVmus/gsn lineage (Vpu and Env region). Importantly, the two distinguishing features of the recombinant are that it lacks a Vpx but does encode Vpu. Prior to this work, phylogenetic inference of the genes around the region of recombination (Vif, Vpx, Vpr and Vpu) would suggest a two-step process (Figure 46, Scenario 1). First, since the Vif and Vpr from HIV-1/SIVcpz and SIVrcm are more phylogenetically related, this suggests that the precursor recombinant would have acquired both the Vpx and Vpr since Vpx lies 5' upstream of Vpr. However, the recombinant HIV-1/SIVcpz ancestor lacked Vpx. The phylogeny strongly argues against the current HIV/SIVcpz Vpr being a misnamed Vpx. In that scenario, I would expect that HIV/SIVcpz Vpr to be more closely related to SIVrcm Vpx than SIVrcm, but that is not the case. Instead, SIVcpz/HIV-1 Vpr clusters with Vpr genes, and clearly separate from Vpx genes, supporting that it has been named accurately as a Vpr. Yet, there is no evidence of Vpx-like sequence erosion between Vif and Vpr. In fact, the first 60-80 bp of Vpr that overlaps into 3' end of Vif is maintained. Therefore, in the second stage, Vpx had to be lost subsequently by another recombination event or mechanism that allowed the Vif/Vpr overlap to be restored (Figure 46). While this might be possible, it is highly unlikely.

Instead, I propose an alternative hypothesis that the recombination was with a SIVmus/gsn lineage and an ancestral SIVrcm that encoded a single Vpr, which existed prior to the birth of Vpx and was incapable of degrading SAMHD1 (Figure 46, Scenario 2). This would explain why the Vif/Vpr overlap is still maintained. More importantly, this means that

HIV-1 Vpr does not degrade SAMHD1 because it never acquired this function. There are two lines of evidence to support the plausible existence of such an ancestral SIVrcm. First, phylogenetic and functional analyses in Chapter Six support that prior to the neofunctionalization of *vpr* and birth of *vpx*, primate lentiviruses had a single *vpr* that was incapable of degrading SAMHD1. Secondly, while none of the extant SIVrcm sequenced to date encode only a single *vpr* gene, there are non-recombinant primate lentiviruses such as SIVolc and SIVsun/SIVlst that fit this description. This is in contrast to an evolutionary scenario where primate lentiviruses had both *vpx* and *vpr*, but *vpx* was lost in some lineages. Furthermore, this implies that the current SIVrcm (Vpx- and Vpr-encoding) has replaced the ancestral single *vpr* SIVrcm (Figure 46). However, I note that this is based on the inference that the acquisition and subfunctionalization of *vpx* and *vpr* is more evolutionarily fit for the virus than having a single *vpr*. Nonetheless, this means that the fate of the ancestral single *vpr* SIVrcm virus lead to either an acquisition of *vpx* (current SIVrcm) or *vpu* (HIV-1/SIVcpz lineage). Together, this strongly suggests that ancestral recombinant of SIVcpz/HIV-1 was much older and likely pre-dated the cross-species transmission into chimpanzees. This implies that the recombination event did not occur in chimpanzees (a recent event), as widely hypothesized.

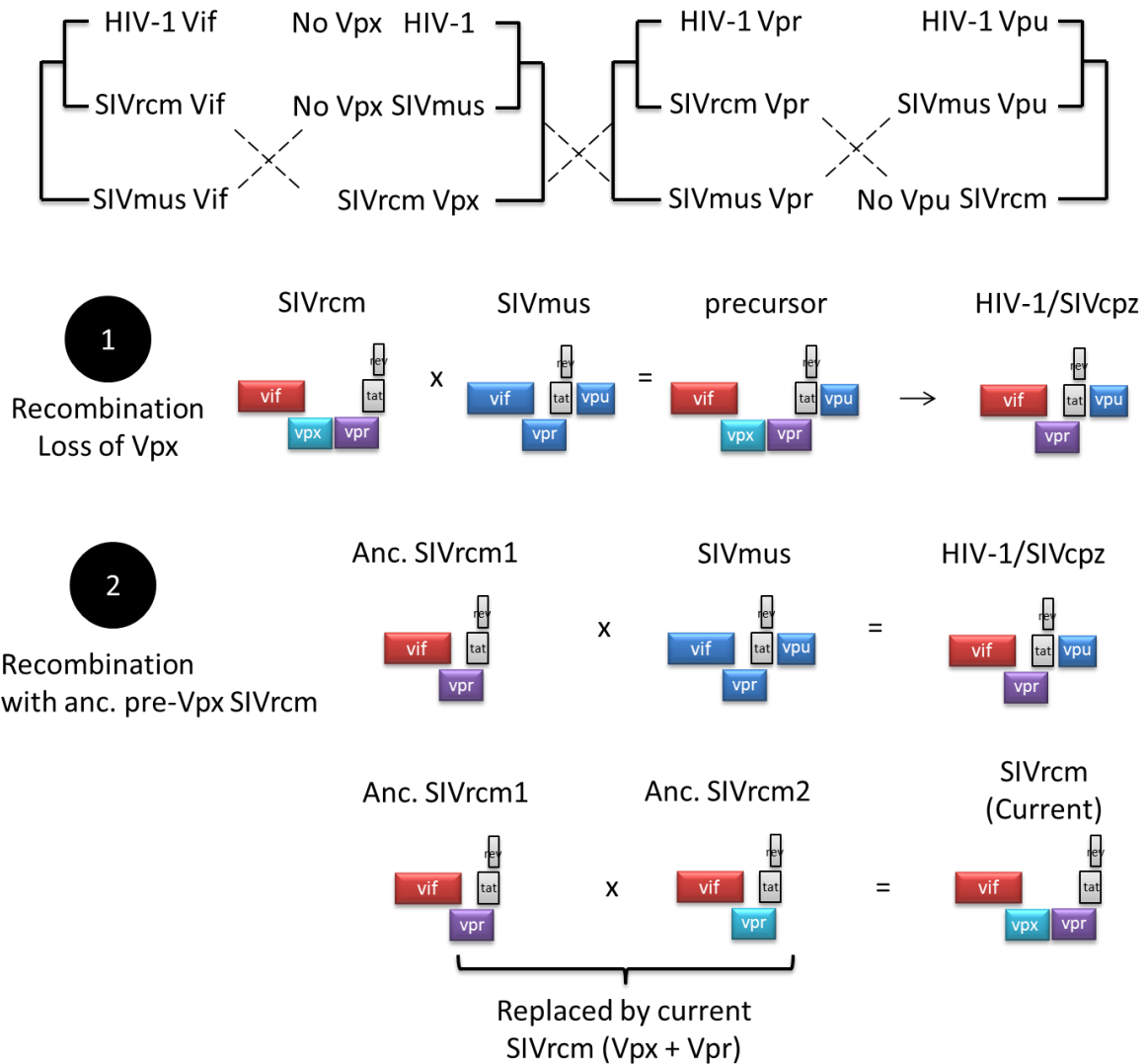


Figure 46

Hypothetical scenarios for the origin of the recombinant precursor of SIVcpz/HIV-1. Phylogenies of Vif, Vpx, Vpr and Vpu (top) show that the precursor of SIVcpz/HIV-1 resulted from multiple recombinations (dotted lines) between SIVrcm and SIVmus/gsn lineages. In scenario 1, the recombination event was followed by the loss of Vpx which maintained/restored the Vif/Vpr overlap. In scenario 2, the recombination was with an ancestral SIVrcm that existed prior to the birth of Vpx. This virus has since been replaced by the Vpx encoding strains. The viral origins of the different segments can be traced by colors: SIVmus (blue), SIVrcm (red), the neofunctional vpr/vpx (cyan).

The discovery of Vpr proteins that can antagonize SAMHD1 raises several immediate research questions. First, what are the viral determinants for Vpr's recognition of SAMHD1? To address this, we will construct chimeric Vpr proteins to assay for a gain of function activity. Our diverse panel of characterized Vpr proteins combined with our *vpr* sequence analyses will allow us to make informative decisions on how to map the phenotype. The expectation is that the 'active' Vpr proteins encode a conserved SAMHD1-interacting motif that is poorly conserved or absent from the 'inactive' Vpr proteins. Secondly, how does the single Vpr protein maintain its ability to degrade SAMHD1 and also cause cell cycle arrest? I have found that SIVagm Vpr can degrade AGM SAMHD1. Previous work from our lab has also found SIVagm Vpr can exert a G2 cell cycle arrest in AGM cells (257). Therefore, mapping the determinants of Vpr will directly impact our understanding of the cell cycle arrest mechanism. For instance, if both functions map to the same region of Vpr, this would suggest that the G2 arrest target could be another SAM-domain containing protein. Alternatively, if Vpr determinants of SAMHD1-binding are distinctly separable from G2 arrest function, this would explain how the neofunctionalization of Vpr occurred. Our contribution here will be a crucial part of the larger goal to identify the unknown cellular protein behind the Vpr cell cycle arrest phenotype.

Exploiting the evolutionary signatures of host restriction factors

Finally, **host antiviral restriction is fundamentally an evolutionary problem**. I have reconstructed two specific examples that convincingly show that host restriction factors are locked in a Red Queen's arms race with viruses. This means that we can exploit the

evolutionary signatures of positive selection to screen for novel host restriction factors. This will involve cross-reference existing interferon stimulated gene databases for genes evolving under positive selection to generate an exclusive list of candidate genes. By distinguishing the bona fide host restriction factors repertoire, we will be poised to characterize antiviral strategies and effectively design complementing therapeutics.

There are two considerations to this approach. First, the host restriction factor activity may be dependent on the virus model system. For instance, although Viperin potentially restricts Influenza virus and HCV, I have found that it does not inhibit HIV-1 at biologically-relevant levels. Second, evolutionary analyses must take deletions/insertions into consideration. For instance, the adaptive evolution of human Tetherin involved a unique deletion. Thus, the strategies and detailed examples featured in this dissertation is a practical guide on how to effectively integrate evolutionary biology with virology.

Closing remarks

In conclusion, the broad themes that emerge from my research are two-fold. First, lentiviruses are able to evolve new functions within existing gene repertoires to counteract rapidly host antiviral genes. Secondly, hosts escape from viral pressure either by single amino acid changes or by deletions of a 'susceptibility domain'. Using a reconstruction of the evolutionary "arms race" between primates and lentiviruses, my thesis research has helped define the rules by which host-virus arms races ensue. Based on my findings, we contend that the host evolutionary framework is a fundamental pillar of antiviral restriction.

REFERENCES

1. **Abbink, T. E., and B. Berkhout.** 2008. HIV-1 reverse transcription initiation: a potential target for novel antivirals? *Virus Res* **134**:4-18.
2. **Adachi, A., H. E. Gendelman, S. Koenig, T. Folks, R. Willey, A. Rabson, and M. A. Martin.** 1986. Production of acquired immunodeficiency syndrome-associated retrovirus in human and nonhuman cells transfected with an infectious molecular clone. *J Virol* **59**:284-291.
3. **Aghokeng, A., E. Bailes, S. Loul, V. Courgnaud, E. Mpoudi-Ngolle, P. Sharp, E. Delaporte, and M. Peeters.** 2007. Full-length sequence analysis of SIVmus in wild populations of mustached monkeys (*Cercopithecus cephus*) from Cameroon provides evidence for two co-circulating SIVmus lineages. *Virology* **360**:407-418.
4. **Allan, J., P. Kanda, R. Kennedy, E. Cobb, M. Anthony, and J. Eichberg.** 1990. Isolation and characterization of simian immunodeficiency viruses from two subspecies of African green monkeys. *AIDS Res Hum Retroviruses* **6**:275-285.
5. **Allan, J., M. Short, M. Taylor, S. Su, V. Hirsch, P. Johnson, G. Shaw, and B. Hahn.** 1991. Species-specific diversity among simian immunodeficiency viruses from African green monkeys. *J Virol* **65**:2816-2828.
6. **Anderson, E. C., and A. M. Lever.** 2006. Human immunodeficiency virus type 1 Gag polyprotein modulates its own translation. *J Virol* **80**:10478-10486.
7. **Anderson, J. L., E. M. Campbell, X. Wu, N. Vandegraaff, A. Engelman, and T. J. Hope.** 2006. Proteasome inhibition reveals that a functional preintegration complex intermediate can be generated during restriction by diverse TRIM5 proteins. *J Virol* **80**:9754-9760.
8. **Andrew, A. J., E. Miyagi, and K. Strebel.** 2011. Differential effects of human immunodeficiency virus type 1 Vpu on the stability of BST-2/tetherin. *J Virol* **85**:2611-2619.
9. **Apetrei, C., D. L. Robertson, and P. A. Marx.** 2004. The history of SIVS and AIDS: epidemiology, phylogeny and biology of isolates from naturally SIV infected non-human primates (NHP) in Africa. *Front Biosci* **9**:225-254.
10. **Arhel, N.** 2010. Revisiting HIV-1 uncoating. *Retrovirology* **7**:96.
11. **Arhel, N. J., and F. Kirchhoff.** 2009. Implications of Nef: host cell interactions in viral persistence and progression to AIDS. *Curr Top Microbiol Immunol* **339**:147-175.
12. **Ariën, K., and B. Verhasselt.** 2008. HIV Nef: role in pathogenesis and viral fitness. *Curr HIV Res* **6**:200-208.
13. **Ariën, K. K., A. Abrahama, M. E. Quiñones-Mateu, L. Kestens, G. Vanham, and E. J. Arts.** 2005. The replicative fitness of primary human immunodeficiency virus type 1 (HIV-1) group M, HIV-1 group O, and HIV-2 isolates. *J Virol* **79**:8979-8990.
14. **Ayinde, D., C. Maudet, C. Transy, and F. Margottin-Goguet.** 2010. Limelight on two HIV/SIV accessory proteins in macrophage infection: is Vpx overshadowing Vpr? *Retrovirology* **7**:35.
15. **Bailes, E., F. Gao, F. Bibollet-Ruche, V. Courgnaud, M. Peeters, P. Marx, B. Hahn, and P. Sharp.** 2003. Hybrid origin of SIV in chimpanzees. *Science* **300**:1713.
16. **Balvay, L., M. Lopez Lastra, B. Sargueil, J. L. Darlix, and T. Ohlmann.** 2007. Translational control of retroviruses. *Nat Rev Microbiol* **5**:128-140.
17. **Bannwarth, S., and A. Gatignol.** 2005. HIV-1 TAR RNA: the target of molecular interactions between the virus and its host. *Curr HIV Res* **3**:61-71.
18. **Barr, S. D., J. R. Smiley, and F. D. Bushman.** 2008. The interferon response inhibits HIV particle production by induction of TRIM22. *PLoS Pathog* **4**:e1000007.
19. **Basler, C., and G. Amarasinghe.** 2009. Evasion of interferon responses by Ebola and Marburg viruses. *J Interferon Cytokine Res* **29**:511-520.

20. **Basler, C., X. Wang, E. Mühlberger, V. Volchkov, J. Paragas, H. Klenk, A. García-Sastre, and P. Palese.** 2000. The Ebola virus VP35 protein functions as a type I IFN antagonist. *Proc Natl Acad Sci U S A* **97**:12289-12294.
21. **Bergamaschi, A., D. Ayinde, A. David, E. Le Rouzic, M. Morel, G. Collin, D. Descamps, F. Damond, F. Brun-Vezinet, S. Nisole, F. Margottin-Goguet, G. Pancino, and C. Transy.** 2009. The human immunodeficiency virus type 2 Vpx protein usurps the CUL4A-DDB1 DCAF1 ubiquitin ligase to overcome a postentry block in macrophage infection. *J Virol* **83**:4854-4860.
22. **Bibollet-Ruche, F., E. Bailes, F. Gao, X. Pourrut, K. L. Barlow, J. P. Clewley, J. M. Mwenda, D. K. Langat, G. K. Chege, H. M. McClure, E. Mpoudi-Ngole, E. Delaporte, M. Peeters, G. M. Shaw, P. M. Sharp, and B. H. Hahn.** 2004. New simian immunodeficiency virus infecting De Brazza's monkeys (*Cercopithecus neglectus*): evidence for a cercopithecus monkey virus clade. *J Virol* **78**:7748-7762.
23. **Bick, M. J., J. W. Carroll, G. Gao, S. P. Goff, C. M. Rice, and M. R. MacDonald.** 2003. Expression of the zinc-finger antiviral protein inhibits alphavirus replication. *J Virol* **77**:11555-11562.
24. **Bieniasz, P. D.** 2004. Intrinsic immunity: a front-line defense against viral attack. *Nat Immunol* **5**:1109-1115.
25. **Bishop, K. N., R. K. Holmes, and M. H. Malim.** 2006. Antiviral potency of APOBEC proteins does not correlate with cytidine deamination. *J Virol* **80**:8450-8458.
26. **Bishop, K. N., M. Verma, E. Y. Kim, S. M. Wolinsky, and M. H. Malim.** 2008. APOBEC3G inhibits elongation of HIV-1 reverse transcripts. *PLoS Pathog* **4**:e1000231.
27. **Blanc, M., W. Y. Hsieh, K. A. Robertson, S. Watterson, G. Shui, P. Lacaze, M. Khondoker, P. Dickinson, G. Sing, S. Rodríguez-Martín, P. Phelan, T. Forster, B. Strobl, M. Müller, R. Riemersma, T. Osborne, M. R. Wenk, A. Angulo, and P. Ghazal.** 2011. Host defense against viral infection involves interferon mediated down-regulation of sterol biosynthesis. *PLoS Biol* **9**:e1000598.
28. **Bogerd, H., B. Doehle, H. Wiegand, and B. Cullen.** 2004. A single amino acid difference in the host APOBEC3G protein controls the primate species specificity of HIV type 1 virion infectivity factor. *Proc Natl Acad Sci U S A* **101**:3770-3774.
29. **Bosco, D. A., E. Z. Eisenmesser, S. Pochapsky, W. I. Sundquist, and D. Kern.** 2002. Catalysis of cis/trans isomerization in native HIV-1 capsid by human cyclophilin A. *Proc Natl Acad Sci U S A* **99**:5247-5252.
30. **Bostik, P., E. S. Noble, A. E. Mayne, L. Gargano, F. Villinger, and A. A. Ansari.** 2006. Central memory CD4 T cells are the predominant cell subset resistant to anergy in SIV disease resistant sooty mangabeys. *AIDS* **20**:181-188.
31. **Bour, S., and K. Strebel.** 1996. The human immunodeficiency virus (HIV) type 2 envelope protein is a functional complement to HIV type 1 Vpu that enhances particle release of heterologous retroviruses. *J Virol* **70**:8285-8300.
32. **Braaten, D., E. K. Franke, and J. Luban.** 1996. Cyclophilin A is required for an early step in the life cycle of human immunodeficiency virus type 1 before the initiation of reverse transcription. *J Virol* **70**:3551-3560.
33. **Bradley, R. K., A. Roberts, M. Smoot, S. Juvekar, J. Do, C. Dewey, I. Holmes, and L. Pachter.** 2009. Fast statistical alignment. *PLoS Comput Biol* **5**:e1000392.
34. **Brennan, G., Y. Kozyrev, and S. L. Hu.** 2008. TRIMCyp expression in Old World primates *Macaca nemestrina* and *Macaca fascicularis*. *Proc Natl Acad Sci U S A* **105**:3569-3574.
35. **Briggs, J. A., and H. G. Kräusslich.** 2011. The molecular architecture of HIV. *J Mol Biol* **410**:491-500.

36. **Cao, W., L. Bover, M. Cho, X. Wen, S. Hanabuchi, M. Bao, D. Rosen, Y. Wang, J. Shaw, Q. Du, C. Li, N. Arai, Z. Yao, L. Lanier, and Y. Liu.** 2009. Regulation of TLR7/9 responses in plasmacytoid dendritic cells by BST2 and ILT7 receptor interaction. *J Exp Med* **206**:1603-1614.
37. **Casartelli, N., M. Sourisseau, J. Feldmann, F. Guivel-Benhassine, A. Mallet, A. G. Marcelin, J. Guatelli, and O. Schwartz.** 2010. Tetherin restricts productive HIV-1 cell-to-cell transmission. *PLoS Pathog* **6**:e1000955.
38. **Centers for Disease Control and Prevention** 2011, posting date. Screening for HIV-Infection During the Refugee Domestic Medical Examination. [Online.]
39. **Chan, Y., T. Chang, C. Liao, and Y. Lin.** 2008. The cellular antiviral protein viperin is attenuated by proteasome-mediated protein degradation in Japanese encephalitis virus-infected cells. *J Virol* **82**:10455-10464.
40. **Charleston, M. A., and D. L. Robertson.** 2002. Preferential host switching by primate lentiviruses can account for phylogenetic similarity with the primate phylogeny. *Syst Biol* **51**:528-535.
41. **Cheng-Mayer, C., and J. A. Levy.** 1988. Distinct biological and serological properties of human immunodeficiency viruses from the brain. *Ann Neurol* **23 Suppl**:S58-61.
42. **Chesebro, B., K. Wehrly, J. Nishio, and S. Perryman.** 1992. Macrophage-tropic human immunodeficiency virus isolates from different patients exhibit unusual V3 envelope sequence homogeneity in comparison with T-cell-tropic isolates: definition of critical amino acids involved in cell tropism. *J Virol* **66**:6547-6554.
43. **Chin, K., and P. Cresswell.** 2001. Viperin (cig5), an IFN-inducible antiviral protein directly induced by human cytomegalovirus. *Proc Natl Acad Sci U S A* **98**:15125-15130.
44. **Christ, F., W. Thys, J. De Rijck, R. Gijssbers, A. Albanese, D. Arosio, S. Emiliani, J. C. Rain, R. Benarous, A. Cereseto, and Z. Debyser.** 2008. Transportin-SR2 imports HIV into the nucleus. *Curr Biol* **18**:1192-1202.
45. **Coleman, C. M., P. Spearman, and L. Wu.** 2011. Tetherin does not significantly restrict dendritic cell-mediated HIV-1 transmission and its expression is upregulated by newly synthesized HIV-1 Nef. *Retrovirology* **8**:26.
46. **Courgnaud, V., B. Abela, X. Pourrut, E. Mpoudi-Ngole, S. Loul, E. Delaporte, and M. Peeters.** 2003. Identification of a new simian immunodeficiency virus lineage with a vpu gene present among different cercopithecus monkeys (*C. mona*, *C. cephus*, and *C. nictitans*) from Cameroon. *J Virol* **77**:12523-12534.
47. **Crooks, G., G. Hon, J. Chandonia, and S. Brenner.** 2004. WebLogo: a sequence logo generator. *Genome Res* **14**:1188-1190.
48. **Damond, F., M. Worobey, P. Campa, I. Farfara, G. Colin, S. Matheron, F. Brun-Vézinet, D. L. Robertson, and F. Simon.** 2004. Identification of a highly divergent HIV type 2 and proposal for a change in HIV type 2 classification. *AIDS Res Hum Retroviruses* **20**:666-672.
49. **de Veer, M. J., M. Holko, M. Frevel, E. Walker, S. Der, J. M. Paranjape, R. H. Silverman, and B. R. Williams.** 2001. Functional classification of interferon-stimulated genes identified using microarrays. *J Leukoc Biol* **69**:912-920.
50. **Deacon, N., A. Tsykin, A. Solomon, K. Smith, M. Ludford-Menting, D. Hooker, D. McPhee, A. Greenway, A. Ellett, C. Chatfield, V. Lawson, S. Crowe, A. Maerz, S. Sonza, J. Learmont, J. Sullivan, A. Cunningham, D. Dwyer, D. Downton, and J. Mills.** 1995. Genomic structure of an attenuated quasi species of HIV-1 from a blood transfusion donor and recipients. *Science* **270**:988-991.
51. **Dehart, J. L., and V. Planelles.** 2008. Human immunodeficiency virus type 1 Vpr links proteasomal degradation and checkpoint activation. *J Virol* **82**:1066-1072.

52. **Der, S. D., A. Zhou, B. R. Williams, and R. H. Silverman.** 1998. Identification of genes differentially regulated by interferon alpha, beta, or gamma using oligonucleotide arrays. *Proc Natl Acad Sci U S A* **95**:15623-15628.
53. **Diop, O., A. Gueye, M. Dias-Tavares, C. Kornfeld, A. Faye, P. Ave, M. Huerre, S. Corbet, F. Barre-Sinoussi, and M. Müller-Trutwin.** 2000. High levels of viral replication during primary simian immunodeficiency virus SIVagm infection are rapidly and strongly controlled in African green monkeys. *J Virol* **74**:7538-7547.
54. **Diop, O., M. Ploquin, L. Mortara, A. Faye, B. Jacquelin, D. Kunkel, P. Lebon, C. Butor, A. Hosmalin, F. Barré-Sinoussi, and M. Müller-Trutwin.** 2008. Plasmacytoid dendritic cell dynamics and alpha interferon production during Simian immunodeficiency virus infection with a nonpathogenic outcome. *J Virol* **82**:5145-5152.
55. **Douglas, J., K. Viswanathan, M. McCarroll, J. Gustin, K. Früh, and A. Moses.** 2009. Vpu directs the degradation of the human immunodeficiency virus restriction factor BST-2/Tetherin via a {beta}TrCP-dependent mechanism. *J Virol* **83**:7931-7947.
56. **Drummond, A. J., and R. Andrew** 2009, posting date. Tracer v1.5. [Online.]
57. **Drummond, A. J., and A. Rambaut.** 2007. BEAST: Bayesian evolutionary analysis by sampling trees. *BMC Evol Biol* **7**:214.
58. **Elde, N., S. Child, A. Geballe, and H. Malik.** 2009. Protein kinase R reveals an evolutionary model for defeating viral mimicry. *Nature* **457**:485-489.
59. **Emerman, M., and H. Malik.** 2010. Paleovirology--modern consequences of ancient viruses. *PLoS Biol* **8**:e1000301.
60. **Engelman, A., and P. Cherepanov.** 2008. The lentiviral integrase binding protein LEDGF/p75 and HIV-1 replication. *PLoS Pathog* **4**:e1000046.
61. **Engelman, A., K. Mizuuchi, and R. Craigie.** 1991. HIV-1 DNA integration: mechanism of viral DNA cleavage and DNA strand transfer. *Cell* **67**:1211-1221.
62. **Evans, D. T., R. Serra-Moreno, R. K. Singh, and J. C. Guatelli.** 2010. BST-2/tetherin: a new component of the innate immune response to enveloped viruses. *Trends Microbiol* **18**:388-396.
63. **Fisher, R. D., H. Y. Chung, Q. Zhai, H. Robinson, W. I. Sundquist, and C. P. Hill.** 2007. Structural and biochemical studies of ALIX/AIP1 and its role in retrovirus budding. *Cell* **128**:841-852.
64. **Fitzgerald, K. A.** 2011. The interferon inducible gene: Viperin. *J Interferon Cytokine Res* **31**:131-135.
65. **Fomsgaard, A., M. C. Müller-Trutwin, O. Diop, J. Hansen, C. Mathiot, S. Corbet, F. Barré-Sinoussi, and J. S. Allan.** 1997. Relation between phylogeny of African green monkey CD4 genes and their respective simian immunodeficiency virus genes. *J Med Primatol* **26**:120-128.
66. **Franke, E. K., H. E. Yuan, and J. Luban.** 1994. Specific incorporation of cyclophilin A into HIV-1 virions. *Nature* **372**:359-362.
67. **Gale, M., and E. M. Foy.** 2005. Evasion of intracellular host defence by hepatitis C virus. *Nature* **436**:939-945.
68. **Gallo, R. C., and L. Montagnier.** 2003. The discovery of HIV as the cause of AIDS. *N Engl J Med* **349**:2283-2285.
69. **Ganser-Pornillos, B. K., M. Yeager, and W. I. Sundquist.** 2008. The structural biology of HIV assembly. *Curr Opin Struct Biol* **18**:203-217.
70. **Gao, F., E. Bailes, D. Robertson, Y. Chen, C. Rodenburg, S. Michael, L. Cummins, L. Arthur, M. Peeters, G. Shaw, P. Sharp, and B. Hahn.** 1999. Origin of HIV-1 in the chimpanzee *Pan troglodytes* troglodytes. *Nature* **397**:436-441.

71. **Gao, F., L. Yue, A. T. White, P. G. Pappas, J. Barchue, A. P. Hanson, B. M. Greene, P. M. Sharp, G. M. Shaw, and B. H. Hahn.** 1992. Human infection by genetically diverse SIVSM-related HIV-2 in west Africa. *Nature* **358**:495-499.
72. **Gao, G., X. Guo, and S. P. Goff.** 2002. Inhibition of retroviral RNA production by ZAP, a CCCCH-type zinc finger protein. *Science* **297**:1703-1706.
73. **Garrus, J. E., U. K. von Schwedler, O. W. Pornillos, S. G. Morham, K. H. Zavitz, H. E. Wang, D. A. Wettstein, K. M. Stray, M. Côté, R. L. Rich, D. G. Myszka, and W. I. Sundquist.** 2001. Tsg101 and the vacuolar protein sorting pathway are essential for HIV-1 budding. *Cell* **107**:55-65.
74. **Gibbs, J. S., A. A. Lackner, S. M. Lang, M. A. Simon, P. K. Sehgal, M. D. Daniel, and R. C. Desrosiers.** 1995. Progression to AIDS in the absence of a gene for vpr or vpx. *J Virol* **69**:2378-2383.
75. **Gifford, R., A. Katzourakis, M. Tristem, O. Pybus, M. Winters, and R. Shafer.** 2008. A transitional endogenous lentivirus from the genome of a basal primate and implications for lentivirus evolution. *Proc Natl Acad Sci U S A* **105**:20362-20367.
76. **Gilbert, C., D. Maxfield, S. Goodman, and C. Feschotte.** 2009. Parallel germline infiltration of a lentivirus in two Malagasy lemurs. *PLoS Genet* **5**:e1000425.
77. **Goff, S. P.** 2004. Retrovirus restriction factors. *Mol Cell* **16**:849-859.
78. **Goffinet, C., I. Allespach, S. Homann, H. Tervo, A. Habermann, D. Rupp, L. Oberbremer, C. Kern, N. Tibroni, S. Welsch, J. Krijnse-Locker, G. Banting, H. Kräusslich, O. Fackler, and O. Keppler.** 2009. HIV-1 Antagonism of CD317 Is Species Specific and Involves Vpu-Mediated Proteasomal Degradation of the Restriction Factor. *Cell Host Microbe* **5**:285-297.
79. **Goffinet, C., I. Allespach, S. Homann, H. M. Tervo, A. Habermann, D. Rupp, L. Oberbremer, C. Kern, N. Tibroni, S. Welsch, J. Krijnse-Locker, G. Banting, H. G. Kräusslich, O. T. Fackler, and O. T. Keppler.** 2009. HIV-1 antagonism of CD317 is species specific and involves Vpu-mediated proteasomal degradation of the restriction factor. *Cell Host Microbe* **5**:285-297.
80. **Goffinet, C., S. Homann, I. Ambiel, N. Tibroni, D. Rupp, O. T. Keppler, and O. T. Fackler.** 2010. Antagonism of CD317 restriction of human immunodeficiency virus type 1 (HIV-1) particle release and depletion of CD317 are separable activities of HIV-1 Vpu. *J Virol* **84**:4089-4094.
81. **Goila-Gaur, R., and K. Strebel.** 2008. HIV-1 Vif, APOBEC, and intrinsic immunity. *Retrovirology* **5**:51.
82. **Goldstone, D. C., V. Ennis-Adeniran, J. J. Hedden, H. C. Groom, G. I. Rice, E. Christodoulou, P. A. Walker, G. Kelly, L. F. Haire, M. W. Yap, L. P. de Carvalho, J. P. Stoye, Y. J. Crow, I. A. Taylor, and M. Webb.** 2011. HIV-1 restriction factor SAMHD1 is a deoxynucleoside triphosphate triphosphohydrolase. *Nature*.
83. **Gorry, P. R., and P. Ancuta.** 2011. Coreceptors and HIV-1 pathogenesis. *Curr HIV/AIDS Rep* **8**:45-53.
84. **Goto, T., S. Kennel, M. Abe, M. Takishita, M. Kosaka, A. Solomon, and S. Saito.** 1994. A novel membrane antigen selectively expressed on terminally differentiated human B cells. *Blood* **84**:1922-1930.
85. **Gueye, A., O. Diop, M. Ploquin, C. Kornfeld, A. Faye, M. Cumont, B. Hurtrel, F. Barré-Sinoussi, and M. Müller-Trutwin.** 2004. Viral load in tissues during the early and chronic phase of non-pathogenic SIVagm infection. *J Med Primatol* **33**:83-97.
86. **Guindon, S., and O. Gascuel.** 2003. A simple, fast, and accurate algorithm to estimate large phylogenies by maximum likelihood. *Syst Biol* **52**:696-704.

87. **Gummuluru, S., C. Kinsey, and M. Emerman.** 2000. An in vitro rapid-turnover assay for human immunodeficiency virus type 1 replication selects for cell-to-cell spread of virus. *J Virol* **74**:10882-10891.
88. **Gupta, R. K., S. Hué, T. Schaller, E. Verschoor, D. Pillay, and G. J. Towers.** 2009. Mutation of a single residue renders human tetherin resistant to HIV-1 Vpu-mediated depletion. *PLoS Pathog* **5**:e1000443.
89. **Gupta, R. K., P. Mlcochova, A. Pelchen-Matthews, S. J. Petit, G. Mattiuzzo, D. Pillay, Y. Takeuchi, M. Marsh, and G. J. Towers.** 2009. Simian immunodeficiency virus envelope glycoprotein counteracts tetherin/BST-2/CD317 by intracellular sequestration. *Proc Natl Acad Sci U S A* **106**:20889-20894.
90. **Göttlinger, H., T. Dorfman, E. Cohen, and W. Haseltine.** 1993. Vpu protein of human immunodeficiency virus type 1 enhances the release of capsids produced by gag gene constructs of widely divergent retroviruses. *Proc Natl Acad Sci U S A* **90**:7381-7385.
91. **Göttlinger, H. G.** 2008. HIV/AIDS: virus kept on a leash. *Nature* **451**:406-408.
92. **Harris, R. S., K. N. Bishop, A. M. Sheehy, H. M. Craig, S. K. Petersen-Mahrt, I. N. Watt, M. S. Neuberger, and M. H. Malim.** 2003. DNA deamination mediates innate immunity to retroviral infection. *Cell* **113**:803-809.
93. **Harris, R. S., S. K. Petersen-Mahrt, and M. S. Neuberger.** 2002. RNA editing enzyme APOBEC1 and some of its homologs can act as DNA mutators. *Mol Cell* **10**:1247-1253.
94. **Hatzioannou, T., D. Perez-Caballero, A. Yang, S. Cowan, and P. D. Bieniasz.** 2004. Retrovirus resistance factors Ref1 and Lv1 are species-specific variants of TRIM5alpha. *Proc Natl Acad Sci U S A* **101**:10774-10779.
95. **Hauser, H., L. A. Lopez, S. J. Yang, J. E. Oldenburg, C. M. Exline, J. C. Guatelli, and P. M. Cannon.** 2010. HIV-1 Vpu and HIV-2 Env counteract BST-2/tetherin by sequestration in a perinuclear compartment. *Retrovirology* **7**:51.
96. **Helbig, K. J., D. T. Lau, L. Semendric, H. A. Harley, and M. R. Beard.** 2005. Analysis of ISG expression in chronic hepatitis C identifies viperin as a potential antiviral effector. *Hepatology* **42**:702-710.
97. **Higgins, J. R., S. Sutjipto, P. A. Marx, and N. C. Pedersen.** 1992. Shared antigenic epitopes of the major core proteins of human and simian immunodeficiency virus isolates. *J Med Primatol* **21**:265-269.
98. **Hirsch, V. M., M. E. Sharkey, C. R. Brown, B. Brichacek, S. Goldstein, J. Wakefield, R. Byrum, W. R. Elkins, B. H. Hahn, J. D. Lifson, and M. Stevenson.** 1998. Vpx is required for dissemination and pathogenesis of SIV(SM) PBj: evidence of macrophage-dependent viral amplification. *Nat Med* **4**:1401-1408.
99. **Holmes, E. C.** 2011. The evolution of endogenous viral elements. *Cell Host Microbe* **10**:368-377.
100. **Howard, B. R., F. F. Vajdos, S. Li, W. I. Sundquist, and C. P. Hill.** 2003. Structural insights into the catalytic mechanism of cyclophilin A. *Nat Struct Biol* **10**:475-481.
101. **Hrecka, K., C. Hao, M. Gierszewska, S. K. Swanson, M. Kesik-Brodacka, S. Srivastava, L. Florens, M. P. Washburn, and J. Skowronski.** 2011. Vpx relieves inhibition of HIV-1 infection of macrophages mediated by the SAMHD1 protein. *Nature* **474**:658-661.
102. **Huelsenbeck, J. P., and F. Ronquist.** 2001. MRBAYES: Bayesian inference of phylogenetic trees. *Bioinformatics* **17**:754-755.
103. **Ikeda, Y., Y. Takeuchi, F. Martin, F. L. Cosset, K. Mitrophanous, and M. Collins.** 2003. Continuous high-titer HIV-1 vector production. *Nat Biotechnol* **21**:569-572.
104. **Ishikawa, J., T. Kaisho, H. Tomizawa, B. Lee, Y. Kobune, J. Inazawa, K. Oritani, M. Itoh, T. Ochi, and K. Ishihara.** 1995. Molecular cloning and chromosomal mapping of a bone

- marrow stromal cell surface gene, BST2, that may be involved in pre-B-cell growth. *Genomics* **26**:527-534.
105. **Iwabu, Y., H. Fujita, M. Kinomoto, K. Kaneko, Y. Ishizaka, Y. Tanaka, T. Sata, and K. Tokunaga.** 2009. HIV-1 accessory protein Vpu internalizes cell-surface BST-2/tetherin through transmembrane interactions leading to lysosomes. *J Biol Chem* **284**:35060-35072.
 106. **Iwasaki, A., and R. Medzhitov.** 2010. Regulation of adaptive immunity by the innate immune system. *Science* **327**:291-295.
 107. **Janeway, C. A.** 1989. Approaching the asymptote? Evolution and revolution in immunology. *Cold Spring Harb Symp Quant Biol* **54 Pt 1**:1-13.
 108. **Janvier, K., A. Pelchen-Matthews, J. B. Renaud, M. Caillet, M. Marsh, and C. Berlioz-Torrent.** 2011. The ESCRT-0 component HRS is required for HIV-1 Vpu-mediated BST-2/tetherin down-regulation. *PLoS Pathog* **7**:e1001265.
 109. **Jia, B., R. Serra-Moreno, W. Neidermyer, A. Rahmberg, J. Mackey, I. Fofana, W. Johnson, S. Westmoreland, and D. Evans.** 2009. Species-specific activity of SIV Nef and HIV-1 Vpu in overcoming restriction by tetherin/BST2. *PLoS Pathog* **5**:e1000429.
 110. **Jiang, D., H. Guo, C. Xu, J. Chang, B. Gu, L. Wang, T. Block, and J. Guo.** 2008. Identification of three interferon-inducible cellular enzymes that inhibit the replication of hepatitis C virus. *J Virol* **82**:1665-1678.
 111. **Jin, M., H. Hui, D. Robertson, M. Müller, F. Barré-Sinoussi, V. Hirsch, J. Allan, G. Shaw, P. Sharp, and B. Hahn.** 1994. Mosaic genome structure of simian immunodeficiency virus from west African green monkeys. *EMBO J* **13**:2935-2947.
 112. **Jolly, C., N. J. Booth, and S. J. Neil.** 2010. Cell-cell spread of human immunodeficiency virus type 1 overcomes tetherin/BST-2-mediated restriction in T cells. *J Virol* **84**:12185-12199.
 113. **Jolly Cjoff, J. E. Phillips-Conroy, T. R. Turner, S. Broussard, and J. S. Allan.** 1996. SIVagm incidence over two decades in a natural population of Ethiopian grivet monkeys (*Cercopithecus aethiops aethiops*). *J Med Primatol* **25**:78-83.
 114. **Jouvenet, N., S. Neil, M. Zhadina, T. Zang, Z. Kratovac, Y. Lee, M. McNatt, T. Hatziioannou, and P. Bieniasz.** 2009. Broad-spectrum inhibition of retroviral and filoviral particle release by tetherin. *J Virol* **83**:1837-1844.
 115. **Jouvenet, N., S. J. Neil, C. Bess, M. C. Johnson, C. A. Virgen, S. M. Simon, and P. D. Bieniasz.** 2006. Plasma membrane is the site of productive HIV-1 particle assembly. *PLoS Biol* **4**:e435.
 116. **Jouvenet, N., S. J. Neil, M. Zhadina, T. Zang, Z. Kratovac, Y. Lee, M. McNatt, T. Hatziioannou, and P. D. Bieniasz.** 2009. Broad-spectrum inhibition of retroviral and filoviral particle release by tetherin. *J Virol* **83**:1837-1844.
 117. **Jouvenet, N., S. M. Simon, and P. D. Bieniasz.** 2009. Imaging the interaction of HIV-1 genomes and Gag during assembly of individual viral particles. *Proc Natl Acad Sci U S A* **106**:19114-19119.
 118. **Jouvenet, N., M. Zhadina, P. D. Bieniasz, and S. M. Simon.** 2011. Dynamics of ESCRT protein recruitment during retroviral assembly. *Nat Cell Biol* **13**:394-401.
 119. **Kaletsky, R., J. Francica, C. Agrawal-Gamse, and P. Bates.** 2009. Tetherin-mediated restriction of filovirus budding is antagonized by the Ebola glycoprotein. *Proc Natl Acad Sci U S A*.
 120. **Keele, B., F. Van Heuverswyn, Y. Li, E. Bailes, J. Takehisa, M. Santiago, F. Bibollet-Ruche, Y. Chen, L. Wain, F. Liegeois, S. Loul, E. Ngole, Y. Bienvenue, E. Delaporte, J. Brookfield, P. Sharp, G. Shaw, M. Peeters, and B. Hahn.** 2006. Chimpanzee reservoirs of pandemic and nonpandemic HIV-1. *Science* **313**:523-526.

121. **Kerns, J., M. Emerman, and H. Malik.** 2008. Positive selection and increased antiviral activity associated with the PARP-containing isoform of human zinc-finger antiviral protein. *PLoS Genet* **4**:e21.
122. **Kik, M. J., J. H. Bos, J. Groen, and G. M. Dorrestein.** 2005. Herpes simplex infection in a juvenile orangutan (*Pongo pygmaeus pygmaeus*). *J Zoo Wildl Med* **36**:131-134.
123. **Kirchhoff, F.** 2010. Immune evasion and counteraction of restriction factors by HIV-1 and other primate lentiviruses. *Cell Host Microbe* **8**:55-67.
124. **Kirchhoff, F.** 2009. Is the high virulence of HIV-1 an unfortunate coincidence of primate lentiviral evolution? *Nat Rev Microbiol* **7**:467-476.
125. **Kobayashi, T., H. Ode, T. Yoshida, K. Sato, P. Gee, S. P. Yamamoto, H. Ebina, K. Strebel, H. Sato, and Y. Koyanagi.** 2011. Identification of amino acids in the human tetherin transmembrane domain responsible for HIV-1 Vpu interaction and susceptibility. *J Virol* **85**:932-945.
126. **Kosakovsky Pond, S., and S. Frost.** 2005. Not so different after all: a comparison of methods for detecting amino acid sites under selection. *Mol Biol Evol* **22**:1208-1222.
127. **Kosakovsky Pond, S., D. Posada, M. Gravenor, C. Woelk, and S. Frost.** 2006. GARD: a genetic algorithm for recombination detection. *Bioinformatics* **22**:3096-3098.
128. **Krishnan, L., K. A. Matreyek, I. Oztop, K. Lee, C. H. Tipper, X. Li, M. J. Dar, V. N. Kewalramani, and A. Engelman.** 2010. The requirement for cellular transportin 3 (TNPO3 or TRN-SR2) during infection maps to human immunodeficiency virus type 1 capsid and not integrase. *J Virol* **84**:397-406.
129. **Kuhl, B. D., R. D. Sloan, D. A. Donahue, T. Bar-Magen, C. Liang, and M. A. Wainberg.** 2010. Tetherin restricts direct cell-to-cell infection of HIV-1. *Retrovirology* **7**:115.
130. **Kuhmann, S. E., N. Madani, O. M. Diop, E. J. Platt, J. Morvan, M. C. Müller-Trutwin, F. Barré-Sinoussi, and D. Kabat.** 2001. Frequent substitution polymorphisms in African green monkey CCR5 cluster at critical sites for infections by simian immunodeficiency virus SIVagm, implying ancient virus-host coevolution. *J Virol* **75**:8449-8460.
131. **Kupzig, S., V. Korolchuk, R. Rollason, A. Sugden, A. Wilde, and G. Banting.** 2003. Bst-2/HM1.24 is a raft-associated apical membrane protein with an unusual topology. *Traffic* **4**:694-709.
132. **Kühl, A., C. Banning, A. Marzi, J. Votteler, I. Steffen, S. Bertram, I. Glowacka, A. Konrad, M. Stürzl, J. T. Guo, U. Schubert, H. Feldmann, G. Behrens, M. Schindler, and S. Pöhlmann.** 2011. The Ebola virus glycoprotein and HIV-1 Vpu employ different strategies to counteract the antiviral factor tetherin. *J Infect Dis* **204 Suppl 3**:S850-860.
133. **Laguet, N., B. Sobhian, N. Casartelli, M. Ringard, C. Chable-Bessia, E. Ségéral, A. Yatim, S. Emiliani, O. Schwartz, and M. Benkirane.** 2011. SAMHD1 is the dendritic- and myeloid-cell-specific HIV-1 restriction factor counteracted by Vpx. *Nature* **474**:654-657.
134. **Le Tortorec, A., and S. J. Neil.** 2009. Antagonism to and intracellular sequestration of human tetherin by the human immunodeficiency virus type 2 envelope glycoprotein. *J Virol* **83**:11966-11978.
135. **Le Tortorec, A., S. Willey, and S. J. Neil.** 2011. Antiviral Inhibition of Enveloped Virus Release by Tetherin/BST-2: Action and Counteraction. *Viruses* **3**:520-540.
136. **Lee, K., Z. Ambrose, T. D. Martin, I. Oztop, A. Mulky, J. G. Julias, N. Vandegraaff, J. G. Baumann, R. Wang, W. Yuen, T. Takemura, K. Shelton, I. Taniuchi, Y. Li, J. Sodroski, D. R. Littman, J. M. Coffin, S. H. Hughes, D. Unutmaz, A. Engelman, and V. N. KewalRamani.** 2010. Flexible use of nuclear import pathways by HIV-1. *Cell Host Microbe* **7**:221-233.

137. **Lemaitre, B., E. Nicolas, L. Michaut, J. M. Reichhart, and J. A. Hoffmann.** 1996. The dorsoventral regulatory gene cassette *spätzle/Toll/cactus* controls the potent antifungal response in *Drosophila* adults. *Cell* **86**:973-983.
138. **Liang, C., and M. A. Wainberg.** 2002. The role of Tat in HIV-1 replication: an activator and/or a suppressor? *AIDS Rev* **4**:41-49.
139. **Liao, C. H., Y. Q. Kuang, H. L. Liu, Y. T. Zheng, and B. Su.** 2007. A novel fusion gene, TRIM5-Cyclophilin A in the pig-tailed macaque determines its susceptibility to HIV-1 infection. *AIDS* **21 Suppl 8**:S19-26.
140. **Lim, E., and M. Emerman.** 2009. Simian immunodeficiency virus SIVagm from African green monkeys does not antagonize endogenous levels of African green monkey tetherin/BST-2. *J Virol* **83**:11673-11681.
141. **Lim, E., O. Fregoso, C. McCoy, F. Matsen, H. Malik, and M. Emerman.** 2012. The Ability of Primate Lentiviruses to Degrade the Monocyte Restriction Factor SAMHD1 Preceded the Birth of the Viral Accessory Protein Vpx. *Cell Host Microbe* **Published online ahead of print.**
142. **Lim, E., H. Malik, and M. Emerman.** 2010. Ancient adaptive evolution of tetherin shaped the functions of vpu and nef in human immunodeficiency virus and primate lentiviruses. *J Virol* **84**:7124-7134.
143. **Lim, E. S., and M. Emerman.** 2011. HIV: Going for the watchman. *Nature* **474**:587-588.
144. **Lim, E. S., and M. Emerman.** 2009. Simian immunodeficiency virus SIVagm from African green monkeys does not antagonize endogenous levels of African green monkey tetherin/BST-2. *J Virol* **83**:11673-11681.
145. **Liégeois, F., B. Lafay, P. Formenty, S. Locatelli, V. Cournaud, E. Delaporte, and M. Peeters.** 2009. Full-length genome characterization of a novel simian immunodeficiency virus lineage (SIVolc) from olive Colobus (*Procolobus verus*) and new SIVwrcPbb strains from Western Red Colobus (*Piliocolobus badius badius*) from the Tai Forest in Ivory Coast. *J Virol* **83**:428-439.
146. **Lodmell, J. S., C. Ehresmann, B. Ehresmann, and R. Marquet.** 2001. Structure and dimerization of HIV-1 kissing loop aptamers. *J Mol Biol* **311**:475-490.
147. **Lopez, L. A., S. J. Yang, H. Hauser, C. M. Exline, K. G. Haworth, J. Oldenburg, and P. M. Cannon.** 2010. Ebola virus glycoprotein counteracts BST-2/Tetherin restriction in a sequence-independent manner that does not require tetherin surface removal. *J Virol* **84**:7243-7255.
148. **Los Alamos HIV sequence database** 2011, posting date. <http://www.hiv.lanl.gov/>. [Online.]
149. **Luban, J., K. L. Bossolt, E. K. Franke, G. V. Kalpana, and S. P. Goff.** 1993. Human immunodeficiency virus type 1 Gag protein binds to cyclophilins A and B. *Cell* **73**:1067-1078.
150. **Maillard, P. V., S. Reynard, F. Serhan, P. Turelli, and D. Trono.** 2007. Interfering residues narrow the spectrum of MLV restriction by human TRIM5alpha. *PLoS Pathog* **3**:e200.
151. **Malim, M., and M. Emerman.** 2008. HIV-1 accessory proteins--ensuring viral survival in a hostile environment. *Cell Host Microbe* **3**:388-398.
152. **Mandl, J., A. Barry, T. Vanderford, N. Kozyr, R. Chavan, S. Klucking, F. Barrat, R. Coffman, S. Staprans, and M. Feinberg.** 2008. Divergent TLR7 and TLR9 signaling and type I interferon production distinguish pathogenic and nonpathogenic AIDS virus infections. *Nat Med* **14**:1077-1087.
153. **Mangeat, B., G. Gers-Huber, M. Lehmann, M. Zufferey, J. Luban, and V. Piguet.** 2009. HIV-1 Vpu neutralizes the antiviral factor Tetherin/BST-2 by binding it and directing its beta-TrCP2-dependent degradation. *PLoS Pathog* **5**:e1000574.

154. **Mangeat, B., P. Turelli, G. Caron, M. Friedli, L. Perrin, and D. Trono.** 2003. Broad antiretroviral defence by human APOBEC3G through lethal editing of nascent reverse transcripts. *Nature* **424**:99-103.
155. **Mansfield, K. G., N. W. Lerch, M. B. Gardner, and A. A. Lackner.** 1995. Origins of simian immunodeficiency virus infection in macaques at the New England Regional Primate Research Center. *J Med Primatol* **24**:116-122.
156. **Mansouri, M., K. Viswanathan, J. Douglas, J. Hines, J. Gustin, A. Moses, and K. Fröh.** 2009. Molecular mechanism of BST2/tetherin downregulation by K5/MIR2 of Kaposi's sarcoma-associated herpesvirus. *J Virol* **83**:9672-9681.
157. **Marcello, T., A. Grakoui, G. Barba-Spaeth, E. S. Machlin, S. V. Kotenko, M. R. MacDonald, and C. M. Rice.** 2006. Interferons alpha and lambda inhibit hepatitis C virus replication with distinct signal transduction and gene regulation kinetics. *Gastroenterology* **131**:1887-1898.
158. **Mariani, R., D. Chen, B. Schröfelbauer, F. Navarro, R. König, B. Bollman, C. Münk, H. Nymark-McMahon, and N. Landau.** 2003. Species-specific exclusion of APOBEC3G from HIV-1 virions by Vif. *Cell* **114**:21-31.
159. **Martinon, F., A. Mayor, and J. Tschopp.** 2009. The inflammasomes: guardians of the body. *Annu Rev Immunol* **27**:229-265.
160. **Martinson, J. J., N. H. Chapman, D. C. Rees, Y. T. Liu, and J. B. Clegg.** 1997. Global distribution of the CCR5 gene 32-basepair deletion. *Nat Genet* **16**:100-103.
161. **Mattijssen, S., and G. J. Pruijn.** 2011. Viperin, a key player in the antiviral response. *Microbes Infect.*
162. **Mañes, S., G. del Real, and C. Martínez-A.** 2003. Pathogens: raft hijackers. *Nat Rev Immunol* **3**:557-568.
163. **McNatt, M., T. Zang, T. Hatzioannou, M. Bartlett, I. Fofana, W. Johnson, S. Neil, and P. Bieniasz.** 2009. Species-specific activity of HIV-1 Vpu and positive selection of tetherin transmembrane domain variants. *PLoS Pathog* **5**:e1000300.
164. **Medzhitov, R.** 2009. Approaching the asymptote: 20 years later. *Immunity* **30**:766-775.
165. **Medzhitov, R., P. Preston-Hurlburt, and C. A. Janeway.** 1997. A human homologue of the Drosophila Toll protein signals activation of adaptive immunity. *Nature* **388**:394-397.
166. **Meyerson, N. R., and S. L. Sawyer.** 2011. Two-stepping through time: mammals and viruses. *Trends Microbiol* **19**:286-294.
167. **Misumi, S., M. Inoue, T. Dochi, N. Kishimoto, N. Hasegawa, N. Takamune, and S. Shoji.** 2010. Uncoating of human immunodeficiency virus type 1 requires prolyl isomerase Pin1. *J Biol Chem* **285**:25185-25195.
168. **Mitchell, R., C. Katsura, M. Skasko, K. Fitzpatrick, D. Lau, A. Ruiz, E. Stephens, F. Margottin-Goguet, R. Benarous, and J. Guatelli.** 2009. Vpu antagonizes BST-2-mediated restriction of HIV-1 release via beta-TrCP and endo-lysosomal trafficking. *PLoS Pathog* **5**:e1000450.
169. **Miyagi, E., A. J. Andrew, S. Kao, and K. Strebel.** 2009. Vpu enhances HIV-1 virus release in the absence of Bst-2 cell surface down-modulation and intracellular depletion. *Proc Natl Acad Sci U S A* **106**:2868-2873.
170. **Miyauchi, K., Y. Kim, O. Latinovic, V. Morozov, and G. B. Melikyan.** 2009. HIV enters cells via endocytosis and dynamin-dependent fusion with endosomes. *Cell* **137**:433-444.
171. **Moore, M. D., W. Fu, O. Nikolaitchik, J. Chen, R. G. Ptak, and W. S. Hu.** 2007. Dimer initiation signal of human immunodeficiency virus type 1: its role in partner selection during RNA copackaging and its effects on recombination. *J Virol* **81**:4002-4011.
172. **Murphey-Corb, M., L. N. Martin, S. R. Rangan, G. B. Baskin, B. J. Gormus, R. H. Wolf, W. A. Andes, M. West, and R. C. Montelaro.** 1986. Isolation of an HTLV-III-related retrovirus from

- macaques with simian AIDS and its possible origin in asymptomatic mangabeys. *Nature* **321**:435-437.
173. **Müller, M., N. Saksena, E. Nerrienet, C. Chappey, V. Hervé, J. Durand, P. Legal-Campodonico, M. Lang, J. Digoutte, and A. Georges.** 1993. Simian immunodeficiency viruses from central and western Africa: evidence for a new species-specific lentivirus in tantalus monkeys. *J Virol* **67**:1227-1235.
 174. **Müller, S., P. Möller, M. J. Bick, S. Wurr, S. Becker, S. Günther, and B. M. Kümmerer.** 2007. Inhibition of filovirus replication by the zinc finger antiviral protein. *J Virol* **81**:2391-2400.
 175. **Neil, S., V. Sandrin, W. Sundquist, and P. Bieniasz.** 2007. An interferon-alpha-induced tethering mechanism inhibits HIV-1 and Ebola virus particle release but is counteracted by the HIV-1 Vpu protein. *Cell Host Microbe* **2**:193-203.
 176. **Neil, S. J., T. Zang, and P. D. Bieniasz.** 2008. Tetherin inhibits retrovirus release and is antagonized by HIV-1 Vpu. *Nature* **451**:425-430.
 177. **Newman, E. N., R. K. Holmes, H. M. Craig, K. C. Klein, J. R. Lingappa, M. H. Malim, and A. M. Sheehy.** 2005. Antiviral function of APOBEC3G can be dissociated from cytidine deaminase activity. *Curr Biol* **15**:166-170.
 178. **Nguyen, K., M. Ilano, H. Akari, E. Miyagi, E. Poeschla, K. Strebel, and S. Bour.** 2004. Codon optimization of the HIV-1 vpu and vif genes stabilizes their mRNA and allows for highly efficient Rev-independent expression. *Virology* **319**:163-175.
 179. **Niederman, T. M., J. V. Garcia, W. R. Hastings, S. Luria, and L. Ratner.** 1992. Human immunodeficiency virus type 1 Nef protein inhibits NF-kappa B induction in human T cells. *J Virol* **66**:6213-6219.
 180. **Nisole, S., C. Lynch, J. P. Stoye, and M. W. Yap.** 2004. A Trim5-cyclophilin A fusion protein found in owl monkey kidney cells can restrict HIV-1. *Proc Natl Acad Sci U S A* **101**:13324-13328.
 181. **Nitta, T., Y. Kuznetsov, A. McPherson, and H. Fan.** 2010. Murine leukemia virus glycosylated Gag (gPr80gag) facilitates interferon-sensitive virus release through lipid rafts. *Proc Natl Acad Sci U S A* **107**:1190-1195.
 182. **Noguchi, C., H. Ishino, M. Tsuge, Y. Fujimoto, M. Imamura, S. Takahashi, and K. Chayama.** 2005. G to A hypermutation of hepatitis B virus. *Hepatology* **41**:626-633.
 183. **Nomaguchi, M., N. Doi, S. Fujiwara, M. Fujita, and A. Adachi.** 2010. Site-Directed Mutagenesis of HIV-1 vpu Gene Demonstrates Two Clusters of Replication-Defective Mutants with Distinct Ability to Down-Modulate Cell Surface CD4 and Tetherin. *Front Microbiol* **1**:116.
 184. **Ohkura, S., M. W. Yap, T. Sheldon, and J. P. Stoye.** 2006. All three variable regions of the TRIM5alpha B30.2 domain can contribute to the specificity of retrovirus restriction. *J Virol* **80**:8554-8565.
 185. **Ono, A., and E. O. Freed.** 2001. Plasma membrane rafts play a critical role in HIV-1 assembly and release. *Proc Natl Acad Sci U S A* **98**:13925-13930.
 186. **Ono, A., and E. O. Freed.** 2005. Role of lipid rafts in virus replication. *Adv Virus Res* **64**:311-358.
 187. **Ono, A., A. A. Waheed, and E. O. Freed.** 2007. Depletion of cellular cholesterol inhibits membrane binding and higher-order multimerization of human immunodeficiency virus type 1 Gag. *Virology* **360**:27-35.
 188. **Ortiz, M., N. Guex, E. Patin, O. Martin, I. Xenarios, A. Ciuffi, L. Quintana-Murci, and A. Telenti.** 2009. Evolutionary Trajectories of Primate Genes Involved in HIV Pathogenesis. *Mol Biol Evol.*
 189. **Ott, D. E.** 2008. Cellular proteins detected in HIV-1. *Rev Med Virol* **18**:159-175.

190. **Ozaki, S., M. Kosaka, S. Wakatsuki, M. Abe, Y. Koishihara, and T. Matsumoto.** 1997. Immunotherapy of multiple myeloma with a monoclonal antibody directed against a plasma cell-specific antigen, HM1.24. *Blood* **90**:3179-3186.
191. **Paiardini, M., I. Pandrea, C. Apetrei, and G. Silvestri.** 2009. Lessons learned from the natural hosts of HIV-related viruses. *Annu Rev Med* **60**:485-495.
192. **Paillart, J. C., M. Shehu-Xhilaga, R. Marquet, and J. Mak.** 2004. Dimerization of retroviral RNA genomes: an inseparable pair. *Nat Rev Microbiol* **2**:461-472.
193. **Pardieu, C., R. Vigan, S. J. Wilson, A. Calvi, T. Zang, P. Bieniasz, P. Kellam, G. J. Towers, and S. J. Neil.** 2010. The RING-CH ligase K5 antagonizes restriction of KSHV and HIV-1 particle release by mediating ubiquitin-dependent endosomal degradation of tetherin. *PLoS Pathog* **6**:e1000843.
194. **Patel, M. R., Y.-M. Loo, S. M. Horner, M. Gale Jr., and H. S. Malik.** 2012. Convergent evolution of escape from hepaciviral antagonism in primates. *PLoS Biology* **In Press**.
195. **Peden, K., M. Emerman, and L. Montagnier.** 1991. Changes in growth properties on passage in tissue culture of viruses derived from infectious molecular clones of HIV-1LAI, HIV-1MAL, and HIV-1ELI. *Virology* **185**:661-672.
196. **Peeters, M., and V. Cournaud.** 2002. Overview of Primate Lentiviruses and Their Evolution in Non-human Primates in Africa. *HIV sequence compendium*:2-23.
197. **Pereira, L. A., K. Bentley, A. Peeters, M. J. Churchill, and N. J. Deacon.** 2000. A compilation of cellular transcription factor interactions with the HIV-1 LTR promoter. *Nucleic Acids Res* **28**:663-668.
198. **Perelman, P., W. E. Johnson, C. Roos, H. N. Seuánez, J. E. Horvath, M. A. Moreira, B. Kessing, J. Pontius, M. Roelke, Y. Rumpler, M. P. Schneider, A. Silva, S. J. O'Brien, and J. Pecon-Slattery.** 2011. A molecular phylogeny of living primates. *PLoS Genet* **7**:e1001342.
199. **Perez-Caballero, D., T. Zang, A. Ebrahimi, M. McNatt, D. Gregory, M. Johnson, and P. Bieniasz.** 2009. Tetherin inhibits HIV-1 release by directly tethering virions to cells. *Cell* **139**:499-511.
200. **Perez-Caballero, D., T. Zang, A. Ebrahimi, M. W. McNatt, D. A. Gregory, M. C. Johnson, and P. D. Bieniasz.** 2009. Tetherin inhibits HIV-1 release by directly tethering virions to cells. *Cell* **139**:499-511.
201. **Perron, M. J., M. Stremlau, M. Lee, H. Javanbakht, B. Song, and J. Sodroski.** 2007. The human TRIM5alpha restriction factor mediates accelerated uncoating of the N-tropic murine leukemia virus capsid. *J Virol* **81**:2138-2148.
202. **Perron, M. J., M. Stremlau, B. Song, W. Ulm, R. C. Mulligan, and J. Sodroski.** 2004. TRIM5alpha mediates the postentry block to N-tropic murine leukemia viruses in human cells. *Proc Natl Acad Sci U S A* **101**:11827-11832.
203. **Pertel, T., S. Hausmann, D. Morger, S. Züger, J. Guerra, J. Lascano, C. Reinhard, F. A. Santoni, P. D. Uchil, L. Chatel, A. Bisiaux, M. L. Albert, C. Strambio-De-Castillia, W. Mothes, M. Pizzato, M. G. Grütter, and J. Luban.** 2011. TRIM5 is an innate immune sensor for the retrovirus capsid lattice. *Nature* **472**:361-365.
204. **Phillips-Conroy, J. E., C. J. Jolly, B. Petros, J. S. Allan, and R. C. Desrosiers.** 1994. Sexual transmission of SIVagm in wild grivet monkeys. *J Med Primatol* **23**:1-7.
205. **Pichlmair, A., and C. Reis e Sousa.** 2007. Innate recognition of viruses. *Immunity* **27**:370-383.
206. **Pickl, W. F., F. X. Pimentel-Muiños, and B. Seed.** 2001. Lipid rafts and pseudotyping. *J Virol* **75**:7175-7183.
207. **Planelles, V., J. B. Jowett, Q. X. Li, Y. Xie, B. Hahn, and I. S. Chen.** 1996. Vpr-induced cell cycle arrest is conserved among primate lentiviruses. *J Virol* **70**:2516-2524.

208. **Plantier, J. C., M. Leoz, J. E. Dickerson, F. De Oliveira, F. Cordonnier, V. Lemée, F. Damond, D. L. Robertson, and F. Simon.** 2009. A new human immunodeficiency virus derived from gorillas. *Nat Med* **15**:871-872.
209. **Pond, S. L., S. D. Frost, and S. V. Muse.** 2005. HyPhy: hypothesis testing using phylogenies. *Bioinformatics* **21**:676-679.
210. **Poss, M., and J. Overbaugh.** 1999. Variants from the diverse virus population identified at seroconversion of a clade A human immunodeficiency virus type 1-infected woman have distinct biological properties. *J Virol* **73**:5255-5264.
211. **Powell, R. D., P. J. Holland, T. Hollis, and F. W. Perrino.** 2011. The Aicardi-Goutieres syndrome gene and HIV-1 restriction factor SAMHD1 is a dGTP-regulated deoxynucleotide triphosphohydrolase. *J Biol Chem.*
212. **Prince, A. M., B. Brotman, D. H. Lee, L. Andrus, J. Valinsky, and P. Marx.** 2002. Lack of evidence for HIV type 1-related SIVcpz infection in captive and wild chimpanzees (*Pan troglodytes verus*) in West Africa. *AIDS Res Hum Retroviruses* **18**:657-660.
213. **Purvis, A.** 1995. A composite estimate of primate phylogeny. *Philos Trans R Soc Lond B Biol Sci* **348**:405-421.
214. **Rambaut, A., D. Posada, K. A. Crandall, and E. C. Holmes.** 2004. The causes and consequences of HIV evolution. *Nat Rev Genet* **5**:52-61.
215. **Regier, D. A., and R. C. Desrosiers.** 1990. The complete nucleotide sequence of a pathogenic molecular clone of simian immunodeficiency virus. *AIDS Res Hum Retroviruses* **6**:1221-1231.
216. **Rice, G. I., J. Bond, A. Asipu, R. L. Brunette, I. W. Manfield, I. M. Carr, J. C. Fuller, R. M. Jackson, T. Lamb, T. A. Briggs, M. Ali, H. Gornall, L. R. Couthard, A. Aeby, S. P. Attard-Montalto, E. Bertini, C. Bodemer, K. Brockmann, L. A. Brueton, P. C. Corry, I. Desguerre, E. Fazzi, A. G. Cazorla, B. Gener, B. C. Hamel, A. Heiberg, M. Hunter, M. S. van der Knaap, R. Kumar, L. Lagae, P. G. Landrieu, C. M. Lourenco, D. Marom, M. F. McDermott, W. van der Merwe, S. Orcesi, J. S. Prendiville, M. Rasmussen, S. A. Shalev, D. M. Soler, M. Shinawi, R. Spiegel, T. Y. Tan, A. Vanderver, E. L. Wakeling, E. Wassmer, E. Whittaker, P. Lebon, D. B. Stetson, D. T. Bonthron, and Y. J. Crow.** 2009. Mutations involved in Aicardi-Goutières syndrome implicate SAMHD1 as regulator of the innate immune response. *Nat Genet* **41**:829-832.
217. **Riddick, N. E., E. A. Hermann, L. M. Loftin, S. T. Elliott, W. C. Wey, B. Cervasi, J. Taaffe, J. C. Engram, B. Li, J. G. Else, Y. Li, B. H. Hahn, C. A. Derdeyn, D. L. Sodora, C. Apetrei, M. Paiardini, G. Silvestri, and R. G. Collman.** 2010. A novel CCR5 mutation common in sooty mangabeys reveals SIVsmm infection of CCR5-null natural hosts and efficient alternative coreceptor use in vivo. *PLoS Pathog* **6**:e1001064.
218. **Rivieccio, M., H. Suh, Y. Zhao, M. Zhao, K. Chin, S. Lee, and C. Brosnan.** 2006. TLR3 ligation activates an antiviral response in human fetal astrocytes: a role for viperin/cig5. *J Immunol* **177**:4735-4741.
219. **Rock, F. L., G. Hardiman, J. C. Timans, R. A. Kastelein, and J. F. Bazan.** 1998. A family of human receptors structurally related to *Drosophila* Toll. *Proc Natl Acad Sci U S A* **95**:588-593.
220. **Rong, L., J. Zhang, J. Lu, Q. Pan, R. P. Lorgeoux, C. Aloysius, F. Guo, S. L. Liu, M. A. Wainberg, and C. Liang.** 2009. The transmembrane domain of BST-2 determines its sensitivity to down-modulation by human immunodeficiency virus type 1 Vpu. *J Virol* **83**:7536-7546.
221. **Rosenwirth, B., A. Billich, R. Datema, P. Donatsch, F. Hammerschmid, R. Harrison, P. Hiestand, H. Jaksche, P. Mayer, and P. Peichl.** 1994. Inhibition of human immunodeficiency virus type 1 replication by SDZ NIM 811, a nonimmunosuppressive cyclosporine analog. *Antimicrob Agents Chemother* **38**:1763-1772.

222. **Sakuma, T., T. Noda, S. Urata, Y. Kawaoka, and J. Yasuda.** 2009. Inhibition of Lassa and Marburg virus production by tetherin. *J Virol* **83**:2382-2385.
223. **Sakuma, T., A. Sakurai, and J. Yasuda.** 2009. Dimerization of tetherin is not essential for its antiviral activity against Lassa and Marburg viruses. *PLoS One* **4**:e6934.
224. **Salemi, M., T. De Oliveira, V. Courgnaud, V. Moulton, B. Holland, S. Cassol, W. M. Switzer, and A. M. Vandamme.** 2003. Mosaic genomes of the six major primate lentivirus lineages revealed by phylogenetic analyses. *J Virol* **77**:7202-7213.
225. **Samson, M., F. Libert, B. J. Doranz, J. Rucker, C. Liesnard, C. M. Farber, S. Saragosti, C. Lapoumeroulie, J. Cognaux, C. Forceille, G. Muyldermans, C. Verhofstede, G. Burtonboy, M. Georges, T. Imai, S. Rana, Y. Yi, R. J. Smyth, R. G. Collman, R. W. Doms, G. Vassart, and M. Parmentier.** 1996. Resistance to HIV-1 infection in caucasian individuals bearing mutant alleles of the CCR-5 chemokine receptor gene. *Nature* **382**:722-725.
226. **Santiago, M. L., C. M. Rodenburg, S. Kamenya, F. Bibollet-Ruche, F. Gao, E. Bailes, S. Meleth, S. J. Soong, J. M. Kilby, Z. Moldoveanu, B. Fahey, M. N. Muller, A. Ayoub, E. Nerrienet, H. M. McClure, J. L. Heeney, A. E. Pusey, D. A. Collins, C. Boesch, R. W. Wrangham, J. Goodall, P. M. Sharp, G. M. Shaw, and B. H. Hahn.** 2002. SIVcpz in wild chimpanzees. *Science* **295**:465.
227. **Sasada, A., A. Takaori-Kondo, K. Shirakawa, M. Kobayashi, A. Abudu, M. Hishizawa, K. Imada, Y. Tanaka, and T. Uchiyama.** 2005. APOBEC3G targets human T-cell leukemia virus type 1. *Retrovirology* **2**:32.
228. **Sastri, J., and E. M. Campbell.** 2011. Recent insights into the mechanism and consequences of TRIM5 α retroviral restriction. *AIDS Res Hum Retroviruses* **27**:231-238.
229. **Sauter, D., M. Schindler, A. Specht, W. N. Landford, J. Münch, K. A. Kim, J. Votteler, U. Schubert, F. Bibollet-Ruche, B. F. Keele, J. Takehisa, Y. Ogando, C. Ochsenbauer, J. C. Kappes, A. Ayoub, M. Peeters, G. H. Learn, G. Shaw, P. M. Sharp, P. Bieniasz, B. H. Hahn, T. Hatziioannou, and F. Kirchhoff.** 2009. Tetherin-driven adaptation of Vpu and Nef function and the evolution of pandemic and nonpandemic HIV-1 strains. *Cell Host Microbe* **6**:409-421.
230. **Sawyer, S., M. Emerman, and H. Malik.** 2004. Ancient adaptive evolution of the primate antiviral DNA-editing enzyme APOBEC3G. *PLoS Biol* **2**:E275.
231. **Sawyer, S., L. Wu, M. Emerman, and H. Malik.** 2005. Positive selection of primate TRIM5 α identifies a critical species-specific retroviral restriction domain. *Proc Natl Acad Sci U S A* **102**:2832-2837.
232. **Sayah, D. M., E. Sokolskaja, L. Berthou, and J. Luban.** 2004. Cyclophilin A retrotransposition into TRIM5 explains owl monkey resistance to HIV-1. *Nature* **430**:569-573.
233. **Scarlatti, G., E. Tresoldi, A. Björndal, R. Fredriksson, C. Colognesi, H. K. Deng, M. S. Malnati, A. Plebani, A. G. Siccardi, D. R. Littman, E. M. Fenyö, and P. Lusso.** 1997. In vivo evolution of HIV-1 co-receptor usage and sensitivity to chemokine-mediated suppression. *Nat Med* **3**:1259-1265.
234. **Schindler, M., J. Münch, O. Kutsch, H. Li, M. Santiago, F. Bibollet-Ruche, M. Müller-Trutwin, F. Novembre, M. Peeters, V. Courgnaud, E. Bailes, P. Roques, D. Sodora, G. Silvestri, P. Sharp, B. Hahn, and F. Kirchhoff.** 2006. Nef-mediated suppression of T cell activation was lost in a lentiviral lineage that gave rise to HIV-1. *Cell* **125**:1055-1067.
235. **Schröder, A. R., P. Shinn, H. Chen, C. Berry, J. R. Ecker, and F. Bushman.** 2002. HIV-1 integration in the human genome favors active genes and local hotspots. *Cell* **110**:521-529.

236. **Schröfelbauer, B., D. Chen, and N. Landau.** 2004. A single amino acid of APOBEC3G controls its species-specific interaction with virion infectivity factor (Vif). *Proc Natl Acad Sci U S A* **101**:3927-3932.
237. **Schubert, H. L., Q. Zhai, V. Sandrin, D. M. Eckert, M. Garcia-Maya, L. Saul, W. I. Sundquist, R. A. Steiner, and C. P. Hill.** 2010. Structural and functional studies on the extracellular domain of BST2/tetherin in reduced and oxidized conformations. *Proc Natl Acad Sci U S A* **107**:17951-17956.
238. **Schubert, U., S. Bour, A. Ferrer-Montiel, M. Montal, F. Maldarell, and K. Strebel.** 1996. The two biological activities of human immunodeficiency virus type 1 Vpu protein involve two separable structural domains. *J Virol* **70**:809-819.
239. **Sebastian, S., and J. Luban.** 2005. TRIM5alpha selectively binds a restriction-sensitive retroviral capsid. *Retrovirology* **2**:40.
240. **Seo, J. Y., R. Yaneva, and P. Cresswell.** 2011. Viperin: A Multifunctional, Interferon-Inducible Protein that Regulates Virus Replication. *Cell Host Microbe* **10**:534-539.
241. **Seo, J. Y., R. Yaneva, E. R. Hinson, and P. Cresswell.** 2011. Human cytomegalovirus directly induces the antiviral protein viperin to enhance infectivity. *Science* **332**:1093-1097.
242. **Serra-Moreno, R., B. Jia, M. Breed, X. Alvarez, and D. T. Evans.** 2011. Compensatory changes in the cytoplasmic tail of gp41 confer resistance to tetherin/BST-2 in a pathogenic nef-deleted SIV. *Cell Host Microbe* **9**:46-57.
243. **Shah, A. H., B. Sowrirajan, Z. B. Davis, J. P. Ward, E. M. Campbell, V. Planelles, and E. Barker.** 2010. Degranulation of natural killer cells following interaction with HIV-1-infected cells is hindered by downmodulation of NTB-A by Vpu. *Cell Host Microbe* **8**:397-409.
244. **Sharova, N., Y. Wu, X. Zhu, R. Stranska, R. Kaushik, M. Sharkey, and M. Stevenson.** 2008. Primate lentiviral Vpx commandeers DDB1 to counteract a macrophage restriction. *PLoS Pathog* **4**:e1000057.
245. **Sharp, P.** 2002. Origins of human virus diversity. *Cell* **108**:305-312.
246. **Sharp, P. M., E. Bailes, M. Stevenson, M. Emerman, and B. H. Hahn.** 1996. Gene acquisition in HIV and SIV. *Nature* **383**:586-587.
247. **Sheehy, A. M., N. C. Gaddis, J. D. Choi, and M. H. Malim.** 2002. Isolation of a human gene that inhibits HIV-1 infection and is suppressed by the viral Vif protein. *Nature* **418**:646-650.
248. **Shehu-Xhilaga, M., S. M. Crowe, and J. Mak.** 2001. Maintenance of the Gag/Gag-Pol ratio is important for human immunodeficiency virus type 1 RNA dimerization and viral infectivity. *J Virol* **75**:1834-1841.
249. **Shi, M., W. Deng, E. Bi, K. Mao, Y. Ji, G. Lin, X. Wu, Z. Tao, Z. Li, X. Cai, S. Sun, C. Xiang, and B. Sun.** 2008. TRIM30 alpha negatively regulates TLR-mediated NF-kappa B activation by targeting TAB2 and TAB3 for degradation. *Nat Immunol* **9**:369-377.
250. **Simons, K., and M. J. Gerl.** 2010. Revitalizing membrane rafts: new tools and insights. *Nat Rev Mol Cell Biol* **11**:688-699.
251. **Skasko, M., Y. Wang, Y. Tian, A. Tokarev, J. Munguia, A. Ruiz, E. B. Stephens, S. J. Opella, and J. Guatelli.** 2011. HIV-1 Vpu antagonizes the innate restriction factor BST-2 via lipid-embedded helix-helix interactions. *J Biol Chem*.
252. **Sliva, K., T. Resch, B. Kraus, C. Goffinet, O. T. Keppler, and B. S. Schnierle.** 2011. The Cellular Anti-viral Restriction Factor Tetherin Does Not Inhibit Poxviral Replication. *J Virol*.
253. **Sodora, D. L., J. S. Allan, C. Apetrei, J. M. Brenchley, D. C. Douek, J. G. Else, J. D. Estes, B. H. Hahn, V. M. Hirsch, A. Kaur, F. Kirchhoff, M. Muller-Trutwin, I. Pandrea, J. E. Schmitz, and G. Silvestri.** 2009. Toward an AIDS vaccine: lessons from natural simian immunodeficiency virus infections of African nonhuman primate hosts. *Nat Med* **15**:861-865.

254. **Souquière, S., F. Bibollet-Ruche, D. L. Robertson, M. Makuwa, C. Apetrei, R. Onanga, C. Kornfeld, J. C. Plantier, F. Gao, K. Abernethy, L. J. White, W. Karesh, P. Telfer, E. J. Wickings, P. Maucière, P. A. Marx, F. Barré-Sinoussi, B. H. Hahn, M. C. Müller-Trutwin, and F. Simon.** 2001. Wild Mandrillus sphinx are carriers of two types of lentivirus. *J Virol* **75**:7086-7096.
255. **Souquière, S., R. Onanga, M. Makuwa, I. Pandrea, P. Ngari, P. Rouquet, O. Bourry, M. Kazanji, C. Apetrei, F. Simon, and P. Roques.** 2009. Simian immunodeficiency virus types 1 and 2 (SIV mnd 1 and 2) have different pathogenic potentials in rhesus macaques upon experimental cross-species transmission. *J Gen Virol* **90**:488-499.
256. **Stetson, D. B., J. S. Ko, T. Heidmann, and R. Medzhitov.** 2008. Trex1 prevents cell-intrinsic initiation of autoimmunity. *Cell* **134**:587-598.
257. **Stivahtis, G. L., M. A. Soares, M. A. Vodicka, B. H. Hahn, and M. Emerman.** 1997. Conservation and host specificity of Vpr-mediated cell cycle arrest suggest a fundamental role in primate lentivirus evolution and biology. *J Virol* **71**:4331-4338.
258. **Stolp, B., M. Reichman-Fried, L. Abraham, X. Pan, S. Giese, S. Hannemann, P. Goulimari, E. Raz, R. Grosse, and O. Fackler.** 2009. HIV-1 Nef interferes with host cell motility by deregulation of Cofilin. *Cell Host Microbe* **6**:174-186.
259. **Strack, B., A. Calistri, S. Craig, E. Popova, and H. G. Göttlinger.** 2003. AIP1/ALIX is a binding partner for HIV-1 p6 and EIAV p9 functioning in virus budding. *Cell* **114**:689-699.
260. **Stremlau, M., C. Owens, M. Perron, M. Kiessling, P. Autissier, and J. Sodroski.** 2004. The cytoplasmic body component TRIM5alpha restricts HIV-1 infection in Old World monkeys. *Nature* **427**:848-853.
261. **Stremlau, M., M. Perron, M. Lee, Y. Li, B. Song, H. Javanbakht, F. Diaz-Griffero, D. J. Anderson, W. I. Sundquist, and J. Sodroski.** 2006. Specific recognition and accelerated uncoating of retroviral capsids by the TRIM5alpha restriction factor. *Proc Natl Acad Sci U S A* **103**:5514-5519.
262. **Stremlau, M., M. Perron, S. Welikala, and J. Sodroski.** 2005. Species-specific variation in the B30.2(SPRY) domain of TRIM5alpha determines the potency of human immunodeficiency virus restriction. *J Virol* **79**:3139-3145.
263. **Suhasini, M., and T. R. Reddy.** 2009. Cellular proteins and HIV-1 Rev function. *Curr HIV Res* **7**:91-100.
264. **Swiecki, M., S. M. Scheaffer, M. Allaire, D. H. Fremont, M. Colonna, and T. J. Brett.** 2011. Structural and biophysical analysis of BST-2/tetherin ectodomains reveals an evolutionary conserved design to inhibit virus release. *J Biol Chem* **286**:2987-2997.
265. **Szretter, K. J., J. D. Brien, L. B. Thackray, H. W. Virgin, P. Cresswell, and M. S. Diamond.** 2011. The interferon-inducible gene viperin restricts West Nile virus pathogenesis. *J Virol*.
266. **Takeda, K., and S. Akira.** 2003. Toll receptors and pathogen resistance. *Cell Microbiol* **5**:143-153.
267. **Takehisa, J., M. Kraus, A. Ayoub, E. Bailes, F. Van Heuverswyn, J. Decker, Y. Li, R. Rudicell, G. Learn, C. Neel, E. Ngole, G. Shaw, M. Peeters, P. Sharp, and B. Hahn.** 2009. Origin and biology of simian immunodeficiency virus in wild-living western gorillas. *J Virol* **83**:1635-1648.
268. **Takehisa, J., M. Kraus, J. Decker, Y. Li, B. Keele, F. Bibollet-Ruche, K. Zammit, Z. Weng, M. Santiago, S. Kamenya, M. Wilson, A. Pusey, E. Bailes, P. Sharp, G. Shaw, and B. Hahn.** 2007. Generation of infectious molecular clones of simian immunodeficiency virus from fecal consensus sequences of wild chimpanzees. *J Virol* **81**:7463-7475.
269. **Takemura, T., and M. Hayami.** 2004. Phylogenetic analysis of SIV derived from mandrill and drill. *Front Biosci* **9**:513-520.

270. **Tareen, S. U., and M. Emerman.** 2011. Human Trim5 α has additional activities that are uncoupled from retroviral capsid recognition. *Virology* **409**:113-120.
271. **Thali, M., A. Bukovsky, E. Kondo, B. Rosenwirth, C. T. Walsh, J. Sodroski, and H. G. Göttinger.** 1994. Functional association of cyclophilin A with HIV-1 virions. *Nature* **372**:363-365.
272. **Thompson, J., T. Gibson, F. Plewniak, F. Jeanmougin, and D. Higgins.** 1997. The CLUSTAL_X windows interface: flexible strategies for multiple sequence alignment aided by quality analysis tools. *Nucleic Acids Res* **25**:4876-4882.
273. **Tokarev, A., M. Skasko, K. Fitzpatrick, and J. Guatelli.** 2009. Antiviral Activity of the Interferon-Induced Cellular Protein BST-2/Tetherin. *AIDS Res Hum Retroviruses* **25**:1197-1210.
274. **Tokarev, A. A., J. Munguia, and J. C. Guatelli.** 2011. Serine-threonine ubiquitination mediates downregulation of BST-2/tetherin and relief of restricted virion release by HIV-1 Vpu. *J Virol* **85**:51-63.
275. **Tosi, A., D. Melnick, and T. Disotell.** 2004. Sex chromosome phylogenetics indicate a single transition to terrestriality in the guenons (tribe Cercopithecini). *J Hum Evol* **46**:223-237.
276. **Towers, G., M. Bock, S. Martin, Y. Takeuchi, J. P. Stoye, and O. Danos.** 2000. A conserved mechanism of retrovirus restriction in mammals. *Proc Natl Acad Sci U S A* **97**:12295-12299.
277. **Tristem, M., C. Marshall, A. Karpas, J. Petrik, and F. Hill.** 1990. Origin of vpx in lentiviruses. *Nature* **347**:341-342.
278. **Tristem, M., A. Purvis, and D. L. Quicke.** 1998. Complex evolutionary history of primate lentiviral vpr genes. *Virology* **240**:232-237.
279. **Tsujimoto, H., R. W. Cooper, T. Kodama, M. Fukasawa, T. Miura, Y. Ohta, K. Ishikawa, M. Nakai, E. Frost, and G. E. Roelants.** 1988. Isolation and characterization of simian immunodeficiency virus from mandrills in Africa and its relationship to other human and simian immunodeficiency viruses. *J Virol* **62**:4044-4050.
280. **Vallari, A., V. Holzmayer, B. Harris, J. Yamaguchi, C. Ngansop, F. Makamche, D. Mbanya, L. Kaptué, N. Ndembi, L. Gürtler, S. Devare, and C. A. Brennan.** 2011. Confirmation of putative HIV-1 group P in Cameroon. *J Virol* **85**:1403-1407.
281. **van 't Wout, A. B., J. V. Swain, M. Schindler, U. Rao, M. S. Pathmajeyan, J. I. Mullins, and F. Kirchhoff.** 2005. Nef induces multiple genes involved in cholesterol synthesis and uptake in human immunodeficiency virus type 1-infected T cells. *J Virol* **79**:10053-10058.
282. **Van Damme, N., D. Goff, C. Katsura, R. Jorgenson, R. Mitchell, M. Johnson, E. Stephens, and J. Guatelli.** 2008. The interferon-induced protein BST-2 restricts HIV-1 release and is downregulated from the cell surface by the viral Vpu protein. *Cell Host Microbe* **3**:245-252.
283. **van der Kuyl, A., C. Kuiken, J. Dekker, and J. Goudsmit.** 1995. Phylogeny of African monkeys based upon mitochondrial 12S rRNA sequences. *J Mol Evol* **40**:173-180.
284. **Van Heuverswyn, F., Y. Li, C. Neel, E. Bailes, B. Keele, W. Liu, S. Loul, C. Butel, F. Liegeois, Y. Bienvenue, E. Ngolle, P. Sharp, G. Shaw, E. Delaporte, B. Hahn, and M. Peeters.** 2006. Human immunodeficiency viruses: SIV infection in wild gorillas. *Nature* **444**:164.
285. **van Rensburg, E. J., S. Engelbrecht, J. Mwenda, J. D. Laten, B. A. Robson, T. Stander, and G. K. Chege.** 1998. Simian immunodeficiency viruses (SIVs) from eastern and southern Africa: detection of a SIVagm variant from a chacma baboon. *J Gen Virol* **79** (Pt 7):1809-1814.
286. **Van Valen, L.** 1973. A new evolutionary law. *Evolutionary theory* **1**:1-30.
287. **Verschoor, E. J., S. Langenhuijzen, I. Bontjer, Z. Fagrouch, H. Niphuis, K. S. Warren, K. Eulenberger, and J. L. Heeney.** 2004. The phylogeography of orangutan foamy viruses supports the theory of ancient repopulation of Sumatra. *J Virol* **78**:12712-12716.

288. **Vigan, R., and S. J. Neil.** 2010. Determinants of tetherin antagonism in the transmembrane domain of the human immunodeficiency virus type 1 Vpu protein. *J Virol* **84**:12958-12970.
289. **Virgen, C. A., Z. Kratovac, P. D. Bieniasz, and T. Hatzioannou.** 2008. Independent genesis of chimeric TRIM5-cyclophilin proteins in two primate species. *Proc Natl Acad Sci U S A* **105**:3563-3568.
290. **Vodicka, M., W. Goh, L. Wu, M. Rogel, S. Bartz, V. Schweickart, C. Raport, and M. Emerman.** 1997. Indicator cell lines for detection of primary strains of human and simian immunodeficiency viruses. *Virology* **233**:193-198.
291. **Waheed, A. A., and E. O. Freed.** 2009. Lipids and membrane microdomains in HIV-1 replication. *Virus Res* **143**:162-176.
292. **Wainberg, M. A., A. Dascal, N. Blain, L. Fitz-Gibbon, F. Boulterice, K. Numazaki, and M. Tremblay.** 1988. The effect of cyclosporine A on infection of susceptible cells by human immunodeficiency virus type 1. *Blood* **72**:1904-1910.
293. **Wang, X., E. Hinson, and P. Cresswell.** 2007. The interferon-inducible protein viperin inhibits influenza virus release by perturbing lipid rafts. *Cell Host Microbe* **2**:96-105.
294. **Warren, K. S., H. Niphuis, Heriyanto, E. J. Verschoor, R. A. Swan, and J. L. Heeney.** 1998. Seroprevalence of specific viral infections in confiscated orangutans (*Pongo pygmaeus*). *J Med Primatol* **27**:33-37.
295. **Warrilow, D., G. Tachedjian, and D. Harrich.** 2009. Maturation of the HIV reverse transcription complex: putting the jigsaw together. *Rev Med Virol* **19**:324-337.
296. **Watanabe, R., G. P. Leser, and R. A. Lamb.** 2011. Influenza virus is not restricted by tetherin whereas influenza VLP production is restricted by tetherin. *Virology* **417**:50-56.
297. **Wertheim, J., and M. Worobey.** 2007. A challenge to the ancient origin of SIVagm based on African green monkey mitochondrial genomes. *PLoS Pathog* **3**:e95.
298. **Wertheim, J. O., and M. Worobey.** 2009. Dating the age of the SIV lineages that gave rise to HIV-1 and HIV-2. *PLoS Comput Biol* **5**:e1000377.
299. **Wilson, S. J., B. L. Webb, L. M. Ylinen, E. Verschoor, J. L. Heeney, and G. J. Towers.** 2008. Independent evolution of an antiviral TRIMCyp in rhesus macaques. *Proc Natl Acad Sci U S A* **105**:3557-3562.
300. **Wolf, D., and S. Goff.** 2008. Host restriction factors blocking retroviral replication. *Annu Rev Genet* **42**:143-163.
301. **Worobey, M., M. Gemmel, D. Teuwen, T. Haselkorn, K. Kunstman, M. Bunce, J. Muyembe, J. Kabongo, R. Kalengayi, E. Van Marck, M. Gilbert, and S. Wolinsky.** 2008. Direct evidence of extensive diversity of HIV-1 in Kinshasa by 1960. *Nature* **455**:661-664.
302. **Wu, C., C. Orozco, J. Boyer, M. Leglise, J. Goodale, S. Batalov, C. L. Hodge, J. Haase, J. Janes, J. W. Huss, and A. I. Su.** 2009. BioGPS: an extensible and customizable portal for querying and organizing gene annotation resources. *Genome Biol* **10**:R130.
303. **Wu, Y.** 2004. HIV-1 gene expression: lessons from provirus and non-integrated DNA. *Retrovirology* **1**:13.
304. **Yamashita, M., and M. Emerman.** 2004. Capsid is a dominant determinant of retrovirus infectivity in nondividing cells. *J Virol* **78**:5670-5678.
305. **Yamashita, M., O. Perez, T. J. Hope, and M. Emerman.** 2007. Evidence for direct involvement of the capsid protein in HIV infection of nondividing cells. *PLoS Pathog* **3**:1502-1510.
306. **Yang, H., J. Wang, X. Jia, M. W. McNatt, T. Zang, B. Pan, W. Meng, H. W. Wang, P. D. Bieniasz, and Y. Xiong.** 2010. Structural insight into the mechanisms of enveloped virus tethering by tetherin. *Proc Natl Acad Sci U S A* **107**:18428-18432.

307. **Yang, S., L. Lopez, H. Hauser, C. Exline, K. Haworth, and P. Cannon.** 2010. Anti-tetherin activities in Vpu-expressing primate lentiviruses. *Retrovirology* **7**:13.
308. **Yang, Z.** 1997. PAML: a program package for phylogenetic analysis by maximum likelihood. *Comput Appl Biosci* **13**:555-556.
309. **Yap, M. W., S. Nisole, and J. P. Stoye.** 2005. A single amino acid change in the SPRY domain of human Trim5alpha leads to HIV-1 restriction. *Curr Biol* **15**:73-78.
310. **Yondola, M. A., F. Fernandes, A. Belicha-Villanueva, M. Uccellini, Q. Gao, C. Carter, and P. Palese.** 2011. Budding capability of the influenza virus neuraminidase can be modulated by tetherin. *J Virol* **85**:2480-2491.
311. **Yoshida, T., S. Kao, and K. Strebel.** 2011. Identification of Residues in the BST-2 TM Domain Important for Antagonism by HIV-1 Vpu Using a Gain-of-Function Approach. *Front Microbiol* **2**:35.
312. **Yu, X. F., S. Ito, M. Essex, and T. H. Lee.** 1988. A naturally immunogenic virion-associated protein specific for HIV-2 and SIV. *Nature* **335**:262-265.
313. **Yuan, X., Z. Matsuda, M. Matsuda, M. Essex, and T. H. Lee.** 1990. Human immunodeficiency virus vpr gene encodes a virion-associated protein. *AIDS Res Hum Retroviruses* **6**:1265-1271.
314. **Zhang, F., W. N. Landford, M. Ng, M. W. McNatt, P. D. Bieniasz, and T. Hatziioannou.** 2011. SIV Nef proteins recruit the AP-2 complex to antagonize Tetherin and facilitate virion release. *PLoS Pathog* **7**:e1002039.
315. **Zhang, F., S. Wilson, W. Landford, B. Virgen, D. Gregory, M. Johnson, J. Munch, F. Kirchhoff, P. Bieniasz, and T. Hatziioannou.** 2009. Nef proteins from simian immunodeficiency viruses are tetherin antagonists. *Cell Host Microbe* **6**:54-67.
316. **Zhang, H., B. Yang, R. J. Pomerantz, C. Zhang, S. C. Arunachalam, and L. Gao.** 2003. The cytidine deaminase CEM15 induces hypermutation in newly synthesized HIV-1 DNA. *Nature* **424**:94-98.
317. **Zhao, G., D. Ke, T. Vu, J. Ahn, V. B. Shah, R. Yang, C. Aiken, L. M. Charlton, A. M. Gronenborn, and P. Zhang.** 2011. Rhesus TRIM5α disrupts the HIV-1 capsid at the inter-hexamer interfaces. *PLoS Pathog* **7**:e1002009.
318. **Zheng, Y. H., A. Plemenitas, C. J. Fielding, and B. M. Peterlin.** 2003. Nef increases the synthesis of and transports cholesterol to lipid rafts and HIV-1 progeny virions. *Proc Natl Acad Sci U S A* **100**:8460-8465.

EFREM SU-EE LIM

Research Interests

Molecular biology of HIV-1

Evolutionary arms race between host restriction factors and retroviruses

Discovery of novel viruses and human pathogens

Education

2007 – 2012	Ph.D. , Microbiology	University of Washington, Seattle, WA, USA
	Thesis: Fundamentals of the Host-Virus Evolutionary Arms Race Laboratory of Michael Emerman	
2005 – 2007	B.S. , Microbiology (Honors)	University of Michigan, Ann Arbor, MI, USA
	Thesis: Quantitative trait locus mapping for susceptibility to Mouse Adenovirus Type I Laboratory of Katherine Spindler	

Work Experience

2012 – Present	Postdoctoral Research Fellow	Washington University, St Louis, MO, USA
	Discovery of novel viruses and human pathogens.	
2007 – 2012	Graduate Research Assistant	University of Washington, Seattle, WA, USA
	Integrated Evolutionary biology with Virology to reconstruct evolutionary arms races between primate host restriction factors and retroviruses. 5 first author publications on 3 host restriction factors.	
	Research expertise includes: Pioneered HIV/SIV tissue culture assays and virus reporter systems, Biosafety Level 3 certified (5 years' experience), extensive molecular engineering of HIV-1 and SIV proviruses, comprehensive evolutionary (PAML, HyPhy) and phylogenetic (Maximum likelihood, Bayesian) analyses of host genes and complex viral sequences.	
2006 – 2007	Undergraduate Research Assistant	University of Michigan, Ann Arbor, MI, USA
	Genotyped and fine-mapped the quantitative trait locus for Mouse Adenovirus Type I susceptibility, and managed and maintained colonies of more than 600 mice. Research led to 1 publication.	
2005	Asia-Pacific Business Knowledge Analyst	Ernst & Young, Shanghai, China
	Chinese-to-English translation and SWOT analysis of market research covering the automotive and manufacturing industries of Greater-China region, generated Director/Partner level analysis reports	
2003 – 2005	Lieutenant (LTA)	Singapore Armed Forces, Singapore
	Platoon Commander, Company 3 rd in command	1 st Battalion, Singapore Infantry Regiment

Awards

2011 - 2012	Helen Riaboff Whiteley Graduate Fellowship Award, University of Washington Dept. of Microbiology, Seattle, WA
2009 - 2011	Fred Hutchinson Cancer Research Center Interdisciplinary Training Fellowship (Dual Mentored by Michael Emerman and Harmit S. Malik)
2010	Young Investigator Award. 17 th Conference on Retroviruses and Opportunistic Infections (CROI)
2009	Neal B. Groman Teaching Award, University of Washington Dept. of Microbiology, Seattle, WA

Publications

1. **Lim, E.S.**, and Emerman, M. (2009) Simian Immunodeficiency Virus SIVagm from African Green Monkeys does not antagonize endogenous levels of African Green Monkey Tetherin/BST-2. *J. Virol.* **83**: 11673-81
 2. Spindler, K., Welton, A., **Lim, E.S.**, Duvvuru, S., Althaus, I., Imperiale, J., Daoud, A., and Chesler, E. (2010) The Major Locus for Mouse Adenovirus Susceptibility Maps to Genes of the Hematopoietic Cell Surface-Expressed LY6 Family. *J. Immunol.* **184**: 3055-62
 3. **Lim, E.S.**, Malik, H.S., and Emerman, M. (2010) Ancient adaptive evolution of Tetherin shaped Vpu and Nef functions in human immunodeficiency virus and primate lentiviruses. *J. Virol.* **84**: 7124-34
 4. **Lim, E.S.** and Emerman, M. (2011) Going for the watchman. *Nature.* **474**(7353): 587-8
 5. **Lim, E.S.**, Fregoso, O.I., McCoy, C.O., Matsen, F.A., Malik, H.S., and Emerman M. (2012) SAMHD1-degrading activity preceded the birth of Vpx in primate lentiviruses. *Cell Host and Microbe*. Published online ahead of print doi:10.1016/j.chom.2012.01.007
 6. **Lim, E.S.**, Wu, L.I., Malik, H.S., and Emerman M. The function and evolution of the restriction factor Viperin in primates was not driven by lentiviruses. *J. Virol.* Under review
-

EDITORIAL ACTIVITIES

2011 – Present Young Investigator Editorial Board, AIDS Research and Human Retroviruses
2009 – Present Co-reviewed publications for Journal of Virology and Nature.

PRESENTATIONS

- 10/11 Basic Sciences Seminar Series, Fred Hutchinson Cancer Research Center. **Oral presentation**
- 9/11 Fred Hutchinson Cancer Research Center Retrovirus Meeting. **Oral presentation**
- 3/11 Keystone Symposia on HIV Evolution, Genomics and Pathogenesis. Whistler, BC. **Poster presentation**
- 9/10 Fred Hutchinson Cancer Research Center Retrovirus Meeting. **Oral presentation**
- 7/10 29th Annual Meeting of the American Society for Virology. Bozeman, MO. **Oral presentation**
- 4/10 Basic Sciences Seminar Series, Fred Hutchinson Cancer Research Center. **Oral presentation**
- 2/10 17th Conference on Retroviruses and Opportunistic Infections. San Francisco, CA. **Oral presentation**
- 2/10 Fred Hutchinson Cancer Research Center Retrovirus Meeting. **Oral presentation**
- 8/09 University of Washington Microbiology Department Retreat. **Poster presentation**
- 5/09 Cold Spring Harbor Laboratory Meeting on Retroviruses. Cold Spring Harbor, NY. **Poster presentation**
- 3/09 Fred Hutchinson Cancer Research Center Retrovirus Meeting. **Oral presentation**
- 8/08 University of Washington Microbiology Department Retreat. **Oral presentation**
-

TEACHING EXPERIENCE

Undergraduate Trainees

Kathryn Hooper. 2010 – 2011. Undergraduate laboratory research, Mary Gates Scholar

Amelia Gallaher. 2009. Summer internships program

Teaching Assistant

2009 Neal B. Groman Teaching Award*, University of Washington Dept. of Microbiology
(* also appears in Awards)

2008 Fundamentals of General Microbiology Laboratory (Micro402). University of Washington

2008 General Microbiology Laboratory (Micro302). University of Washington

Lectures

2010 Prokaryotic Recombinant DNA Techniques (Micro431). University of Washington

2010 Prokaryotic Recombinant DNA Techniques (Micro431). University of Washington

REFERENCES

Dr. Michael Emmerman (Ph.D Advisor)

Fred Hutchinson Cancer Research Center, Department of Human Biology and Basic Sciences
University of Washington, Department of Microbiology
Email: memerman@fhcrc.org

Dr. Harmit S. Malik (Ph.D Co-mentor)

Fred Hutchinson Cancer Research Center, Division of Basic Sciences
University of Washington, Department of Genome Sciences
Howard Hughes Medical Institute
Email: hsmalik@fhcrc.org

Dr. Julie Overbaugh (Ph.D Committee member)

Fred Hutchinson Cancer Research Center, Division of Human Biology and Public Health Sciences
Email: joverbau@fhcrc.org

Dr. Shiu-lok Hu (Ph.D Committee member)

University of Washington, Department of Pharmaceutics and Microbiology
Washington National Primate Research Center
Email: hus@uw.edu